New Tools for Stereoselectivity and Orthogonality in Automated Glycan Assembly for Conjugate Vaccine Development

Inaugural-Dissertation

to obtain the academic degree

Doctor rerum naturalium (Dr. rer. nat.)

submitted to the Department of Biology, Chemistry, Pharmacy

Freie Universität Berlin

by

Sabrina Omoregbee-Leichnitz (geb. Leichnitz)

2022

This work was performed between May 2019 and May 2022 under the direction of Prof. Dr. Peter H. Seeberger in the Department of Biomolecular Systems, at Max Planck Institute of Colloids and Interfaces.

1st reviewer: Prof. Dr. Peter H. Seeberger

2nd reviewer: Prof. Dr. Kevin Pagel

Date of defense: 14.10.2022

IV

Acknowledgements

Herewith I certify that I have prepared and written my thesis independently and that I have not used any sources and aids other than those indicated by me. I also declare that I have not submitted the dissertation in this or any other form to any other institution as a dissertation.

_____

Sabrina Omoregbee-Leichnitz

Table of Contents

Abstract

Carbohydrates represent the most diverse and prevalent class of biomolecules in nature and are essential in a wide variety of biological processes. Antigenic glycans at the surface of microbes have the potential to be developed into glycoconjugate vaccines. The **Automated Glycan Assembly** (AGA) approach can provide those glycans rapidly in a solid-supported synthesis. Challenges in the synthesis of glycans by AGA arise from their complex structures, which require both strict regio- and stereocontrol, but also from technical limitations of the current AGA synthesizer. The goal of my research was to expand capabilities of AGA by introducing new orthogonal protecting groups and developing new strategies for 1,2-*cis* stereoselective glycosylations to give access to materials for research on infectious diseases.

The first part of this dissertation focuses on **orthogonality** and the expansion of the protecting group portfolio in AGA (Chapter 3). The introduction of microwave-assistance to the AGA synthesizer enabled a larger temperature range (-40 to 100 °C) and the development of a mannose building block with four orthogonal protecting groups. When utilized in the microwave-assisted platform, this building block allowed 1) on-resin global deprotection and 2) the synthesis of glycan structures with up to four branches. In parallel, photo-labile 4,4-difluoro-4-bora-3*a*,4*a*-diaza-*s*-indacene (BODIPY) protecting groups were developed. A BODIPY protecting group bearing a boron difluoride unit provided the optimal compromise between glycosylation-stability and photo-lability by green light irradiation. This protecting group enabled a solution-phase consecutive glycan assembly without intermediate purification up to a trisaccharide.

The second part of this dissertation describes studies on factors that influence the **stereoselectivity** for 1,2-*cis* glycosylations (Chapter 4). The influence of positional and electronic effects in acyl and ether groups on the efficacy for remote participation were investigated. An array of uniquely substituted building blocks was synthesized followed by the evaluation in model glycosylations and cold-ion IR spectroscopy. The obtained mechanistic insights helped to design building blocks for the formation of α-(1→3)-galactosidic linkages.

In Chapter 5, the new knowledge and developed methods were utilized to synthesize a conjugation-ready glycan library of the *Porphorymonas gingivalis* lipopolysaccharide (LPS). *P. gingivalis* has an immense social and medical impact as it is the major cause of chronical periodontitis and is associated with several systemic diseases. The improvement of our basic understanding of interactions between human immune system and LPS may allow for treatment and prevention strategies. Twelve LPS fragments of *P. gingivalis* were screened for IgG and IgA binding in human saliva and serum using glycan microarray studies, which enabled the identification of 5-amino-pentyl α-D-Galp-(1→6)-α-D-Glcp-(1→4)-α-L-Rhap-(1→3)-2-β-D-GalNAc as a potential **glycoconjugate vaccine candidate** against *P. gingivalis*.

Zusammenfassung

Kohlenhydrate sind die vielfältigsten und verbreitetsten Biomoleküle in der Natur und sind essentiell für eine Vielzahl an Abläufen in Organsimen. Oberflächen-Glykane von Pathogenen können als Antigene dienen und haben Potential für die Entwicklung von Glykokonjugatimpfstoffen. Die **automatische Festphasensynthese** (engl. *Automated Glycan Assembly*, AGA) kann diese Glykane schnell bereitstellen. Syntheseschwierigkeiten von Glykanen im AGA kommen vor allem durch ihre Komplexität, die strenge Einhaltung von Regio- und Stereokontrolle voraussetzt, aber auch durch technische Grenzen der AGA-Synthesemaschinen zustande. Das allgemeine Ziel meiner Forschung war die Verbesserung des AGA-Repertoire durch die Einführung von orthogonalen Schutzgruppen und die Entwicklung von neuen Strategien für 1,2-*cis*-stereoselektive Glykosylierungen.

Der erste Teil dieser Dissertation fokussiert sich auf die **Orthogonalität** und die Erweiterung des Schutzgruppen-Portfolios (3. Kapitel). Die Einführung von Mikrowellen-assistenz in die AGA-Synthesemaschine ermöglichte eine größere Temperaturspanne (-40 bis 100 °C) und die Entwicklung eines komplett orthogonalen Mannose-Bausteines. Dieser Baustein erlaubte zum einen die globale Entschützung am Harz und zum anderen den Aufbau von Strukturen mit bis zu vier Verzweigungen. Außerdem wurden photo-labile BODIPY-Schutzgruppen entwickelt. Eine BODIPY-Schutzgruppe mit einer Bordifluorid-Einheit bot einen guten Kompromiss zwischen Glykosylierungs-Stabilität und Photoreaktivität bei grünem Licht. Dies ermöglichte eine fortlaufende Glykan-Herstellung ohne intermediäre Aufreinigungen bis zum Trisaccharid.

Der zweite Teil der Dissertation beschreibt Studien zu Einflussfaktoren auf die **Stereoselektivität** von 1,2-*cis*-Glykosylierungen (4. Kapitel). Es wurden elektronische Effekte von Acyl- und Ether-Gruppen und der Effekt ihrer Position auf die Effizienz von Fern-Beteiligung untersucht. Dies wurde durch die Synthese einer Vielzahl an substituierten Bausteinen, ihrer Evaluation in Test-Glykosylierungen und Kalt-Ionen-Spektroskopie verwirklicht. Die so erhaltenen mechanistischen Einblicke halfen dabei, Bausteine für die Bildung von α-(1→3)-galactosidischen Bindungen zu entwickeln.

Das erlernte Wissen und die entwickelten Methoden wurden im 5. Kapitel für die Synthese einer Glykan-Bibliothek aus konjugations-bereiten Teilen der LPS-Wiederholungseinheit von *Porphyromonas gingivalis* verwendet. *P. gingivalis* hat einen großen sozialen und medizinischen Impakt, da es der Hauptauslöser von chronischer Parodontitis ist und mit verschiedenen systemischen Krankheiten in Verbindung steht. Mikroarray-Studien zur Überprüfung von IgG- und IgA-Bindung aus Speichel und Serum ermöglichten die Identifizierung eines potentiellen **Glykokonjugat-Impfstoff-Kandidaten** (-D-Galp-(1→6)-α-D-Glcp-(1→4)-α-L-Rhap-(1→3)-2-β-D-GalNAc) gegen *P. gingivalis*.

Abbreviations

Ac	Acetyl
AD	Alzheimer's disease
ADDP	1,1'-(Azodicarbonyl)dipiperidine
AGA	Automated Glycan Assembly
Aβ	Amyloid-β
Bn	Benzyl
BODIPY	4-difluoro-4-bora-3*a*,4*a*-diaza-*s*-indacene
Bz	Benzoyl
Cbz	Benzyl chloroformate
CDI	Carbonyldiimidazole
ClAc	Chloroacetate
COVID-19	Coronavirus disease 2019
CP	Chronic periodontitis
CPS	Capsular polysaccharide
CRM197	Corynebacterium diphtheria Mutant CRM197
DCE	Dichloroethane
DDQ	2,3-Dichloro-5,6-dicyano-1,4-benzoquinone
DEAD	Diethyl azodicarboxylate
DFT	Density functional theory
DMAP	Dimethylamino pyridine
DMP	2,6-dimethylphenyl
DMS	Dimethyl sulfone
DMSO	Dimethyl sulfoxide
DMTST	Dimethyl(methylthio)sulfonium trifluoromethanesulfonate
DNA	Deoxyribonucleic acid
Engl.	English
Equiv.	Equivalents
ESI	Electrospray ionization
Et	Ethyl
Fmoc	Fluorenylmethyloxycarbonyl
Fmoc	9-Fluorenylmethyl carbonate
FT-IR	Fourier-transform-infrared
Fuc	Fucose
Gal	Galactose
GalNAc	N-Acetylgalactosamine
Glc	Glucose
GPI	Glycosylphosphatidylinositol
HPLC	High-performance liquid chromatography
HRMS	High-resolution mass spectrometry
IgG/A/M	Immunoglobulin G/A/M
***i*Pr**	*iso*-Propyl
IR	Infrared
Lat.	Latin
LED	Light-emitting diode
Lev	Levulinyl
LG	Leaving group

LPS	Lipopolysaccharide
LRMS	low resolution mass spectrometry
MALDI	Matrix-assisted laser desorption-ionization
Man	Mannose
Mbp	1-(*tert*-butyl)-4-methyl phenyl
Me	Methyl
mRNA	Messenger ribonucleic acid
MS	Mass spectrometry
MW	Microwave
NAP	2-Naphthylmethyl ether
nESI	Nanoelectrospray ionization
NHS	*N*-Hydroxysuccinimide
NIS	*N*-Iodosuccinimide
NMR	Nuclear magnetic resonance
NP	Normal phase
PG	Protecting group
Ph	Phenyl
Piv	Pivaloyl
PPAD	Peptidyl-arginine deiminase
Rha	Rhamnose
RP	Reversed phase
SARS-CoV-2	Severe acute respiratory syndrome coronavirus type 2
S$_N$	Nucleophilic substitution
TBAF	Tetra-n-butylammonium fluoride
_t_Bu	*tert*-Butyl
TCA	Trichloroacetyl
TEA	Triethylamine
Tf	Triflate
TFA	Trifluoroacetic acid
TFAA	Trifluoracetic anhydride
TfOH	Triflic acid
THF	Tetrahydrofuran
TLC	thin-layer chromatography
TMS	(Trimethyl)silyl
TOF	Time-of-flight
Tol	Tolyl
tPG	Temporary protecting group
Trt	Trityl
Ts	Tosyl
UV	Ultraviolet

1   Motivation and Background

1.1   General Aspects of Carbohydrate Synthesis

Carbohydrates are found in all forms of living organisms. The global biomass is constituted by two thirds of carbohydrates, especially in form of photosynthesis products such as cellulose and the exoskeleton component chitin.[1] Therefore, carbohydrates are an important energy source, carbon dioxide storage and regenerative raw material. They are also essential for a variety of important roles in living organisms, including structural definition, nutrition, signalling, cell adhesion and host-pathogen interactions.[2] Polysaccharides of pathogens enable interactions with the host and play an important role in infectious diseases and immune responses.[3] Rapid access to homogeneous carbohydrate material provides precious materials for many research fields such as immunology, oncology and material science.

Carbohydrates, including oligosaccharides and polysaccharides (also known as glycans), are composed of monosaccharide units that are connected *via* glycosidic linkages. Compounds consisting of a large number of monosaccharides linked *via* a glycosidic bond, are called polysaccharides, while compounds from three to ten monosaccharide units are considered to be oligosaccharides.[4]

Polysaccharides are besides nucleic acids and proteins the major biopolymers in nature. However, carbohydrates stand out for their complexity and diversity compared to other biomolecules. While nucleotides and peptides are linear, carbohydrates often are branched. Most monosaccharide units contain four hydroxyl groups that can serve as anchor points for further chain growth. Furthermore, each glycosidic linkage is a stereogenic center, in contrast to the phosphate diester that connects nucleotides and the amide bond that connects amino acids in peptides. Therefore, stereo- and regiocontrol are inevitable for the synthesis of defined glycans.

The belated progress in glycosciences, compared to peptides and nucleic acids, originates from the complexity of carbohydrates and its synthetic challenges. Traditional approaches rely on chemoenzymatic methods, extraction from natural sources and conventional chemical methods. Each step requires separation from enzyme, buffer, metal and any incomplete sequence.[5] Isolation from natural sources is difficult as carbohydrates are typically obtained in small amounts and as complex heterogeneous mixtures.[6] Access to defined structures in useful quantities without contamination relies on synthetic carbohydrates. Therefore, the progress in glycosciences is dependent on chemical strategies for synthetic carbohydrates.

The chemical synthesis of carbohydrates involves a series of sequential steps (Figure 1.1): the building block synthesis (A), the glycan assembly (B) including glycosylation reaction and selective deprotection, the global deprotection (C) followed by purification and characterization.

Suitable protected building blocks are synthesized from monosaccharides using protecting group manipulations (Figure 1.1A). Protecting groups (PGs) are chosen according to the orthogonality principle to achieve regiocontrol, which is further discussed in Chapter 3. Differences in reactivity of typical ether, ester, acetal, carbonate or silyl ether protecting groups can be used to selectively deprotect a specific position at the saccharide. In a glycosylation reaction (Figure 1.1B), the anomeric carbon of a completely protected monosaccharide (glycosyl donor) bearing a leaving group (LG) is activated using a promoter. Afterwards, a nucleophilic attack by an unprotected hydroxyl group of another monosaccharide (glycosyl acceptor) takes place. Glycosyl donors are typically glycosyl halides, thioglycosides, glycosyl phosphates or imidates. Stereocontrol of this reaction is often the most challenging aspect of the assembly of monosaccharides. It can be achieved by protecting group participation, chiral auxiliaries, steric hindrance and solvent or additive effects. This aspect is further discussed in Chapter 4. After the subsequent oligosaccharide assembly steps, protecting groups are removed in a global deprotection that typically includes the hydrolysis of ester and carbonate PGs (e.g. using sodium methoxide) and the reductive cleavage of ether PGs (e.g. using H_2 and palladium on carbon) to afford the unprotected oligosaccharide.
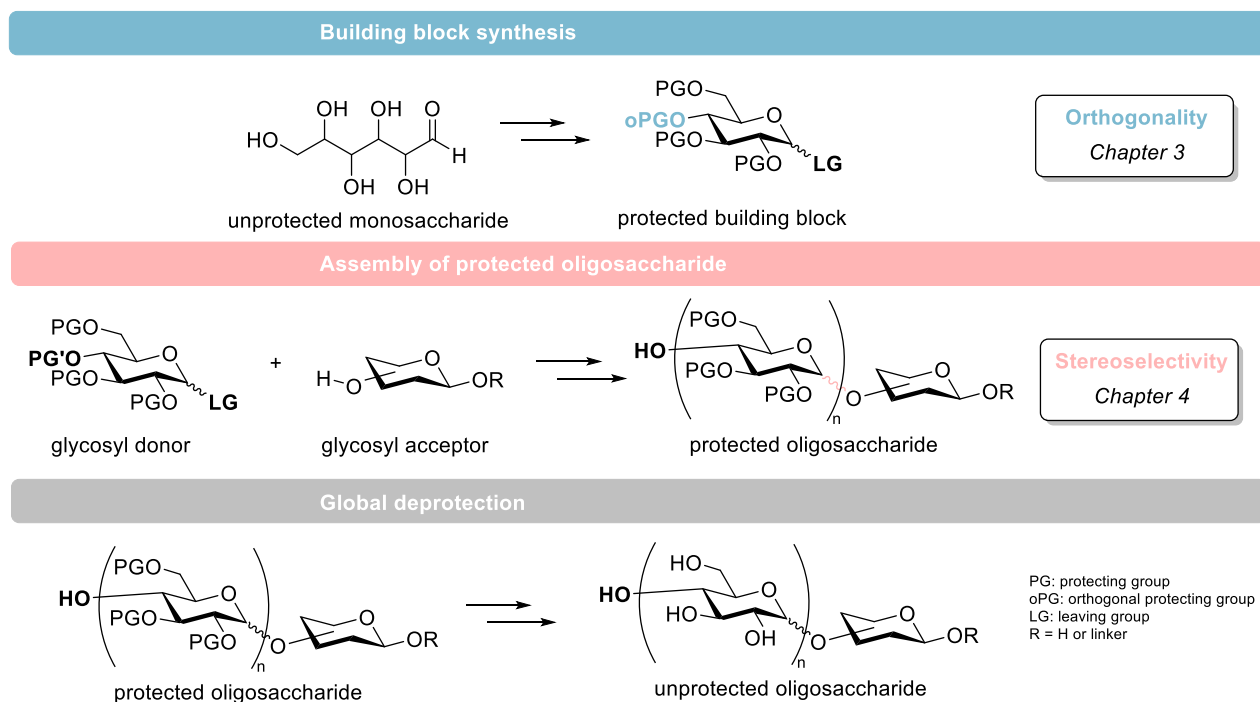
Figure 1.1. Sequential steps of the synthesis of glycans.

The synthesis of carbohydrates requires multiple stereoselective glycosylation steps, protecting group manipulations and purification procedures (as illustrated in Figure 1.1). This often results in several months of work employing traditional approaches in solution-phase. In order to accelerate the synthesis of carbohydrates, several strategies have been developed in the past, including enzymatic or chemoenzymatic, convergent, one-pot, tag-assisted and solid-supported synthesis. This work focuses on the automated solid-supported synthesis.

1.2   The Automated Glycan Assembly Approach

The Automated Glycan Assembly (AGA)[7] approach is a method for the automated solid-phase synthesis of glycans. Challenges of oligosaccharide synthesis, such as time, labor-intensity, and reliability, were encountered by this approach. AGA completes the set of automated biomolecule synthesis besides the well-established solid-supported synthesis of homogeneous oligonucleotides[8] and peptides[9]. The scope of the current AGA technology includes mannose-polysaccharides up to 151-mers[16], complex stereochemically challenging starch polysaccharides[10], glycans with different building blocks and one branch such as Lewis type antigens[11], blood group determants[12] or CPS antigens[13], flourine-labeled glycans[14], keratan sulfate and generally sulfated oligosaccharides[15], plant oligosaccharides[16], and oligogalactofuranosides[17].
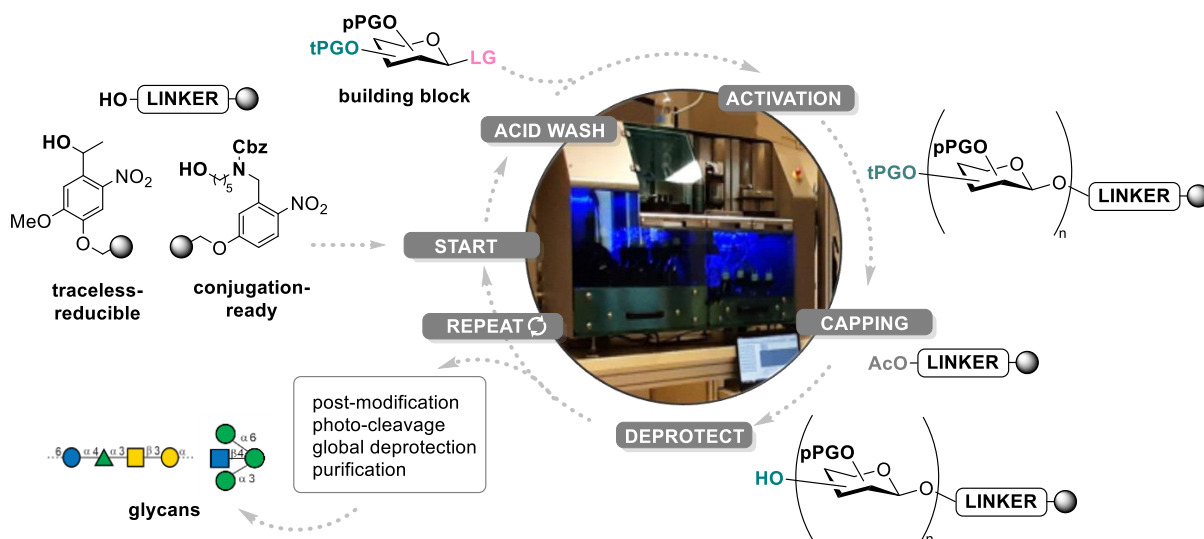
Figure 1.2. Overview of the AGA coupling cycle including acid wash, activation, capping, and deprotection. A traceless-reducible or conjugation-ready linker is used to couple building blocks containing a temporary protecting group (**tPG**), permanent protecting groups (**pPG**) and a leaving group (**LG**, -SR or glycosyl phosphates) for the assembly of a growing oligomer chain, to get glycans after optional post-modification, photo-cleavage, global deprotection and purification.

In AGA, a solid-support (Merrifield polystyrene resin) equipped with a traceless-reducible or conjugation-ready linker is used to couple building blocks and assemble a growing oligomer chain (Figure 1.2). The solid-support is used as an anchor for the growing oligomer

and enables the removal of excess reagents by washing. This saves time-consuming intermediate purification steps. The building blocks are monosaccharides that bear a temporary protecting group (tPG, e.g. 9-fluorenylmethyl carbonate (Fmoc) and levulinoyl esters (Lev)) and permanent protecting groups (pPG, e.g. benzyl (Bn) ethers or benzoyl (Bz) esters). The temporary protecting group is removed from the resin-bound oligomer to allow for subsequent chain growth in the following coupling cycle. After the coupling of the first building block, the coupling cycle consists of an acidic wash (TMSOTf), activation and glycosylation (NIS/TfOH for thioglycosides or TMSOTf for glycosyl phosphates), capping (Ac$_2$O, pyridine), and deprotection (e.g. piperidine for Fmoc). This cycle can be repeated until the desired glycan length is achieved. A post-modification step is optional, e.g. for the introduction of sulfate or phosphate functionalities. The process is completed after final cleavage from the support in a flow photo-reactor using UV light (366 nm, halogen or LED lamp) followed by global deprotection including ester deprotection by methanolysis and reductive hydrogenolysis and final purification of the free glycan.

Technical limitations of the current AGA synthesizer restrict assembly speed as well as the diversity of the glycans prepared by it. Therefore, process optimization is ongoing to enable a more efficient synthesis of even more complex glycans in a larger scale.

1.3 Synthetic Glycans in Conjugate Vaccines

Glycans play an important role in infectious diseases – mainly due to antigenic glycan structures at the surface of pathogens.[2] Infectious diseases, caused by bacteria, viruses and parasites, are a major global health problem. The discovery of penicillin by Alexander Fleming in 1928[18] and further research on antibiotics, antivirals and antiparasitics saved millions of lives so far, but also resulted in a major problem of anti-drug resistance. Instead of disease treatment, the prevention by immunization is an effective way to fight and eradicate infectious diseases. The first mucosal immunization approach by the Chinese physician Wan Quan in 1549[19] and the successful immunization against smallpox by the English physician Edward Jenner in 1796[20] was the starting point for the development of vaccines. Edward Jenner found that induced infection with mild cowpox caused immunity to the lethal smallpox virus, which is the origin of the word vaccine (lat. *Vaccinus*, "from the cow").[20] Following vaccine development and governmental immunization programs almost eradicated smallpox and polio in the 20th century and prevented many deadly infections, such as those caused by tetanus.[21]

The improved understanding of the human immune system and pathogen biology is the basis of the development of effective modern vaccine technologies for the generation of active immunity against infectious diseases. Vaccine technologies include the use of attenuated or

killed organisms, the use of subunits, such as toxins, proteins, virus-like particles or cell surface glycans, or the use of viral vectors and nucleic acids, such as messenger ribonucleic acid (mRNA) vaccines (Figure 1.3). Synthetic glycoconjugate vaccines are an attractive option, because of culturing challenges, rapid protein mutation, host-similarity risks in protein-based subunit vaccines as well as laborious isolation of native polysaccharides.[22]
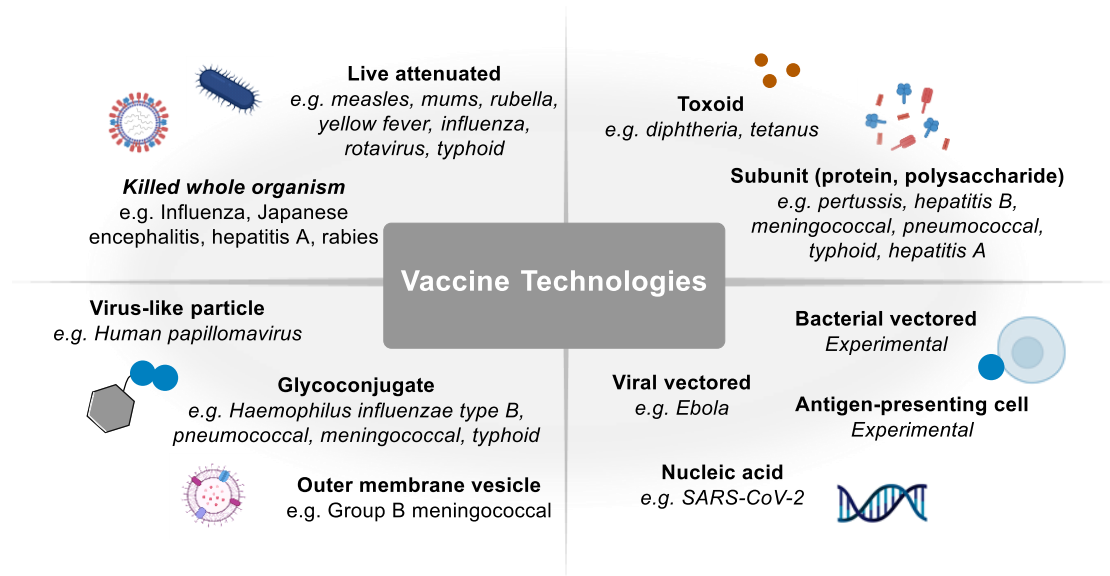
Figure 1.3. Different types of vaccines and examples of pathogens against which certain vaccines are licensed.

Infection with pathogens usually results in a potent immune response that is generated by the recognition of antigens, such as proteins and glycans. The goal of vaccination is mainly to achieve a long-term protection by the induction of antibodies (such as IgG, IgA and IgM) against those antigens mediated by B and T cells (Figure 1.4). The role of T cells in protection against infectious diseases is poorly characterized, but their role in providing help for the development of B cells and antibody production in lymph nodes is known. While proteins are thymus-dependent antigens that can induce immunological memory, glycans are thymus-independent antigens and thus cannot elicit immunological memory by stimulation of neonatal B cells. Only zwitterionic polysaccharides are known to be T cell dependent, as their charges play an essential role in immune system activation.[23] Despite the remarkable success of polysaccharide vaccines, such as against *Neisseria meningitides* and *Streptococcus pneumonia*, polysaccharides were not effective in protecting infants mainly due to their T cell independency.[24]

To overcome immunogenicity problems with polysaccharides and to induce a T cell mediated immune response, glycans can be conjugated to a carrier protein, such as a tetanus toxoid, diphtheria toxoid or a detoxified variant of diphtheria toxoid (cross-reacting material (CRM 97)).[25] Possible conjugation strategies include reductive amination of the anomeric carbon of the free-reducing end to lysine side chains of the carrier, multipoint attachment *via* carbodiimide coupling of uronic acids or cyanogen bromide activation of vicinal hydroxyl

groups, or thioether formation between thiolated polysaccharide fragments and haloacylated carrier proteins.[26] The conjugate-vaccine is processed by dendritic cells, which leads to the presentation of the glycan epitopes to T-helper cells by the major histocompatibility complex (MHC). Afterwards, cellular and cytokine-mediated signals induce maturation and proliferation of glycan-specific B cells and memory response. Several licensed glycoconjugate vaccines have shown to be highly efficient in the prevention of infectious diseases, such as pneumococcal conjugate vaccines (e.g. Prevnar13, Pfizer) or conjugate vaccines against *Haemophilus influenza* type b.[27]
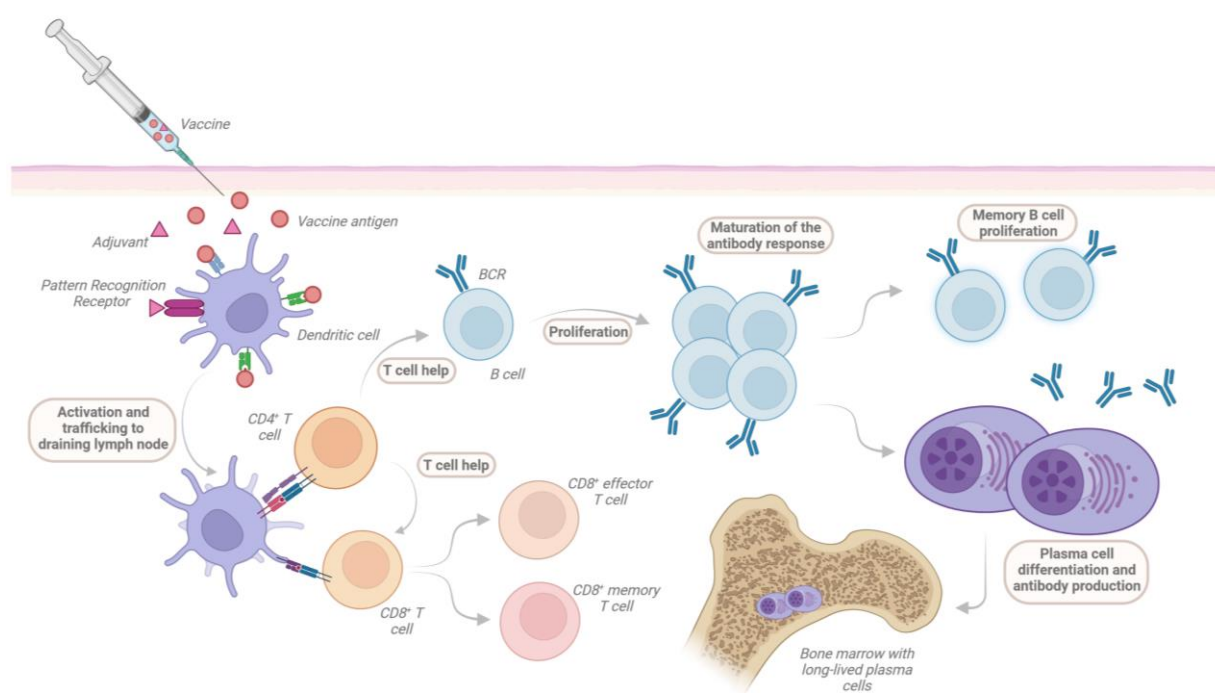
Figure 1.4. Schematic representation of the generation of an immune response to a vaccine with a conventional protein antigen. Modified from *Nat. Rev. Immunology* **2021,** *21* (2), 83-100.[22]

The common way to obtain carbohydrates for glycoconjugate vaccines is the isolation from cultured bacteria. However, this limits the development and production of glycoconjugate vaccines to pathogens that can be cultured. Furthermore, the isolation is often difficult: some labile polysaccharides can decompose during the isolation, depolymerization can be challenging, production of the correct glycan in sufficient amounts requires complex process optimization, and trace impurities are not avoidable. The use of synthetic carbohydrates for glycoconjugate vaccines is the better alternative in terms of purity, production process, costs and variability. The first marketed semi-synthetic glycoconjugate vaccine, QuimiHib, was developed against *Haemophilus influenza* type b in Cuba. It relies on the use of synthetic oligosaccharides coupled to an expressed tetanus toxoid protein. The substitution of expressed carrier proteins by a synthetic carrier, such as liposomes[28] from glycolipids, oligosaccharide-bound virosomes[29] and gold nanoparticles[30] is desirable to give fully

synthetic glycoconjugate vaccines. Those synthetic constructs have potential to no longer require an adjuvant.

The identification and analysis of glycans at the pathogen surface provide target structures for glycan synthesis and synthetic glycoconjugate vaccines. Glycans with different lengths, arrangement of the repeating unit, stereochemistry and covalent modifications can be synthesized to elucidate the importance of structural components on the immunogenicity and optimize the vaccine.[31] The immunogenicity of the synthesized compounds can then be tested for binding of antibodies from sera or other body fluids containing IgA, IgG or IgM. Glycan microarray studies are a useful tool to screen antibody binding.[32] For that, conjugation-ready glycans are immobilized on glass slides. The immobilization usually takes advantage of amine functionalized linkers at the synthetic glycan that is coupled to NHS-activated carboxyl-functionalized glass slides or thio-functionalized linkers that can be coupled to epoxy-functionalized glass slides. With this technique, glycan microarrays that carry hundreds of different sugars in small spots can be screened.

Access to defined bacterial glycans has been the bottleneck for the use of glycan microarrays and thus the development of glycoconjugate vaccines. However, there is a great need for an improved understanding of the immunological basis for vaccination and for the development of new vaccines against problematic pathogens. Rapid access to defined glycans and their evaluation helps to control pathogens, especially outbreaks that threaten global health security such as recently experienced with COVID-19[33] or Ebola.[34] Therefore, the development of efficient, fast, reliable and inexpensive methods for the synthesis of glycans is of high importance for progress in the prevention and control of infectious diseases.

2 Scientific Goals

The development of automated methods to access synthetic glycans is a milestone in carbohydrate research. The progress of glycan synthesis is hampered due to the high complexity of glycans. New methods for stereo- and regiocontrol, functionalization and efficiency of glycosidic bond formation at the solid-support are frequently developed to access diverse and complex glycans for conjugate vaccine development.

Standard Automated Glycan Assembly (AGA) synthesizers are restricted to temperatures from -40 to 30 °C. This limits the exploration of diverse chemical reactions on glycans, including functionalization and protecting group manipulations. The expansion of the temperature range from -40 to 100 °C in AGA will enable new transformations with higher energy barriers. Another aspect, that limits the progress in glycoscience is the challenging stereoselective formation of 1,2-*cis* glycosidic linkages. However, many relevant glycan structures bear 1,2-*cis* glycosidic linkages, such as several bacterial surface glycan components, that have immunogenic properties.
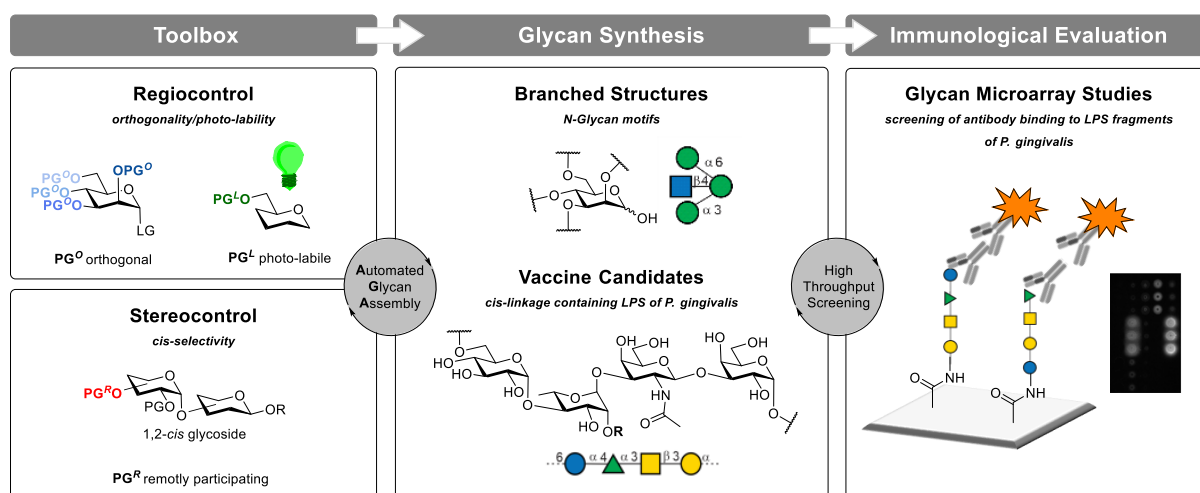
Figure 1.5. Overview of the scientific goals of this thesis. The aim is to improve the glycan discovery process including the expansion of the AGA toolbox for the efficient synthesis of glycan libraries and the immunological evaluation of synthesized vaccine candidate libraries by high throughput screenings using glycan microarray studies.

This work approached challenging regio- and stereocontrol problems to improve the process of the construction of glycan libraries and following studies on structure-property relationships (Figure 1.5). The dissertation is divided into three specific aims:

1. **Expansion of the protecting group portfolio in AGA.** This includes the introduction of microwave-assistance to the AGA synthesizer for a wider temperature range as well as the development of a total orthogonal mannose building block. This building block is applied to AGA for the synthesis of branched structures which serves as a starting point for researchers to synthesize and explore complex mannose structures. Furthermore, photo-labile 4,4-difluoro-4-bora-3*a*,4*a*-diaza-*s*-indacene (BODIPY)

9

protecting groups are developed for the reagent-free deprotection of glycans in solution-phase using visible light.

2. **Investigation and optimization of 1,2-*cis*-selective glycosylations in AGA.** This includes the investigation of effects of location and electronics in acyl protecting groups on the efficiency of remote participation. For that, numerous substituted building blocks are designed, synthesized, and evaluated by test-glycosylations. The glycosyl oxocarbenium ion intermediate is investigated by cold-ion IR spectroscopy in order to get a deeper understanding into the glycosylation mechanism.

3. **Application – bacterial glycan synthesis and evaluation.** The developed methods for 1,2-*cis*-selective galactosylations and orthogonality are applied to the synthesis of fragments of the tetrasaccharide repeating unit of the lipopolysaccharide (LPS) of the bacterium *Porphyromonas gingivalis (P. gingivalis)*. The LPS fragments of *P. gingivalis* are screened for antibody-binding using glycan microarray studies. Saliva and serum samples of periodontitis patients infected with *P. gingivalis* as well as treated and dental healthy individuals are checked for IgG and IgA binding by the synthesized LPS structures. This method is used to evaluate the potential of the fragments as conjugate vaccine candidates against *P. gingivalis*.

The aim of this dissertation is to further develop efficient strategies for the reliable creation of 1,2-*cis*-linkages by AGA and to further expand the capabilities of automated glycan synthesis by developing methods for the selective manipulation of orthogonal protecting groups. These methods will then be used as a means for the synthesis of branched structures e.g. *N*-glycan motifs, as well as a library of different fragments of the LPS repeating unit of *P. gingivalis*. The synthesized library of LPS fragments will then be subsequently screened for antibody binding using glycan microarray studies. Therefore, the overall aim is to accelerate the discovery process of glycans and their role in nature.

3   Orthogonality: A Total Orthogonal Mannose Building Block and Photo-Cleavable BODIPY Protecting Groups

Part of this Chapter has been published in:

Danglad Flores, J.[‡]; **Leichnitz, S.**[‡]; Sletten, E. T.[‡]; Joseph, A. A.; Bienert, K.; Le Mai Hoang, K.; Seeberger, P. H., Microwave-assisted Automated Glycan Assembly. *J. Am. Chem. Soc.* **2021**, 143 (23), 8893–8901.[35] https://doi.org/10.1021/jacs.1c03851. Reproduced in part from Ref.[35] with permission from the American Chemical Society (© 2021, ACS).

[‡]These authors contributed equally. The total orthogonal building block **3.07** was developed and compounds **3.17** and **3.22-3.28** were synthesized and characterized by **Sabrina Leichnitz**. The microwave-assisted AGA system was developed and built by Dr. José Danglad Flores, compound **3.18-3.21** for the proof-of-principle of the machine were synthesized and characterized by Dr. Eric Thomas Sletten.

Sletten, E. T.; Danglad Flores, J.; **Leichnitz, S.**; Joseph, A. A.; Seeberger, P. H., Expedited synthesis of mannose-6-phosphate containing oligosaccharides, *Carbohydrate. Res.* **2022**, *511*, 108489.[36] https://doi.org/10.1016/j.carres.2021.108489.

Parts of this Chapter are in preparation for the manuscript:

Leichnitz, S; Winter, A.; Seeberger, P. H., Green Light Labile BODIPY Protecting Groups for the Synthesis of Glycans.

3.1 Introduction

3.1.1 The Concept of Orthogonality in Oligosaccharide Synthesis

Protecting groups are essential for the synthesis of complex natural products. Especially in oligosaccharide synthesis, protecting groups play an important role, since the monomeric building blocks usually contain up to five hydroxyl functional groups with minute differences in reactivity. In some cases, they also contain carboxylate and amino functional groups. Differentiation of functional groups on carbohydrate rings predominantely relies on the dissimilar steric and electronic environments of the ring structure (Figure 3.1). Even though, primary alcohols are the most reactive hydroxyl groups and axial secondary alcohols are slightly less reactive than equatorial hydroxyl groups, total regiocontrol in the synthesis and functionalization of oligosaccharides requires a cautious protecting group strategy.
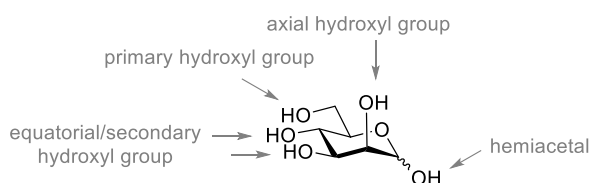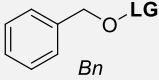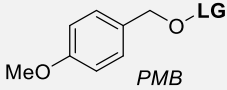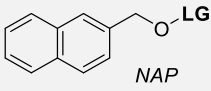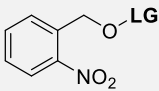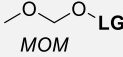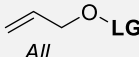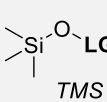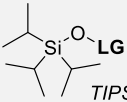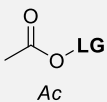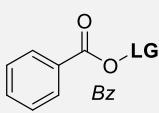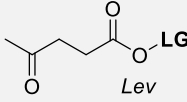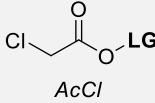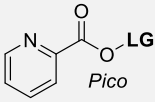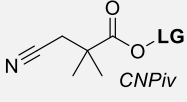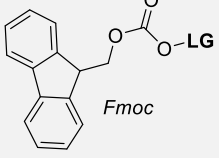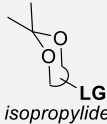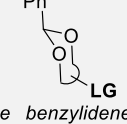
Figure 3.1. Discrimination of carbohydrate alcohols.

Protecting groups mask reactive functional groups – either permanently (maintained the entire synthesis), or temporarily. Besides masking, protecting groups can have a significant effect on the overall reactivity of a molecule by their electronic (e.g. inductive effects) and steric effects, they can improve the solubility in organic solvents, which aid the purification ease, and also have an influence on the stereochemical outcome of glycosylation reactions (see Chapter 4). Carbohydrates, unlike peptides and oligonucleotides, are often branched molecules. Therefore, the chemical synthesis of branched oligo- and polysaccharides requires more than one temporary protecting group. Orthogonal protecting groups enable selective unmasking of one hydroxyl group without affecting other protected functional groups at other positions of the same molecule.

In the past, a large set of orthogonal protecting groups was developed for the synthesis of carbohydrates.[37] Common protecting groups are benzyl, allyl, silyl ethers, esters, carbonates and acetals as well as ketals for diol protection. Based on the chemical properties of the protecting group, it is labile or stable under specific circumstances, such as basic or acidic conditions, reduction or oxidation, light or specific reagents (examples see Table 3.1).

Table 3.1. Common protecting groups in carbohydrate synthesis and corresponding cleavage conditions.[37]

Category	Example	Cleavage Conditions
Benzyl ethers	*Bn*	reduction (e.g. H_2, Pd-C)
	PMB	reduction (e.g. H_2, Pd-C)
		oxidation (e.g. DDQ or CAN)
		acids (e.g. TFA)
2-Naphthylmethyl ethers	*NAP*	reduction (e.g. H_2, Pd-C),
		oxidation (e.g. DDQ or CAN)
		acids (TFA) or HF-pyridine
2-*O*-(*o*-nitrobenzyl) ether	NO_2	irradiation with light
Alkyl ethers	*MOM*	H_2, Pd-C or HCl
Allyl ethers	*All*	e.g. Wilkinson's catalyst, acid, Tetrakis(triphenylphosphine)palladium(0)
		e.g. *t*-BuOK, NIS, H_2O
Silyl ethers	*TMS* *TIPS*	Fluoride (e.g. TBAF, HF-pyridine)
		acids
Esters	*Ac* *Bz*	Bases (e.g. NaOMe, MeOH)
		Zirconium hyride
	Lev	Bases (e.g. NaOMe, MeOH)
		Hydrazine acetate
	AcCl	Bases (e.g. NaOMe, MeOH)
		Thiourea
	Pico	Cu(OAc)$_2$, MeOH
	CNPiv	Pd(OH)$_2$/C, TEA
Carbonates	*Fmoc*	Bases (e.g. piperidine, TEA)
Acetals and ketals	*isopropylidene* *benzylidene*	Acids (e.g. TsOH or AcOH)
		Selective ring opening (e.g. BH_3, TMSOTf or SiEt$_3$, TFAA, TFA)

3.1.2 Photo-Cleavable Protecting Groups

Standard orthogonality strategies are based on the lability and stability to specific chemical conditions. One category of protecting groups, photo-labile ones, are unique tools for the masking of specific functional groups.[38] Photo-removable groups are useful in the synthesis of glycans, as their cleavage can be carried out without any reagents, which greatly reduces required resources and can spare an additional purification step after deprotection. Moreover, photo-caged glycans can be used in purification and analytics. Especially in biological research, this could be used for the detection of biological processes or the release of an active compound by light radiation. Photo-cleavable protecting groups, which usually absorb at visible light, most preferably red light (~600-1000 nm) are desirable, because the biological window tissues have maximal light transmittance and minimal photo-toxicity.[39] Photo-cleavable protecting groups have been frequently used to mask functional groups such as proteins[40], and pharmaceuticals[41] so far. However, the majority of the chromophores of the most popular photo-cleavable protecting groups absorb in the ultraviolet region, such as o-nitrobenzyl-[42], phenacyl[43], acridinyl[44], benzoinyl[45], and o-hydroxynaphthyl[46] structures (Figure 3.2). The photo-deprotection of these groups is often slow and ultraviolet light is limited in its tissue penetration properties as well as causes photo-toxic cell damage.
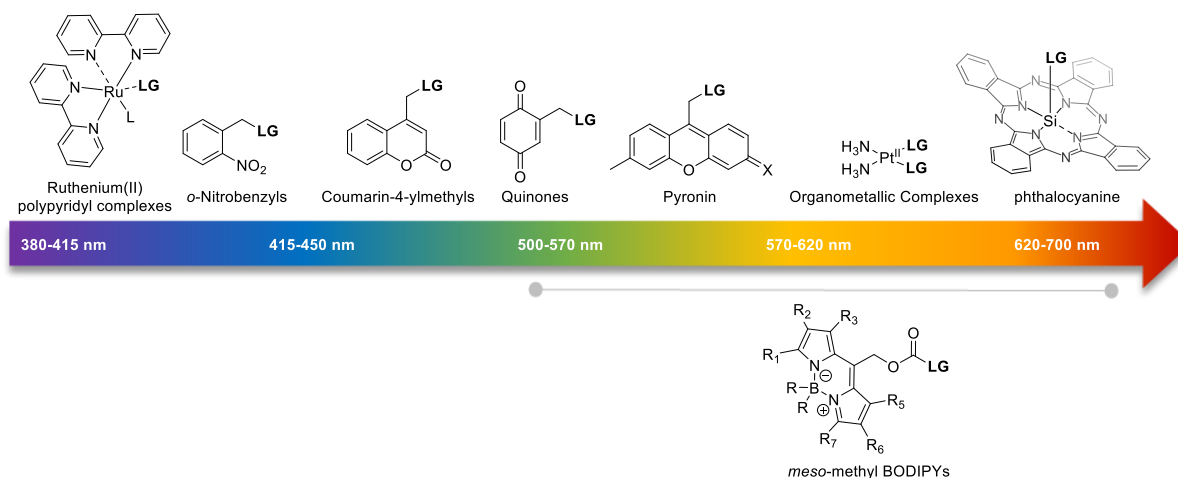
Figure 3.2. Overview over the most popular photo-cleavable protecting groups with an absorption maximum between 380 and 700 nm and absorption range of different reported *meso*-methyl BODIPY protecting groups.

In general, visible-light is too low in energy for bond cleavage. However, some examples are known for visible-light-absorbing photo-cleavable protecting groups, such as organometallic ruthenium complexes[47], pyroninchromophores[48], cyanines and coumarin-based chromophores like 7-diethylamino-4-(thio)coumarinylmethyl group[49] (Figure 3.2). Most importantly, 4,4-difluoro-4-bora-3a,4a-diaza-s-indacene (BODIPY) protecting groups were described (general structure see Figure 3.2) as excellent chromophores which absorb in the visible region for S_0-S_1 transitions. They are thermally stable in the dark and are synthetically

accessible. Furthermore, they have tunable absorptions due to many substitution options and show fast and efficient release of simple leaving groups.[50]

The photo-cleavage of *meso*-methyl BODIPY protecting groups is believed to occur in a photo-chemical S_N1 reaction *via* a carbocation intermediate and subsequent nucleophilic attack of the solvent (Figure 3.3). Experimental and theoretical findings suggest that the triplet excited state releases the leaving group and generates the carbocation in its triplet state.[50b] The Jablonski diagram in Figure 3.3 shows, that the singlet excited state S_1 is formed by light absorption, and then is deactivated by fluorescence. Radiationless relaxation and intersystem crossing (ISC) give the triplet excited state (T_1) and release the leaving group.
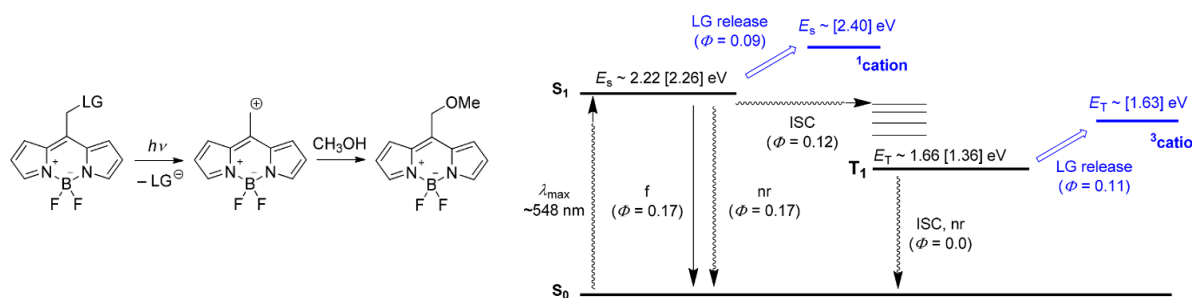
Figure 3.3. Proposed mechanism of the photo-release of a leaving group (**LG**) from the BODIPY cage and Jablonski diagram of photo-chemistry of *meso*-methyl BODIPY **LG** release.[50b]

BODIPY groups are promising photo-cleavable protecting groups for carbohydrates due to their high tolerance towards chemical reagents. They have been used for labelling of glycans[51] but not yet in protecting group strategies for the synthesis of glycans.

3.1.3 Orthogonal Protecting Groups in AGA

Besides the general requirements for orthogonal protecting groups, the choice of temporary orthogonal protecting groups in AGA is limited by many factors:

- The required deprotection temperature needs to be achievable by the AGA synthesizer,
- The deprotection time needs to be reasonable to ensure an efficient AGA process,
- All required reactants, reagents and side products must be soluble,
- The protecting group needs to be stable under different conditions during the AGA process, since large excess of reagents are used.

The technical limitations of the current AGA instruments[7a] allow a temperature range of -40 °C to 40 °C. Unfortunately, many deprotection reactions require a higher energy barrier than achievable in the instrument, thus eliminating many common protecting groups for routine use in AGA. Furthermore, acidic conditions play a vital role in AGA (activation, acidic wash, and capping) making acid-labile groups such as silyl and acetal protecting groups, not viable

options. Therefore, AGA is restricted to just two types of routinely used temporary protecting groups: 9-fluorenylmethyl carbonate (Fmoc) and levulinoyl esters (Lev).[52] Thus, to date access to highly branched glycans is challenging in AGA due to lack of other temporary protecting groups. In addition, functionalizations like sulfation or phosphorylation of glycans usually requires specialized instrumentation and very long reaction times.[15a, 53]

3.1.4 Project Aim

The aim of this Chapter is to develop an efficient method for oligosaccharide synthesis with great regiocontrol towards the expansion of the AGA toolbox. Concepts developed here, are microwave-assistance in AGA, total orthogonal protection of monosaccharide, and BODIPY photo-cages which in turn are used as starting point for the synthesis of complex branched and functionalized glycan structures.

This Chapter describes the expansion of the portfolio of orthogonal temporary protecting groups for regiocontrol in oligosaccharide synthesis enabled by microwave-assisted AGA (MW-AGA) and the development of a total orthogonal mannose building block. This building block is used to synthesize diverse mannose structures including on-resin fully deprotected structures, such as the *P. falciparum* mannose trisaccharide portion of a GPI anchor, as well as highly branched structures, such as bisecting *N*-glycan motifs.

Furthermore, the design of photo-labile BODIPY protecting groups and their synthesis followed by its application in glycan synthesis are described. The main aim is to introduce the visible-light absorbing photo-cages to glycan synthesis. Photo-deprotection can be a useful tool to simplify or reduce the required intermediate purification, similar to methods such as the solid-supported AGA or one-pot glycosylations.

3.2   Results

3.2.1   The New Microwave-Assisted AGA System

In order to expand the protecting group portfolio available for AGA, but also to introduce the option of functionalization to improve the efficiency of the whole process, a system with faster temperature adjustment and a higher temperature range is required. The reaction temperature of the standard AGA instruments[7a] (-40 to 40 °C) was adjusted using a dynamic temperature control system connected to a jacketed reaction vessel. This thermoregulation system is inefficient when significant temperature differences are required during a synthesis.[54] To overcome that, a MW-AGA instrument was developed[35] using dual thermoregulation by integration of a microwave generator and a jacketed reaction vessel (Figure 3.4A).[1]
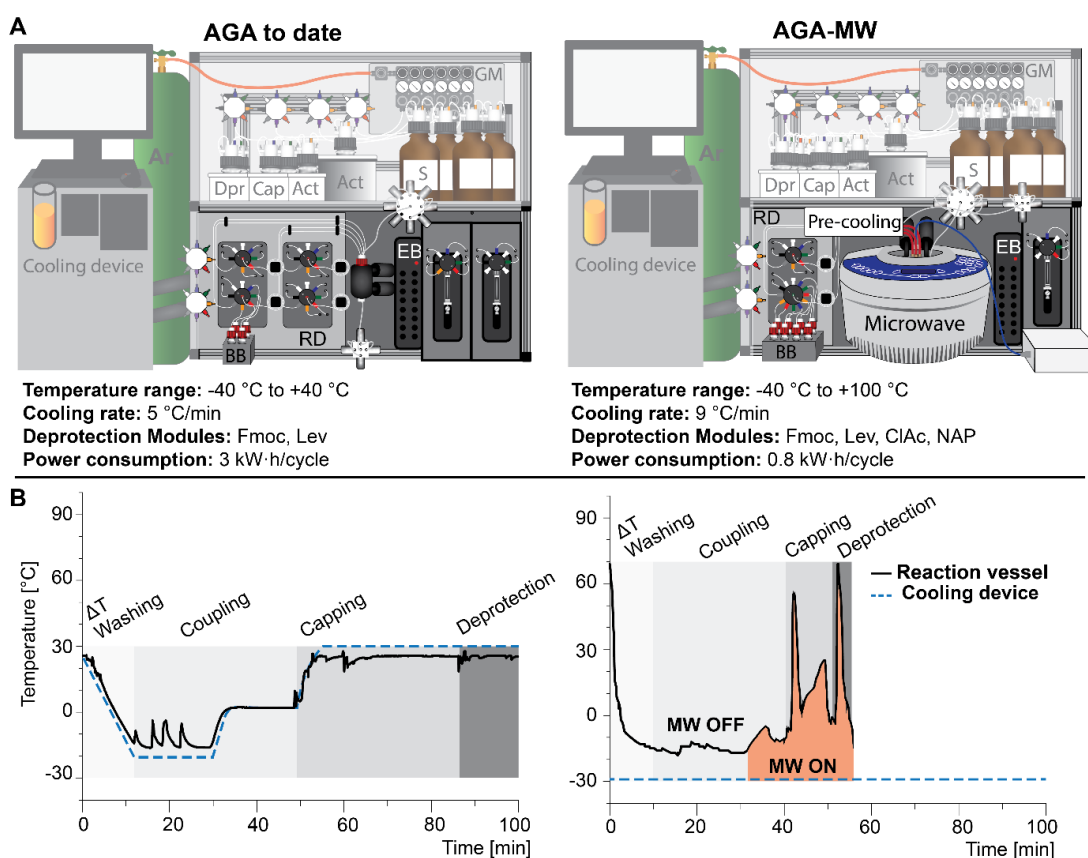
Figure 3.4. Comparison of the previous state of the art and MW-AGA system. (A) Pictorial representation and technical data (EB = electronic board, SP = syringe pump, GM = gas manifold, and RD = reagents distribution). (B) Temperature profile inside the reaction vessel during one coupling/capping/deprotection cycle of **3.20** (right) compared to that of one cycle in a standard AGA instrument. Reprinted with permission from *J. Am. Chem. Soc.* **2021**, 143, 23, 8893–8901 (https://doi.org/10.1021/jacs.1c03851).[35] Copyright 2021 American Chemical Society.

Upon initiation, the fritted reaction vessel containing the solid-support is cooled to the lowest temperature required during the synthesis using a circulating coolant (Figure 3.4B). The temperature in the reaction vessel is then adjusted by microwave radiation. Throughout the

---

[1] The dual thermoregulation system was developed and built by Dr. José Danglad Flores.

heating phase, the temperature of the microwave-inert coolant in the jacket is unchanged and allows for rapid return to low temperatures.

This permits almost instant temperature changes over a wide range (-40 to +100 °C) with minimal energy consumption. This new instrument significantly shortened the time required for the synthesis modules and expands the portfolio of orthogonal temporary protecting groups as well as glycan modifications.

3.2.2 Design and Synthesis of the Orthogonal Mannose Building Block 3.07

The ability to adjust the temperature in the MW-AGA system to higher temperatures created new opportunities for the use of orthogonal protecting groups that were previously not amenable to AGA. In order to create heavily branched glycans, ideally four orthogonal protecting groups are required. For this purpose, totally orthogonal protected mannose building block **3.07** was designed.

A few other completely orthogonal building blocks have been reported[55], yet none are amendable to AGA as the requirements for application in AGA (described in Chapter 3.1.3) cannot be fulfilled. Therefore, the protecting groups and their positions were chosen carefully for optimal performance in AGA. From the plethora of protecting groups that have been developed for solution phase chemistry, Fmoc, Lev, 2-naphthylmethyl ether (NAP), and chloroacetate ester (ClAc) were selected as orthogonal protecting groups[52, 55a] to be used for AGA.
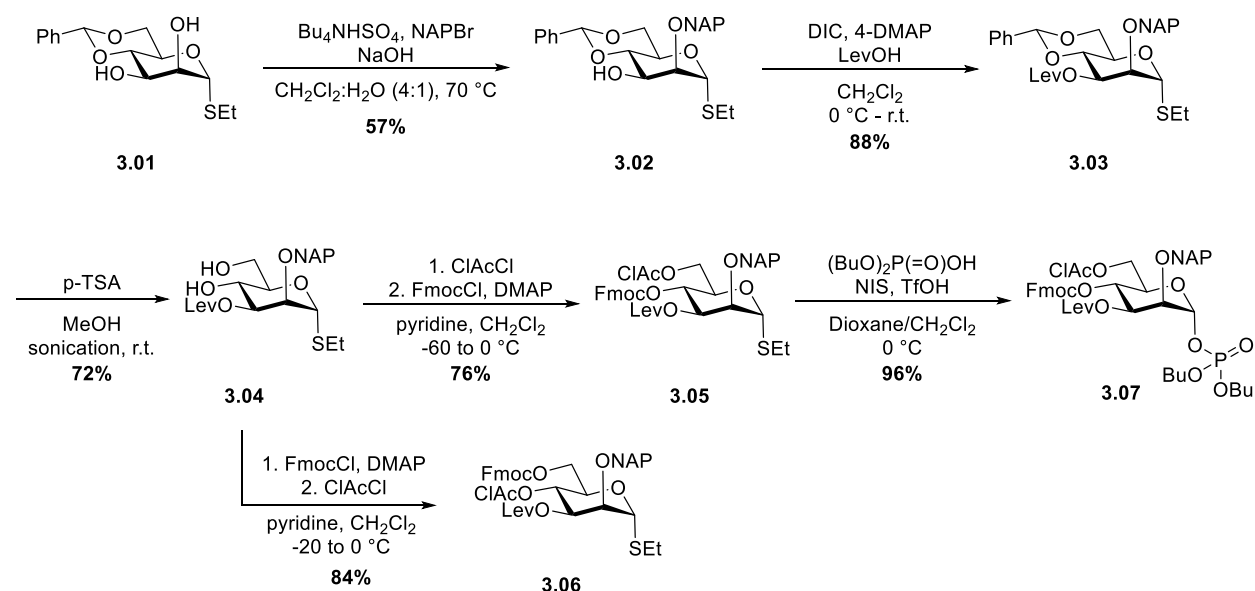
Scheme 3.1. Synthesis of orthogonal mannose building block **3.06** and **3.07**. More detailed reaction conditions are shown in the experimental section.

Two mannose building blocks **3.06** and **3.07**, bearing those four groups, were synthesized and tested for orthogonality and application in AGA (Scheme 3.1). Both building blocks were synthesized starting from commercially available ethyl 4,6-O-benzylidene-1-thio-

α-D-mannopyranoside **3.01**. NAP was selectively installed at the C2-OH position to give **3.02** using a limited amount of alkylating agent, sodium hydroxide as a base and tetrabutylammonium hydrogen sulfate as a phase-transfer catalysis, while the selectivity is mainly based on the higher acidity of C2-OH as well as steric hindrance at C3-OH by the benzylidene protecting group.[56] Afterwards, Lev was installed under STEGLICH esterification conditions, followed by acid hydrolysis of the benzylidene group. The free primary C6-OH group was then selectively protected, either with ClAc to give **3.05** or Fmoc to give **3.06** followed by protection of the last free C4-OH using either the acid chloride or chloroformate to form an ester or carbonate. Furthermore, thioglycoside **3.05** was converted to glycosyl phosphate to give the total orthogonal building block **3.07** (6 steps, overall yield 78%).

Common deprotection conditions[37b, 57] of each protecting group were chosen or had to be modified to ensure stability of the other present protecting groups (Figure 3.5). The Fmoc group is usually deprotected using piperidine. It was found that repeated exposure of the Lev group to piperidine resulted in side reactions. Also, the ClAc group is sensitive to nucleophiles, such as piperidine that can undergo a nucleophilic substitution of the chloride. The simple switch to triethylamine ensured the stability of the Lev and ClAc group. All present groups were stable under previously reported deprotection conditions for the Lev group using hydrazine acetate[37b] as well as deprotection conditions for the ClAc group using thiourea.[55a] Now capable of reaching 80 °C in the MW-AGA system – which was not achievable in the earlier standard AGA system – the deprotection of the ClAc group using thiourea was facilitated in 45 minutes. It was found that the Fmoc was best positioned at the C4-OH position in orthogonal building block **3.05**. The high electrophilic character of ClAc caused migration to the primary C6-OH position in building block **3.06** upon a C6-Fmoc cleavage (Scheme 3.2).
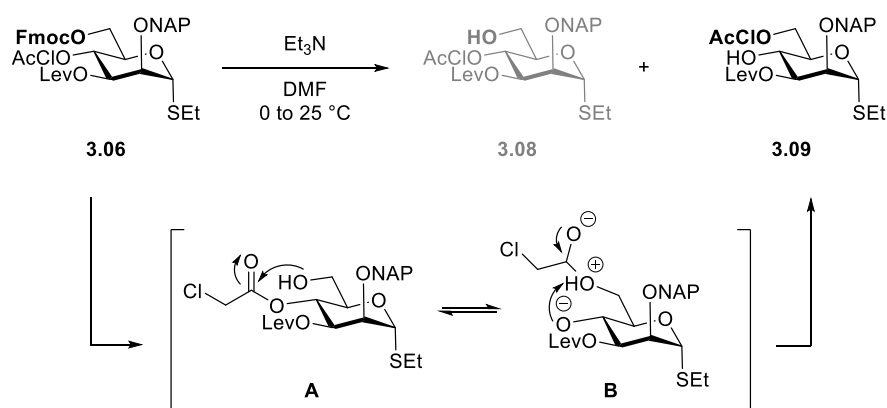
Scheme 3.2. Migration and its proposed mechanism of the chloroacetyl group to the primary alcohol group at C6 during Fmoc deprotection, which resulted in the exclusion of structure **3.06**.

Bearing mainly electron-withdrawing ester and carbamate groups (Fmoc, ClAc and Lev), the reactivity of the orthogonal mannose building block **3.05** as an acceptor in glycosylation reactions was increased by installing the electron-donating NAP group at C2-OH position and conversion of the thioglycoside **3.05** into glycosyl phosphate **3.07**. While acidic conditions[58]

failed to selectively cleave the NAP ether in the presence of Lev, AcCl, and Fmoc, the NAP group was successfully deprotected in the presence of all other protecting groups under reductive conditions using DDQ. To date, NAP ethers have been used in AGA[59] but their cleavage is very slow, sometimes incomplete and accompanied by side-products, arising from debenzylation. While in the previous system the NAP group removal required unpractical 240 minutes using DDQ/MeOH/water in DCE at 40 °C, the MW-AGA system provides more practical and reliable NAP deprotections in 60 minutes at 60 °C using DDQ/MeOH in DCE. The Lev group was positioned at the C3-OH as C3-ester groups are reported to assist with strong α-selectivity.[10, 60]

Module		Conditions	T[°C]	Time [min]
Glycosylation		BB in CH_2Cl_2 then NIS,TfOH in CH_2Cl_2/dioxane	-20 to 0 / -20 to -5	To date 25 / AGA-MW 13
Capping		10% Ac_2O, 2% MsOH in CH_2Cl_2 [a]	25 / 30	35 / 12
Deprotection	Fmoc	20% piperidine or Et_3N in DMF	25 / 60	5 / 1
	Lev	7% $N_2H_4·HOAc$ in CH_2Cl_2/py/HOAc/H_2O	25 / 35	90 / 15
	NAP	2% DDQ in DCE/MeOH/H_2O [b]	40 / 60	240 / 60
	ClAc	5% thiourea in EGME/py	- / 80	Not available / 45
Post-Assembly	Sulfation	$SO_3·py$ (20 equiv/OH) or $SO_3·TMA$ in DMF [c]	50 / 90	540 / 30
	Methanolysis	CH_3ONa in MeOH (0.5 M)/THF 1:9	- / 25	Not available / 480

[a]AGA-MW: double concentration. [b]AGA-MW: only DCE and MeOH. [c]Traditional AGA: $SO_3·py$ in py/DMF, AGA-MW:$SO_3·TMA$ in DMF.

Figure 3.5. Comparison of modules in the standard system (without microwave) and the MW-AGA system and overview over the deprotection conditions. Reprinted with permission from *J. Am. Chem. Soc.* **2021**, 143, 23, 8893–8901 (https://doi.org/10.1021/jacs.1c03851).[35] Copyright 2021 American Chemical Society.

3.2.3 Oligosaccharides Synthesized from Orthogonal Building Block 3.07

To illustrate the concept, α-(1,2), α-(1,3), α-(1,4) and α-(1,6)-tetramannosides **3.22-3.25** were assembled from building block **3.07** (Figure 3.6, yields: α-(1,2) **3.22** 19%, α-(1,3) **3.23** 12%, α-(1,4) **3.24** 18%, α-(1,6) **3.25**, 18%) with excellent regio- and stereoselectivity.
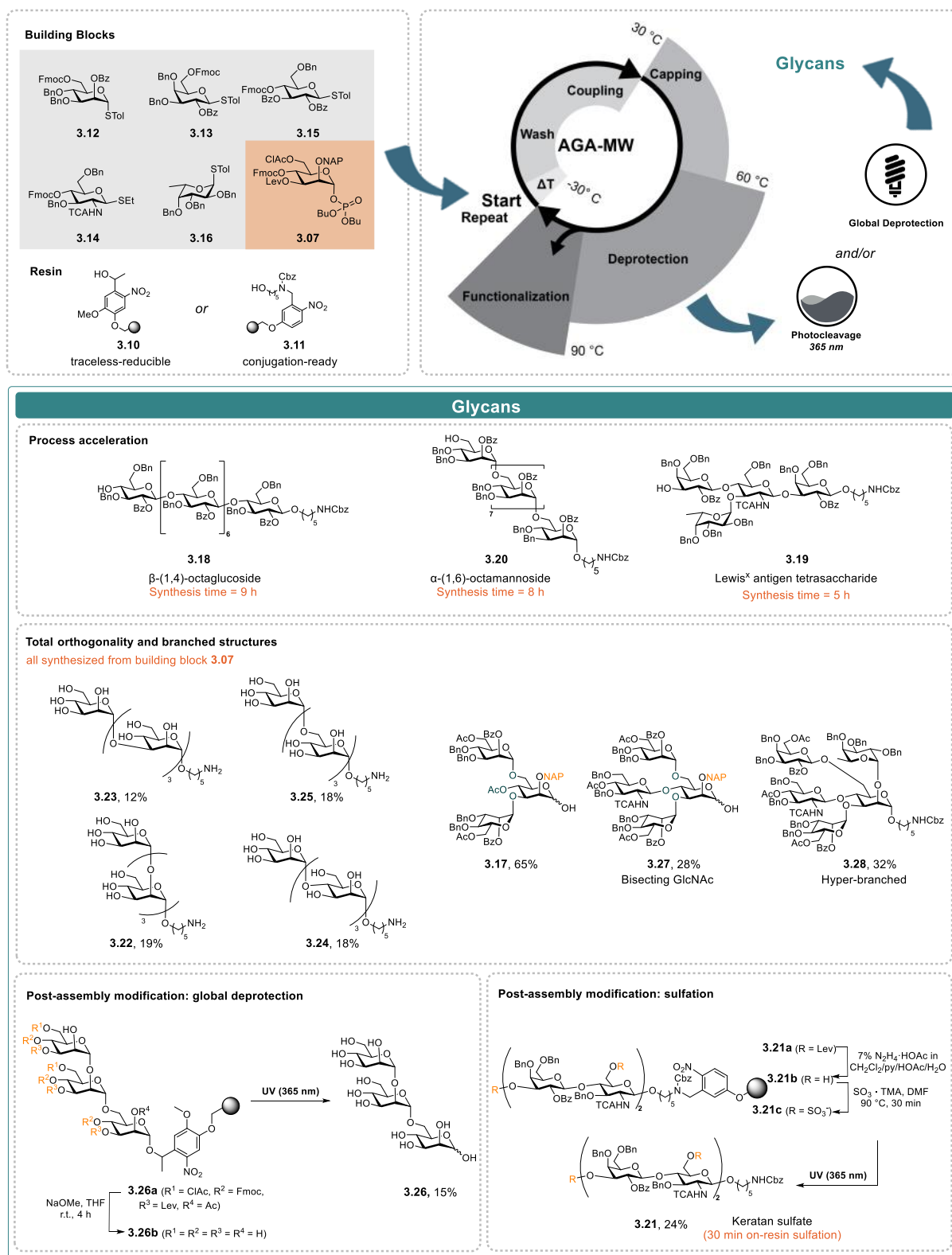
Figure 3.6. Oligosaccharides **3.18-3.28** prepared to highlight the capabilities of the MW-AGA synthesizer. Time in parenthesis notes synthesis time using a standard AGA instrument. Oligosaccharides **3.22-3.28** were synthesized from orthogonal mannose building block **3.07**. More detailed reaction conditions are shown in the experimental section. In parts adapted with permission from *J. Am. Chem. Soc.* **2021**, 143, 23, 8893–8901 (https://doi.org/10.1021/jacs.1c03851).[35] Copyright 2021 American Chemical Society.

Encouraged by these results, *P. falciparum* GPI anchor mannose trisaccharide portion **3.26**[61] containing both α-(1,2) and α-(1,6) linkages was achieved on polystyrene resin

equipped with traceless-reducible photo-labile linker **3.10**. For that, the NAP group at the first sugar unit was removed and acetylated before extending at C6-position and then the C2-position. After the assembly, solid-support-bound unprotected oligosaccharide was prepared by removing the remaining NAP ether, followed by methanolysis using sodium methoxide. The global deprotection on solid-support was confirmed by on-resin FT-IR.

3.26a (R^1 = ClAc, R^2 = Fmoc, R^3 = Lev, R^4 = Ac)

NaOMe, THF rt, 4 h

3.26b (R^1 = R^2 = R^3 = R^4 = H)

3.26, 15%
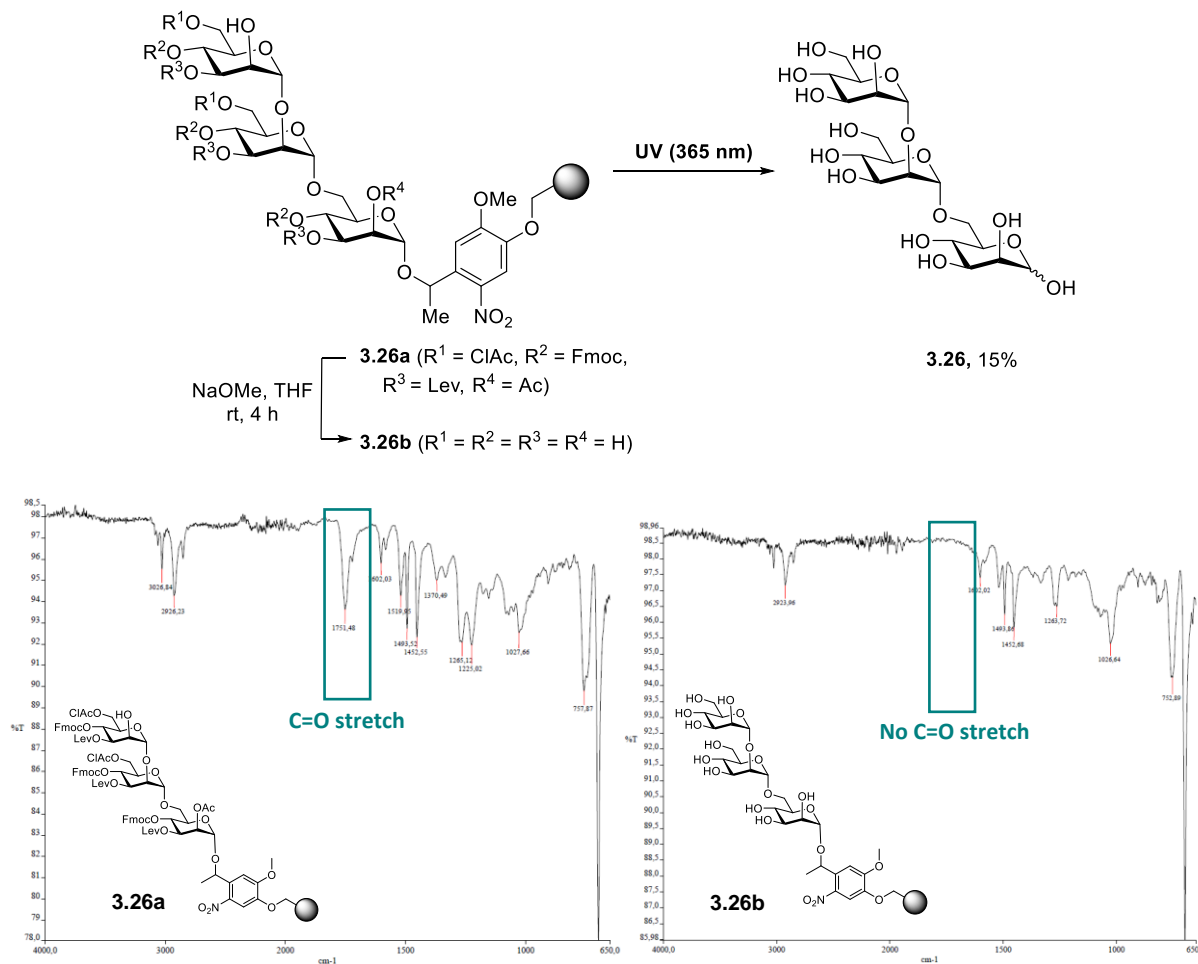
Figure 3.7. FT-IR spectrum of the resin containing **3.26** before (**3.26a**) and after (**3.26b**) on-resin methanolysis. 20-30 beads of resin were ground using a mortar. The ground beads were suspended in CH$_2$Cl$_2$ and applied on a Perkin-Elmer 1600 FTIR spectrometer. Spectra were taken after evaporation of the CH$_2$Cl$_2$.

Photo-cleavage of the linker released the trisaccharide product **3.26** from the solid-support (yield 15%). This oligosaccharide is the first example of a natural, unmodified glycan produced by AGA without any manual protecting group manipulations. Otherwise this could be done only by either fully enzymatic or chemoenzymatic approaches. The syntheses of **3.22-3.25** as well as **3.26** also demonstrate that a single building block such as **3.07** can give many possible combinations of oligosaccharides.

Synthesis of Highly Branched Glycans

Naturally occurring glycans are often branched. Chorella viruses for example contain three branches on a single monosaccharide unit.[62] For artificial systems, the creation of highly

branched glycans where every hydroxyl group serves as a point of modulation are also desirable. Orthogonally protected mannose building block **3.07** served in the assembly of branched structures including a portion of bisecting *N*-glycan **3.27** (Figure 3.6, yield 28%) and hyperbranched structure **3.28**. Characterization of **3.28** by NMR spectroscopy gave rise to concerns, as the ^{1}H NMR spectrum at 23 °C (Figure 3.8) is crowded and seemed to suggest a failed synthesis.
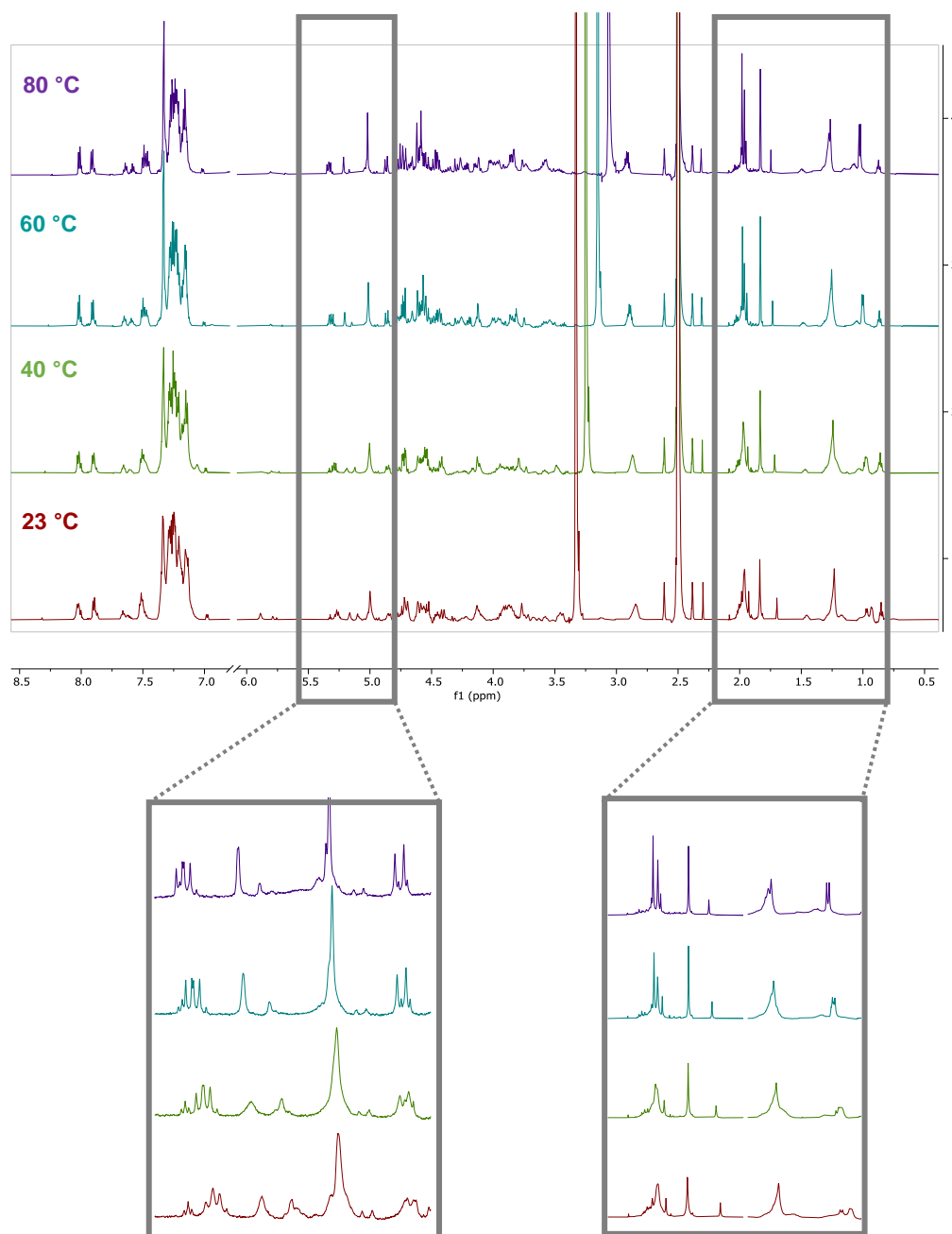
Figure 3.8. Comparison of ^{1}H NMR spectra (600 MHz, [D$_6$]-DMSO) of **3.28** at different temperatures (23 to 80 °C) and extracts from specific regions. Spectra at elevated temperature are showing more defined signals due to faster rotation of rotamers. Reprinted with permission from *J. Am. Chem. Soc.* **2021**, 143, 23, 8893–8901 (https://doi.org/10.1021/jacs.1c03851).[35] Copyright 2021 American Chemical Society.

23

The C6-methyl group of fucose that is expected as a doublet signal at around 1.0 ppm for example showed many different signals suggesting the presence of many different compounds and thus poor regio- or stereoselectivity. This was resolved by NMR analysis of the same sample at elevated temperature (Figure 3.8). At 60 °C, a clear doublet signal at 1.0 ppm appeared for the fucose C6-methyl group and at 80 °C all expected signals are observed and a clean spectrum of **3.28** was obtained. This observation shows that such densely functionalized, protected oligosaccharides adopt structures containing different rotamers. The raised temperature leads to faster rotations. Therefore, spectra at higher temperature do not show the signals of each energetically favored rotamer. The same effect has been found for other glycan structures before.[63]

3.2.4 Synthesis of Carbohydrate BODIPY Photo-cages

Photo-cleavable BODIPY protected glycans **3.29a-d** were synthesized and further evaluated for their applicability in glycan synthesis (Figure 3.9). Here, the influence of boron substituents (methyl for **3.29a-b**, fluoro for **3.29c** and cyano for **3.29d**) on the efficiency of photo-deprotection and glycosylation stability were of interest.
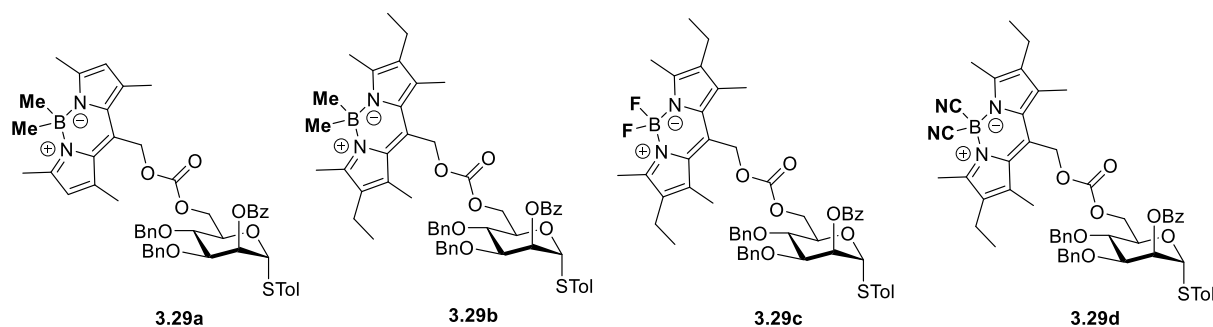
Figure 3.9. BODIPY protecting group at a representative mannose building block bearing different substituents at the boron atom (methyl for **3.29a**, fluoro for **3.29b** and cyano for **3.29c**).

Carbonates **3.29a-c** were synthesized using methylimidazolium BODIPY precursors **3.31a-c** in good yields. In contrast, similar alkoxycarbonylimidazole precursors did not give any formation of carbonates **3.29a-b** (Scheme 3.3).

3.31a[1] (R^1 = Me, R^2 = H)
3.31b[1] (R^1 = Me, R^2 = Et)
3.31c[1] (R^1 = F, R^2 = Et)

Pyridine, 4-DMAP

THF
0 °C - r.t.

3.29a (R^1 = Me, R^2 = H), 49%
3.29b (R^1 = Me, R^2 = Et), 65%
3.29c (R^1 = F, R^2 = Et), 67%
3.29d (R^1 = CN, R^2 = Et), 97%

TMSCN, SnCl$_4$
CH$_2$Cl$_2$, 0 °C - r.t.
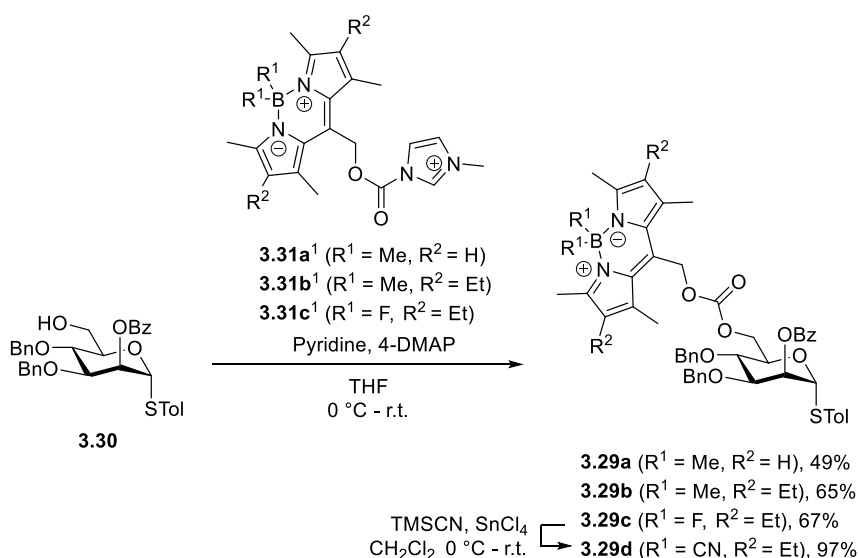
Scheme 3.3. Synthetic route to BODIPY-sugar **3.29a-d** starting from C6-OH building block **3.30**. [1]Methylimidazolium BODIPY precursors **3.31a-c** were provided by Prof. Dr. Arthur Winter (Department of Chemistry, Iowa State University). More detailed reaction conditions are shown in the experimental section.

The synthesis of CN-BODIPY sugar **3.29d** was more challenging than the synthesis of F-BODIPY and Me-BODIPY sugars, because the cyano groups seem to strongly deactivate the BODIPY-alcohol **3.33** and thus reduce its nucleophilicity. Therefore, a comparable imidazolium CN-BODIPY precursor was not possible to synthesize[2] and further strategies that

---

[2] Prof. Dr. Arthur Winter (Department of Chemistry, Iowa State University) provided the methylimidazolium precursors.

include the activation of the sugar alcohol **3.30** using carbonyldiimidazole (CDI) or triphosgen to alkoxycarbonylimidazole **3.31** or chloroformate **3.32** failed (Scheme 3.4). Instead, CN-BODIPY sugar **3.29d** was synthesized by substituting the fluoro-substitutent in **3.29c** by cyanide using TMSCN and SnCl$_4$ (Scheme 3.3).
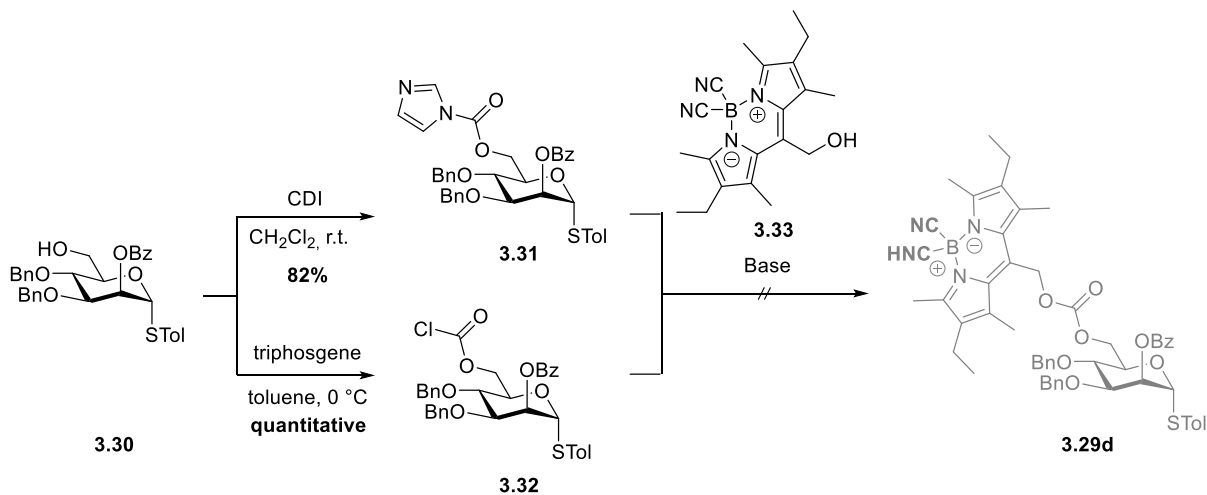
Scheme 3.4. Failed attempts to couple CN-BODIPY alcohol **3.33** to alkoxycarbonylimidazol sugar **3.31** or chloroformate **3.32**. More detailed reaction conditions are shown in the experimental section.

Upon synthesis, **3.29a** was then used to test the photo-deprotection set-up and solvents. Being known that the C$_{arom}$2 and C$_{arom}$6 positions of the BODIPY core are reactive to electrophilic aromatic substitution by iodonium ions in *N*-iodosuccinimide (NIS), a commonly used activator in glycan synthesis, **3.29a** will not be applicable to glycan synthesis. Therefore, **3.29b-d** were designed with ethyl-groups for the prevention of this possible side-reaction. Synthesized BODIPY-sugars **3.29b-d** absorb green light (λ_{max}(**3.29c**) = 517 nm, λ_{max}(**3.29b**) = 538 nm, λ_{max}(**3.29d**) = 550 nm) as shown in the UV/Vis spectra in Figure 3.10.
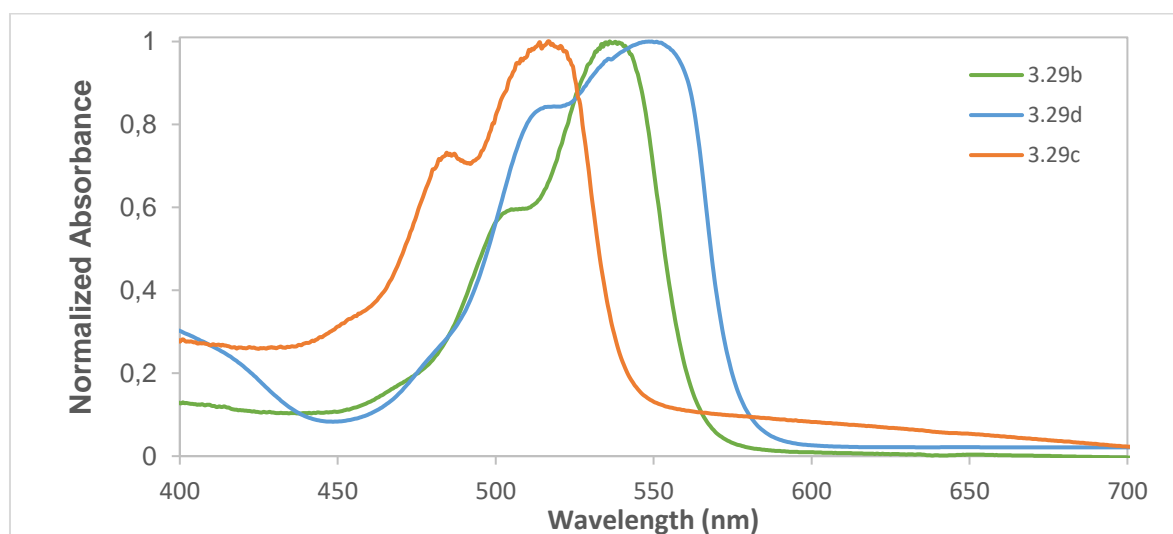
Figure 3.10. Normalized absorbance of **3.29b-d** in MeOH/CHCl$_3$ (3:2).

3.2.5 Photo-Cleavage Experiments of BODIPY-Protected Building Blocks

The photo-deprotection of synthesized BODIPY building blocks was carried out using a white halogen lamp set-up or a green LED set-up at room temperature (Scheme 3.5). The mixture was prevented from warming up using a water filter for the white halogen lamp and ventilation for the green LED lamp. The deprotection yield was determined by quantitative ^{1}H NMR spectroscopy, using dimethyl sulfone (DMS) as an internal standard.
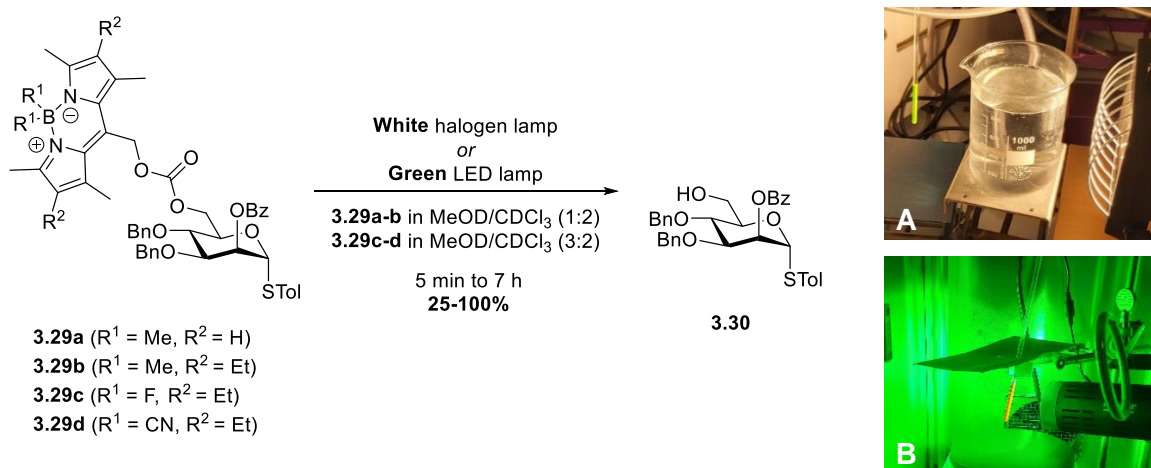
Scheme 3.5. Photo-deprotection reactions of **3.29a-d** and set-up using a white halogen lamp (**A**) or a green LED lamp (**B**). More detailed reaction conditions are shown in the experimental section.

The photo-deprotection of **3.29a** was screened in four solvents (Table 3.2). The addition of methanol increased the efficiency of the deprotection. This finding is in accordance with the proposed photo-chemical S_N1 mechanism *via* a carbocation intermediate[50b], that can be attacked by nucleophilic solvents such as methanol (Figure 3.3). However, the BODIPY building blocks, especially the Me-BODIPY building blocks **3.29a-b**, are not well soluble in pure methanol. Therefore, a mixture of chloroform and methanol was a good compromise using a 1:2 (MeOD/CDCl$_3$) mixture for less polar **3.29a-b** and a 3:2 (MeOD/CDCl$_3$) mixture for more polar F-BODIPY and CN-BODIPY building blocks **3.29c-d**.

Table 3.2. Photo-deprotection yields of **3.29a** (~1.6 mM) using a white halogen lamp in different solvents determined by quantitative ^{1}H NMR spectroscopy (DMS as internal standard).

Solvent	Yield
CDCl$_3$	94%
MeOD	100%
CDCl$_3$/MeOD	100%
DMSO	92%

The photo-deprotection experiments of **3.29b-d** using the white halogen lamp set-up showed a strong dependence of the photo-induced cleavage on the substituent at the boron atom (Figure 3.11, Me > F > CN).
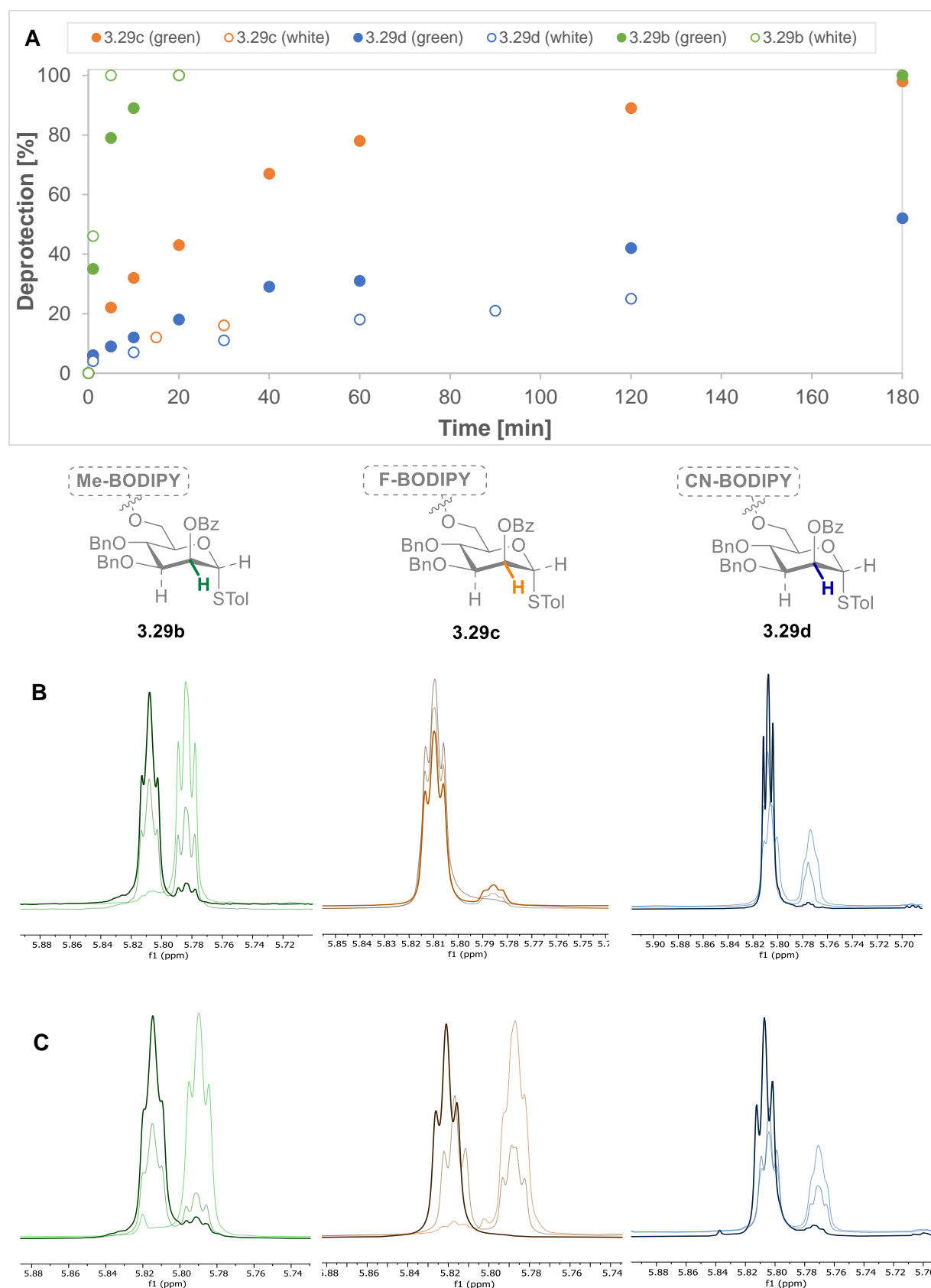
Figure 3.11. (**A**) Yield of the photo-deprotection by time of **3.29b-d** using a white halogen lamp or a green LED lamp determined by quantitative ^{1}H NMR analysis comparing the integral of H-2 and DMS as an internal standard. (**B**) H-2 region in superimposed ^{1}H NMR spectra of photo-deprotection of **3.29b** (0 min, 1 min, 5 min), **3.29c** (0 min, 15 min, 30 min) and **3.29d** (0 min, 120 min, 7 h) using a white halogen lamp, following the increase of deprotected product (high-field shifted). (**C**) H-2 region in superimposed ^{1}H NMR spectra of photo-deprotection of **3.29b** (0 min, 1 min, 20 min), **3.29c** (0 min, 20 min, 180 min) and **3.29d** (0 min, 60 min, 180 min) using a green LED lamp, following the increase of deprotected product (high-field shifted).

While the Me-BODIPY building block **3.29b** was fully deprotected after only five minutes, the deprotection of F-BODIPY building block **3.29c** and CN-BODIPY building block **3.29d** was significantly slower and not even completed after seven hours. The simple switch to a green LED light source (525 nm) increased the efficiency of the deprotection of F-BODIPY building block **3.29c** immensely and the deprotection was completed after 180 minutes. Though **3.29c** is not as labile as Me-BODIPY building block **3.29b**, it is still in an acceptable range for application in glycan synthesis. Interestingly, the deprotection of Me-BODIPY building block **3.29b** and CN-BODIPY building block **3.29d** could not be significantly accelerated using the green light source. Therefore, CN-BODIPY building block **3.29d** is irrelevant for the application in glycan synthesis with a deprotection yield of only 52% after 180 minutes.

3.2.6 Glycosylations of BODIPY-Protected Building Blocks

After verifying the photo-lability of synthesized BODIPY-sugars **3.29b-d**, their applicability for glycan synthesis was investigated. To have synthetic utility, not only an efficient photo-release is required for the use of BODIPY-building blocks, but they also need to be stable under glycosylation conditions.

Therefore, synthesized BODIPY-sugars **3.29b-d** were subjected to glycosylation reactions with acceptor **3.34** (Scheme 3.6). The BODIPY building blocks with electron withdrawing groups at the boron atom - F-BODIPY donor **3.29c** and CN-BODIPY donor **3.29d** - are stable to standard NIS/TfOH glycosylation conditions. On the other hand, Me-BODIPY donor **3.29b**, with the best photo-deprotection results, is not stable under several glycosylation conditions (Scheme 3.6). To avoid decomposition due to the high acidity of triflic acid, milder TMSOTf was used to promote the leaving group activation in combination with NIS. However, the same decomposition was observed again. By buffering the glycosylation mixture using non-nucleophilic base 2,4,6-tri-*tert*-butylpyrimidine or by using the milder promoter system dimethyl(methylthio)sulfonium trifluoromethanesulfonate (DMTST), the chemical deprotection of the Me-BODIPY group could not be suppressed.

These results show that the application of photo-labile BODIPY protecting groups to glycan synthesis requires a good balance between photo-lability and chemo-stability. Strongly photo-labile Me-BODIPY groups tend to decompose under catalytic amounts of triflic acid and other promoters, while less photo-labile F- and CN-BODIPY are fully stable under glycosylation conditions and provide high glycosylation yields. Since the photo-deprotection of CN-BODIPY building block is too slow for a possible application in glycan synthesis and Me-BODIPY building block is not stable under glycosylation conditions, these two motifs are not interesting for glycan synthesis.
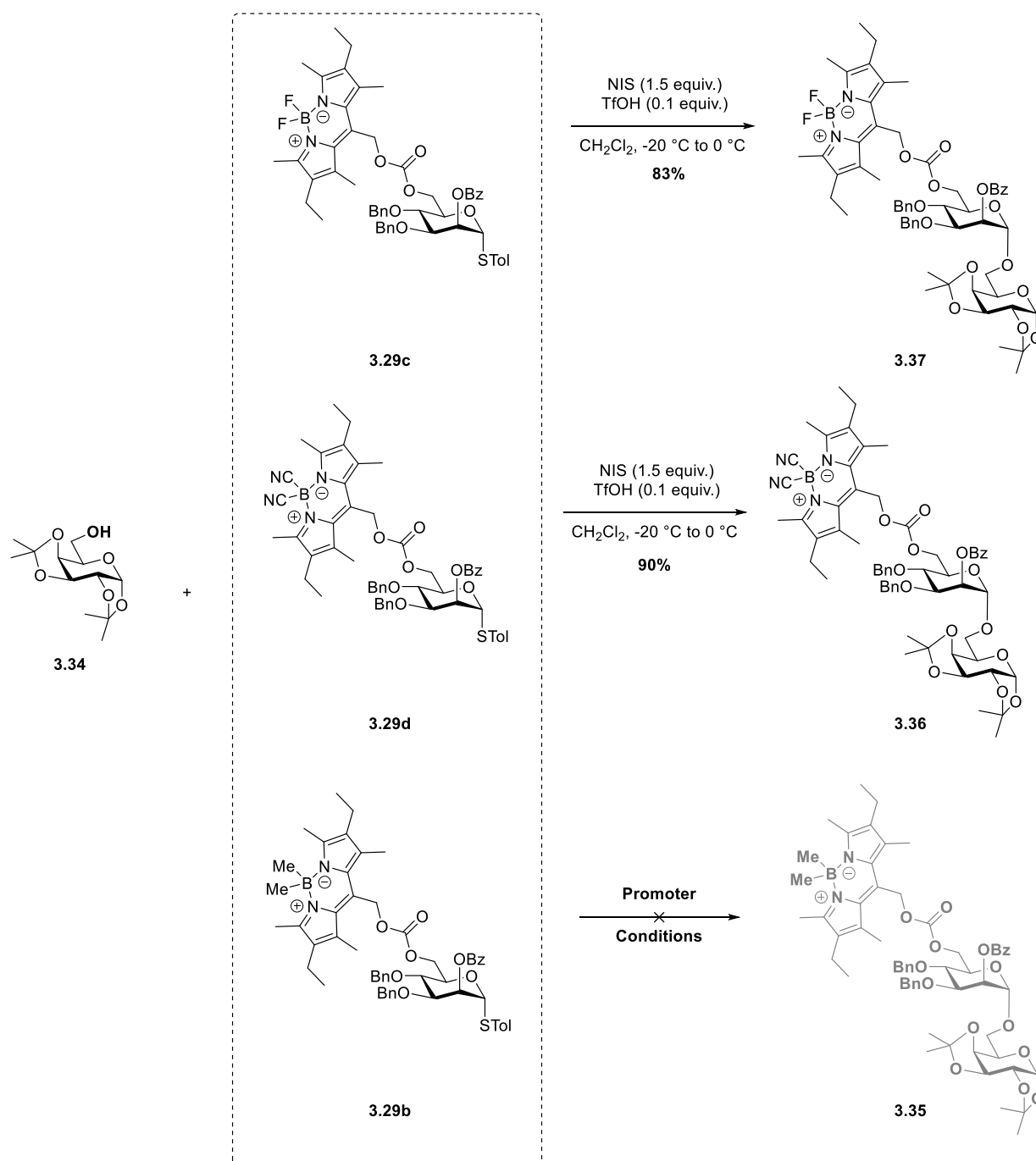
Attempt	Promoter	Conditions
1	NIS (1.5 equiv.), **TfOH** (0.1-0.2 equiv.),	CH₂Cl₂, -20 °C to 0 °C, 0.5 h to 1 h, no light
2	NIS (1.5 equiv.), **TMSOTf** (0.1-0.2 equiv.)	CH₂Cl₂, -20 °C to 0 °C, 0.5 h to 1 h, no light
3	NIS (1.5 equiv.), **TMSOTf** (0.2 equiv.), **2,4,6-tri-*tert*-butylpyrimidine** (0.2 equiv. or 4.0 equiv.),	CH₂Cl₂, -20 °C to 0 °C, 0.5 h to 2 h, no light
4	**DMTST** (3.0 equiv.), **2,4,6-tri-*tert*-butylpyrimidine** (4.0 equiv.)	-10 °C to r.t., 2 to 12 h, no light
5	**DMTST**	-10 °C to r.t., 2 to 12 h, no light

Scheme 3.6. Glycosylation of BODIPY-building blocks **3.29b-d** and acceptor **3.34**. While F-BODIPY donor **3.29c** and CN-BODIPY donor **3.29d** are stable to standard glycosylation conditions, Me-BODIPY donor **3.29b** with the best photo-deprotection results is not stable under several glycosylation conditions and promoters. More detailed reaction conditions are shown in the experimental section.

However, F-BODIPY building block can be deprotected in three hours using green light and is practical to be used as a donor for glycosylations. Therefore, F-BODIPY building block **3.29c** provides the right balance between glycosylation-stability and photo-reactivity.

Several strategies have been developed in the past to avoid the intermediate purification in the consecutive coupling of building blocks to achieve desired and defined oligosaccharides. This includes solid-supported AGA[7a, 35], but also one-pot strategies[64] as well as poly(tetrafluoroethylene)-assisted purification[65] and latent-active glycosylation[66]. Also a consecutive glycan assembly approach has been recently presented using photo-labile 2-(2-nitrophenyl)-propyloxycarbonyl protecting groups.[67] However, those photo-labile protecting groups require UV light irradiation for photolysis, which bares the risk of partial deprotection of many other protecting groups, such as benzyl ethers, NAP groups and silyl groups and thus reduction of yield. Given the stability of the F-BODIPY protecting group under glycosylation conditions as well as their photo-lability under green light, the opportunity of a consecutive glycan assembly without intermediate purification and the risk of benzyl ether deprotection is provided.
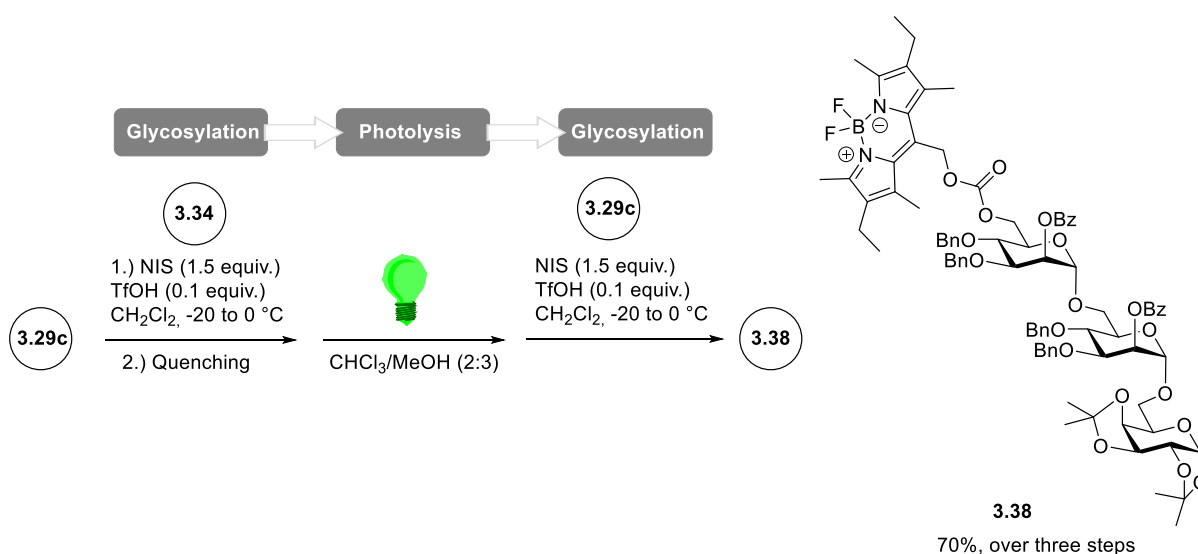
Scheme 3.7. Consecutive assembly of oligosaccharides using F-BODIPY building block **3.29** and green light for photolysis. More detailed reaction conditions are shown in the experimental section.

To prove the concept, F-BODIPY building block **3.29c** was tested for the applicability in a consecutive photo-glycan assembly (Scheme 3.7). F-BODIPY building block **3.29c** (one equivalent) was used to glycosylate acceptor **3.34**. After quenching (0.1 equivalent pyridine, aqueous sodium thiosulfate), evaporation of the separated organic phase followed by dissolving the crude residue in a chloroform-methanol mixture (2:3), the reaction mixture was subjected to photolysis using green light irradiation for three hours. C6-deprotected disaccharide **3.37** was successfully obtained and directly used after co-evaporation with toluene for the next glycosylation with F-BODIPY building block **3.29c** (one equivalent) to give trisaccharide **3.38** with a yield of 70% over three steps and only one purification step.

3.3   Conclusion and Outlook

In summary, orthogonality concepts for oligosaccharide synthesis were developed with strong regiocontrol. A total orthogonal mannose building block was designed and used in a new microwave-assisted oligosaccharide synthesizer. Furthermore, photo-labile BODIPY protecting groups were investigated for their application in a consecutive glycan assembly approach.

The new microwave-assisted oligosaccharide synthesizer enabled the extension of the protecting group portfolio in AGA from just two types of routinely used temporary protecting groups, Fmoc and Lev to ClAc and NAP. The new AGA instrument combines microwave irradiation and constant cooling to allow for fast adjustments of temperatures from -40 up to +100 °C. Previously, some carbohydrate transformations were performed using microwave radiation[68] and even cooled microwave reactors.[69] However, microwave heating has not been implemented to regulate several steps during an oligosaccharide synthesis or for AGA.[69a] The ability to heat and cool reactions quickly and reliably, enables new chemical strategies for oligosaccharide assembly. Now, access to glycans with and without modifications is possible. The design of total orthogonal building block **3.07**, bearing the Fmoc, Lev, ClAc and NAP groups enabled the synthesis of highly branched structures such as *N*-glycan motifs, which has been demonstrated by the synthesis of **3.17** and **3.22-3.28**. The total orthogonal mannose building block will act as a tool for carbohydrate chemists for the quick access to mannose structures with branches and functionalizations, without synthesizing several building blocks for different connections. The application of **3.07** to further glycan synthesis has recently been demonstrated for mannose-6-phosphate containing oligosaccharides[36]. This will help in the future to synthesize relevant *N*-glycan structures. It will also help to synthesize differently coupled and functionalized mannose structures such as PI-88 – a heparanase and angiogenesis inhibitor with anti-metastatic[70] effects. Structures synthesized using total orthogonal building block **3.07** can also be fully deprotected on solid-support so that completely deprotected oligosaccharides are released upon photo-cleavage from the solid-support, which avoids the extra global deprotection step. The new set of protecting groups will not only be used for mannose structures, but is applicable for other monosaccharide units as well. This would allow the new AGA synthesizer to prepare even more complex glycans rapidly. The application of the ClAc protecting group in the synthesis of vaccine candidates against *P. gingivalis* for example will be shown in Chapter 5. For that, ClAc was used as a temporary and also a remotely participating group in glucose to provide *cis*-glucosidic linkages.

A set of BODIPY-protected carbamate building blocks were synthesized and evaluated for their photo-lability and glycosylation-stability. F-BODIPY building block **3.29c** provides the right compromise between glycosylation-stability and photo-reactivity. The concept of a

consecutive glycan assembly approach was demonstrated by the synthesis of trisaccharide **3.38** with a yield of 70% over three steps. On the basis of these results, BODIPY-protecting groups can be optimized for even faster photolysis without losing chemostablity. Since the wavelength of the absorption of the BODIPY-protecting groups can be tuned by various substituents in the range between 450 nm (green) to 700 nm (red)[50a] another level of orthogonality can be investigated using different BODIPY groups with different absorption, so that deprotection of specific groups could occur by irradiation with light of different wavelengths.

4 Stereocontrol: Selective Formation of 1,2-*cis* Linkages

Parts of this Chapter are in preparation for the manuscript: Greis, K.[‡]; **Leichnitz, S.**[‡]; Kirschbaum, C.; Meijer, G.; von Helden, G.; Seeberger, P. H.; Pagel, K., The Effect of Electron Density in Acyl Protecting Groups on the Selectivity of Galactosylations.

[‡]These authors contributed equally. Building blocks were synthesized and characterized by **Sabrina Leichnitz** as well as glycosylation reactions for alpha/beta-ratio determination and AGA experiments. Cold-ion IR experiments and density functional theory calculations were carried out by Kim Greis.

Part of this Chapter is published in: Greis, K.; Kirschbaum, C.; **Leichnitz, S.**; Gewinner, S.; Schöllkopf, W.; von Helden, G.; Meijer, G.; Seeberger, P. H.; Pagel, K., Direct Experimental Characterization of the Ferrier Glycosyl Cation in the Gas Phase. *Org. Lett.* **2020**, *22* (22), 8916-8919.[71] https://doi.org/10.1021/acs.orglett.0c03301.

4.1   Introduction

4.1.1   Glycosylation Reactions – Mechanism and Stereocontrol

The predominant reason for challenges in the synthesis of carbohydrates, such as tetrasaccharide repeating unit of the lipopolysaccharide of *P. gingivalis* described in Chapter 5, is the stereocontrol of glycosylation reactions. Especially the formation of certain 1,2-*cis* glycosidic linkages in AGA remains challenging. In AGA, total stereocontrol is required, because a purification after the glycosylation steps during the synthesis is not possible at the solid-support. To overcome this problem, a deeper understanding of the glycosylation mechanism is required.
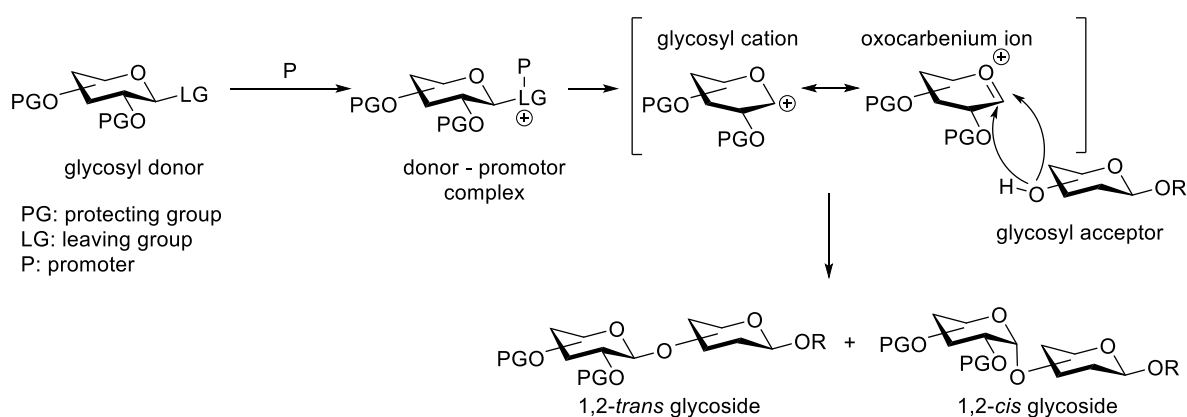
Scheme 4.1. General mechanism for glycosylation reactions.

The generally accepted mechanism of glycosylation reactions proceeds *via* a planar key transient cationic species – the glycosyl oxocarbenium ion (Scheme 4.1). This species can be attacked by a glycosyl acceptor in a nucleophilic fashion from the top or bottom phase, which either leads to the 1,2-*trans* glycoside or the 1,2-*cis* glycoside.

1,2-*Trans*-glycosidic linkages are efficiently incorporated by taking advantage of C2 neighboring group participation (Scheme 4.2). Stereoselective formation of 1,2-*cis*-glycosidic linkages remains challenging as anomeric mixtures are typically formed when neighboring group participation is missing.[37b, 72]
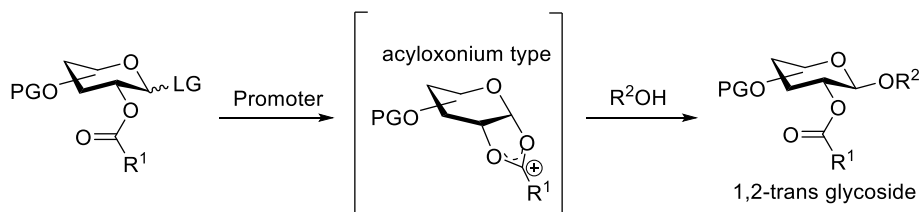
Scheme 4.2. Neighboring group participation using acyl groups for the formation of 1,2-*trans* glycosides.

Several strategies for the stereoselective synthesis of 1,2-*cis*-glycosides have been described taking advantage of solvent effects, effects of additives, hydrogen bonds, chiral auxiliaries, steric hindrance or remote participation (Figure 4.1).[72-73] However, the application of these methods on AGA are challenging, because the protecting groups have to fit the coupling-deprotection scheme and most methods require additional manipulations.
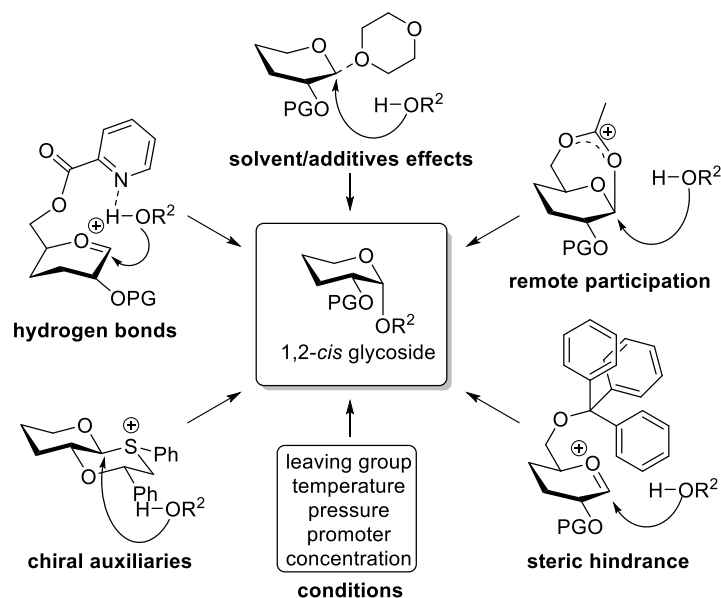
Figure 4.1. Various methods used for the formation of 1,2-*cis* glycosidic linkages.

Remote participation has been used in AGA before, but only moderate yields and selectivity were obtained for galactose building blocks.[72] On the other hand, great progress has been made recently in the automated assembly of starch and glycogen polysaccharides.[10] To that end, the stereoselective installation of multiple 1,2-*cis*-glucosidic linkages was achieved using glucose building blocks with remote ester groups in the C3- and C6-position. These results are encouraging for further investigations on general factors that enable a quick design of building blocks for the efficient incorporation of 1,2-*cis*-glycosidic linkages in AGA by remote participation. However, every monomer, including glucose, mannose and galactose, show individual glycosylation results, reactivities and confirmations. The lack of a universal glycosylation method that controls the stereoselectivity shows the importance of understanding the glycosylation mechanism, characterizing glycosyl oxocarbenium ions and investigating effects of protecting groups on the structure of the intermediates. Most importantly, structural insights into the intermediates improve our understanding of the glycosidic bond formation.

4.1.2 Cold-Ion IR Spectroscopy – Investigation of Remote Participation

Cold-ion infrared (IR) spectroscopy is a useful tool to investigate the gas-phase structure of glycosyl cations and the participation of protecting groups. This enables a deeper insight into the glycosylation mechanism.[74] The method combines mass spectrometry (MS) and IR spectroscopy, which provides a very sensitive option by interrogating the vibrational modes of

isolated molecules in the controlled environment of the gas phase. In the cold-ion IR experiment (Figure 4.2) isolated molecular ions are generated using nanoelectronspray ionization (*n*ESI). They are then selected based on mass-to-charge values, accumulated in a linear ion trap and picked up by superfluid helium droplets, where they are rapidly cooled to the internal temperature of the droplets (0.37 K). Irradiation with intense, narrow-bandwidth IR radiation from the free-electron laser of the Fritz-Haber-Institute (FHI) can lead to the ejection of ions, if the wavelength is in resonance with a vibrational excitation of the ion. Thereby, the monitoring of the ejection efficiency as a function of the wavelength is possible and provides a characteristic IR spectrum that can be compared to a density functional theory (DFT) simulated spectrum of the ion.[74]
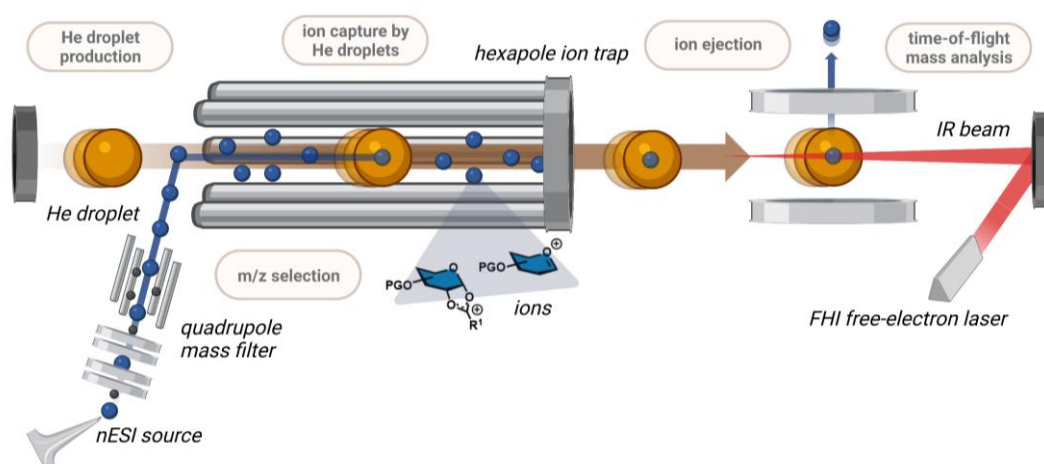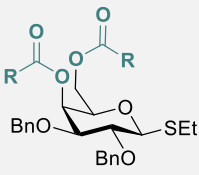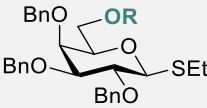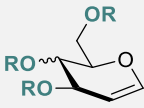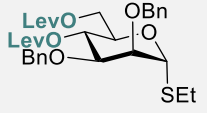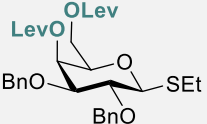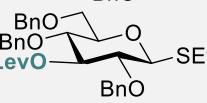
Figure 4.2. Schematic experimental setup of the cold-ion IR experiment. Modified from *Angew. Chem. Int. Ed.* **2017**, 56, 11248-11251.[74]

This method was used[75] to present a detailed structural characterization of the acyloxonium cation, which is the main intermediate in neighboring group participation (Scheme 4.2). In this way, direct evidence for remote participation of acetyl groups at C4 and C6 in galactose building blocks was provided.[76]

4.1.3   Project Aim

A better understanding of the glycosylation mechanism and the investigation of intermediates paves a way to fine-tune the efficiency of remote participation in AGA. The aim is to use mechanistic findings for the design of new 1,2-*cis* selective building blocks for AGA. Here, mainly the effect of electron density is investigated, which includes the synthesis of model building blocks, test reactions with different nucleophiles to determine the ratio between 1,2-*cis* and 1,2-*trans* linkages and the comparison of cryogenic infrared spectra of the dioxolenium-type intermediates with density functional theory calculations. Investigations focus on the effect of electron density in acyl protecting groups on the selectivity of galactosylations, the effect of ether groups with sigma electron donor and acceptor properties on galactosylations, electronic effects in glucals and galactals as well as the influence of Lev groups in galactose, glucose and mannose (Table 4.1).

Table 4.1. Overview on the aspects and structural classes that are investigated for the improvement of 1,2-*cis* linkage formation by remote participation.

	Acyl Groups	Ether Groups	Glucals and Galactals	Lev Groups
Structures				
Aspects	Position (C4-OH or C6-OH)	Influence of electron density Sigma electron donor or acceptor		Influence of Lev ester groups Position (C3-OH, C4-OH or C6-OH)
Monomer	Galactose	Galactose	Galactose Glucose	Galactose Glucose Mannose

4.2 Results

4.2.1 The Effect of Electron Density in Acyl Protecting Groups in Galactose Synthesis

For the systematic investigation on how electron density in acyl protecting groups influences the stereoselectivity of galactosylations, galactose building blocks bearing the electron withdrawing pivaloyl (trimethylacetyl, Piv) group (**4.06-4.08a**) and the electron withdrawing trifluoroacetyl (TFA) group (**4.06-4.08b**) were synthesized (Scheme 4.3). The investigations did not only focus on the electron density, but also on the preferred position of the acyl group in galactose. Therefore, Piv and TFA groups were installed at C4-OH, C6-OH and both positions, while the remaining hydroxyl groups are benzylated.

The selective introduction of the Piv and TFA groups at C4-OH and C6-OH position is based on benzylidene protected building block **4.02**. Regioselective ring opening of the benzylidene resulted in the three different alcohol building blocks **4.03-4.05**. These building blocks are useful for introducing a variety of protecting groups at C4-OH, C6-OH and both positions for diverse investigations. Here, the Piv group was introduced using pivaloyl chloride in pyridine, the TFA group by using trifluoroacetic anhydride and but also the Lev group for investigations that are discussed in section 4.3.3 using STEGLICH esterification conditions.
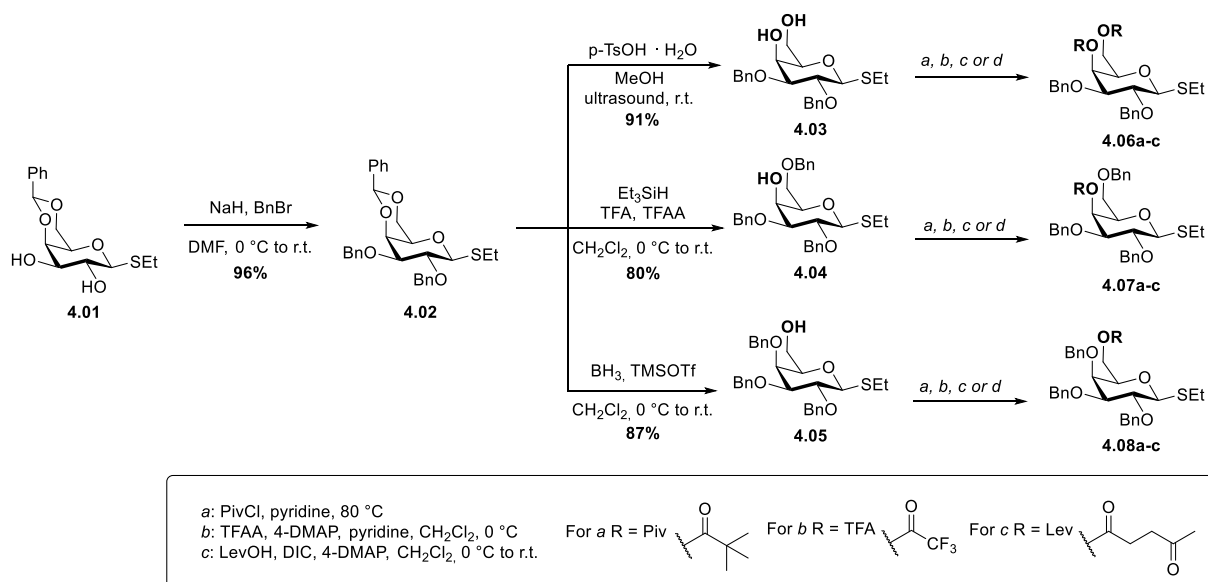
Scheme 4.3. Synthetic route to C4-OH/C6-OH acyl substituted galactose building blocks **4.06a-c**, **4.07a-c** and **4.08a-c**. More detailed reaction conditions are shown in the experimental section.

Stereochemical Outcome

Building blocks equipped with Piv (**4.06-4.08a**) and TFA (**4.06-4.08b**) were employed in glycosylation reactions (Figure 4.3). Four different nucleophiles based on the HSAB principle, from soft (trifluoroethanol) to hard (primary benzylalcohol), were used to further understand the influence of the remote participating groups on the stereochemical outcome of glycosylations with different acceptors. In general, soft nucleophiles lead to a high α-selectivity, while harder nucleophiles provide poor α-selectivity. This is a trend that was previously reported[77]. As glycosyl alcohols are soft nucleophiles[78], the observed trend is desirable for the synthesis of α-glycosidic bonds in the context of oligosaccharide synthesis.
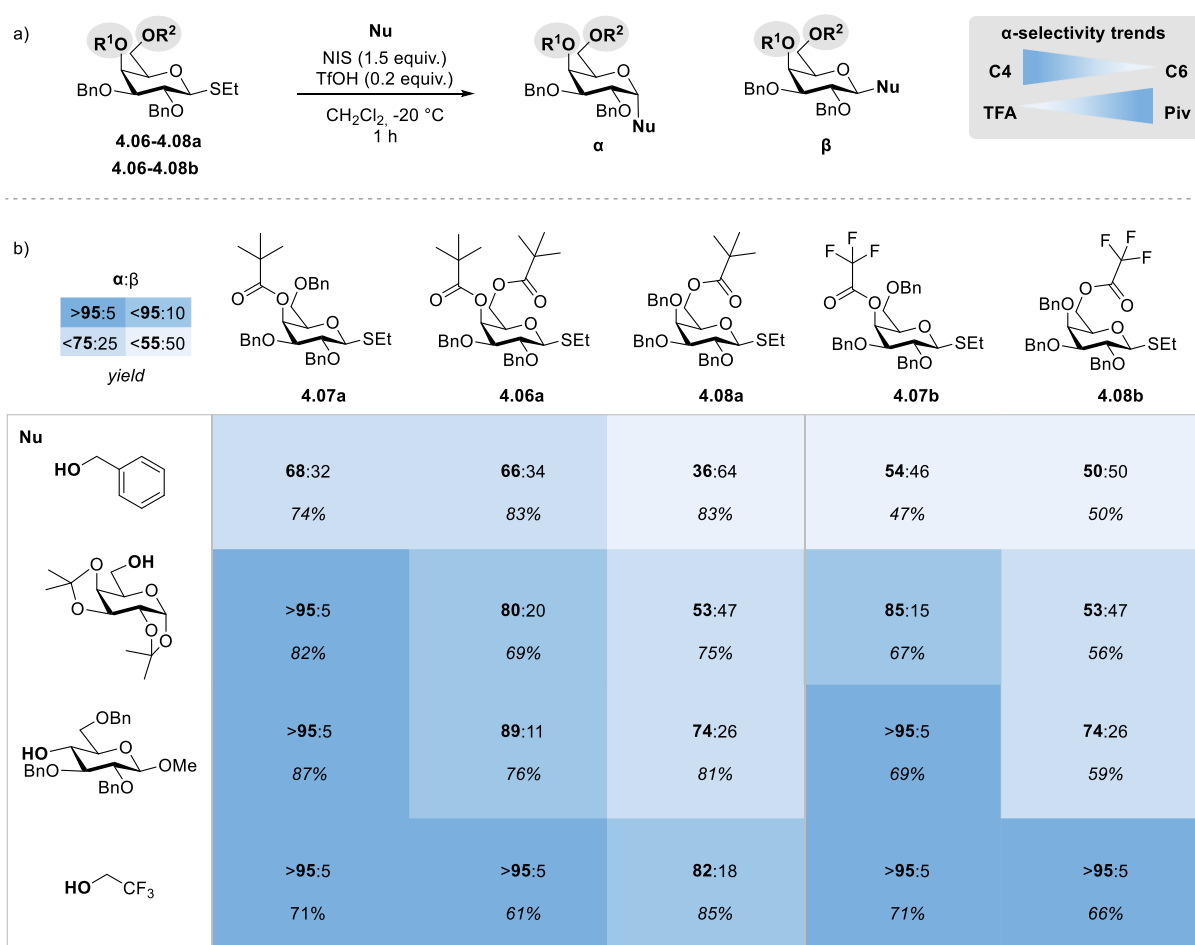
Figure 4.3. (a) Glycosylation conditions of glycosyl donors carrying either Piv, TFA or Bn protecting groups at the C4-OH and C6-OH positions (**R$_{1/2}$**). (b) Stereochemical outcome of the glycosylation reactions of the respective donors with different acceptors (**Nu**).

The glycosylation studies show that the α-selectivity is higher for building block **4.07a** and **4.07b** with an acyl protecting group at C4-OH, compared to those with the protecting group at C6-OH. Even with the primary hard sugar acceptor, the 1,2-*cis*-selectivity is highly distinct. Building block **4.08a** and **4.08b** with acyl protecting groups at C6 show no 1,2-*cis*-selectivity for primary sugar acceptors. Therefore, the active participation of acyl-groups at the mechanism of C6-ester groups must be questioned. Interestingly, for **4.06a**, which bears Piv

at C4-OH and C6-OH position, the α-selectivity is lower than for C4-Piv building block **4.07a**, although an inverse trend has been reported[79] for similar acetyl building blocks. Most likely the sterical bulk of the Piv group may explain this observation.

A clear trend is not only found for the preferred position of the acyl group at galactose, which is clearly the C4-OH position. Also, the electron density of the acyl groups has an immense impact on the stereochemical outcome of the reaction. For building blocks carrying the acyl group at the C4-OH position, the electron-rich Piv building block **4.07a** provides high α-selectivity. The electron-withdrawing TFA group **4.07b** on the other hand, provides significant lower α-selectivity. These results show that an increase in the electron density on the carbonyl oxygen of the acyl group tends to lead to the formation of a covalent bond with the positively charged anomeric carbon in the intermediate state. This results in a better shielding of the β-side and thus high α-selectivity. The high α-selectivity for **4.07a** for soft as well as hard nucleophiles suggests that the origin of the increased α-selectivity of C4-acylated pivaloylated building blocks is remote participation of the C4-acyl group. High α-selectivity of **4.07b** for at least soft nucleophiles indicates, that remote participation must also play a role in building blocks with electron withdrawing acyl groups at C4 as well, but it is significantly weaker. The high α-selectivity of C4-Piv building block **4.07a** in glycosylations with primary and secondary sugar alcohols suggests that building blocks with this substitution motif are promising for AGA. It is important to highlight the high yield of the coupling reactions of **4.07a** with sugars, which is an important requirement for AGA.

Cold-Ion IR Studies

In addition to the investigation of the stereochemical outcome of the synthesized building blocks in glycosylation reactions with different nucleophiles, the intermediates of the glycosylations - the glycosyl cations - were structurally characterized by cryogenic IR spectroscopy and DFT calculations[3]. Thioglycoside precursors were subjected to in-source fragmentation conditions after nano-electrospray ionization. Only the pivaloylated building blocks were ionized leading to the cleavage of the leaving group to form the desired glycosyl cation intermediates. Trifluoroacetylated molecules did not fragment sufficiently or decomposed by losing TFA. Therefore, only pivaloylated building blocks **4.06-4.08a** were analyzed by cold-ion IR spectroscopy. The experimental spectra show mainly the fingerprint region and the functional group region. The fingerprint region, that is located between 1000 and 1400 cm^{-1} is predominantly populated by C–O and C–C stretching as well as C–H bending vibrations and is usually challenging to model[80]. The region of functional groups is located

---

[3] Cold-ion IR spectra were recorded and DFT calculations were carried out by M. Sc. Kim Greis, group of Prof. Dr. Kevin Pagel, Fritz Haber Institut Berlin.

between 1400 and 1800 cm^{-1} and contains most of the diagnostic vibrations of the investigated ions, such as dioxolenium v(O–C–O) and carbonyl stretches v(C=O).

The cold-ion IR spectra of **4.06-4.08a** are shown in Figure 4.4

Figure 4.4. For **4.07a**, C4-dioxolenium structures are the lowest in energy according to DFT simulations. The simulated spectra match the experimental resolved signals for the dioxolenium intermediate at 1090–1110, 1540, and 1558 cm^{-1} well (Figure 4.4a,e – blue structures and signals).
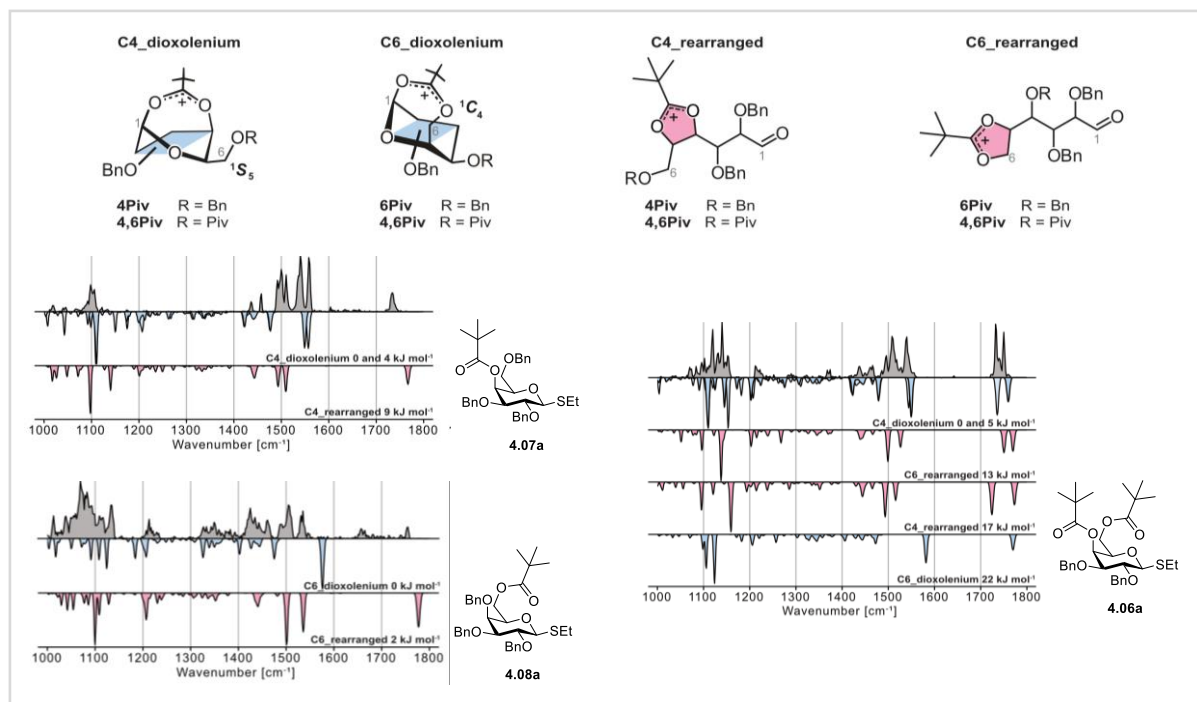
Figure 4.4. Cryogenic infrared spectra of **4.07a**, **4.08a**, and **4.06a** galactosyl cations (**gray**). Computed infrared spectra are shown in the inverted traces in (**blue**) for the dioxolenium species and in (**red**) for the rearranged species.[4]

The observed signals at 1492–1510 cm^{-1} for **4.07a** as well as the carbonyl stretch at 1734 cm^{-1} are showing that most likely a rearranged species is present, where the acyl group attacks the C5-atom (Figure 4.4a, e, red structures and signals). Previously, it was suggested that acyl groups may attack the C5-atom in glycosyl cations leading to ring opening and the free aldehyde.[77] The cold-ion IR spectra of **4.07a** proved the presence of the C4-dioxolenium structure and it is in accordance with the high α-selectivity that was observed in glycosylation reactions. The formation of the C4-rearrangement product is unique to the employed gas-phase conditions. There were no side products in the glycosylation reactions observed that could give evidence for the presence of this species in solution phase. For **4.08a**, the simulated C6-dioxolenium structure does not match the experimental spectrum. Therefore, C6-acyl

---

[4] Cold-ion IR spectra were recorded and DFT calculations were carried out by M. Sc. Kim Greis, group of Prof. Dr. Kevin Pagel, Fritz Haber Institut Berlin as well as the graphic content in Figure **4.4**.

participation is does not exist for Piv groups, which is also in accordance with the poor α-selectivity of these building blocks. For **4.06a**, the experimental IR signature is similar to **4.07a**. Therefore, the observed α-selectivity is mainly caused by remote participation of the C4-Piv group at C4.

Application in AGA

The glycosylation studies as well as the cold-ion IR spectra give important insights into the glycosylation mechanism of galactosylations. It was demonstrated that the efficiency of remote participation can be fine-tuned by the right choice of position and nature of the protecting group. The studies showed, that electron-rich C4-pivaloylated galactose building blocks show high α-selectivity for several nucleophiles – especially for sugar nucleophiles, yields and α-selectivity are excellent. According to these findings, α-selective building block **4.12** was developed for the application in AGA. In order to enable elongation in AGA, temporary Fmoc protecting group was installed at C3-OH position.

The synthetic route for galactose building block **4.12** (Scheme 4.4) is similar to building block **4.07a** described earlier. Only an additional step for the selective NAP introduction to **4.09** was required for the installation of the temporary Fmoc group at the end of the synthetic route. NAP was regioselectively introduced at C3-OH *via* a stannylene ketal intermediate that enhances the nucleophilicity of the oxygen at C3. Treatment with 2,3-dichloro-5,6-dicyano-1,4-benzochinone (DDQ) and subsequent Fmoc protection followed by the conversion of the thioglycoside into a glycosyl phosphate afforded target building block **4.12** (81%, overall eight steps).
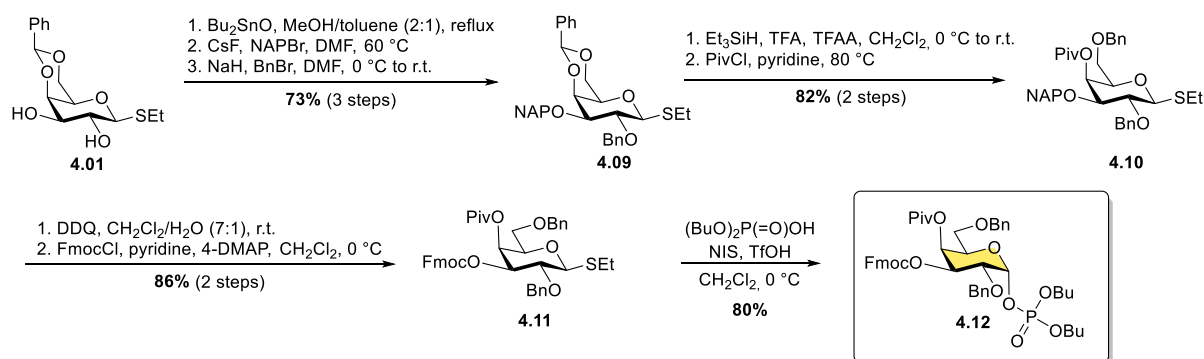
Scheme 4.4. Synthetic route to α-galactose building block **4.12**, which was developed based on the results of glycosylation studies and cold-ion IR studies and can be applied in AGA. More detailed reaction conditions are shown in the experimental section.

The use of thioglycoside **4.11** in AGA resulted in low yields, because the glycosylation at C3 position is sterically hindered by the bulky Piv group. The more reactive phosphate leaving group at C1 in **4.12** ensured high yields. To prove the high 1,2-*cis* selectivity and applicability in AGA, **4.12** was employed to AGA to assemble the α(1,3)-galactose trisaccharide **4.14** with a yield of 69% and total α-selectivity (Figure 4.5), which was verified by

coupled ^{1}H,^{13}C HSQC NMR spectroscopy and analytical HPLC. While the free reducing end mutarotates, all building blocks are coupled *via* 1,2-*cis* glycosidic linkages.
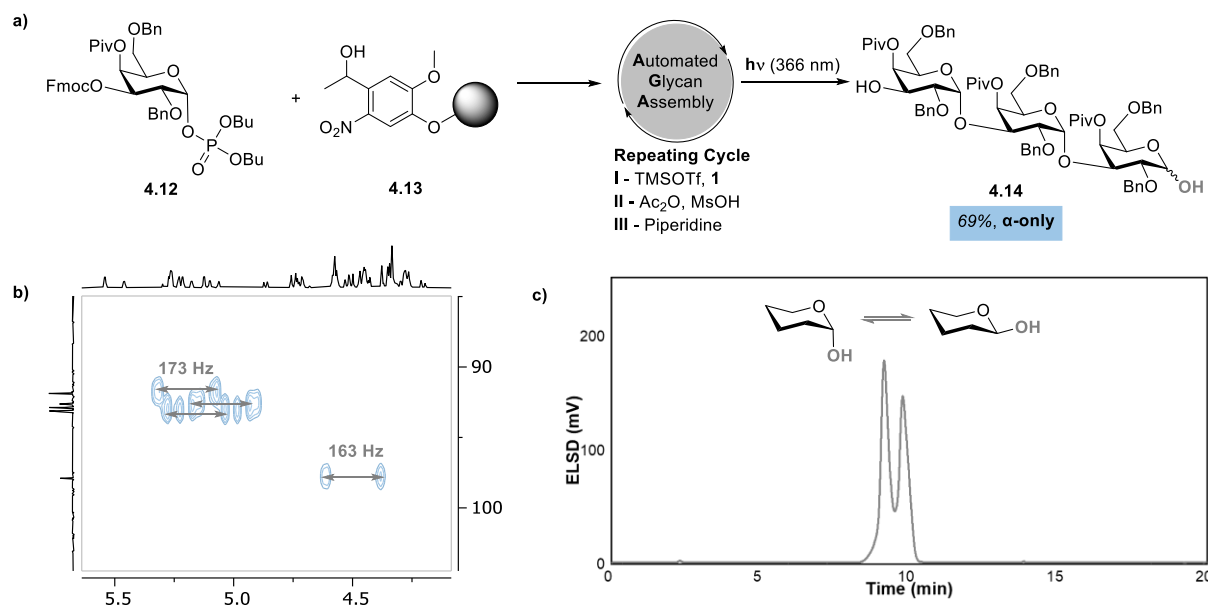
Figure 4.5. AGA (a) employing C4-piv galactosyl building block **4.12** leads to an α(1,3)-D-trigalactopyranoside **4.14** with a yield of 69% in six hours using solid-support **2**. While the free reducing end mutarotates, the coupled ^{13}C,^{1}H HSQC (anomeric region) (b) and the HPLC profile (c) confirm total α-selectivity. More detailed reaction conditions are shown in the experimental section.

The here shown study on the effect of electron density in acyl protecting groups on the selectivity of galactosylations shows that electron donating substituents on participating acyl protecting groups increase the α-selectivity of glycosylation reactions. This was demonstrated for Piv groups. In opposite, electron withdrawing substituents, such as the TFA group, deactivate remote participation and therefore decrease the selectivity of galactosylations. It was also shown, that C4 substituents are responsible for remote participation in galactose and C6 substituents do not provide efficient remote participation. This was shown in glycosylation reactions with different nucleophiles as well as in cold-ion IR studies. The obtained mechanistic knowledge is the basis to design building blocks for the application in AGA. Guiding principles are provided to fine-tune the selectivity and efficiency of building blocks. This will help to improve the efficiency of the formation of 1,2-*cis* linkages in order to access oligosaccharides containing 1,2-*cis* linkages such as blood group systems[81] or bacterial lipopolysaccharide antigens[82].

4.2.2 Through-Bond Communication of *σ*-Bond-Donor/Acceptor Ethers in Galactose

A non-classical remote participation of benzyl groups at C6 in galactose has been observed in previous cold-ion IR studies.[76] This non-classical remote participation could be responsible for the previously observed α-selectivity of benzylated galactose.[72, 76] Here, the effect of through-bond communication on relative donor abilities of *σ*-bonds of remote

45

substituents is investigated. Fluorine-rich remote ether-substituents are sigma electron acceptors, which would lead to a decrease of the orbital overlap of the oxygen at C6 and the anomeric carbon atom (Figure 4.6). In opposite to that, silicon ether-substituents are known to be sigma electron donors and the β-silicon effect can lead to an increase of the orbital overlap and a stabilization of an oxocarbenium ion. Computational studies on this through-bond communication have previously been described.[83] Therefore, the synthesis of model galactose building blocks with sigma electron acceptor and sigma electron donor substitutes at C6-OH position is presented here and further investigations on the selectivity of its glycosylations.
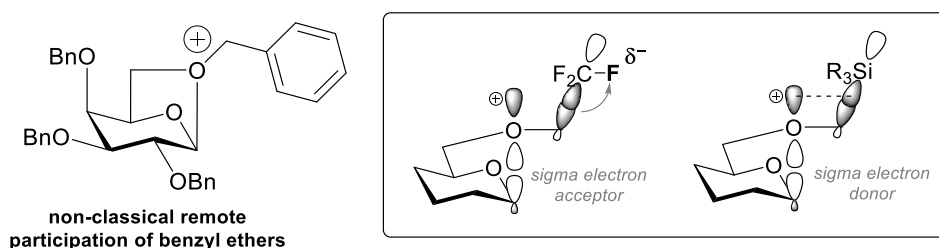
Figure 4.6. Non-classical remote participation of benzyl ethers and sigma electron effect of fluorine-rich and silicon remote participating groups for the investigation of σ-bond acceptor and donor effects on remote participation.

Synthesis

Target compound **4.15** was synthesized in a WILLIAMSON ether synthesis with a yield of 14% using (trimethylsilyl)methyl trifluoromethanesulfonate as an electrophile and C6 deprotected **4.05** as a nucleophile (Scheme 4.5). However, the formation of several side products was observed, that were not further characterized. The formation of side products in the substitution reactions at (halomethyl)silanes has been described before.[84] It was shown that rearrangement reactions can take place as well as coordination of the alkoxide at the silicon atom, as silicon is a good Lewis acid. An alternative procedure using (bromomethyl)-TMS as electrophile failed to produce **4.15**. Instead, side product **4.16** was obtained with a yield of 88%. A proposed mechanism for the formation of product **13** is depicted in Scheme 4.5. It is possible, that the alkoxide group attacks a methyl group of the TMS reagent and bromide would be eliminated to obtain **4.16**.
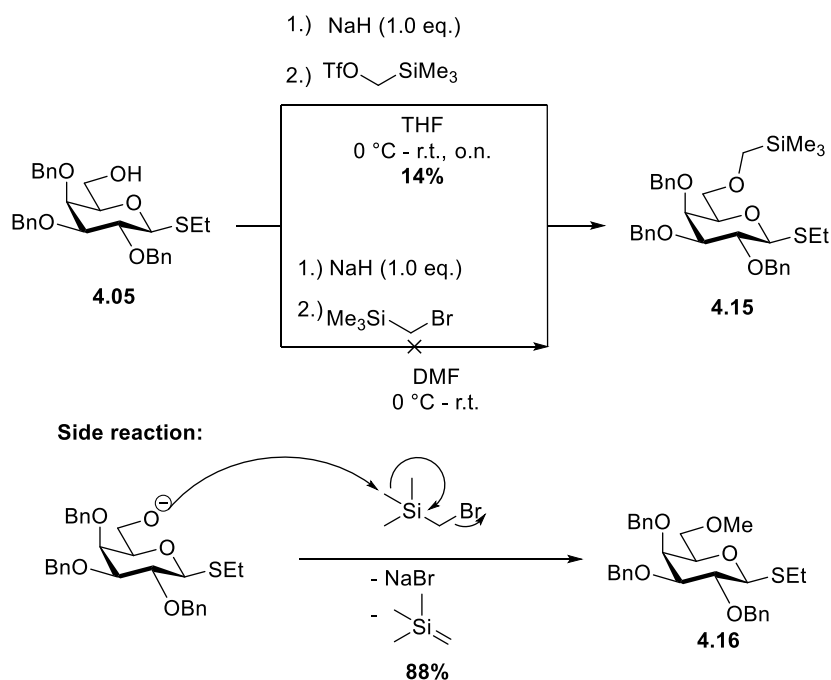
Scheme 4.5. Synthesis of σ electron donor building block **4.15** and undesired side reaction using (bromomethyl)-TMS. More detailed reaction conditions are shown in the experimental section.

The introduction of fluorinated ether groups at C6-OH is challenging, because the electron withdrawing character of fluorine changes the behavior of reagents for the common WILLIAMSON ether synthesis in terms of polarity and nucleophilicity. Shielding effects of fluorine for example prevented the synthesis of nonafluorinated **4.17**, but it was possible to synthesize its methylenetrifluoromethyl analogue. For the synthesis of compound **4.17**, the C6-OH in building block **4.05** was used as a nucleophile and nonafluoro-4-iodobutane was used as an electrophile (Figure 4.7).
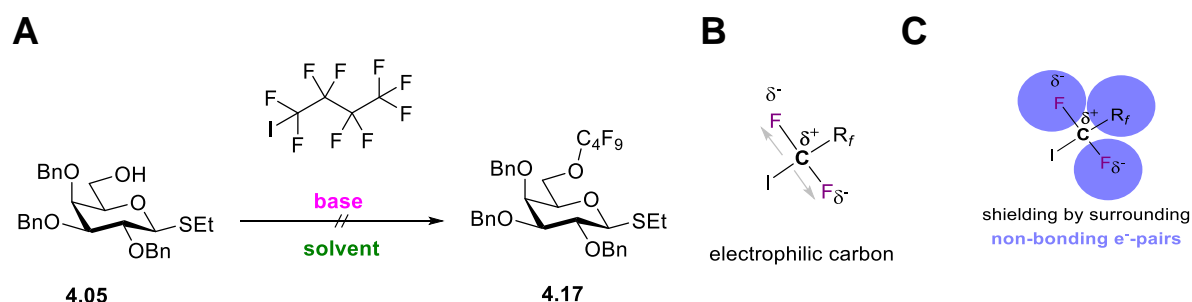
Figure 4.7. Failed synthetic route for the synthesis of compound **4.17** (**A**), substituent effects of fluorine on S_N2 process showing the electron withdrawing character of the fluorine (**B**) and shielding (**C**). More detailed reaction conditions are shown in the experimental section.

For the nucleophilic substitution, several conditions were applied using different bases for the deprotonation of the hydroxyl group (cesium carbonate, sodium hydride and potassium hydroxide), different solvents and temperatures as well as neat conditions using nonafluoro-4-iodobutane as a solvent. However, none of the conditions gave the desired product. In theory, the nucleophilic substitution in R_FCF_2-Hal systems should be highly favored due to the electron withdrawing character of the fluorine substituents and thus the high electrophilicity of the carbon center. However, nucleophilic substitution of a halogen atom in R_FCF_2-Hal systems are

difficult, due to a combination of steric effects and shielding of the carbon skeleton by surrounding non-bonding pairs on fluorine (Figure 4.7B,C).[85] As the synthesis of highly fluorinated **4.17** failed, trifluoroethanolether **4.18** was attempted. Target compound **4.18** was obtained using the C6 atom of galactose as an electrophile with a yield of 16% over eight steps starting from acetone-D-galactose **16** (Scheme 4.6, strategy 4). Original strategy 1 to obtain **4.18** using C6-OH galactose derivative **4.05** failed due to an intramolecular side reaction.
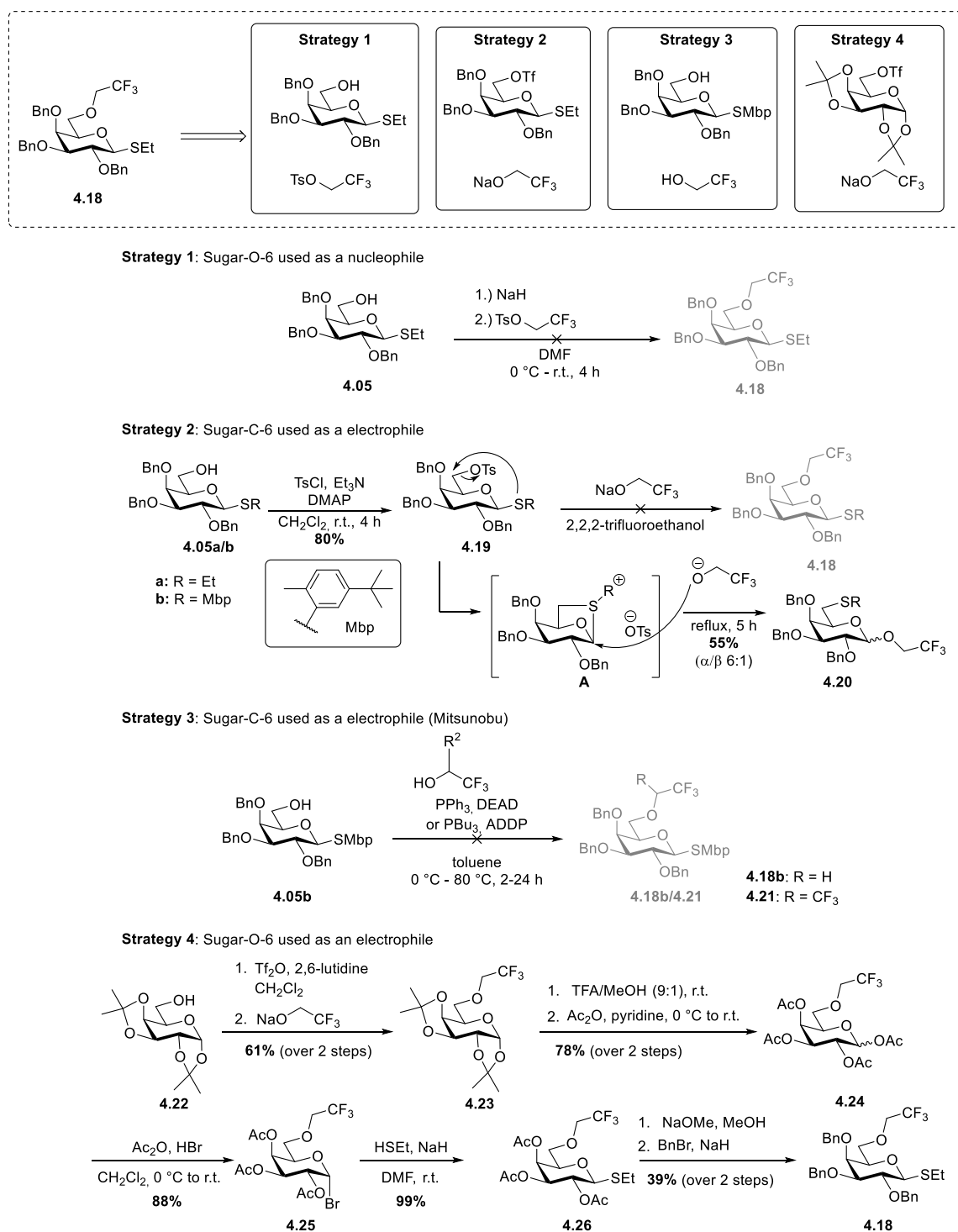
Scheme 4.6. Synthesis of fluorinated ether-substituted galactose building block **4.18**. While strategies 1-3 failed, the use of the C6-OH as nucleophile was successful. More detailed reaction conditions are shown in the experimental section.

Successful strategy 4. Triflated **4.22** was treated with 2,2,2-trifluroethoxide and the triflate leaving group was replaced by the trifluoroethoxide in a nucleophilic substitution. After obtaining the desired trifluoroethoxide group at position C6, six more steps were conducted to get the desired benzylated thioglycoside **4.18** with a yield of 16% over eight steps. Acetal derivative **4.23** was deprotected under acidic conditions followed by acetylation to afford compound **4.23** (78%, 2 steps). Afterwards, **4.23** was treated with hydrobromic acid to obtain the α-galactopyranosyl bromide **4.25** with a yield of 88%. Ethylthiolate was used to substitute the α-bromide to obtain the β-thioglycoside **4.26** in quantitative yield. Common thioglycosylation conditions using boron trifluoride etherate did not lead to any conversion. This could be caused by coordination of the boron trifluoride to a fluorine atom at the trifluorethoxide group at position C6. Another reason could be a lower reactivity of **4.24** in glycosylation reactions due to the electron withdrawing character of the trifluoroethoxy group. The oxocarbenium ion would not be stabilized well by the oxygen atom at position C6 due to its low electron density. Afterwards, methanolysis was conducted for the deprotection of the acetyl groups followed by a benzylation using benzyl bromide with a yield of 39% over two steps to obtain the desired product **4.18**.

Failed strategy 1. Another attempted strategy failed using the C6-OH of **4.05** as a nucleophile and tosylated 2,2,2-trifluoroethanol as an electrophile. Compound **4.05** was deprotonated using sodium hydride in order to nucleophilically substitute the tosyl leaving group. However, the alkoxide at position C6 attacked the sulfur atom of the tosyl group at in a nucleophilic fashion.

Failed strategy 2. Following a strategy using the C6-atom as an electrophile, the tosyl leaving group was introduced at the C6 atom of **4.05a** to obtain **4.19** with a yield of 80%. Treatment of **4.19** with 2,2,2-trifluoroethoxide did not afford the desired product **4.18**. Instead, the migration product 4.20 was obtained, which can be explained by the proposed mechanism that is shown in **Scheme 4.6**. The sulfur atom at the thioethyl group can compete as a nucleophile with the trifluoroethoxide and can undergo an intramolecular substitution at the C6 atom. This intramolecular reaction would lead to the substitution of the tosyl group at postion C6 by sulfur and the formation of intermediate **A**. Intermediate **A** can be attacked in a nucleophilic fashion by the trifluoroethoxide at position C6 or C1. As the anomeric position C1 is more reactive, the nucleophilic substitution takes place at the C1 atom, so that **4.19** is formed, where the thioethyl group is migrated to the C6 atom.

The nucleophilicity of the sulfur atom in thioglycosides is a common problem in carbohydrate chemistry, because the thio group can act as a competing nucleophile in nucleophilic substitutions. A common example for this is the aglycon transfer of thioglycosides in glycosylation reactions. It was shown that sterically hindered groups at the sulfur of thioglycosides, such as the 2,6-dimethylphenyl (DMP) group or the Mbp group can effectively

block the aglycon transfer.[86] The effective blocking of the aglycon transfer is a result of steric hindrance of the nucleophilic sulfur atom. Therefore, Mbp-thioglycoside **4.05b** was used instead of ethyl-thioglycoside **4.05a** with the aim to avoid the intramolecular substitution reaction of the sulfur at the C6-atom. Nevertheless, the unwanted migration was observed again. Usually, the use of the tosyl group at the C6-OH at thioglycosides is common for the introduction of azide groups at the C6-atom.[87] However, trifluoroethoxide is less nucleophilic than azide due to the strong electron withdrawing effect of the fluorine atoms, which results in a low electron density at the alkoxy group. Therefore, harsh reaction conditions had to be used, which could induce the unwanted nucleophilic substitution reaction. This is a possible reason, why nucleophilic substituions at the C6-atom of thioglycosides are working with azides, whereas those with trifluoroethoxide as nucleophiles are not.

Failed strategy 3. The MITSUNOBU approach enables the etherification of hydroxyl groups with acidic alcohols under milder conditions than the WILLIAMSON approach. The synthesis of polyfluorinated ethers using the MITSUNOBU approach has already been conducted previously.[88] 2,2,2-Trifluoroethanol, 1,1,1,3,3,3-hexafluoro-2-propanol and other fluorinated alcohols were coupled with primary, secondary and tertiary alcohols. The fluoroalcohol, due to its acidity acted as the proton donor and nucleophile in the reaction. Therefore, the MITSUNOBU approach was applied on the synthesis of compound **4.18b**. No conversion of the starting materials was observed. Therefore, it was assumed that the aciditiy of 2,2,2-trifluoroethanol (pK_a = 12.4[89]) is not high enough for the reaction. MITSUNOBU reactions are working well with phenol (pK_a = 10.0[90]), which is more acidic than 2,2,2-trifluoroethanol. Thus, the more acidic fluoroalcohol 1,1,1,3,3,3-hexafluoro-2-propanol (pK_a = 9.3[91]) was used. However, this reaction did not lead to any product formation as well.

Stereochemical Outcome

Building blocks **4.15** and **4.18** were employed in glycosylation reactions (Figure 4.8) with C6-OH sugar nucleophile and were compared to C6-acyl building blocks **4.08a** and **4.08b**. Similar to previously observed α-selectivity of benzylated galactose[72, 76], both C6-ether substituted building blocks **4.15** and **4.18** show a slight tendency for 1,2-*cis*-linkage formation (60% α-product, 40% β-product). However, no sigma electron effect was observed, as the 1,2-*cis*-selectivity for σ-bond acceptor and donor substituents is similar. It was hypothesized that fluorine-rich remote ether-substituents are sigma electron acceptors and lead to a decrease of the orbital overlap of the oxygen at C6 and the anomeric carbon atom. Furthermore, it was hypothesized that silicon ether-substituents are sigma electron donors and the β-silicon effect can lead to an increase of the orbital overlap and a stabilization of an oxocarbenium ion. Those hypotheses could not be supported with the glycosylation results of **4.15** and **4.18** due to their similar selectivity.

Interestingly, the comparison to **4.08a** and **4.08b** shows that ether substituents at C6-position in galactose result in higher α-selectivity than acyl substituents. Most likely, ether groups at C6-position of galactose more likely are participating in a non-classical manner than acyl groups at C6-position. This is in accordance with previous findings regarding a non-classical remote participation of fully benzylated galactose by cold-ion IR spectroscopy[76] and the results from Chapter 4.2.1, where it was shown, that C6-acyl groups are not remotely participating in glycosylation reactions.
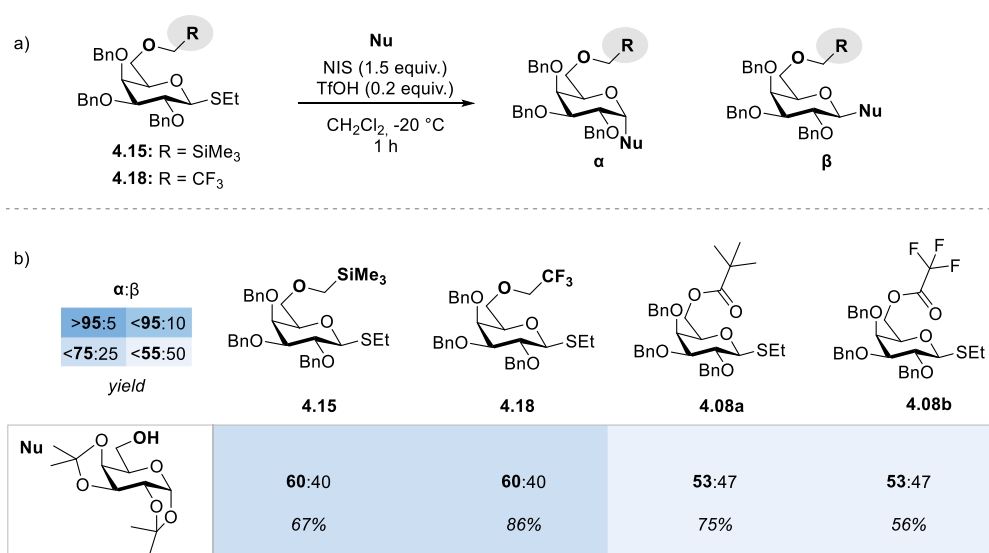
Figure 4.8. (a) Glycosylation conditions of glycosyl donors carrying either fluorine-rich and silicon remote ether groups for the investigation of σ-bond acceptor and donor effects on remote participation. (b) Stereochemical outcome of the glycosylation reactions of the respective donors with fluorine-rich **4.18** and silicon **4.15** remote ether groups compared to building blocks with electron-rich **4.08a** and electron-poor **4.08b** acyl protected building blocks.

Cold-Ion IR Studies

The cold-ion IR spectra of compound **4.15** and **4.18** (Figure 4.9) were recorded and DFT simulations were conducted by Kim Greis of the Pagel[5] group. The spectra do not match the DFT simulated spectra. Therefore, more theoretical work needs to be done in future to understand the cold-ion IR spectra of **4.18** and **4.15** and their influence on glycosylation reactions.

---

[5] M. Sc. Kim Greis, group of Prof. Dr. Kevin Pagel, Fritz Haber Institut Berlin.
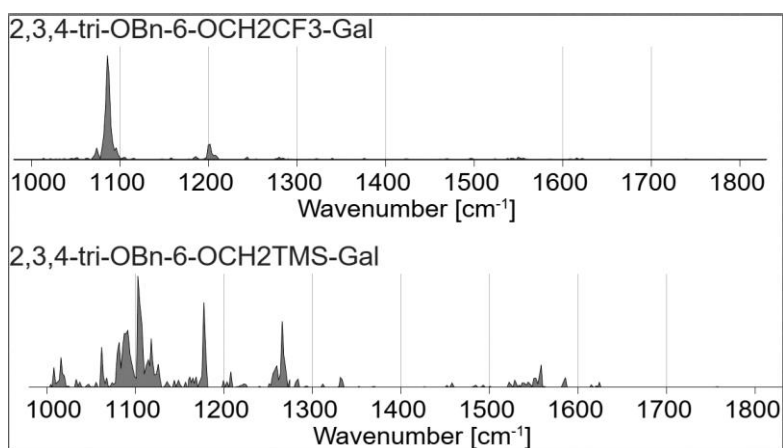
Figure 4.9. Cold-ion IR spectra of compound **4.18** (line 1) and **4.15** (line 2).

4.2.3 The Effect of Lev Protecting Groups in Galactose and Mannose

Synthesis

For the systematic investigation on how Lev protecting groups influence the stereoselectivity of mannosylations and galactosylations, several Lev containing building blocks were synthesized. The synthesis of Lev containing galactose building blocks has been described in section 4.31 (Scheme 4.3). Similar to the synthesis of acyl protected galactose building blocks **4.06-08c**, Lev containing mannose building blocks **4.32-4.34** were synthesized based on the regioselective ring opening of benzylidene protected building block **4.28** (Scheme 4.7).
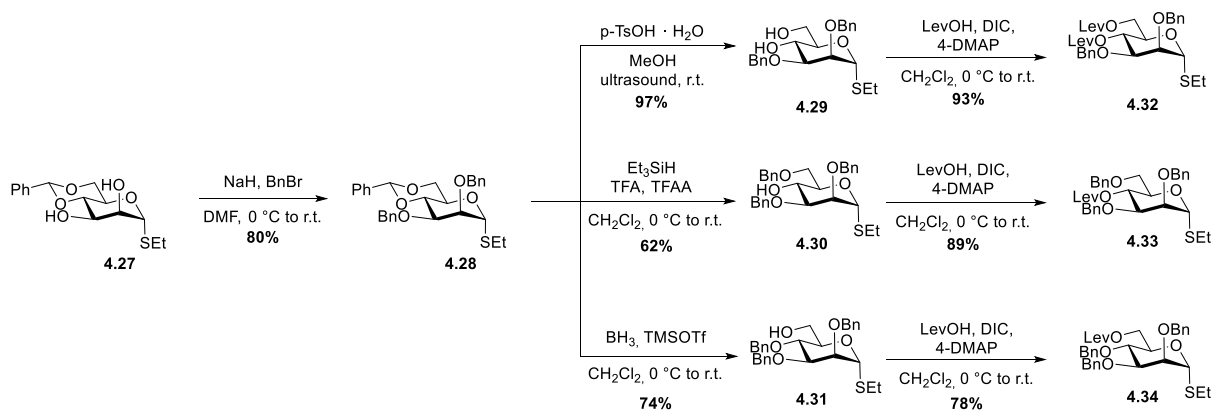
Scheme 4.7. Synthetic route to C4/C6-Lev substituted mannose building blocks **4.32-4.34.** More detailed reaction conditions are shown in the experimental section.

52

Stereochemical Outcome

C4-OLev and/or C6-OLev galactose building blocks **4.06-4.08c** and corresponding mannose building blocks **4.32-4.34** were employed in glycosylation reactions (Figure 4.10) with a C6-OH sugar nucleophile.

Interestingly, C4-OLev galactose building block **4.07c** does not show stereoselectivity. This is contrary to the results found in section 4.2.1 that showed excellent α-selectivity for galactose building blocks with electron donating acyl groups at C4-OH position. Moreover, the C6-OLev galactose building block **4.08c** even shows β-selectivity (81% β-product), which suggests a different glycosylation mechanism for Lev building blocks. Since the 1,2-*cis* selectivity for galactose building blocks was already well studied in section 4.2.1, further optimizations and investigations on Lev substituted galactose building blocks were not conducted. However, the β-selectivity of C6-OLev galactose building block **4.08c** encouraged for further studies on C4-OLev and/or C6-OLev mannose building blocks **4.32-4.34**, since *cis*-glycosidic *β*-mannosides (e.g. *N*-glycans) are of high biological interest, but difficult to achieve.
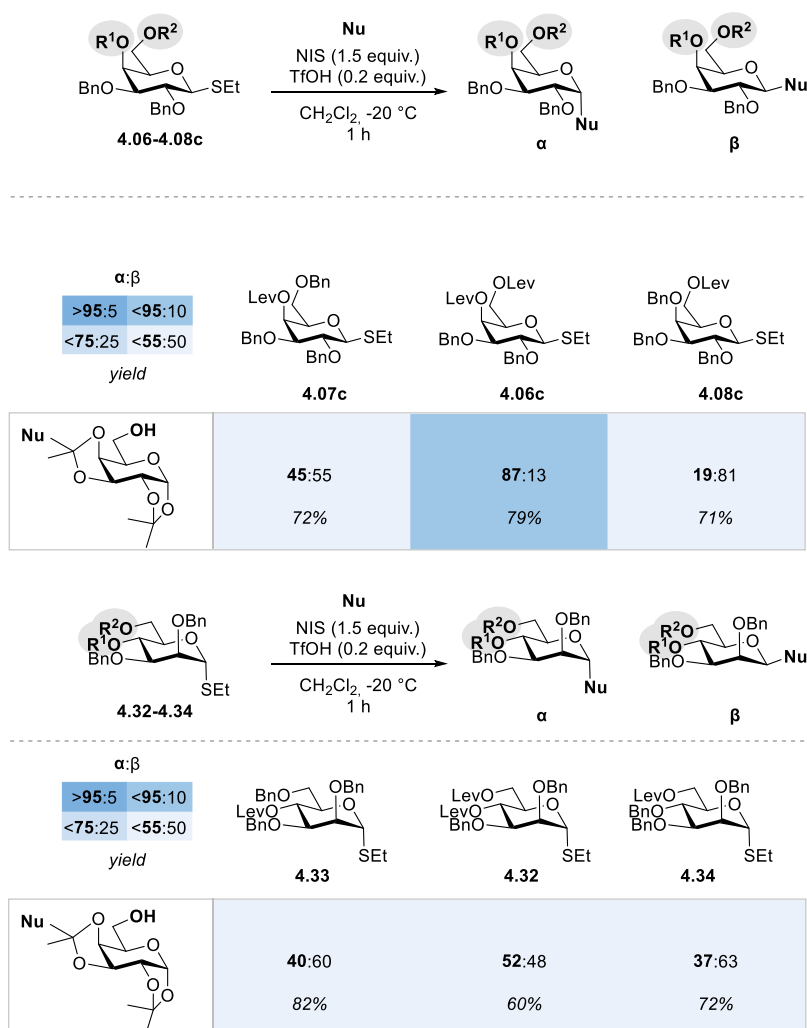
Figure 4.10. Glycosylation conditions of glycosyl galactose and mannose donors carrying Lev groups and stereochemical outcome of the glycosylation reactions of the respective donors.

β-Mannosides are highly unfavoured due to the anomeric effect that favours α-products. Previously developed methods for β-mannosylations are difficult to be applied in AGA as special reagents are needed and the biphasic reaction conditions are often not comparable to reactions that were optimized for solution phase. Solution phase β-mannosylation methods include for example Ag-silicate promoted glycosylations of α-halides, the use of chiral auxiliaries, inversions or intramolecular aglycone delivery.[92] Glycosylation results using remote participation for 1,2-*cis* selectivity, however, has proven in the past to be comparable to AGA-glycosylation results in the case of galactose and glucose.

Indeed, Lev mannose building blocks **4.32-4.34** show unusual low α-selectivity in glycosylations and slight β-selectivity (60% β-product for **4.33**). This supports the hypothesis that Lev substituted mannose building blocks undergo a different glycosylation mechanism than proposed for classical remote participation of acyl groups. The low α-selectivity for **4.07c** supposes that the carbonyl oxygen of the ester unit in Lev substituents does not participate and does not form a dioxolenium intermediate. The β-tendency of **4.33** and **4.34** even gave rise to the imagination of other modes of participation that might include a remote anchimeric assistance of the Lev-ketone. This has already been postulated for glucose before.[93] DFT calculations as well as cold-ion IR studies could give clarity on the mechanism and will help to further increase the interaction of the Lev group with the anomeric center in order to optimize the β-selectivity for mannosylations. Testing different protecting groups with ketone groups with different distances to the anomeric center would be a starting point for further studies.

4.2.4 Synthesis of Glucal and Galactal Building Blocks for Future Investigations

The Ferrier glycosylation of glucals and galactals is a special case of glycosylation reactions and usually yields 2,3-unsaturated glycosides (Scheme 4.8). The intermediate of the Ferrier glycosylation has recently been captured using cold-ion IR spectroscopy.[71]
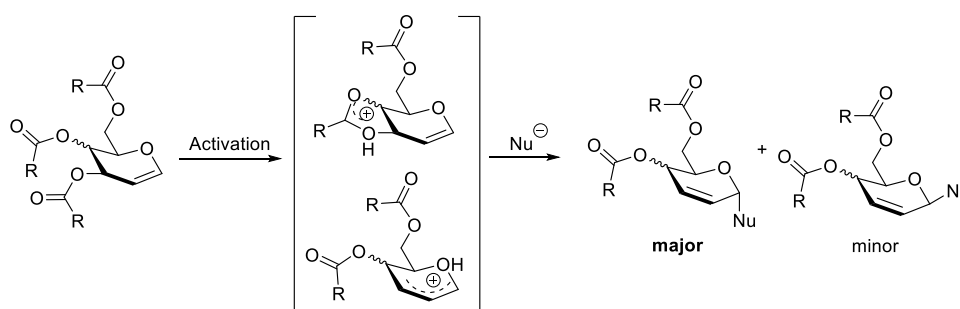
Scheme 4.8. Ferrier rearrangement reaction. Activation of the acylated glucal or galactal leads to Ferrier cations that can then be attacked by a nucleophile (Nu). R can be an electron withdrawing or electron donating substituent.

To better understand the mechanism and factors that influence the stereoselectivity of this reaction (mainly alpha for acetylated glucals and galactals), a series of glucals **4.42a-i** and

galactals **4.44a-i** were synthesized bearing electron withdrawing or electron donating substituents (Figure 4.11).

Conditions

a: PivCl, pyridine
b: TFAA, 4-DMAP, pyridine
c: LevOH, DIC, 4-DMAP
d: BnBr, NaH
e: Ac$_2$O, py
f: BzCl, py
g: p-nitrobenzoic acid, DIC, 4-DMAP
h: PFPCl, 4-DMAP, py
i: ClAcCl, py

	OPiv	OTFA	OLev	OBn	OAc
Glucal:	**4.42a** (55%)	**4.42b** (decomposed)	**4.42c** (70%)	**4.42d** (77%)	**4.42e** (77%)
Galactal:	**4.44a** (55%)	**4.44b** (decomposed)	**4.44c** (65%)	**4.44d** (84%)	**4.44e** (89%)

	OBz	OAcCl
Glucal:	**4.42f** (85%)	**4.42i** (87%)
Galactal:	**4.44f** (64%)	**4.44i** (49%)

4.42h (32%)
4.44h (45%)

4.42g (44%)
4.44g (54%)

Figure 4.11. Synthetic route to glucals **4.41a-i** and galactals **4.41a** with several different acyl and ether groups with EWGs and EDGs. More detailed reaction conditions are shown in the experimental section.

4.3 Conclusion and Outlook

Progress in the glycosciences is mainly limited by challenges in the stereoselective formation of 1,2-*cis* glycosidic linkages. Many relevant glycan structures bear 1,2-*cis* glycosidic linkages, such as several bacterial surface glycan components, that have immunogenic properties. A better understanding of the glycosylation mechanism and the investigation of intermediates open options to fine-tune the efficiency of remote participation in AGA. Here, the effect of electron density in ester or ether substituted monosaccharides was investigated, which included the synthesis of model building blocks, test reactions with sugar acceptors to determine the ratio between 1,2-*cis* and 1,2-*trans* linkages and the comparison of cold-ion IR spectra of the dioxolenium-type intermediates with DFT calculations.

The aim was to use mechanistic findings for the design of new 1,2-*cis* selective building blocks for AGA. This study on the effect of electron density in acyl protecting groups on the selectivity of glycosylations of galactose shows that Piv protecting groups increase the α-selectivity of glycosylation reactions. In opposite, electron withdrawing TFA groups deactivate

remote participation and therefore decrease the selectivity of galactosylations. It was also shown, that C4 substituents are responsible for remote participation in galactose and C6 substituents do not provide efficient remote participation.

On the other hand, it was found that ether substituents at C6-position in galactose result in higher α-selectivity than acyl substituents. Most likely, ether groups at C6-position of galactose are participating in a non-classical manner. This effect is independent from σ-donor or –acceptor substituents at the ether group as demonstrated for trifluoroethanol ether and (trimethylsilyl)methyl ether at C6-OH of galactose.

Furthermore, interesting β-selectivities for C6-OLev- and C4-OLev-subsituted mannose building blocks have been observed. This β-tendency gives rise to the imagination of other modes of participation that might include a remote anchimeric assistance of the Lev-ketone. Testing different protecting groups with ketone functionalities with different distances to the anomeric center, as well as cold-ion IR studies and DFT calculations would clarify the glycosylation mechanism of Lev-substituted building blocks.

This mechanistic insight will help in the future to design building blocks for the application in AGA. Guiding principles are provided to fine-tune the selectivity and efficiency of building blocks. This will help to improve the efficiency of the formation of 1,2-*cis* linkages in order to access oligosaccharides containing 1,2-*cis* linkages. The insights were used in the following Chapter to synthesize fragments of the LPS tetrasaccharide repeating unit of *P. gingivalis* by AGA.

5 Automated Synthesis and Investigation of the Lipopolysaccharide of *Porphyromonas Gingivalis*

5.1   Introduction

5.1.1   *Porphyromonas Gingivalis* – Characteristics and Virulence Factors

Porphyromonas gingivalis (P. gingivalis) is a Gram-negative, anaerobic, rod-shaped bacterium, that colonizes the oral epithelium and is an important component of subgingival microbiomes.[94] Besides *Tannerella forsythia* and *Treponema denticola*, it is part of the so called "red complex" that includes the main pathogens in the development of chronic periodontitis (CP). CP is an inflammatory disease in periodontal tissues that can induce destruction of periodontal tissue, and alveolar bone and tooth loss.[95] Dental plaque, a biofilm formed by aggregation of various microorganisms, is an important factor for the development of periodontal disease. Colonization by *P. gingivalis* causes changes in the subgingival microbiota, which results in dysbiosis, causing bacterial imbalances and exacerbating inflammation.[96]

P. gingivalis has developed survival strategies throughout its evolution. This includes the ability to engineer its environment and modify the host's immune response in order to persist in host tissues. These mechanisms include the alteration of signaling pathways of inflammation, the complement system, the cell cycle, apoptosis, as well as the interaction with various host receptors.[97] Studies have demonstrated that *P. gingivalis* strains vary in their virulence, with some strains being classified as virulent, e.g. strains W50, ATCC 49417 and A7A1 and others being classified as avirulent, e.g. strains 381, 33277 and 23A4. W50 is worldwide the most common type of *P. gingivalis*.[98]

Among surface components of the bacterial envelope, polysaccharides such as the K-antigen (capsule) and the lipopolysaccharide (LPS) are essential for virulence and immunogenicity of *P. gingivalis.*[99] The main virulence factors include its own structural components (lipopolysaccharide (LPS), fimbriae, heat shock proteins) and secretory components (gingipains and outer membrane vesicles).

Fimbriae are crucial for binding to eukaryotic cells and other species of bacteria, e.g. for biofilm formation.[100] The heat shock protein 60 of *P. gingivalis* is remarkably immunogenic and is critically connected to *P. gingivalis*-induced autoimmune diseases.[101] Gingipains (lysine-gingipain (Kgp) and arginine-gingipain (Rgp)) are a group of proteases. Gingipains play essential roles in host colonization, defense deactivation, tissue destruction and nutrient acquisition. The LPS can trigger the innate immune response *via* activation of Toll-like receptors.[102]

Outer membrane vesicles of *P. gingivalis* (Figure 5.1) are enriched in many virulence factors including the LPS and proteins such as well-studied gingipains and the peptidyl-arginine deiminase (PPAD). Outer membrane vesicles participate in biofilm development, host

interaction, colonization, and immune defense evasion.[103] They are double-layer spherical membrane-like structures with a diameter of about 50-250 nm and due to their size, they can easily penetrate deep tissues compared to the parent bacterium. They are released into the hosts tissue and can be internalized into host-cells.[104]
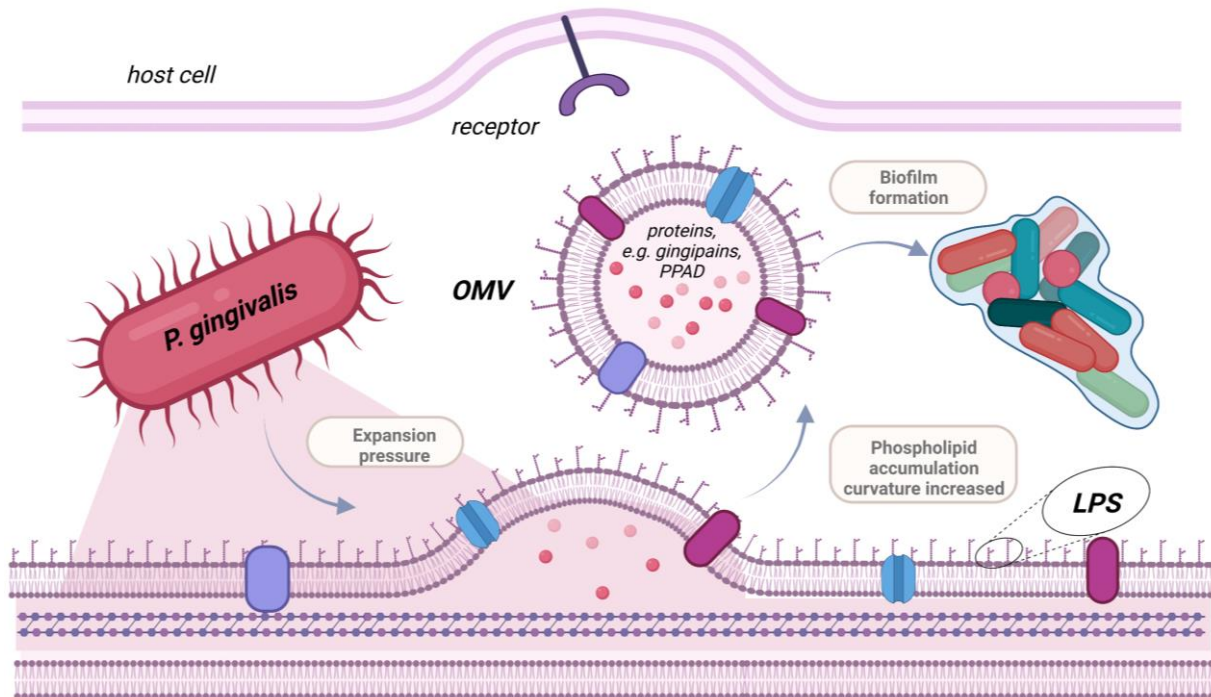
Figure 5.1. Schematic representation of the *P. gingivalis* outer and inner membrane, production of outer membrane vesicles (OMVs) and their interaction to other bacteria as well as host cells. Modified from *Front. Cell. Infect. Microbiol.* **2021**, *10*. [103b]

5.1.2 Porphyromonas Gingivalis and Systemic Diseases

Periodontal diseases are very prevalent and constitute a major public health problem. According to the World Health Organization, 10-15% of adults worldwide suffer from severe periodontal diseases.[105] Moreover, a relationship between periodontal and systemic disease has been increasingly described in the literature - starting in 1900 with mainly clinical experience reported by the British Doctor William Hunter[106], later supported by epidemiological studies as well as *in vitro* and animal model experiments.[94b, 107] Regarding the described connection to systemic diseases, periodontal disease has immense social impact and poses a huge challenge towards global health care. Since *P. gingivalis* is the major cause for periodontal diseases[95], it is an important target in research on systemic diseases. Therefore, a significant amount of research and extensive analysis of *P. gingivalis* over the past decades resulted in evidence of its role in atherosclerosis, Alzheimer's disease, rheumatoid arthritis, cancer, diabetes and adverse pregnancy outcomes.[94b]

The ability of *P. gingivalis* to travel to distant sites might participate in *P. gingivalis*-associated systemic disorder. *P. gingivalis* in local periodontal tissue can enter the vasculature through ulcerated epithelium and lymph vessels by brushing and chewing.[108] This was indicated by the detection of *P. gingivalis* in synovial fluid and plasma[109] as well as by isolation of *P. gingivalis* from human atherosclerotic plaque tissues, mouse lungs, human Alzheimer's brains, aortic endothelial cells, pancreatic tumor cells and human myeloid dendritic cells. Periodontal bacteria also have been found in cardiovascular disease plaques and the detection rate of *P. gingivalis* has been 100%.[110]

Atherosclerosis

Epidemiologic evidence has suggested that CP is a risk factor for cardiovascular diseases. Cardiovascular diseases, including atherosclerosis, myocardial infarction, abdominal aortic aneurysms, and hypertension involve the heart and blood vessels. They are the most common cause of death throughout the world.[94b, 111] The relationship between *P. gingivalis* and cardiovascular diseases has been deeply studied and especially in the case of atherosclerosis significant evidence and possible mechanisms have been found. The pathological basis of atherosclerosis is the progressive accumulation of mainly lipids, calcium, and macrophages at the artery wall. The pathogenesis mechanisms of atherosclerosis are complex, including the activation of endothelial cells and platelets, recruitment of leukocytes, migration and proliferation of smooth muscle cells, and formation of a lipid core, along with thrombosis and plaque instability. *P. gingivalis* can affect the function of all these cells.[94b]

Alzheimer's Disease

Alzheimer's disease (AD), the most common type of dementia, is a chronic neurodegenerative disease where patients suffer from progressive memory loss, disorientation and cognitive performance deficits.[112] The number of dementia cases is projected to reach more than 140 million by 2050 and thus AD is a major challenge for global health and social care.[113] Until now, the current understanding of AD pathogenesis is limited, which hinders efficient treatment and prevention. However, epidemiological studies, animal experiments and other evidence have strengthened support for the possible relevance of *P. gingivalis* in AD pathogenesis. For example, DNA, LPS and gingipains of *P. gingivalis* have been identified in AD brains and oral *P. gingivalis* infection in mice resulted in an increased production of amyloid-β_{1-42} ($A\beta_{1-42}$) plaques.[110f] The pathology of AD is based on Aβ plaques, neurofibrillary tangles and microglia-mediated neuroinflammation. Studies suggest, that infection with *P. gingivalis* can lead to direct disruption of the blood-brain barrier, or bacteria find leaky regions without a blood-brain barrier, invade peripheric nerves or invade immune cells followed by brain recruitment and finally enter into the brain causing neuroinflammation.[114] In addition to the direct role of *P. gingivalis*, the release of inflammatory molecules from infected host cells,

such as a set of cytokines and their immune response may also be involved in AD pathogenesis. Another theory is the suppression of the host's adaptive immune system, which could allow *P. gingivalis* to prevent the entry of immune cells into the brain, or an increased blood-brain barrier permeability, or the inhibition of the local IFN-γ response.[94b, 115]

Rheumatoid Arthritis

Another connection of *P. gingivalis* infection was found to rheumatoid arthritis as different animal models revealed that *P. gingivalis* increased the incidence and progression of rheumatoid arthritis.[116] Furthermore, a meta-analysis found higher rheumatoid arthritis prevalence in periodontitis patients[117] and non-surgical periodontal therapy in individuals with rheumatoid arthritis and CP was associated with improvements of disease activity in rheumatoid arthritis.[94b, 118] One of the pathological bases of rheumatoid arthritis are autoantibodies against citrullinated proteins. *P. gingivalis* is the only microorganism known, which expresses peptidyl-arginine deiminase (PPAD) – an enzyme that carries out the conversion of arginine into citrulline (Scheme 5.1).
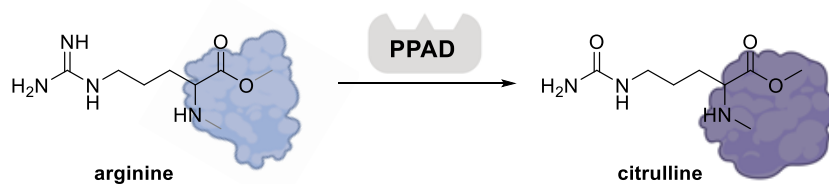
Scheme 5.1. Possible cause of rheumatoid arthritis by the expression of peptidyl-arginine deiminase (PAD) that induces the conversion of arginine into citrulline.

5.1.3   Strategies for Controlling Porphyromonas Gingivalis

The current CP control measures heavily rely on the mechanical removal of dental plaque, which disrupts the disease-triggering dysbiotic biofilm. This includes toothbrushing, interdental cleaning, frequent professional dental cleaning, but also pocket reduction surgery, regenerative surgery, laser therapy and local or systemic antimicrobials.[119]

Many researchers try to explore whether controlling *P. gingivalis* can be a potential treatment of systemic diseases (Figure 5.2). Proposed approaches include broad-spectrum antibiotics and specific inhibitors. Doxycycline and metronidazole resulted in significant reduction in atherosclerotic lesions in mice.[120] Small molecule gingipain inhibitors have been found to block gingipain-induced neurodegeneration, suggesting that it could be used to treat *P. gingivalis* brain colonization and neurodegeneration in AD.[110f, 121]

However, pre-immunization could reduce the ability of the bacteria to translocate to remote tissues. For a successful periodontal vaccine, immunity in the oral cavity should be

induced, which is difficult with traditional vaccination methods. Advances in mucosal vaccination strategies might give the option for periodontal disease control.[122] The intranasal route is a major mucosal route and the nasal influenza vaccine was the pioneering application in humans.[123] Sublingual immunization with a recombinant vaccine that contains *P. gingivalis* heat shock protein 60 or nasal immunization with outer membrane vesicles prior to *P. gingivalis* injection significantly reduced arteriosclerotic lesions in mice.[124] The nasal immunization with outer membrane vesicles in mice resulted in the detection of a significant increase in *P. gingivalis* specific IgA in the nasal lavage fluid and saliva of mice, as well as serum IgG and IgA.[122d] Among the mentioned encouraging results, it is of high interest to provide novel therapeutic strategies for systemic diseases caused by *P. gingivalis* and many studies are ongoing.
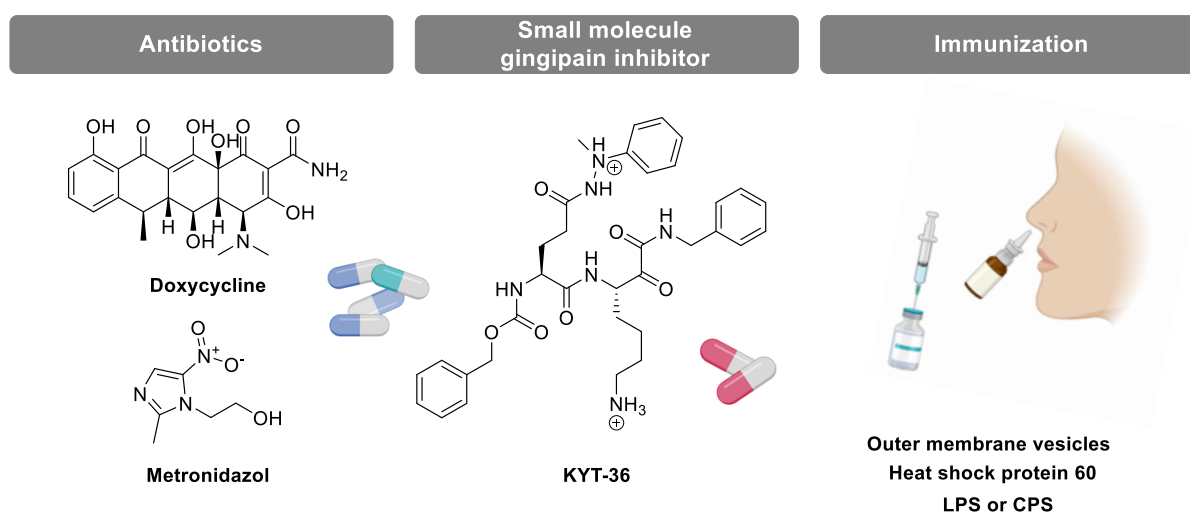
Figure 5.2. Overview of proposed approaches for the control of *P. gingivalis*, including antibiotics, small molecule gingipain inhibitors and mucosal immunization.

5.1.4 The LPS of Porphyromonas Gingivalis: A Potential Vaccine Candidate

The peptidoglycan layer of gram-negative bacteria, such as *P. gingivalis*, is surrounded by an outer membrane (Figure 5.1). Generally, miscellaneous surface exposed molecules on intact bacteria are of medicinal interest, as they can activate the hosts immune system. Gram-negative bacteria additionally release outer membrane vesicles that contain components from the outer membrane, such as the LPS, but also the underlying periplasm. Those outer membrane vesicles can be internalized into host cells. After lysis of the outer membrane vesicle, various antigens from the outer membrane and the underlying periplasm may be processed by antigen-presenting cells leading to the induction of an adaptive immune response including *P. gingivalis*-specific antibody production.[125]

The LPS is the major component of the outer bacterial membrane. It is a complex glycolipid that is composed of three covalently linked domains (Figure 5.3): The lipid A or

endotoxin, the central oligosaccharide core and the O-antigen, which is the most external part of this molecule.[126] The glycan part in the O-antigen (O-LPS) of *P. gingivalis* W50 is built from the tetrasaccharide repeating sequence [→6)-α-D-Glcp-(1→4)-α-L-Rhap-(1→3)-β-D-GalNAc-(1→3)-α-D-Galp-(1→] and bears a monophosphoethanolamine residue at position C2 of the α-rhamnose in a nonstoichiometric (approximately 60%) amount (Figure 5.3).[127] The LPS of *P. gingivalis* is a significant antigen in periodontitis patients, which offers opportunities for the development of a carbohydrate-based conjugate vaccine.[128]
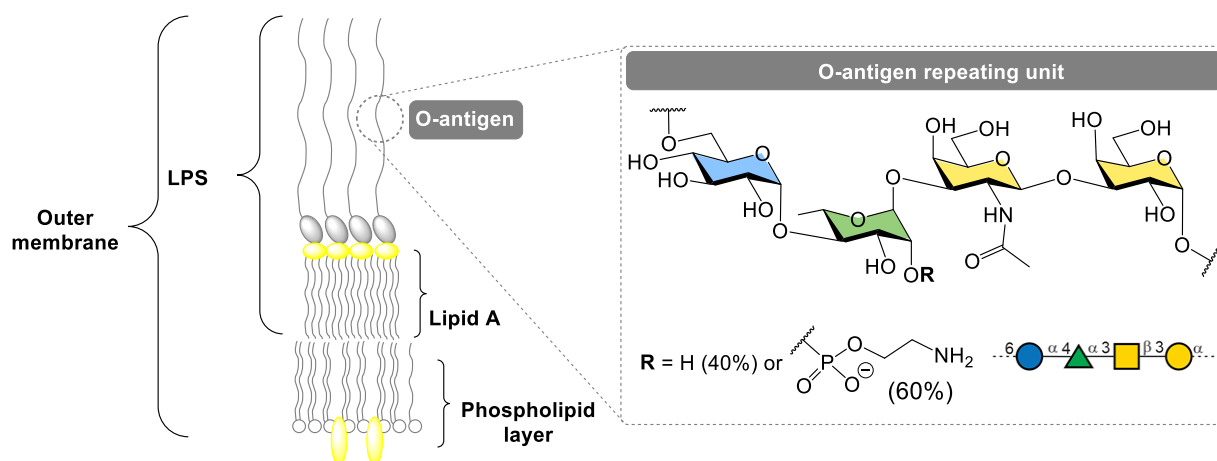
Figure 5.3. Schematic representation of the outer membrane and chemical structure of the O-antigen repeating unit of *P. gingivalis* LPS (W50 strain).

5.1.5   Project Aim

As described in Chapter 4, the main reason for challenges in the synthesis of carbohydrates is the stereocontrol of glycosylation reactions. Especially the formation of 1,2-*cis* glycosidic linkages in AGA remains challenging. However, an efficient synthesis of the tetrasaccharide repeating unit in the LPS of *P. gingivalis* requires stereocontrol, because two of the four units are connected *via* 1,2-*cis*-glycosidic linkages. Here, the stereoselective synthesis in AGA of LPS fragments is described as well as the identification of a potential vaccine candidate using glycan microarray studies. Saliva and serum of periodontitis patients as well as dental healthy or treated periodontitis patients are investigated for IgG and IgA antibodies that bind to fragments of the LPS of *P. gingivalis*. Antibody-binding glycans have the potential for improving the understanding of the interaction of *P. gingivalis* with the human immune system and for the development of a vaccine against *P. gingivalis*. This would not only have an impact on the development of millions of periodontitis cases, but also according to recent studies, on the development of systemic diseases such as rheumatoid arthritis, atherosclerosis and Alzheimer's disease.

5.2 Results

5.2.1 Design and Synthesis of the Building Blocks for the LPS Repeating Unit

The synthesis of a library of different fragments of the LPS of *P. gingivalis* is important for the systematic investigation of its biological and immunological roles. The importance of the order of glycans in the LPS repeating unit and the antibody-binding to specific fragments has not yet been researched. Therefore, the synthesis of many LPS glycan parts is important for further high throughput screenings on antibody binding using glycan microarray studies. AGA is the method of choice for the library synthesis, because many defined glycan fragments with the same glycosylation pattern are desired. AGA provides a tool for the fast and reliable synthesis of many similar conjugation-ready structures as soon as the ideal coupling conditions of a specific building block are identified.
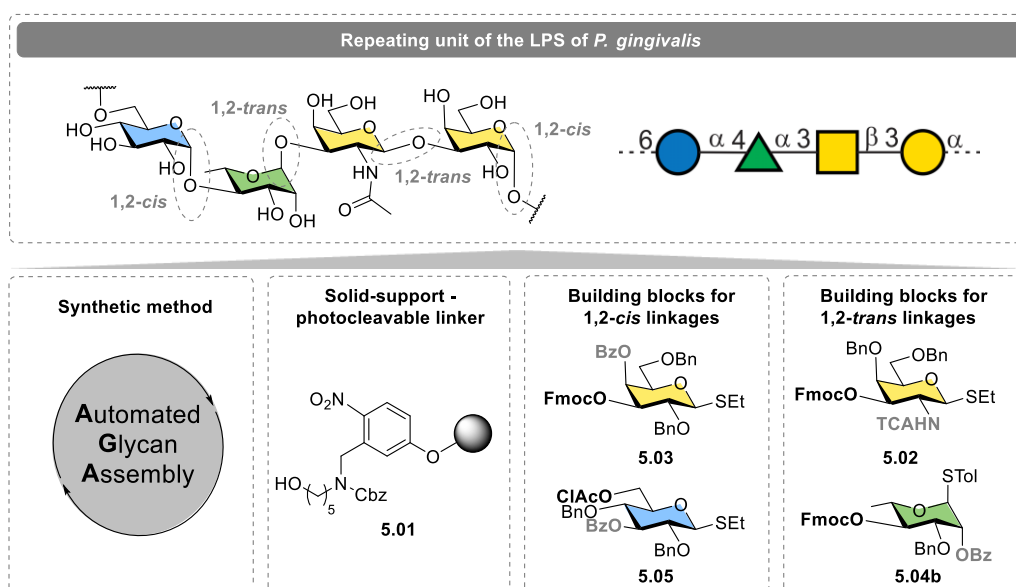
Figure 5.4. Strategy for the synthesis of conjugation-ready LPS fragments of *P. gingivalis* in AGA using building blocks **5.02-5.05** and solid-support **5.01**. Participating groups for stereocontrol are highlighted in **grey**.

A retrosynthetic analysis was performed on conjugation-ready tetrasaccharide combinations of the repeating unit of the LPS of *P. gingivalis*. This resulted in a strategy using building blocks **5.02-5.05** and the Merrifield resin **5.01** equipped with a photo-cleavable aminopentanol linker in AGA (Figure 5.4). In general, Fmoc was chosen as a temporary protecting group for chain elongation due to its efficient standard deprotection in AGA as described in Chapter 3. The trichloroacetyl (TCA) group at C2-amine in commercial GalNAc building block **5.02** and the benzoyl ester at C2-OH in rhamnose building block **5.04b** were chosen to ensure the stereoselective formation of 1,2-*trans* linkages taking advantage of neighboring group participation.

Previous studies by our group demonstrated that starch and amylose polysaccharides can be efficiently assembled with high *cis*-selectivity, if the glucose building block had a

benzoyl protecting group at C3-OH.[10] Cold-ion IR studies[129] as well as studies in Chapter 4 support that high *cis*-selectivity can be achieved for galactose building blocks with an acyl group at C4-OH. Therefore, the stereoselective formation of 1,2-*cis* linkages in galactose and glucose was planned to be ensured by remote participation of the benzoyl group at C4-OH in galactose building block **5.03** and at C3-OH in glucose building block **5.05**. Benzoyl esters were generally chosen for remote participation, as they are easy to remove in post-synthesis methanolysis. In addidtion, migration rearrangement is less likely compared to acetyl esters.

Galactose building block 5.03

The synthetic route to galactose building block **5.03** (Scheme 5.2) relies on the regioselective introduction of a temporary protecting group at C3-OH (Fmoc) and a remote participating ester group at C4-OH (benzoyl). Starting from commercial benzylidene protected building block **5.07**, NAP was regioselectively introduced at C3-OH *via* a stannylene ketal intermediate that enhances the nucleophilicity of C3-oxygen, followed by benzylation of C2-oxygen in a WILLIAMSON ether synthesis to give **5.08**. Regioselective ring opening was achieved using triethylsilane, trifluoracetic acid and trifluoracetic anhydride taking advantage of the sterical hinderance at the C4-*O*-benzyl cation intermediate that cannot be reduced by bulky triethylsilane and the easily accessible C6-*O*-benzyl cation intermediate[130] formed by the initial acid complexation with C4-oxygen. Protection of the free C4-OH resulted in **5.09**. Treatment with DDQ and subsequent Fmoc protection afforded target building block **5.03** (seven steps, overall yield 77%).
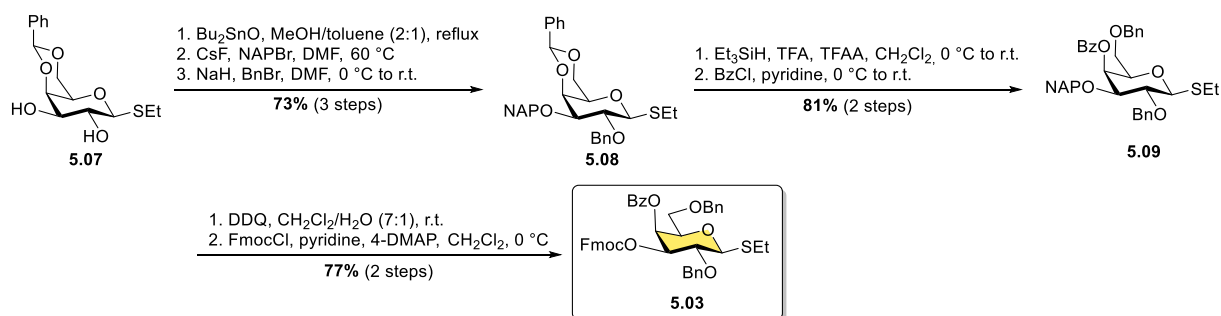
Scheme 5.2. Synthetic route to α-galactose building block **5.03**. More detailed reaction conditions are shown in the experimental section.

Rhamnose building blocks 5.04a and 5.04b

The synthesis of rhamnose building blocks **5.04a** and **5.04b** (Scheme 5.3) requires the introduction of the temporary Fmoc protecting group at C4-OH position as well as a participating ester group at C2-OH. Here, a benzoyl group was chosen for building block **5.04b** or a Lev group that would further allow branching or functionalization at C2-OH in the case of building block **5.04a**. The synthesis of both building blocks **5.04a-b** started from peracetylated rhamnose **5.10** followed by thioglycosylation and ester methanolysis resulting in **5.11**. The 2,3-*cis*-hydroxyl groups were selectively protected with the isopropylidene protecting group

followed by the introduction of the NAP group at C4-OH by Williamson ether synthesis giving **5.12**. The isopropylidine group was hydrolyzed and the benzyl group was regioselectively introduced at C3-OH *via* a stannylene ketal intermediate that enhances the reactivity of the equatorial oxygen. The C2-OH atom was esterificated using levulinic acid under Steglich conditions or benzoyl chloride followed by oxidative NAP cleavage using DDQ and subsequent Fmoc protection to provide target building block **5.04a** (10 steps, overall yield 87%) or **5.04b** (ten steps, overall yield 89%).
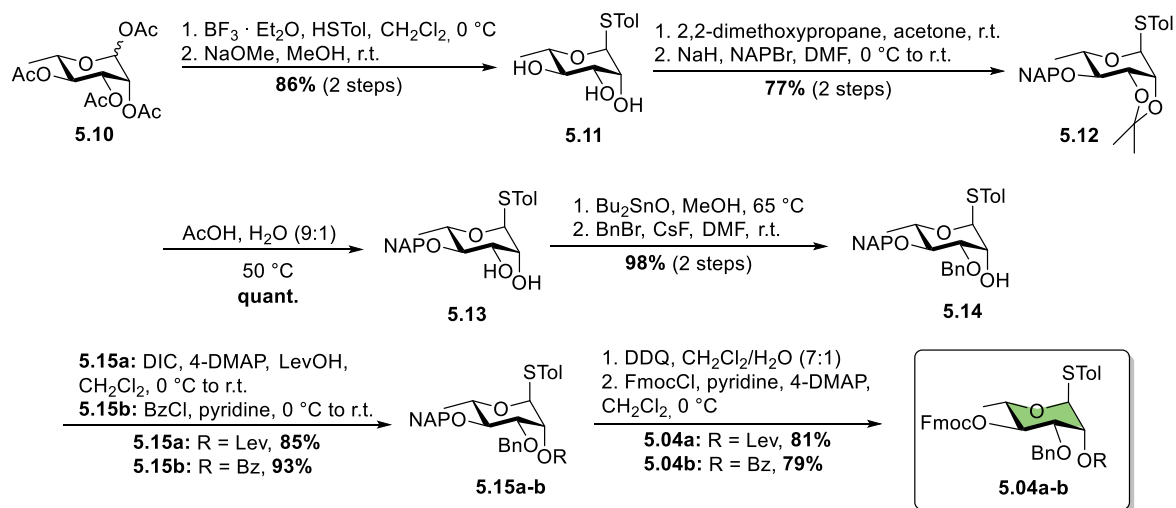
Scheme 5.3. Synthetic route to rhamnose building block **5.04a** and **5.04b**. More detailed reaction conditions are shown in the experimental section.

Glucose building block 5.05

The synthetic route for glucose building block **5.05** (Scheme 5.4) relies on the regioselective introduction of a temporary protecting group at C6-OH (ClAc) and a remote participating ester group at C3-OH (benzoyl).
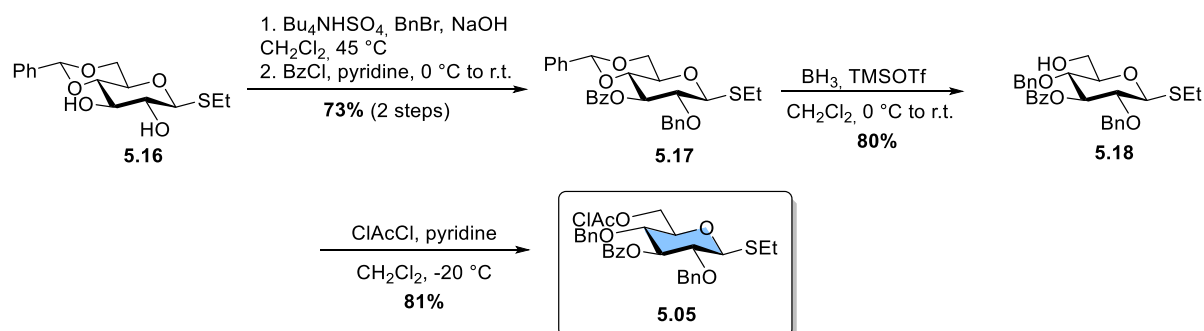
Scheme 5.4. Synthetic route to α-glucose building block **5.05**. More detailed reaction conditions are shown in the experimental section.

Starting from commercial benzylidene protected building block **5.16**, a benzyl group was selectively installed at the C2-OH position. For that, a limited amount of alkylating benzyl bromide was used with sodium hydroxide as a base and tetrabutylammonium hydrogen sulfate as a phase-transfer catalyst. Similar to mannose building block **3.02** in Chapter 3, the

selectivity is mainly based on the high acidity of C2-OH as well as steric hindrance at C3-OH by the benzylidene protecting group.[56] Subsequently, the benzoyl group was installed at C3-OH using benzoyl chloride followed by selective ring opening of the benzylidene unit by using BH_3 and TMSOTf. Then, the C6-OH group was esterificated using chloroacetyl chloride giving glucose building block **5.05** (four steps, overall yield 78%).

5.2.2 Automated Glycan Assembly of LPS Fragments

The set of building blocks **5.02-5.05** and Merrifield resin **5.01** were used in AGA to get access to different arrangements of the LPS glycan sequence of *P. gingivalis*. A library of conjugation-ready parts of the LPS of *P. gingivalis* **LPS1-11** (Scheme 5.5) was synthesized according to the strategy described in Figure 5.4 in order to identify its immunogenic epitope. This includes four tetrasaccharide combinations **LPS1-4**, as well as tri-, di- and monosaccharide structural fragments **LPS5-11**.
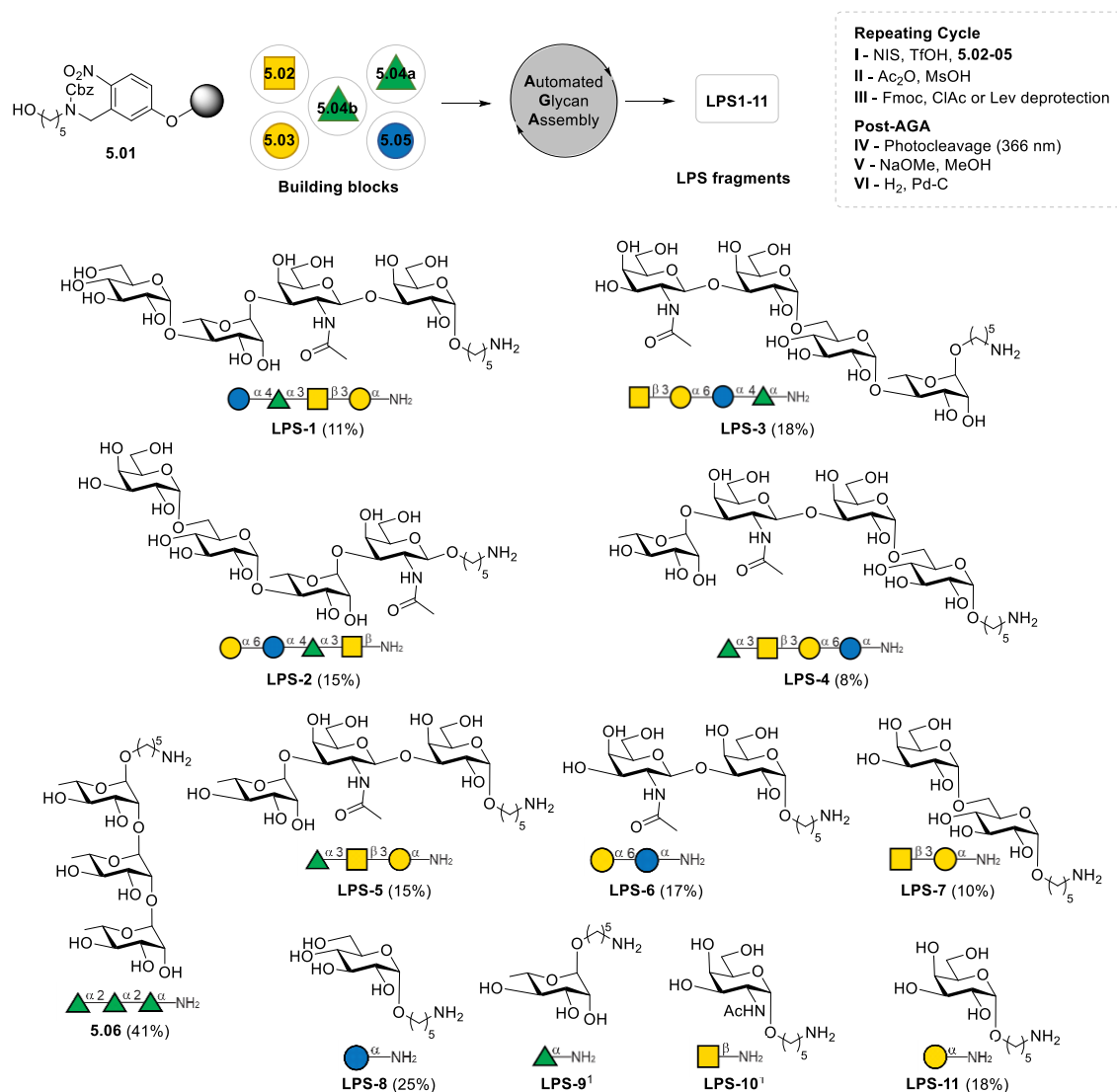
Scheme 5.5. AGA of conjugation-ready parts of the LPS of *P. gingivalis* **LPS1-11** (yield) and rhamnose structure **5.06** for comparison. Detailed coupling conditions (**I**) are described in Table 5.1. [1]**LPS-9** and **LPS-10** were obtained from the glycan base of the Max Planck Institute. More detailed reaction conditions are shown in the experimental section.

Automated Glycan Assembly Cycles and Post-AGA

As soon as the ideal coupling conditions of a specific building block are identified, a large number of combinatorial fragments of polysaccharides can be synthesized using AGA. Previous studies[131] have shown that galactose and galactosamine building blocks for example exhibit very low activation temperatures and give better performance at those temperatures. Therefore, galactose building block **5.03** and *N*-acetylgalactosamine building block **5.02** provided good coupling results starting at -40 °C, while glucose **5.05** and rhamnose **5.04a-b** were less reactive and gave good coupling results starting at -20 °C with a longer reaction time at 0 °C. Glycosylation conditions summarized in Table 5.1 provided optimal performance of synthesized building blocks **5.02-5.05** in AGA.

Table 5.1. Optimized glycosylation conditions of building blocks **5.02-5.05** for AGA.

Building block	t_1 (min)	T_1 (°C)	t_2 (min)	T_2 (°C)
Galactose **5.03**	10	-40	50	-10
*N-A*cetylgalactosamine **5.02**	30	-40	20	-20
Rhamnose **5.04a-b**	10	-20	30	0
Glucose **5.05**	5	-20	30	0

The main limiting factor of the LPS library synthesis is *N*-acetylgalactosamine building block **5.02**. It is very sensitive to factors such as temperature, humidity and stability of the glycosidic bond. Therefore, the reproducibility of an efficient coupling is problematic. The change to a phosphate leaving group did not increase the coupling efficiency, while double to triple glycosylation cycles enabled the reliable coupling of **5.02** up to the tetrasaccharide stage. Also, couplings of C3-OH at galactose and galactosamine are known to be challenging due to the sterical hindrance by groups at the axial C4-position.[132] Double deprotection cycles after the coupling of galactose **5.03** or galactoseamine **5.02** were required to achieve full deprotection of the Fmoc group followed by double glycosylation cycles of the respective 1,3-coupled building block. Further deprotections (Lev at **5.04a**, ClAc at **5.05** and Fmoc at **5.04a-b**) as well as capping steps, photo-cleavage from solid-support and global deprotection followed standard procedures[133] previously reported. Following the optimized glycosylation conditions and the described peculiarities, **LPS1-11** were synthesized in common AGA-yields (8-25%).

Stereoselectivity of α-Galactose Building Block 5.03 and α-Glucose Building Block 5.05

The TCA group at C2-amine in commercial GalNAc building block **5.02** and the benzoyl ester or the Lev ester at C2-OH in rhamnose building block **5.04a/b** ensured the stereoselective formation of 1,2-*trans* linkages taking advantage of neighboring group participation. This resulted in excellent stereocontrolled formation of Rha-α(1→3) and GalNAc-β(1→3) linkages.

The stereoselective formation of 1,2-*cis* linkages in galactose was systematically investigated in Chapter 4 as well as previous cold-ion IR studies[129]. In the context of Chapter 4 developed building block **4.12** was employed to the synthesis of the LPS fragments in AGA and gave excellent *cis*-stereoselectivity to soft sugar acceptors and high *cis*-stereoselectivity when coupled to the primary alcohol nucleophile of the aminopentanol linker (α/β 9:1). However, post-AGA removal of the Piv group using methanolysis conditions (NaOMe, MeOH in CH_2Cl_2) was not completed after a reasonable time (Scheme 5.6). The three methyl groups at the Piv group sterically hinder the nucleophilic attack of the methoxide, which causes a very slow deprotection of the Piv group. In contrast, benzoyl building block **5.03** resulted in excellent *cis*-stereoselectivity in glycosylations with soft sugar acceptors, but lower *cis*-selectivity (α/β 4:1) when coupled to the linker alcohol. However, the efficient deprotection (2 h) of the benzoyl group under methanolysis conditions rationalize the preferred use of **5.03**.
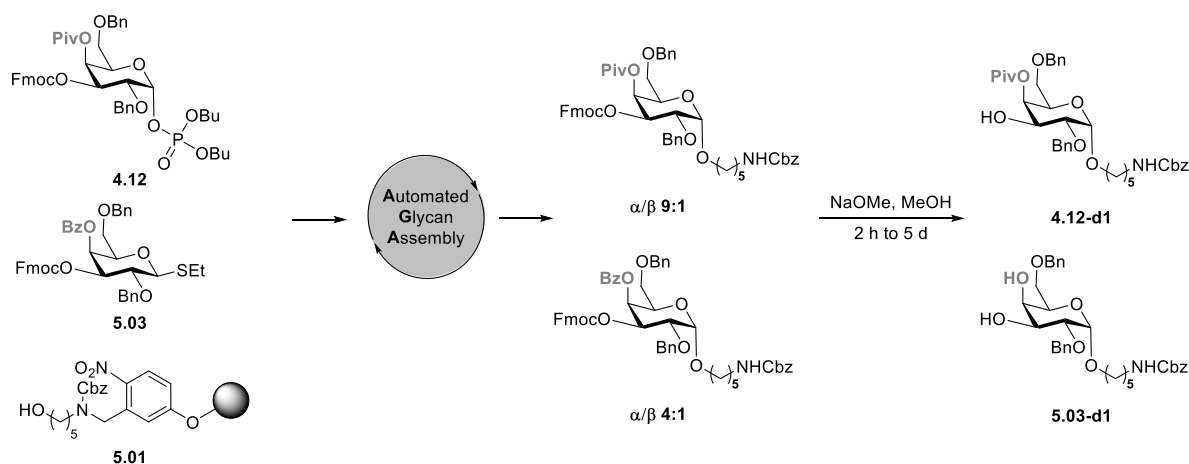
Scheme 5.6. Piv building block **4.12** vs. Bz building block **5.03** for the stereoselective formation of *cis*-linkages and following methanolysis. More detailed reaction conditions are shown in the experimental section.

The stereoselective formation of 1,2-*cis* linkages in glucose was enabled by remote participation of the benzoyl group[10] at C3 in glucose building block **5.05** that I developed. Glucose building block **5.05** gives excellent *cis*-stereoselectivity for soft sugar acceptors (α-only) as well as for the hard aminopentanol nucleophile (α/β 20:1).

Generally, α-glucose building block **5.05** as well as α-galactose building block **5.03** provide excellent *cis*-stereoselectivity when used as a donor for soft sugar nucleophiles. The yield of the LPS fragment synthesis is reduced when those building blocks needed to be

directly coupled to the aminopentanol linker, because total *cis*-stereoselectivity could not be achieved for both building blocks. However, the retention time in RP-HPLC of the isomers directly coupled to the linker are significantly different so that the isolation of the α-isomer after the synthesis was ensured (Figure 5.5).
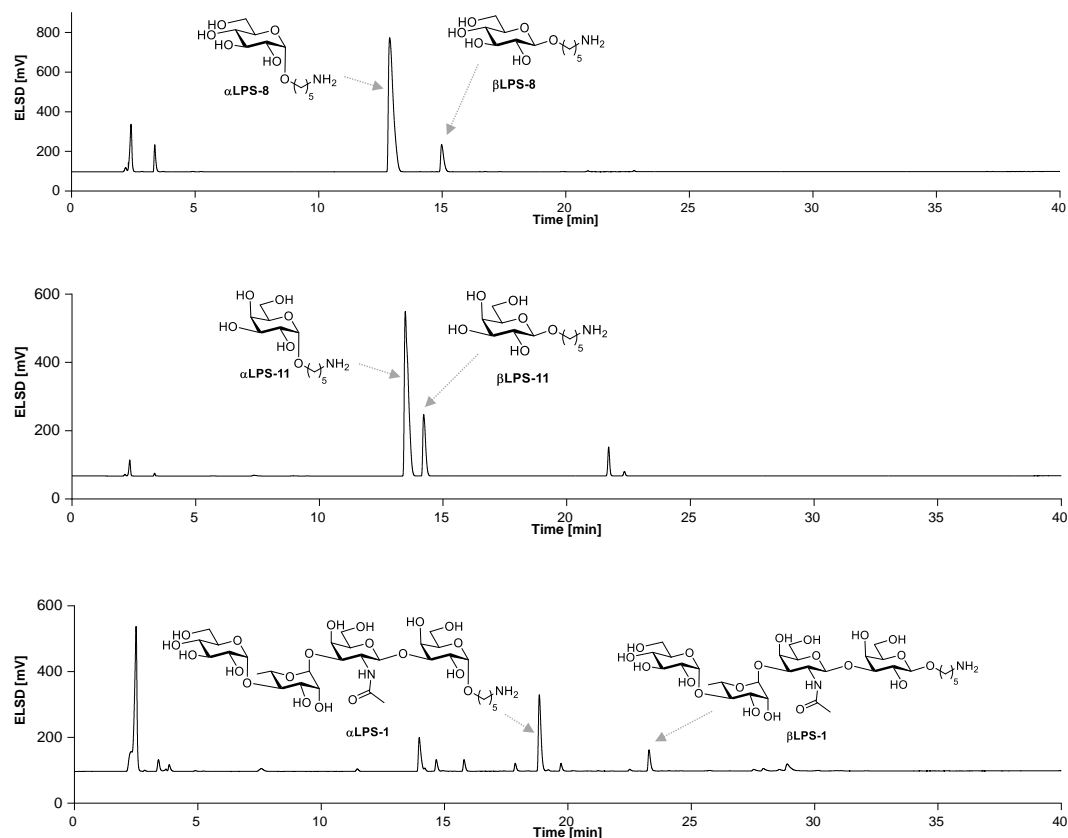
Figure 5.5. Crude RP-HPLC ELSD signals show exemplarily the *cis*-stereoselectivity of building block **5.03** and **5.05** to the linker and sugar nucleophiles. The β-isomer, when coupled to the linker, provides significantly longer retention times allowing for purification.

The purity and the correct stereochemistry at the anomeric center is shown in Figure 5.6 for the tetrasaccharides **LPS1-4**. Coupled ^{1}H, ^{13}C NMR spectroscopy proofs the three α-linkages at rhamnose, glucose and galactose ($^1J_{CH}$ 170 to 175) and the single β-linkage at galactosamine ($^1J_{CH}$ 161 to 165).
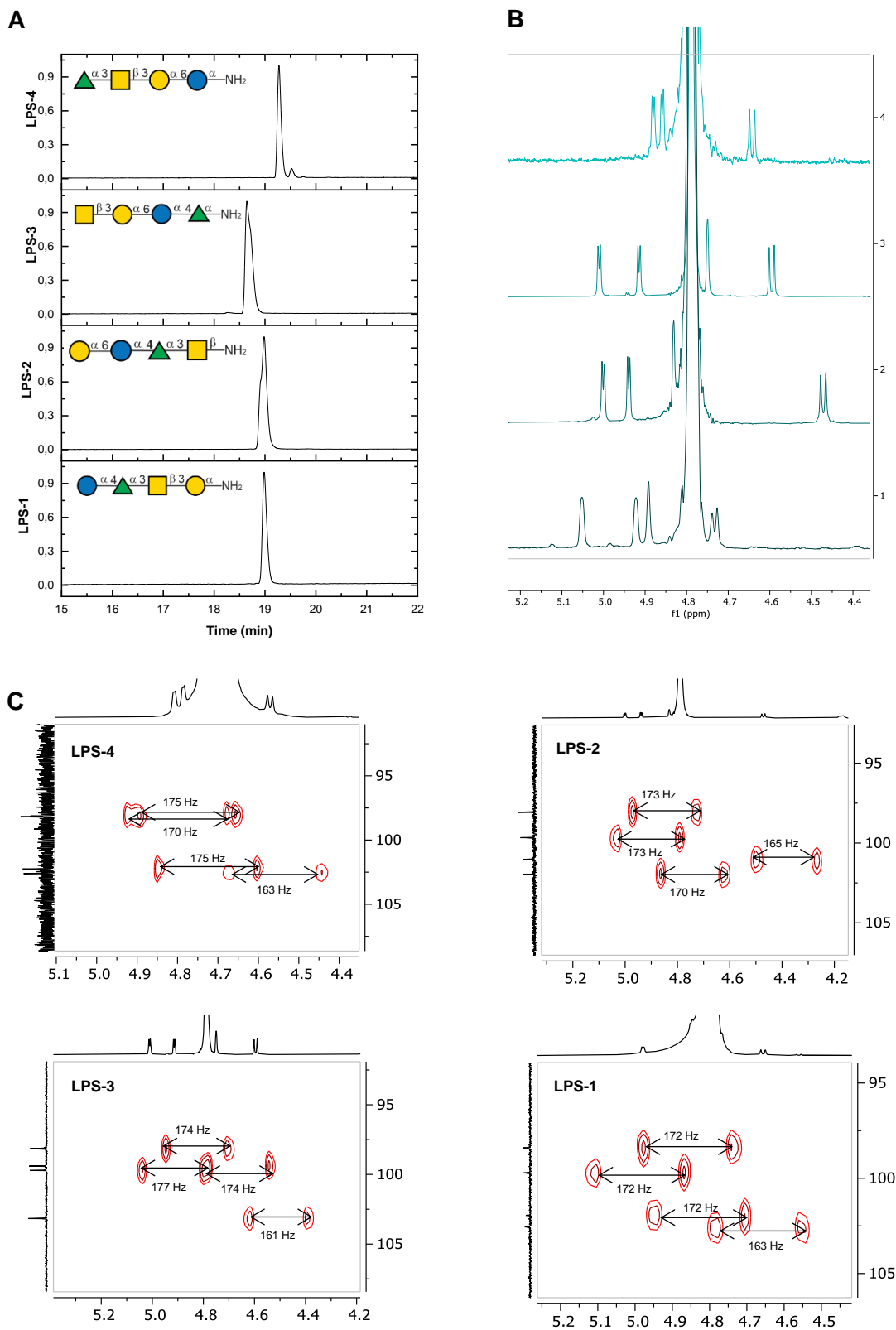
Figure 5.6. Extract from the normalized ELSD signals of the purified tetrasaccharide **LPS1-4** (**A**) and anomeric region of the ^{1}H NMR spectra of the purified tetrasaccharides **LPS1-4** (**B**) showing the different retention times and chemical shifts as well as confirming the purity of each glycan structure. (**C**) Extract from the coupled ^{1}H, ^{13}C NMR spectra (axis in ppm) of the anomeric region of the synthesized tetrasaccharides **LPS1-4** proving the desired stereochemistry.

5.2.3 Glycan Microarray Studies

The rapid synthesis of a library of LPS fragments by AGA in combination with following high throughput glycan microarray studies is a fast and efficient tool to identify an active epitope. The determination of the active epitope is essential for the design of conjugate vaccines, because the identified antigen will be responsible for the generation of specific antibodies after immunization in order to produce a protective immune response. In previous studies[122d], *P. gingivalis* infected patients showed to form IgG and IgA antibodies in blood and saliva against pathogen-specific antigens.

Here, human sera and saliva from *P. gingivalis* infected patients were used to screen antibodies against the synthetic glycan library **LPS1-11** to determine whether LPS fragments are potential leads for vaccine development. Samples were taken from a pool of patients at the Charité Zahnklinik (provided by Prof. Dr. Henrik Dommisch). The dental status of three groups of patients was defined as: healthy (20 patients, no clinical indications for CP), infected (16 patients, CP stage III or stage IV[134]) and recovered from CP (six patients). Recovered patients were treated from CP stage III or stage IV at the Charité Zahnklinik by resective and regenerative surgery and execution of two to four professional dental cleanings per year. While *P. gingivalis* was identified in the dental plaque of all patients, the bacterial amount was generally higher for chronical periodontitis patients (mean(cT) of 18.52) and recovered patients (mean(cT) of 21.70) compared to healthy individuals (mean(cT) of 24.71, Table 5.2).

Table 5.2. CT values (PCR) of the three patient groups (dental healthy, chronical periodontitis and recovered from chronical periodontitis). Patients with outlaying high antibody-binding in microarray studies are marked in *orange*.

Dental status: Healthy		Dental status: CP		Dental status: Recovered from CP	
Mean(cT) = 24.71		Mean(cT) = 18.52		Mean(cT) = 21.70	
Sample	cT	Sample	cT	Sample	cT
P-H-00	21.82	P-D-01	28.14	P-T-01	*21.09*
P-H-01	*21.90*	P-D-02	23.42	P-T-02	21.95
P-H-02	24.30	P-D-03	16.15	P-T-03	22.13
P-H-03	25.32	P-D-04	19.90	P-T-04	23.65
P-H-04	25.72	P-D-05	18.55	P-T-05	16.15
P-H-05	25.08	P-D-06	22.93	P-T-06	25.22
P-H-06	24.94	P-D-07	*17.62*		
P-H-07	30.85	P-D-08	18.66		
P-H-08	24.52	P-D-09	*17.35*		
P-H-09	22.15	P-D-10	23.54		
P-H-10	25.74	P-D-11	14.53		
P-H-11	23.33	P-D-12	19.23		
P-H-12	24.17	P-D-13	16.71		
P-H-13	25.25	P-D-14	17.94		
P-H-14	24.72	P-D-15	16.72		
P-H-15	25.01	P-D-16	*14.51*		
P-H-16	25.04				
P-H-17	24.76				
P-H-18	25.96				
P-H-19	23.59				

The synthetic conjugation-ready LPS fragments of *P. gingivalis* were immobilized on NHS-activated carboxyl-functionalized glass slides in triplicates (Figure 5.7A,B). Additionally,

a positive glycan control containing the α(1→2)-trirhamnose (**5.06**) was used in the assay, because most humans develop antibodies against this pathogen-associated glycan.[32]

Figure 5.7. Determination of human IgG and IgA antibodies binding to synthetic LPS-fragments **LPS1-11** and positive control **5.06**. (**A**) Fluorescence signals indicating IgG antibody binding in saliva of one exemplary chronic periodontitis patient, (**B**) fluorescence signals indicating IgA antibody binding in saliva of one exemplary healthy, and (**C**) associated printing pattern. (**D-G**) Mean fluorescence intensity (MFI) indicating IgG or IgA titer of bound human IgG or IgA antibodies in saliva or serum to glycan library.

73

The glycan microarray analysis of saliva compared to serum generally showed IgG antibody binding to the same LPS-fragments **LPS-4**, **LPS-2**, **LPS-9**, **LPS-7**, **LPS-5** as well as the positive control **5.06** (Figure 5.7D,E). While only saliva of CP patients with high bacterial load show IgG antibody binding to the listed LPS glycan structures, also serum of healthy and treated individuals contain IgG antibodies against those structures. It is generally known, that human sera contain antibodies against rhamnose structures as well as α-galactose structures, because those units are common motifs at bacterial surfaces.[135] The specific binding of antibodies in saliva of chronical periodontitis patients to some LPS-glycan structures is an evidence for the active mucosal IgG antibody production in the advanced affection of *P. gingivalis* in CP. IgG antibodies against positive control **5.06** in saliva were also observed in healthy individuals, but significantly less than in chronical periodontitis patients and recovered chronical periodontitis patients, which supports this result. Generally, it is known, that salivary antibodies reflect both mucosal and systemic immunity.[136]
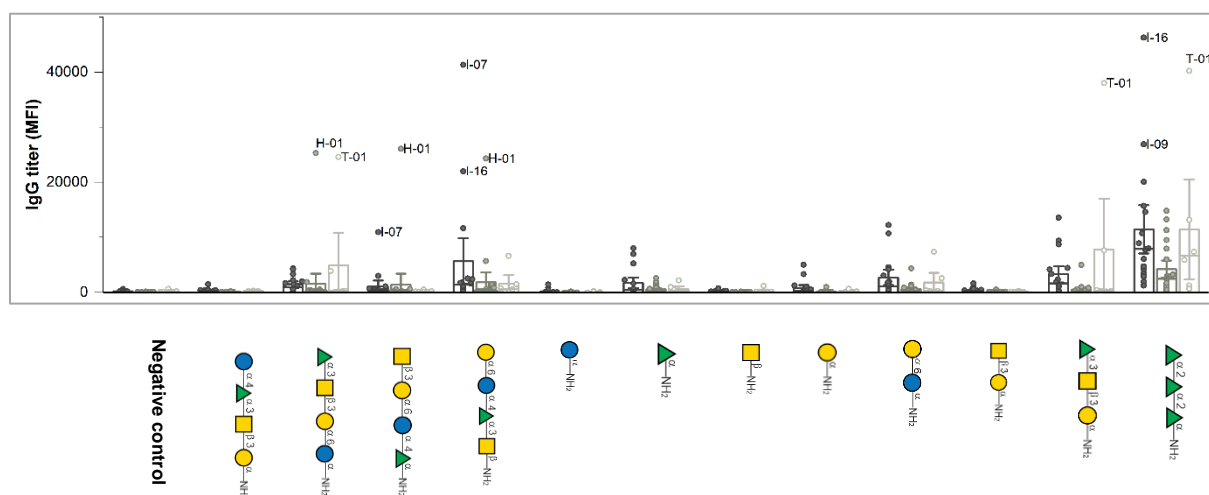
Figure 5.8. Mean fluorescence intensity (MFI) indicating IgG titer of bound human IgG antibodies in saliva to glycan library with labeled outliers.

The glycan microarray studies using saliva show a few outlying data points (Figure 5.8). CP patients I-07, I-09 and I-16 for example have the highest MFI to specific glycans and at the same time the highest bacterial load according to the low cT value (Table 5.2) as well as particularly distinct clinical indications for CP including significant damage to the attachment apparatus, deep periodontal lesions and deep intrabony defects. This shows, that the stage of periodontitis and bacterial load is proportional to the IgG titer. CP treated patient T-01 also shows IgG binding to specific glycans, while the remaining treated patient group is generally comparable with healthy individuals. Interestingly, the frequent professional dental cleaning was skipped for more than ten months in case of T-01. Therefore, the high IgG titer for T-01 could be a first sign of a resurgence of the infection, while clinical indications for CP were not visible yet. Further time-dependent screenings on treated patients before and after the professional dental cleaning and after a longer period of time without such cleaning could give

an idea about a potential of early diagnosis for high CP risk or CP resurgence using the here described glycan array studies.

The epitopes that show binding to IgG antibodies in saliva and blood are generally LPS-fragments with a terminal α(1→3)-rhamnose unit (**LPS-4**, **LPS-5** and **LPS-9**, Figure 5.9) or a terminal α(1→6)-galactose unit (**LPS-2**, **LPS-7** and **LPS-11**, Figure 5.10).

Figure 5.9 compares the mean fluorescence intensity (MFI) indicating IgG titer of bound human IgG antibodies in saliva to terminal α(1→3)-rhamnose LPS-fragments. Interestingly, **LPS-5** trisaccharide shows higher IgG antibody binding than **LPS-4** tetrasaccharide, even though higher molecular weight glycan antigens are known to elicit a better immune response than lower molecular weight fragments.[137] On the other hand, **LPS-5** trisaccharide shows higher amounts of IgG antibody binding than to rhamnose monomer **LPS-9**. This indicates, that observed IgG antibody binding to **LPS-5** is not only attributed to general antibodies against common bacterial rhamnose motifs, but more likely also to the actual LPS-fragment of *P. gingivalis*. These values, however, have low statistical significance (P ≤ 0.1), likely due to the different cT values inside each group. More significant results would probably be received in a larger CP group (n > 16). Nevertheless, the statistical significance of the stronger IgG binding observed for CP patients to **LPS-5** compared to low IgG binding for healthy and recovered patients is high (P ≤ 0.01) and is a clear evidence for the active mucosal IgG antibody production in the advanced affection of *P. gingivalis* in CP against **LPS-5**.
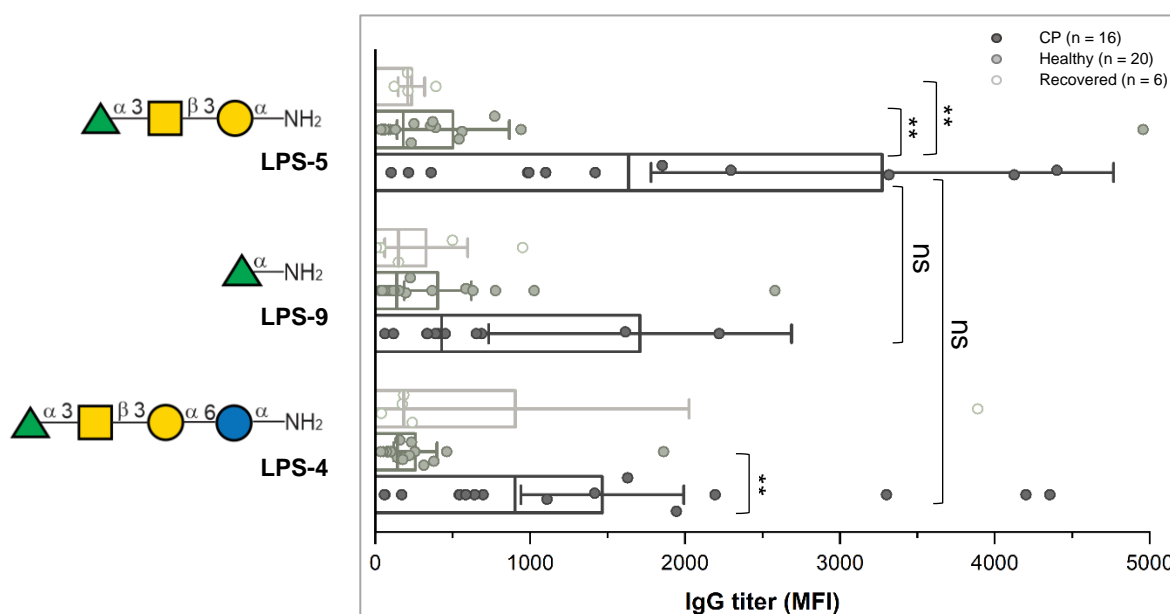
Figure 5.9. Determination of human antibodies in saliva binding to terminal α(1→3)-rhamnose glycans. P-T-01 and P-H-01 are masked. **P ≤ 0.01, ns – not significant, two-sided unpaired *t* test.

Figure 5.10 compares the bound human IgG antibodies in saliva to terminal α(1→6)-galactose LPS-fragments. **LPS-2** tetrasaccharide exhibits the strongest IgG interaction observed in these studies. Conversely, disaccharide **LPS-7** and monosaccharide **LPS-11** bind

significantly less IgG (P ≤ 0.05). This suggests that all four parts of the LPS repeating unit have an impact on the binding to IgG. The antibody binding not just arises from binding of general α(1→6)-galactose antibodies. Furthermore, IgG binding in CP saliva to **LPS-2** is significantly higher than in healthy dental patients (P ≤ 0.05). This supports the assumption, that epitope **LPS-2** is specific for *P. gingivalis.* The glycan microarray studies show that the order of the four tetrasaccharide fragments **LPS1-4** in the LPS repeating unit of *P. gingivalis* is important for the binding to IgG antibodies. α(1→6)-Galactose terminal LPS-fragment **LPS-2** shows the highest amount of bound IgG antibodies in this study.
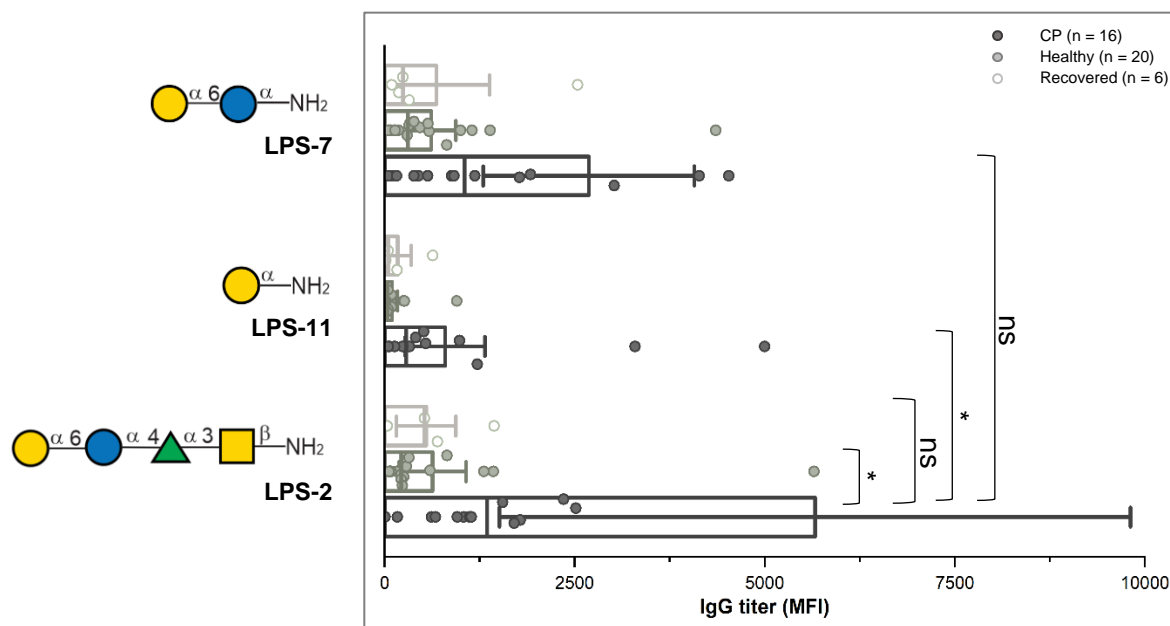
Figure 5.10. Determination of human IgG antibodies in saliva binding to terminal α(1→6)-galactose glycans. P-T-01 and P-H-01 are masked. *P ≤ 0.05, ns – not significant, two-sided unpaired *t* test.

As IgA antibodies are the predominant mucosal antibody species[138], it was also screened for IgA antibody binding (Figure 5.7F,G). Here, approximately ten-fold lower MFI for IgA antibody binding was observed, compared to IgG binding. Saliva samples showed stronger binding, which is expectable due to the high IgA content in saliva.[138] Only positive control rhamnose structures **LPS-9** and **5.06** as well as α-galactose dimer **LPS-7** show significant binding of IgA in saliva and serum – structures that are common for many bacteria.[32] There is also no significant difference observed between CP patients and dental healthy and recovered individuals. Dental healthy individuals actually show slightly higher IgA levels against the common bacteria glycan structures. The screening for IgG antibodies using a fluorescent-labeled secondary antibody (Fc-AF 647) in glycan microarray studies is commonly used to evaluate the immunogenicity of glycans and has already provided reliable results.[23b, 139] The screening of IgA antibodies has been included in very few glycan microarray studies.[140] Therefore, little is known on the IgA binding strength, to the immobilized glycans as well as the competition to IgG binding. However, it was clearly observed that IgA does not bind to antigen

structures that are specific for *P. gingivalis* and only IgG antibodies seem to be actively produced against **LPS-2** in the case of a severe form of CP.

5.3 Conclusion and Outlook

Here, the stereoselective synthesis of a library of fragments from the LPS of *P. gingivalis* by AGA was described. An α-selective glucose and galactose building block were designed to overcome challenges in the formation of 1,2-*cis*-glycosidic in AGA. Thereby, an efficient synthesis of vaccine candidates against *P. gingivalis* was possible. Automation of the antigen synthesis process enabled the fast access to a glycan library for high-throughput screening of antibody binding and determination of the immunogenic epitope of the LPS.

Synthetic LPS fragments were immobilized onto glass slides and microarray screenings for IgG and IgA in saliva and serum of CP patients as well as recovered CP patients and dental healthy patients were performed. The studies revealed that α(1→6)-galactose terminal LPS-tetrasaccharide **LPS-2** is recognized exclusively by salivary IgG from CP patients. Therefore, it is the lead epitope antigen for the development of a glycoconjugate vaccine to protect from high *P. gingivalis* loads and thus protection from *P. gingivalis* associated diseases such as Rheumatoid Arthritis, Alzheimer's disease and Artheorsclerosis. **LPS-2** will be used to immunize mice and antibody production will be investigated in order to evaluate the effectiveness as a vaccine. Due to the primary oral epithelium colonialization of *P. gingivalis*, immunity in the oral cavity should be induced. Advances in mucosal vaccination strategies might provide the option for periodontal disease control. Immobilizing **LPS-2** on liposomes could be a promising strategy to develop a mucosal vaccine against *P. gingivalis*. Further mucosal and traditional immunization studies as well as conjugation strategies for mucosal application need to be developed and are enabled by the here described rapid synthesis of antigen candidates of *P. gingivalis* by AGA.

6   Experimental Section

6.1   General Information

All **chemicals** were reagent grade and used as supplied unless otherwise noted. All **solvents** for chemical reactions were commercially purchased in p.a. quality. If stated, they were dried in a Solvent Dispensing System (J.C. Meyer). For HPLC and MS spectrometry, solvents with corresponding quality were used. Water was used from a Milli Q-station from Millipore. **The automated syntheses** were performed on home-built synthesizers developed at the Max Planck Institute of Colloids and Interfaces.

Reaction completion, identity, and purity of all compounds were determined by low resolution mass spectrometry (**ESI-LRMS**) or analytical thin-layer chromatography (**TLC**). TLC was performed on Merck silica gel 60 F_{254} plates (0.25 mm). Compounds were visualized by UV irradiation (254 nm) or stained (*p*-Anisaldehyde Stain: 3.7 mL *p*-anisaldehyde, 135 mL ethanol, 5 mL sulfuric acid, 1.5 mL glacial acetic acid or Hanessian's Stain: 235 mL of distilled water, 12 g of ammonium molybdate, 0.5 g of ceric ammonium molybdate, and 15 mL sulfuric acid). **Flash column chromatography** was performed on Kieselgel 60 with 230-400 mesh (Sigma-Aldrich, St. Louis, USA) or C_{18}-reverse phased silica gel, fully endcapped (Sigma-Aldrich, St. Louis, USA). Analysis and purification by normal and reverse phase **HPLC** and ESI-LRMS was performed by using an Agilent 1200 series. Products were **lyophilized** using a Christ Alpha 2-4 LD plus freeze dryer. ^{1}H, ^{13}C, COSY and HSQC **NMR spectra** were recorded in parts per million (δ) relative to the resonance of the solvent on a Varian 400-MR (400 MHz), Varian 600-MR (600 MHz), or Bruker Biospin AVANCE700 (700 MHz) spectrometer. Assignments were supported by COSY and HSQC experiments. High resolution mass spectra (**HRMS**) were obtained using 6210 ESI-TOF mass spectrometer (Agilent) and **MALDI-TOF** autoflexTM (Bruker) instruments. **IR spectra** were recorded on a Perkin-Elmer 1600 FTIR spectrometer. **Optical rotations** were measured by using a Perkin-Elmer 241 and Unipol L1000 polarimeter, with concentrations expressed in g/100 mL.

Amberlite IR-120 (Across Organics) protonic exchange resin was rinsed with THF, water, methanol and dichloromethane before use. Palladium on carbon was removed from reaction mixtures by filtration with Rotilabo syringe filters (Roth), PTFE filters (pore size: 0.45 µm).

6.2 Materials and Conditions for Automated Synthesis

6.2.1 Materials and Measurements

Solvents used for dissolving all building blocks and making of various solutions were taken from Solvent Dispensing System (J.C. Meyer). Wash solvents were HPLC grade. The building blocks were purchased from GlycoUniverse GmbH & CO KGaA or synthesized if stated. Prior to automated synthesis, the building blocks were weighed and co-evaporated three times with anhydrous toluene and dried for at least 1 hour under high vacuum prior to use. All solutions were freshly prepared and kept under argon during the automation process. Isolated yields of products were calculated on the basis of resin loading. Functionalized resins were synthesized as previously reported[141] and resin loading (0.3 mmol/g for conjugation-ready resin and 0.4 mmol/g for traceless-reducible resin) was determined following a published protocol.[142] Resin was placed in the reaction vessel and was swollen in dichloromethane for 20 min at room temperature before starting the first module. During this time, all reagent lines involved in the synthesis were washed and primed.

6.2.2 Preparation of Stock Solutions

Building Block Solution 1 (for thioglycosides): Thioglycoside building block was dissolved in 1 mL (per cycle) of anhydrous CH_2Cl_2.

Building Block Solution 2 (for glycosyl phosphates): Glycosyl phosphate building block (0.06 mmol, 4.7 equiv. per cycle) was dissolved in 1 mL (per cycle) of anhydrous CH_2Cl_2.

Acidic Wash Solution: TMSOTf (0.45 mL, 0.31 mmol) was added to 40 mL of anhydrous CH_2Cl_2.

Activator Solution 1 (for thioglycosides): Recrystallized NIS (1.58 g, 0.16 mmol) was dissolved in 45 mL of a 2:1 mixture of anhydrous CH_2Cl_2/dioxane, followed by addition of triflic acid (55 µL, 0.001 mmol). The solution was kept under ice-bath cooling for the duration of the automated run.

Activator Solution 2 (for glycosyl phosphates): TMSOTf (0.9 mL, 0.62 mmol) was added to 40 mL of anhydrous CH_2Cl_2.

Pre-capping Solution: Pyridine (10 mL) was added to 90 mL of DMF.

Capping Solution: Methanesulfonic acid (1.2 mL, 18.5 mmol), acetic anhydride (6 mL, 63.5 mmol) were added to 50 mL of anhydrous CH_2Cl_2.

Concentrated Capping Solution: Methanesulfonic acid (2.4 mL, 37 mmol), acetic anhydride (12 mL, 127 mmol) were added to 50 mL anhydrous CH_2Cl_2.

Lev Deprotection Solution: $N_2H_4 \cdot HOAc$ (725 mg, 7.87 mmol) was dissolved in 50 mL of a 4:1:0.25 mixture of pyridine/acetic acid/water.

Fmoc Deprotection Solution 1: Piperidine (20 mL) was added to 80 mL anhydrous DMF.

Fmoc Deprotection Solution 2: Et_3N (20 mL) was added to 80 mL anhydrous DMF.

NAP Deprotection Solution: DDQ (910 mg, 4.00 mmol) was dissolved in 40 mL of a 4:1 mixture of DCE/methanol. The solution was protected from light by aluminium foil for the duration of the automated run.

ClAc Deprotection Solution: Thiourea (2.5 g, 32.84 mmol) was dissolved in 55 mL of a 10:1 mixture of 2-methoxyethanol/pyridine.

Sulfation Solution: $SO_3 \cdot TMA$ (900 mg, 6.5 mmol) was added to 16 mL of DMF and sonicated until dissolved.

Methanolysis Solution: A solution of sodium methoxide in methanol (1 mL, 0.5 M) was added to 9 mL THF.

6.2.3   Modules for Automated Synthesis

Initiation: The resin loaded in the reaction vessel is washed with DMF, THF, and CH_2Cl_2 (3 x 3 mL for 15 s, respectively). The resin is then swollen in 2 mL CH_2Cl_2 for 20 minutes while the temperature of the reaction vessel is cooled to the lowest temperature required throughout the synthesis.

Module I - Acidic Washing: Once the temperature of the reaction vessel has adjusted to the desired temperature of the subsequent glycosylation by the cooling device, 1 mL of the **Acidic Wash Solution** is delivered to the reaction vessel through the precooling device (set at -20 °C). After three minutes, the solution is drained. Finally, the resin is washed with 3 mL CH_2Cl_2 (bubbling = 15 s) and drained.

Module IIa – Glycosylation (for thioglycosides): Upon draining the CH_2Cl_2 in the reaction vessel, 1 mL of **Building Block Solution 1** containing the appropriate building block is delivered from the building block storing component to the reaction vessel through the precooling device (set at -20 °C). After the temperature reaches the desired temperature (T_1), **Activator Solution 1** (1 mL) is delivered to the reaction vessel from the respective activator storing component to the reaction vessel through the precooling device (set at -20 °C). The glycosylation mixture is incubated for the selected duration (t_1) at the desired T_1, then by microwave irradiation (max power = 120 W) the reaction temperature is linearly ramped to T_2 (rate = 4 °C/min). Once T_2 is reached, it is maintained by microwave irradiation and the reaction mixture is incubated for an additional time (t_2). Once the incubation time is finished, the reaction mixture is drained and the resin is washed with CH_2Cl_2 (1 x 2 mL for 15 s), then dioxane (1 x

2 mL for 15 s), and finally CH_2Cl_2 (2 x 2 mL for 15 s). During the module, the active cooling element is maintained at the lowest temperature required throughout the synthesis.

Module IIb – Glycosylation (for glycosyl phosphate): Upon draining the CH_2Cl_2 in the reaction vessel, **Building Block Solution 1** (1 mL) containing the appropriate building block is delivered from the building block storing component to the reaction vessel through the precooling device (set at -20 °C). After the temperature again reaches the desired temperature (T_1), **Activator Solution 2** (1 mL) is delivered to the reaction vessel from the respective activator storing component to the reaction vessel through the precooling device (set at -20 °C). The glycosylation mixture is incubated for the selected duration (t_1) at the desired T_1, then by microwave irradiation (max power = 180 W) the reaction temperature is linearly ramped to T_2 (rate = 4 °C/min). Once T_2 is reached, it is maintained by microwave irradiation and the reaction mixture is incubated for an additional time (t_2). Once the incubation time is finished, the reaction mixture is drained and the resin is washed with DCE (1 x 2 mL for 5 s). During the module, the active cooling element is maintained at the lowest temperature required throughout the synthesis.

Module IIIa - Capping: The resin is washed with DMF (2 x 3 mL for 15 s). Then **Pre-capping Solution** (2 mL) is delivered and under microwave irradiation the reaction temperature is adjusted to and maintained at 50 °C for one minute (max power = 5 W). The resin is then washed with CH_2Cl_2 (3 x 2 mL for 15). Upon washing, **Capping Solution (**4 mL) is delivered and the temperature is adjusted and maintained 25 °C by microwave irradiation (max power = 100 W). The resin and the reagents are incubated for 8 min. The solution is then drained from the reactor vessel and the resin is washed with CH_2Cl_2 (3 x 3 mL for 15 s). During the entire module, the active cooling element is maintained at the lowest temperature required throughout the synthesis.

Module IVa - Fmoc Deprotection 1: The resin is first washed with DMF (3 x 3 mL for 15 s), and then **Fmoc Deprotection Solution 1** (2 mL) is delivered to the reaction vessel. The temperature of the reagents inside the reactor vessel is then adjusted to and maintained at 60 °C by microwave irradiation (max power = 60 W). After 1 min the reaction solution is drained and the resin is washed with DMF (3 x 3 mL for 15 s) and CH_2Cl_2 (5 x 3 mL for 15 s). During the module, the active cooling element is maintained at the lowest temperature required throughout the synthesis. After this module the resin is ready for the next glycosylation cycle.

Module IVb - Lev Deprotection: The resin is washed with CH_2Cl_2 (3 x 2 mL for 15 s), and then **Lev Deprotection Solution** (2 mL) is delivered to the reaction vessel. The temperature of the reagents inside the reactor vessel is then adjusted to and maintained at 25 °C by microwave irradiation (max power = 180 W). After 5 min, the reaction solution is drained from the reactor vessel and the resin is washed with CH_2Cl_2 (3 x 2 mL for 15 s). Then, of fresh **Lev**

Deprotection Solution (2 mL) is delivered and the process is repeated twice more. Then, the resin is washed with DMF, THF, and CH_2Cl_2 (3 x 3 mL for 15 s, respectively). During the module, the active cooling element is maintained at the lowest temperature required throughout the synthesis. After this module the resin is ready for the next glycosylation cycle.

Module IVc - Fmoc Deprotection 2: The resin is first washed with DMF (3 x 3 mL for 15 s), and then **Fmoc Deprotection Solution 2** (2 mL) is delivered to the reaction vessel. The temperature of the reagents inside the reactor vessel is then adjusted to and maintained at 60 °C by microwave irradiation (max power = 60 W). After 5 min the reaction solution is drained and the resin is washed with DMF (3 x 2 mL for 15 s). Then, fresh **Fmoc Deprotection Solution 2** (2 mL) is delivered and the process is repeated twice more. Then, the resin is washed with DMF (3 x 3 mL) and CH_2Cl_2 (3 x 3 mL) for 15 s each time. During the module, the active cooling element is maintained at the lowest temperature required throughout the synthesis. After this module the resin is ready for the next glycosylation cycle.

Module IVd – NAP Deprotection: The resin is first washed with CH_2Cl_2 (3 x 2 mL for 15 s) then **NAP Deprotection Solution** (2 mL) was delivered to the reaction vessel. The temperature of the reagents inside the reactor vessel is then adjusted to and maintained at 60 ºC by microwave irradiation (max power = 180 W). After 30 min, the reaction solution is drained from the reactor vessel. The resin is washed with CH_2Cl_2 (3 x 2 mL for 15 s). Then, fresh **NAP Deprotection Solution** (2 mL) is delivered and the process is repeated twice more. Then, the resin is washed with DMF, THF, and CH_2Cl_2 (3 x 3 mL for 120 s, respectively). During the module, the active cooling element is maintained at the lowest temperature required throughout the synthesis. After this module the resin is ready for the next glycosylation cycle.

Module IVe – ClAc Deprotection: The resin is first washed with CH_2Cl_2 (3 x 2 mL for 15 s) then **ClAc Deprotection Solution** (2 mL) was delivered to the reaction vessel. The temperature of the reagents inside the reactor vessel is then adjusted to and maintained at 90 °C by microwave irradiation (max power = 180 W). After 22 min, the reaction solution is drained from the reactor vessel. The resin is washed with DMF (3 x 2 mL for 15 s). Then fresh **ClAc Deprotection Solution** (2 mL) is delivered and the process is repeated twice more. Then, the resin is washed with DMF (3 x 3 mL for 15 s) and CH_2Cl_2 (5 x 3 mL for 15 s). During the module, the active cooling element is maintained at the lowest temperature required throughout the synthesis. After this module the resin is ready for the next glycosylation cycle.

Module VI – Methanolysis: The resin was washed with CH_2Cl_2 (3 x 2 mL for 15 s) then **Methanolyis Solution** (2 mL) was delivered to the reaction vessel at room temperature. After 1 h the reaction solution is drained from the reactor vessel. The incubation in **Methanolysis Solution** was repeated three more times. Then, the resin is washed with 10% aqueous citric acid, DMF, THF, and CH_2Cl_2 (3 x 3 mL for 120 s, respectively).

6.2.4 Post-synthesizer Manipulation

Cleavage from Solid-Support (Method A-1): Protected Oligosaccharides

After automated synthesis, the resin was removed from the reaction vessel, suspended in CH_2Cl_2 (20 mL), and photo-cleaved in a continuous-flow photo-reactor. A Vapourtec E-Series easy-MedCHem, equipped with a UV-150 Photo-chemical reactor having a UV-150 Medium-Pressure Mercury Lamp (arc length 27.9 cm, 450 W) surrounded by a long-pass UV filter (Pyrex, 50% transmittance at 305 nm) was used. A Pump 11 Elite Series (Harvard Apparatus syringe pump at a flow rate of 0.8 mL/min was used to pump the mixture through a FEP tubing (i.d. 3.0 inch, volume: 12 mL) at 20 °C. The reactor was washed with 20 mL CH_2Cl_2 at a flow rate of 2.0 mL/min. The output solution was filtered to remove the resin and the solvent was evaporated *in vacuo*. Crude was then analyzed by MALDI.

Cleavage from Solid-Support (Method A-2): Deprotected Oligosaccharides

After automated synthesis, the resin was removed from the reaction vessel, suspended in a 10:1 mixture of THF/water (20 mL), and photo-cleaved in a continuous-flow photo-reactor. A Vapourtec E-Series easy-MedCHem, equipped with a UV-150 Photo-chemical reactor having a UV-150 LED lamp (365 nm) was used. A Pump 11 Elite Series (Harvard Apparatus syringe pump at a flow rate of 2 mL/min was used to pump the mixture through a FEP tubing (i.d. 3.0 inch, volume: 12 mL) at 20 °C. The reactor was washed with 20 mL of a 10:1 mixture of THF/water at a flow rate of 2.0 mL/min, followed by water, acetonitrile and CH_2Cl_2. The output solution was filtered to remove the resin and the solvent was evaporated *in vacuo*. Crude was then analyzed by MALDI.

Deprotection of Oligosaccharides

AGA-synthesized and photo-cleaved product was subjected to methanolysis and hydrogenolysis. The hydrogenolysis product was purified by RP-HPLC and lyophilized on a Christ Alpha 2-4 LD plus freeze dryer to afford the final deprotected compound.

Methanolysis (Method C): To a solution of protected oligosaccharide in MeOH:CH_2Cl_2 (2 mL, 1:1), sodium methoxide (0.5 M solution in MeOH, 2.2 equiv. per ester group) was added. The mixture was stirred at room temperature for 2 h. Then Amberlite IR-120 (H^+ form) was added to quench. After neutralization, the reaction mixture was filtered and the solvent was removed in vacuo. The crude compound was used for hydrogenolysis without further purification.

Hydrogenolysis (Method D): The crude compound obtained after methanolysis was dissolved in 4 mL of EtOAc:t-BuOH:H_2O (2:1:1). Pd/C (10%) was added to the solution and the suspension was stirred in a H_2 bomb with 60 psi pressure over night. The insoluble material was removed by a CHROMAFIL ®Xtra, RC 0.45 syringe filter. The solid was washed once with t-BuOH and several times with water. The filtrate was collected and concentrated in vacuo.

6.2.5 Analytical NP/RP-HPLC and purification

Analytical NP-HPLC of Crude Material (Method B-1)

Analytical NP-HPLC was conducted on an Agilent 1200 Series system. A YMC-Diol-300-NP column (150 mm x 4.60 mm I.D.) was used with a flow rate of 1.00 mL/min and hexane/EtOAc as eluent (20% EtOAc in hexane for 5 min, 20 $\rightarrow$ 100% EtOAc in hexane over 35 min, 100% EtOAc for 10 min).

Analytical NP-HPLC of Crude Material (Method B-2)

Analytical NP-HPLC was conducted on an Agilent 1200 Series system. A YMC-Diol-300-NP column (150 mm x 4.60 mm I.D.) was used at a flow rate of 1.00 mL/min with hexane/EtOAc as eluent (20% EtOAc in hexane for 5 min, 20 $\rightarrow$ 55% EtOAc in hexane over 35 min, 55 $\rightarrow$ 100% EtOAc in hexane over 35 min, 100% EtOAc for 10 min).

Preparative NP-HPLC of Crude Material (Method B-3)

Analytical NP-HPLC was conducted on an Agilent 1200 Series system. A YMC-Diol-300-NP column (150 mm x 20 mm I.D.) was used at a flow rate of 15.00 mL/min with hexane/EtOAc as eluent (20% EtOAc in hexane for 5 min, 20 $\rightarrow$ 55% EtOAc in hexane over 35 min, 100% EtOAc for 10 min).

Preparative NP-HPLC of Crude Material (Method B-4)

Analytical NP-HPLC was conducted on an Agilent 1200 Series system. A YMC-Diol-300-NP column (150 mm x 20 mm I.D.) was used at a flow rate of 15.00 mL/min with hexane/EtOAc as eluent (20% EtOAc in hexane for 5 min, 20 $\rightarrow$ 100% EtOAc in hexane over 35 min, 100% EtOAc for 10 min).

Analytical/preparative RP-HPLC of Crude Material (Method E-1)

Crude products were dissolved in water and analyzed/purified using analytical/preparative HPLC. A Thermo-Scientific Hypercarb column (150 mm x 4.60 mm I.D.) was used for analytical RP-HPLC with a flow rate of 0.70 mL/min with water (0.1% HCO_2H)/acetonitrile as eluents (100% H_2O (0.1% HCO_2H) for 5 min, 0 $\rightarrow$ 30% acetonitrile in H_2O (0.1% HCO_2H) over 30 min, 30 $\rightarrow$ 100% acetonitrile in H_2O (0.1% HCO_2H) over 5 min, 100% acetonitrile for 5 min).

Analytical/preparative RP-HPLC of Crude Material (Method E-2)

Crude products were dissolved in water and analyzed/purified using analytical/preparative HPLC. A Thermo-Scientific Hypercarb column (150 mm x 4.60 mm I.D.) was used for analytical RP-HPLC with a flow rate of 0.70 mL/min with H_2O (0.1% HCO_2H)/acetonitrile as eluents (100% H_2O (0.1% HCO_2H) for 5 min, 0 $\rightarrow$ 10% acetonitrile in H_2O (0.1% HCO_2H) over 30 min, 10 $\rightarrow$ 100% acetonitrile in H_2O (0.1% HCO_2H) over 5 min, 100% acetonitrile for 5 min).

6.3 Preparation and Characterization of Compounds in Chapter 3

6.3.1 Automated Glycan Assembly of Total Orthogonal Building Block 3.07

5-Amino-pentyl α-D-mannopyranosyl-(1→4)-α-D-mannopyranosyl-(1→4)-α-D-mannopyranosyl-(1→4)-α-D-tetramannopyranoside (3.24)

Repeat	Building Blocks	Modules	Notes	
1x	**3.07** (2 x 4.7 equiv.)	**I** – Acidic Wash		
		IIb – Glycosylation with glycosyl phosphate – 2 cycles	-20 °C (T$_1$) 30 min (t$_1$)	0 °C (T$_2$) 10 min (t$_2$)
		III – Capping **IVc** – Fmoc Deprotection		
3x	**3.07** (4.7 equiv.)	**I** – Acidic Wash		
		IIb – Glycosylation with glycosyl phosphate	-20 °C (T$_1$) 30 min (t$_1$)	0 °C (T$_2$) 10 min (t$_2$)
		III – Capping **IVc** – Fmoc Deprotection		

Protected **3.24** (15 mg, 0.007 mmol, crude yield: 52%) was obtained as a colorless oil after photo-cleavage from solid-support following **Method A-1**. Deprotection of **3.24** following **Method C** and **D** and purification by reverse-phase HPLC (**Method E-1**, t$_R$ = 17.3 min) afforded deprotected compound **3.24** (1.8 mg, 0.002 mmol, 18%) as a white solid after lyophilization.

¹H NMR (700 MHz, D$_2$O): δ 5.28 – 5.24 (m, 3H), 4.88 (d, J = 1.8 Hz, 1H), 4.07 (dd, J = 3.3, 1.9 Hz, 1H), 4.03 (dd, J = 3.4, 1.9 Hz, 2H), 3.99 – 3.66 (m, 22H), 3.57 (dt, J = 10.0, 6.2 Hz, 1H), 3.04 – 3.00 (m, 2H), 1.75 – 1.62 (m, 4H), 1.52 – 1.41 (m, 2H) ppm. **¹³C NMR** (176 MHz, D$_2$O): δ 101.4, 101.3, 99.6, 74.3, 74.1, 74.1, 73.7, 72.3, 72.2, 71.2, 71.1, 70.8, 70.8, 70.7, 70.7, 70.6, 70.4, 70.3, 67.6, 66.5, 61.0, 61.0, 60.9, 39.4, 28.0, 26.8, 22.4 ppm. **HRMS** (QToF): Calcd for C$_{29}$H$_{53}$NO$_{21}$ [M + H]$^+$ 752.3183; found 752.3205.

5-Amino-pentyl α-D-mannopyranosyl-(1→3)-α-D-mannopyranosyl-(1→3)-α-D-mannopyranosyl-(1→3)-α-D-tetramannopyranoside (3.23)

Repeat	Building Blocks	Modules	Notes	
1x	**3.07** (2 x 4.7 equiv.)	**I** – Acidic Wash		
		IIb – Glycosylation with glycosyl phosphate – 2 cycles	-20 °C (T$_1$) 30 min (t$_1$) 0 °C (T$_2$) 10 min (t$_2$)	
		III – Capping **IVb** – Lev Deprotection		
3x	**3.07** (4.7 equiv.)	**I** – Acidic Wash		
		IIb – Glycosylation with glycosyl phosphate	-20 °C (T$_1$) 30 min (t$_1$) 0 °C (T$_2$) 10 min (t$_2$)	
		III – Capping **IVb** – Lev Deprotection		

Protected **3.23** (26 mg, 0.010 mmol, crude yield: 74%) was obtained as a colorless oil after photo-cleavage from solid-support following **Method A-1**. Deprotection of **3.23** following **Method C** and **D** and purification by reverse-phase HPLC (**Method E-1**, t$_R$ = 18.0 min) afforded deprotected compound **3.23** (1.2 mg, 0.002 mmol, 12%) as a white solid after lyophilization.

^{1}H NMR (700 MHz, D$_2$O): δ 5.15 (d, J = 1.8 Hz, 1H), 5.13 (d, J = 1.7 Hz, 1H), 5.12 (d, J = 1.9 Hz, 1H), 4.86 (d, J = 1.4 Hz, 1H), 4.26 – 4.23 (m, 1H), 4.12 – 4.07 (m, 2H), 4.06 – 4.00 (m, 2H), 3.96 – 3.73 (m, 12H), 3.71 – 3.62 (m, 2H), 3.57 (dt, J = 9.4, 5.9 Hz, 1H), 3.02 (t, J = 7.6 Hz, 2H), 1.75 – 1.62 (m, 4H), 1.54 – 1.40 (m, 2H) ppm. **^{13}C NMR** (176 MHz, D$_2$O): δ 102.3, 102.2, 102.2, 99.6, 78.3, 78.1, 78.1, 73.6, 73.5, 73.4, 72.9, 70.4, 70.0, 69.7, 69.7, 67.5, 66.9, 66.2, 66.1, 66.1, 61.1, 61.0, 61.0, 60.9, 39.4, 28.0, 26.6, 22.5 ppm. **HRMS** (QToF): Calcd for C$_{29}$H$_{53}$NO$_{21}$ [M + H]$^+$ 752.3183; found 752.3218.

5-Amino-pentyl α-D-mannopyranosyl-(1→6)-α-D-mannopyranosyl-(1→6)-α-D-mannopyranosyl-(1→6)-α-D-tetramannopyranoside (3.25)

Repeat	Building Blocks	Modules	Notes	
1x	**3.05** (2 x 6.5 equiv.)	**I** – Acidic Wash		
		IIa – Glycosylation with thioglycoside – 2 cycles	-20 °C (T$_1$)	10 min (t$_1$)
			0 °C (T$_2$)	35 min (t$_2$)
		III – Capping		
		IVe – ClAc Deprotection		
3x	**3.05** (6.5 equiv.)	**I** – Acidic Wash		
		IIa – Glycosylation with thioglycoside	-20 °C (T1)	10 min (t1)
			0 °C (T2)	35 min (t2)
		III – Capping		
		IVe – ClAc Deprotection		

Protected **3.25** (22 mg, 0.008 mmol, crude yield: 58%) was obtained as a colorless oil after photo-cleavage from solid-support following **Method A-1**. Deprotection of **3.25** following **Method C** and **D** and purification by reverse-phase HPLC (**Method E-1**, t$_R$ = 18.8 min) afforded deprotected compound **3.25** (1.8 mg, 0.002 mmol, 18%) as a white solid after lyophilization.

¹H NMR (600 MHz, D$_2$O): δ 4.88 (d, J = 1.8 Hz, 1H), 4.86 (d, J = 1.9 Hz, 1H), 4.86 (d, J = 1.8 Hz, 1H), 4.83 (d, J = 1.8 Hz, 1H), 4.00 – 3.65 (m, 24H), 3.62 (t, J = 9.7 Hz, 1H), 3.54 (dt, J = 9.9, 6.1 Hz, 1H), 3.00 – 2.93 (m, 2H), 1.72 – 1.61 (m, 4H), 1.49 – 1.35 (m, 2H) ppm. **¹³C NMR** (151 MHz, D$_2$O): δ 99.8, 99.3, 99.2, 72.6, 70.8, 70.7, 70.6, 70.6, 70.5, 70.0, 69.9, 69.9, 67.6, 66.7, 66.5, 66.5, 66.5, 65.5, 65.5, 65.4, 60.8, 39.3, 28.0, 26.6, 22.5 ppm. **HRMS** (QToF): Calcd for C$_{29}$H$_{53}$NO$_{21}$ [M + H]$^+$ 752.3183; found 752.3209.

5-Amino-pentyl α-D-mannopyranosyl-(1→2)-α-D-mannopyranosyl-(1→2)-α-D-mannopyranosyl-(1→2)-α-D-tetramannopyranoside (3.22)

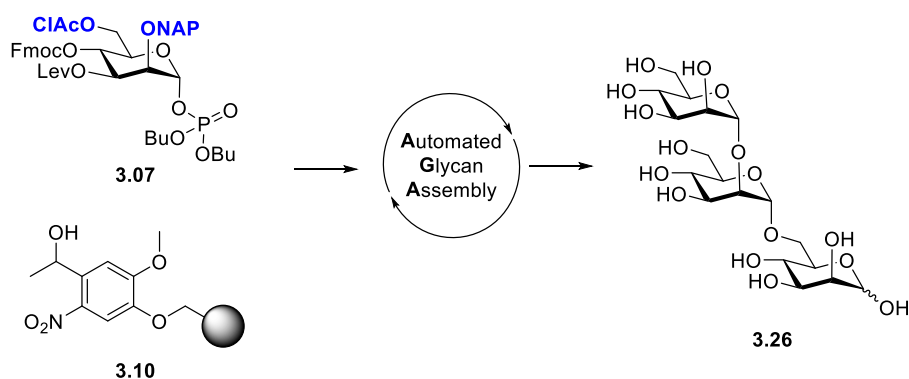| Repeat	Building Blocks	Modules	Notes	
4x	**3.07** (2 x 4.7 equiv.)	**I** – Acidic Wash		
		IIb – Glycosylation with glycosyl phosphate – 2 cycles	-20 °C (T$_1$)	30 min (t$_1$)
			0 °C (T$_2$)	10 min (t$_2$)
		III – Capping		
		IVd – NAP Deprotection		

Protected **3.22** (17 mg, 0.007 mmol, crude yield: 51%) was obtained as a colorless oil after photo-cleavage from solid-support following **Method A-1**. Deprotection of **3.22** following **Method C** and **D** and purification by reverse-phase HPLC (**Method E-1**, t$_R$ = 15.0 min) afforded deprotected compound **3.22** (1.9 mg, 0.003 mmol, 19%) as a white solid after lyophilization.

^{1}H NMR (600 MHz, D$_2$O): δ 5.27 (d, *J* = 1.9 Hz, 1H), 5.25 (d, *J* = 1.9 Hz, 1H), 5.06 (d, *J* = 1.9 Hz, 1H), 5.01 (d, *J* = 1.9 Hz, 1H), 4.10 – 4.01 (m, 3H), 3.96 – 3.78 (m, 9H), 3.78 – 3.56 (m, 13H), 3.55 – 3.47 (m, 1H), 3.00 – 2.94 (m, 2H), 1.71 – 1.58 (m, 4H), 1.46 – 1.36 (m, 2H) ppm.
^{13}C NMR (151 MHz, D$_2$O): δ 102.1, 100.6, 100.5, 97.9, 85.8, 79.5, 78.8, 78.5, 73.2, 73.1, 72.7, 70.2, 70.1, 69.9, 69.8, 67.5, 67.0, 66.9, 66.9, 66.7, 61.8, 61.0, 60.9, 38.7, 27.9, 26.4, 22.4 ppm.
HRMS (QToF): Calcd for C$_{29}$H$_{53}$NO$_{21}$ [M + H]$^+$ 752.3183; found 752.3214.

α-D-Mannopyranosyl-(1→2)-α-D-mannopyranosyl-(1→6)-D-mannopyranose (3.26)

Repeat	Building Blocks	Modules	Notes	
1x	**3.07** (2 x 4.7 equiv.)	**I** – Acidic Wash		
		IIb – Glycosylation with glycosyl phosphate – 2 cycles	-20 °C (T_1) 0 °C (T_2)	30 min (t_1) 10 min (t_2)
		IVd – NAP Deprotection **III** – Capping **IVe** – ClAc Deprotection		
1x	**3.07** (4.7 equiv.)	**I** – Acidic Wash		
		IIb – Glycosylation with glycosyl phosphate	-20 °C (T_1) 0 °C (T_2)	30 min (t_1) 10 min (t_2)
		III – Capping **IVd** – NAP Deprotection		
1x	**3.07** (2 x 4.7 equiv.)	**I** – Acidic Wash		
		IIb – Glycosylation with glycosyl phosphate – 2 cycles	-20 °C (T_1) 0 °C (T_2)	30 min (t_1) 10 min (t_2)
		III – Capping **IVd** – NAP Deprotection **VI** - Methanolysis		

Photo-cleavage from solid-support using **Method A-2** followed by purification by reverse-phase HPLC (**Method E-2**, t_R = 21.6 min) afforded deprotected compound **3.26** (1.2 mg, 0.002 mmol, 15%) as a white solid after lyophilization.
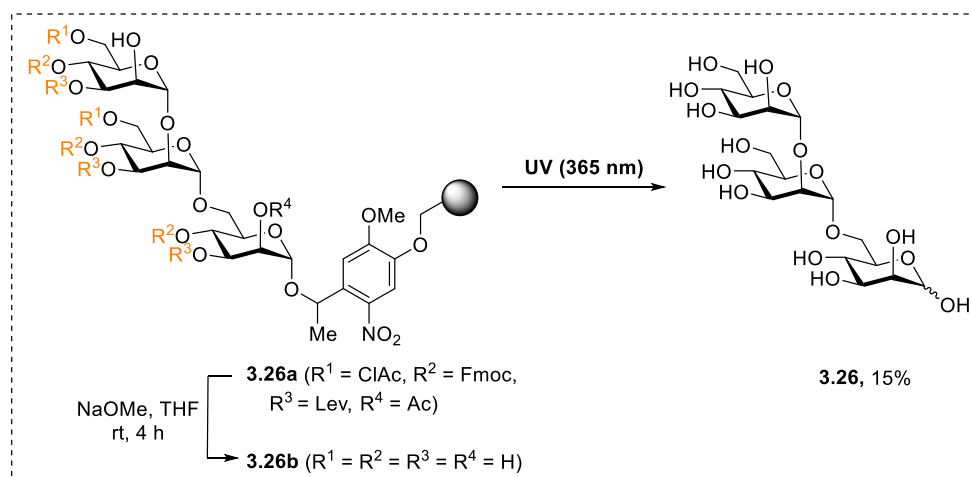
^{1}H NMR (700 MHz, D$_2$O, α-isomer): δ 5.17 (d, J = 1.9 Hz, 1H), 5.14 (d, J = 1.9 Hz, 1H), 5.05 (d, J = 2.2 Hz, 1H), 4.08 (dd, J = 3.4, 1.8 Hz, 1H), 4.03 (dd, J = 3.5, 1.8 Hz, 1H), 4.00 – 3.69 (m, 14H), 3.66 – 3.62 (m, 2H) ppm. **^{13}C NMR** (176 MHz, D$_2$O, α-isomer): δ 102.3, 98.7, 94.2, 78.5, 73.2, 72.7, 71.1, 70.7, 70.6, 70.4, 70.3, 70.2, 69.9, 66.9, 66.7, 66.0, 61.1, 60.9 ppm. **HRMS** (QToF): Calcd for C$_{18}$H$_{32}$O$_{16}$Na [M + Na]$^+$ 527.1583; found 527.1586.

6-*O*-Acetyl-2-*O*-benzoyl-3,4-di-*O*-benzyl-α-D-mannopyranosyl-(1→3)-[6-*O*-acetyl-2-*O*-benzoyl-3,4-di-*O*-benzyl-α-D-mannopyranosyl-(1→6)]-2-*O*-acetyl-2-*O*-(2-naphthalenylmethyl)-D-mannopyranose (3.17)
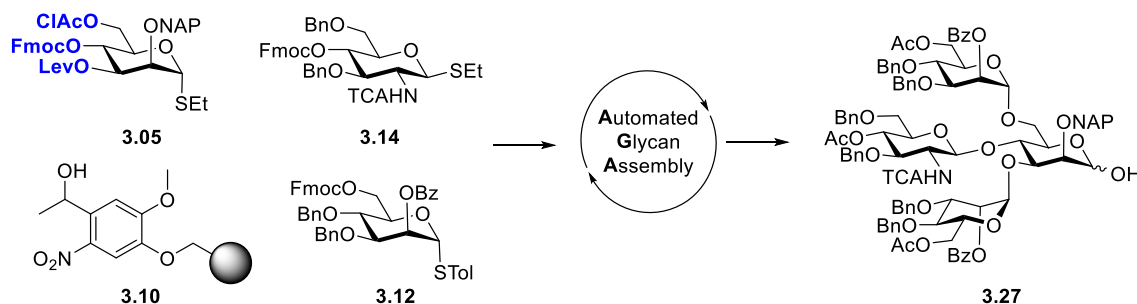

Repeat	Building Blocks	Modules	Notes	
1x	**3.05** (2 x 6.5 equiv.)	**I** – Acidic Wash		
		IIa – Glycosylation with thioglycoside – 2 cycles	-20 °C (T_1)	10 min (t_1)
			0 °C (T_2)	35 min (t_2)
		IVc – Fmoc Deprotection		
		III – Capping		
		IVb – Lev Deprotection		
		IVe – ClAc Deprotection		
1x	**3.12** (3 x 6.5 equiv.)	**I** – Acidic Wash		
		IIa – Glycosylation with thioglycoside – 3 cycles	-20 °C (T_1)	10 min (t_1)
			-10 °C (T_2)	25 min (t_2)
		IVa – Fmoc Deprotection (6 cycles)		
		III – Capping (4 cycles)		

Photo-cleavage from solid-support using **Method A-1** followed by purification by normal-phase HPLC (**Method B-3**, t_R = 22.7 min) afforded compound **3.17** (14 mg, 0.011 mmol, 65%) as a colorless oil.

¹H NMR (400 MHz, CDCl$_3$): δ 8.09 – 8.01 (m, 5H), 7.75 – 7.56 (m, 7H), 7.52 – 7.39 (m, 6H), 7.36 – 7.16 (m, 19H), 5.60 (s, 1H), 5.48 (s, 1H), 5.39 (t, *J* = 10.0 Hz, 1H), 5.24 (s, 1H), 5.11 (s, 1H), 5.01 – 4.67 (m, 7H), 4.65 – 4.42 (m, 6H), 4.37 – 3.95 (m, 8H), 3.92 – 3.78 (m, 5H), 2.18 (s, 3H), 2.05 (s, 3H), 1.91 (s, 3H) ppm. **¹³C NMR** (101 MHz, CDCl$_3$): δ 171.2, 170.8, 170.4, 165.8, 165.6, 138.2, 138.0, 137.7, 135.2, 133.5, 133.5, 133.2, 133.1, 130.0, 130.0, 128.7, 128.6, 128.6, 128.5, 128.5, 128.5, 128.2, 128.0, 127.9, 127.8, 127.8, 127.0, 126.3, 126.1, 125.8, 99.5, 97.6, 92.7, 78.2, 77.8, 77.4, 76.0, 75.3, 75.2, 73.8, 73.7, 73.2, 71.6, 71.5, 70.5, 70.1, 70.0, 69.3, 69.0, 68.9, 68.0, 63.4, 63.3, 21.1, 21.0, 20.7 ppm. **HRMS** (QToF): Calcd for C$_{77}$H$_{78}$O$_{21}$Na [M + Na]⁺ 1361.4928; found 1361.4954.

6-*O*-Acetyl-2-*O*-benzoyl-3,4-di-*O*-benzyl-α-D-mannopyranosyl-(1→3)-[4-*O*-acetyl-3,6-di-*O*-benzyl-2-deoxy-2-*N*-trichloroacetyl-β-D-glucopyranosyl-(1→4)]-[6-*O*-acetyl-2-*O*-benzoyl-3,4-di-*O*-benzyl-α-D-mannopyranosyl-(1→6)]-2-*O*-(2-naphthalenylmethyl)-D-mannopyranose (3.27)
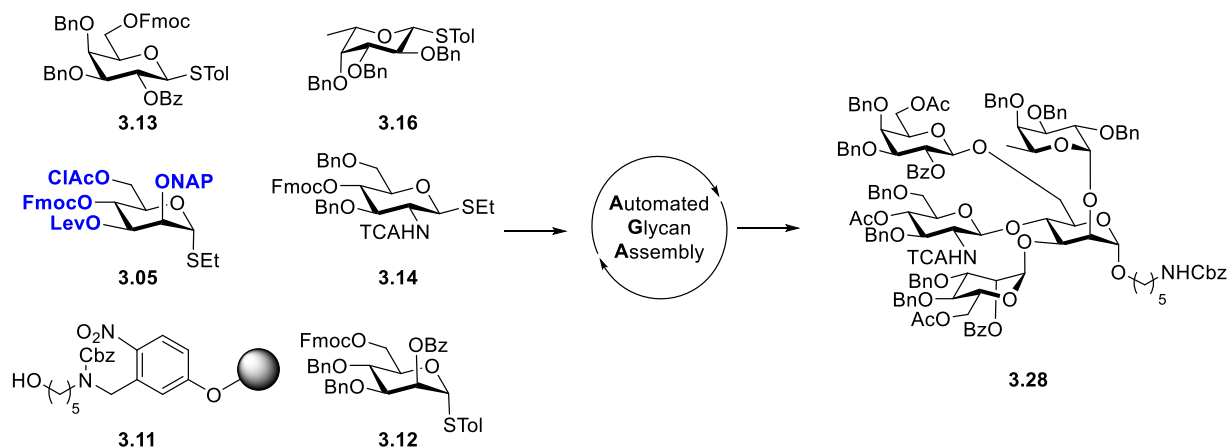

Repeat	Building Blocks	Modules	Notes	
1x	**3.05** (2 x 6.5 equiv.)	**I** – Acidic Wash		
		IIa – Glycosylation with thioglycoside – 2 cycles	-20 °C (T$_1$) 0 °C (T$_2$)	10 min (t$_1$) 35 min (t$_2$)
		III – Capping **IVc** – Fmoc Deprotection		
1x	**3.14** (6.5 equiv.)	**I** – Acidic Wash		
		IIa – Glycosylation with thioglycoside – 2 cycles	-20 °C (T$_1$) -10 °C (T$_2$)	10 min (t$_1$) 45 min (t$_2$)
		III – Capping **IVb** – Lev Deprotection **IVe** – ClAc Deprotection		
1x	**3.12** (3 x 6.5 equiv.)	**I** – Acidic Wash		
		IIa – Glycosylation with thioglycoside – 3 cycles	-20 °C (T$_1$) -10 °C (T$_2$)	10 min (t$_1$) 25 min (t$_2$)
		IVa – Fmoc Deprotection (6 cycles) **III** – Capping (4 cycles)		

Photo-cleavage from solid-support using **Method A-1** followed by purification by normal-phase HPLC (**Method B-3**, t$_R$ = 21.6 min) afforded compound **3.27** (8 mg, 0.004 mmol, 28%) as a colorless oil.

^{1}H NMR (600 MHz, CDCl$_3$, α-isomer): δ 8.11 – 8.06 (m, 4H), 7.65 – 7.56 (m, 5H), 7.47 – 7.39 (m, 7H), 7.36 – 7.11 (m, 31H), 5.86 (s, 1H), 5.74 – 5.70 (m, 1H), 5.39 (d, *J* = 2.0 Hz, 1H), 5.34 (t, *J* = 9.4 Hz, 1H), 5.16 – 5.06 (m, 3H), 4.94 (d, *J* = 10.7 Hz, 1H), 4.87 (d, *J* = 11.2 Hz, 1H), 4.81 – 4.70 (m, 5H), 4.65 – 4.58 (m, 6H), 4.55 – 4.49 (m, 4H), 4.41 (dd, *J* = 11.4, 5.0 Hz, 2H), 4.37 – 4.31 (m, 3H), 4.25 – 4.09 (m, 7H), 3.92 – 3.85 (m, 6H), 2.06 (s, 3H), 1.91 (s, 3H), 1.80 (s, 3H) ppm. **^{13}C NMR** (176 MHz, CDCl$_3$, α-isomer): δ 169.9, 169.6, 169.2, 165.0, 164.5, 137.1, 136.9, 136.9, 136.6, 134.1, 132.1, 132.0, 128.9, 128.9, 128.9, 128.8, 128.8, 127.6, 127.6, 127.4, 127.4, 127.4, 127.4, 127.3, 127.3, 127.3, 127.2, 127.1, 127.0, 127.0, 126.9, 126.9, 126.9, 126.8, 126.8, 126.7, 126.7, 126.6, 98.4, 97.6, 96.5, 96.5, 91.6, 77.1, 76.7, 74.9, 74.1, 72.7, 72.6, 72.1, 70.5, 70.3, 69.4, 69.0, 68.9, 68.2, 68.0, 67.9, 66.8, 62.3, 62.2, 19.9, 19.8, 19.6 ppm. **HRMS** (QToF): Calcd for C$_{99}$H$_{100}$Cl$_3$NO$_{26}$ [M + Na]$^+$ 1846.5491; found 1846.5565.

***N*-Benzyloxycarbonyl-5-amino-pentyl 2,3,4-tri-*O*-benzyl-α-L-fucopyranosyl-(1→2)-[6-*O*-acetyl-2-*O*-benzoyl-3,4-di-*O*-benzyl-α-D-mannopyranosyl-(1→3)]-[4-*O*-acetyl-3,6-di-*O*-benzyl-2-deoxy-2-*N*-trichloroacetyl-β-D-glucopyranosyl-(1→4)]-[6-*O*-acetyl-2-*O*-benzoyl-3,4-di-*O*-benzyl-β-D-galactopyranosyl-(1→6)]-α-D-mannopyranoside (3.28)**

| Repeat	Building Blocks	Modules	Notes	
1x	**3.05** (2 x 6.5 equiv.)	**I** – Acidic Wash		
		IIa – Glycosylation with thioglycoside – 2 cycles	-20 °C (T_1) 10 min (t_1)	0 °C (T_2) 35 min (t_2)
		III – Capping		
		IVc – Fmoc Deprotection		
1x	**3.14** (6.5 equiv.)	**I** – Acidic Wash		
		IIa – Glycosylation with thioglycoside – 2 cycles	-20 °C (T_1) 10 min (t_1)	-10 °C (T_2) 45 min (t_2)
		III – Capping		
		IVb – Lev Deprotection		
1x	**3.12** (3 x 6.5 equiv.)	**I** – Acidic Wash		
		IIa – Glycosylation with thioglycoside	-20 °C (T_1) 10 min (t_1)	0 °C (T_2) 25 min (t_2)
		IVe – ClAc Deprotection		
1x	**3.13** (3 x 6.5 equiv.)	**I** – Acidic Wash		
		IIa – Glycosylation with thioglycoside – 3 cycles	-30 °C (T_1) 10 min (t_1)	-10 °C (T_2) 25 min (t_2)
		IVd – NAP Deprotection		
1x	**3.16** (3 x 6.5 equiv.)	**I** – Acidic Wash		
		IIa – Glycosylation with thioglycoside – 3 cycles	-30 °C (T_1) 10 min (t_1)	-10 °C (T_2) 25 min (t_2)
		IVa – Fmoc Deprotection (6 cycles)		
		III – Capping (4 cycles)		

Photo-cleavage from solid-support using **Method A-1** followed by purification by normal-phase HPLC (**Method B-3**, t_R = 22.8 min) afforded compound **3.28** (12 mg, 0.005 mmol, **32%**) as a colorless oil.

¹H NMR (600 MHz, [D₆]-DMSO): δ 8.02 (dd, *J* = 8.2, 1.6 Hz, 2H), 7.91 (dd, *J* = 8.2, 1.3 Hz, 2H), 7.66 – 7.62 (m, 1H), 7.61 – 7.55 (m, 1H), 7.48 (dt, *J* = 17.4, 7.8 Hz, 5H), 7.35 – 7.31 (m, 12H), 7.30 – 7.19 (m, 27H), 7.19 – 7.13 (m, 10H), 5.33 (dd, *J* = 10.2, 8.0 Hz, 1H), 5.22 (d, *J* = 2.2 Hz, 1H), 5.04 – 5.00 (m, 3H), 4.87 (d, *J* = 11.6 Hz, 1H), 4.80 – 4.41 (m, 22H), 4.37 – 4.19

(m, 5H), 4.17 – 4.09 (m, 3H), 4.05 – 3.81 (m, 12H), 3.78 – 3.71 (m, 2H), 3.63 – 3.54 (m, 3H), 2.94 – 2.88 (m, 2H), 1.98 (s, 3H), 1.96 (s, 3H), 1.83 (s, 3H), 1.30 – 1.24 (m, 8H), 1.03 (d, $J =$ 6.2 Hz, 3H) ppm. **^{13}C NMR** (151 MHz, [D_6]-DMSO, as per HSQC): δ 128.6, 128.5, 132.7, 132.3, 127.8, 127.1, 127.1, 126.7, 126.7, 71.2, 98.3, 95.2, 64.5, 73.3, 100.1, 73.6, 70.5, 100.2, 99.1, 69.5, 73.2, 71.6, 70.7, 70.4, 73.5, 72.0, 72.0, 62.3, 61.8, 61.7, 72.6, 69.3, 77.4, 65.9, 73.4, 79.0, 75.0, 77.9, 71.3, 55.9, 71.1, 77.2, 71.5, 39.7, 20.2, 19.8, 28.2, 27.8, 15.8 ppm. **HRMS** (QToF): Calcd for $C_{128}H_{137}Cl_3N_2O_{32}Na$ [M + Na]$^+$ 2341.8112; found 2341.8408.

### 6.3.2 Synthesis of Orthogonal Building Block 3.07

Ethyl 4,6-*O*-benzylidene-2-*O*-(2-naphthalenylmethyl)-1-thio-α-D-mannopyranoside (3.02)
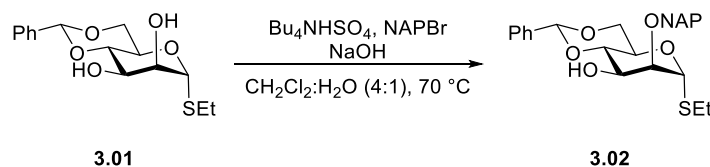
To a suspension of diol **3.01** (20.0 g, 64.03 mmol, 1.0 equiv.) in CH_2Cl_2 (300 mL) was added Bu_4NHSO_4 (3.0 g, 12.17 mmol, 0.2 equiv.), followed by addition of 2-(bromomethyl)naphthalene (15.6 g, 70.43 mmol, 1.1 equiv.). An aqueous solution of NaOH (4.0 g in 100 mL) was added and the biphasic solution was refluxed at 70 °C overnight. The mixture was allowed to cool down to room temperature and the aqueous phase was extracted with CH_2Cl_2. The combined organic phase was washed with citric acid solution, dried over Na_2SO_4, filtered and concentrated. Compound **3.02** (16.8 g, 36.32 mmol, 57%) was obtained as a white solid after purification by column chromatography (SiO$_2$, Hex/EtOAc 3:1).

R$_f$ = 0.44 (Hex/EtOAc 3:1). **^{1}H NMR** (400 MHz, CDCl$_3$): δ 7.91 – 7.79 (m, 4H), 7.59 – 7.44 (m, 5H), 7.44 – 7.31 (m, 3H), 5.59 (s, 1H), 5.42 (d, J = 1.2 Hz, 1H), 4.98 – 4.78 (m, 2H), 4.31 – 4.16 (m, 2H), 4.13 – 4.05 (m, 1H), 4.04 – 3.94 (m, 2H), 3.94 – 3.82 (m, 1H), 2.70 – 2.51 (m, 2H), 2.48 (d, J = 7.9 Hz, 1H), 1.23 (t, J = 7.4 Hz, 3H) ppm. **^{13}C NMR** (101 MHz, CDCl$_3$): δ 137.4, 134.9, 133.3, 133.2, 129.3, 128.7, 128.4, 128.1, 127.9, 127.1, 126.4, 126.4, 126.3, 125.9, 102.3, 82.6, 80.2, 79.9, 73.4, 69.2, 68.7, 64.0, 25.4, 15.0 ppm. **[α]$_D$** 31.11 cm^{-1} (*c* 1, CHCl$_3$). **IR** (film): 3470, 3385, 3318, 2931, 2906, 2876, 1702, 1600, 1510, 1455, 1422, 1383, 1271, 1244, 1209, 1168, 1088, 1057, 1048, 1035, 972, 749 cm^{-1}. **HRMS** (QToF): Calcd for C$_{26}$H$_{28}$O$_5$SNa [M + Na]$^+$ 475.1550; found 475.1552.

Ethyl 4,6-*O*-benzylidene-2-*O*-levulinyl-2-*O*-(2-naphthalenylmethyl)-1-thio-α-D-mannopyranoside (3.03)
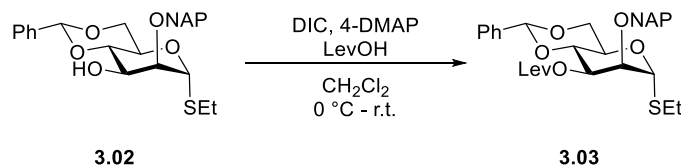
To a solution of **3.02** (15.8 g, 34.91 mmol, 1.0 equiv.) and levulinic acid (7.1 mL, 69.82 mmol, 2.0 equiv.) in anhydrous CH_2Cl_2 (50 mL) was added dropwise a premixed solution of DIC (16.1 mL, 104.7 mmol, 3.0 equiv.) and DMAP (0.9 g, 6.98 mmol, 0.2 equiv.) in anhydrous CH_2Cl_2 (20 mL) at 0 °C. The reaction was stirred at room temperature overnight. The reaction mixture was filtered through Celite, the filtrate was washed with aqueous $NaHCO_3$ and the aqueous phase was extracted with CH_2Cl_2. The combined organic phase was dried over Na_2SO_4, filtered and concentrated. Compound **3.03** (17.0 g, 30.87 mmol, 88%) was obtained as a yellow syrup after purification by column chromatography (SiO_2, Hex/EtOAc 3:1).

R_f = 0.25 (Hex/EtOAc 3:1). ^1H NMR (400 MHz, $CDCl_3$): δ 7.88 – 7.81 (m, 4H), 7.55 (dd, J = 8.5, 1.8 Hz, 1H), 7.52 – 7.44 (m, 4H), 7.39 – 7.32 (m, 3H), 5.58 (s, 1H), 5.33 (d, J = 1.5 Hz, 1H), 5.23 (dd, J = 9.9, 3.5 Hz, 1H), 4.83 (q, J = 12.0 Hz, 2H), 4.34 – 4.21 (m, 3H), 4.14 (dd, J = 3.5, 1.4 Hz, 1H), 3.90 (t, J = 10.0 Hz, 1H), 2.66 – 2.48 (m, 6H), 2.08 (s, 3H), 1.21 (t, J = 7.5 Hz, 3H) ppm. ^{13}C NMR (101 MHz, $CDCl_3$): δ 206.5, 172.2, 137.4, 135.2, 133.3, 133.2, 129.2, 128.5, 128.4, 128.1, 127.8, 127.3, 126.4, 126.4, 126.3, 126.2, 101.3, 83.3, 79.2, 76.5, 73.7, 71.2, 68.8, 64.6, 37.8, 29.9, 28.0, 25.5, 14.9 ppm. **[α]$_D$** 32.53 cm^{-1} (*c* 1, $CHCl_3$). **IR** (film): 2930, 1741, 1719, 1365, 1206, 1180, 1157, 1097, 1014, 753, 700 cm^{-1}. **HRMS** (QToF): Calcd for $C_{31}H_{34}O_7SNa$ [M + Na]$^+$ 573.1917; found 573.1921.

Ethyl 2-*O*-levulinyl-2-*O*-(2-naphthalenylmethyl)-1-thio-α-D-mannopyranoside (3.04)
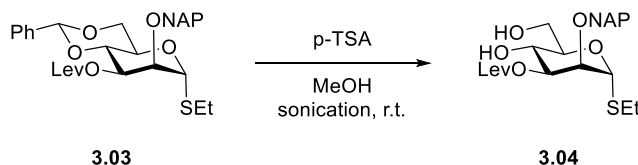
To a suspension of **3.03** (16.5 g, 36.46 mmol, 1.0 equiv.) in MeOH (100 mL) was added *p*-TSA (3.1 g, 18.23 mmol, 0.5 equiv.). The reaction mixture was sonicated for one hour at room temperature before pyridine (5 mL) was added. The solvent was removed and the residue was redissolved in ethyl acetate, washed with water, dried over Na_2SO_4, filtered and concentrated. Compound **3.04** (12.2 g, 26.37 mmol, 72%) was obtained as a colorless oil after purification by column chromatography (SiO_2, Hex/EtOAc 1:1 to 2:3).

R_f = 0.25 (Hex/EtOAc 2:3). **¹H NMR** (400 MHz, CDCl₃): δ 7.87 – 7.77 (m, 4H), 7.54 – 7.44 (m, 3H), 5.35 (d, J = 1.5 Hz, 1H), 5.08 (dd, J = 9.8, 3.3 Hz, 1H), 4.88 – 4.70 (m, 2H), 4.17 (t, J = 9.7 Hz, 1H), 4.11 – 4.02 (m, 1H), 3.98 (dd, J = 3.4, 1.5 Hz, 1H), 3.90 (s, 2H), 2.74 – 2.37 (m, 6H), 2.12 (s, 3H), 1.23 (t, J = 7.4 Hz, 3H) ppm. **¹³C NMR** (101 MHz, CDCl₃): δ 207.4, 172.8, 135.2, 133.2, 133.1, 128.3, 127.9, 127.7, 126.8, 126.3, 126.1, 125.9, 82.1, 77.5, 74.7, 73.0, 72.4, 66.9, 62.7, 38.1, 29.8, 28.1, 25.2, 14.7 ppm. **[α]**$_D$ 5.33 cm⁻¹ (c 1, CHCl₃). **IR** (film): 3456, 2928, 1720, 1365, 1159, 1083, 774 cm⁻¹. **HRMS** (QToF): Calcd for C₂₄H₃₀O₇SNa [M + Na]⁺ 485.1604; found 485.1605.

Ethyl 6-*O*-(2-chloroacetyl)-4-*O*-fluorenylmethoxycarbonyl-2-*O*-levulinyl-2-*O*-(2-naphthalenylmethyl)-1-thio-α-D-mannopyranoside (3.05)
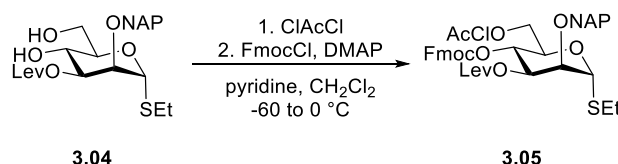

To a solution of **3.04** (2.0 g, 4.32 mmol, 1.0 equiv.) and anhydrous pyridine (1.75 mL, 21.62 mmol, 5.0 equiv.) in anhydrous CH₂Cl₂ (20 mL) at -60 °C was added chloroacetyl chloride (0.38 mL, 4.76 mmol, 1.1 equiv.). The reaction was stirred for 10 min, aqueous citric acid solution (2 mL) was added and the mixture was allowed to warm to room temperature. Water was added and the aqueous phase was extracted with CH₂Cl₂. The combined organic phase was dried over Na₂SO₄, filtered and concentrated. The residue (R_f = 0.53 (Hex/AcOEt 2:3)) was dissolved in anhydrous CH₂Cl₂ (30 mL) and anhydrous pyridine (1.75 mL, 21.62 mmol, 5.0 equiv.) was added followed by a solution of FmocCl (1.7 g, 6.47 mmol, 1.5 equiv.) in anhydrous CH₂Cl₂ (20 mL) at 0 °C. DMAP (53 mg, 0.43 mmol, 0.1 equiv.) was added and the reaction mixture was stirred for one hour at 0 °C. Aqueous citric acid solution (10 mL) was added and the mixture was allowed to warm to room temperature. The aqueous phase was extracted with CH₂Cl₂ and the combined organic phase was dried over Na₂SO₄, filtered and concentrated. Compound **3.05** (2.5 g, 3.28 mmol, 76%) was obtained as a white solid after purification by column chromatography (SiO₂, Hex/EtOAc 9:1 to 3:1).

R_f = 0.26 (Hex/EtOAc 3:1). **¹H NMR** (400 MHz, CDCl₃): δ 7.87 – 7.72 (m, 6H), 7.64 – 7.57 (m, 2H), 7.54 – 7.45 (m, 3H), 7.44 – 7.38 (m, 2H), 7.35 – 7.28 (m, 2H), 5.38 – 5.30 (m, 2H), 5.22 (dd, J = 10.1, 3.2 Hz, 1H), 4.89 – 4.74 (m, 2H), 4.50 – 4.24 (m, 6H), 4.10 (d, J = 2.1 Hz, 2H), 4.06 (dd, J = 3.2, 1.6 Hz, 1H), 2.69 – 2.52 (m, 2H), 2.49 – 2.34 (m, 4H), 2.00 (s, 3H), 1.24 (t, J = 7.4 Hz, 3H) ppm. **¹³C NMR** (101 MHz, CDCl₃): δ 206.2, 171.9, 167.3, 154.5, 143.4, 143.3, 141.4, 141.4, 135.1, 133.3, 133.2, 129.2, 128.4, 128.4, 128.1, 128.0, 127.8, 127.4, 127.3, 127.0, 126.4, 126.2, 126.1, 125.4, 125.4, 125.2, 120.2, 120.2, 82.4, 73.2, 71.8, 70.8, 70.5,

68.6, 64.2, 46.7, 40.9, 37.6, 29.8, 29.8, 27.9, 25.5, 14.9 ppm. **[α]$_D$** 8.93 cm^{-1} (*c* 1, CHCl$_3$). **IR** (film): 2958, 1754, 1720, 1451, 1364, 1261, 1156, 1101, 989, 760, 744 cm^{-1}. **HRMS** (QToF): Calcd for C$_{41}$H$_{41}$SO$_{10}$ClNa [M + Na]$^+$ 783.2001; found 783.2043.

Dibutoxyphosphoryloxy 6-*O*-(2-chloroacetyl)-4-*O*-fluorenylmethoxycarbonyl-2-*O*-levulinyl-2-*O*-(2-naphthalenylmethyl)-α-ᴅ-mannopyranoside (3.07)
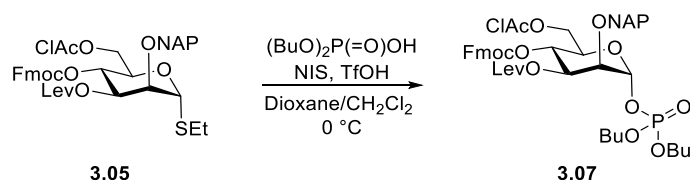

To a solution of thioglycoside **3.05** (1.0 g, 1.31 mmol, 1.0 equiv.) and dibutyl hydrogen phosphate (0.52 mL, 2.63 mmol, 2.0 equiv.) in anhydrous CH$_2$Cl$_2$ (6 mL) a solution of NIS (530 mg, 2.36 mmol, 1.8 equiv.) and TfOH (35 μL, 0.39 mmol, 0.3 equiv.) in anhydrous CH$_2$Cl$_2$/dioxane (1:1, 4 mL) was added dropwise at 0 °C. The reaction was stirred at the same temperature for 2 h. The reaction mixture was diluted with CH$_2$Cl$_2$ (10 mL) and 10% sodium thiosulfate solution was added. The bilayer mixture was extracted with CH$_2$Cl$_2$, dried over Na$_2$SO$_4$, filtered and concentrated. Compound **3.07** (1.2 g, 1.26 mmol, 96%) was obtained as a white solid after purification by column chromatography (SiO$_2$, Hex/EtOAc 2:1).

R$_f$ = 0.23 (Hex/EtOAc 3:1). **^{1}H NMR** (400 MHz, CDCl$_3$): δ 7.86 – 7.74 (m, 6H), 7.60 (t, *J* = 7.3 Hz, 2H), 7.54 – 7.46 (m, 3H), 7.45 – 7.36 (m, 2H), 7.33 (dd, *J* = 8.7, 3.7 Hz, 2H), 5.68 (dd, *J* = 6.4, 2.0 Hz, 1H), 5.43 – 5.28 (m, 2H), 4.86 – 4.82 (m, 2H), 4.48 – 4.25 (m, 5H), 4.26 – 4.20 (m, 1H), 4.10 (d, *J* = 3.1 Hz, 2H), 4.07 – 3.95 (m, 5H), 2.50 – 2.36 (m, 4H), 2.01 (s, 3H), 1.65 – 1.54 (m, 4H), 1.42 – 1.30 (m, 4H), 0.92 (q, *J* = 7.5 Hz, 6H) ppm. **^{13}C NMR** (101 MHz, CDCl$_3$): δ 205.2, 172.3, 167.3, 155.1, 143.4, 142.2, 134.8, 133.8, 128.5, 128.1, 127.8, 127.4, 127.3, 127.2, 126.4, 126.3, 126.1, 125.4, 125.2, 119.8, 95.9, 75.1, 73.8, 70.6, 70.5, 70.0, 69.9, 68.2, 63.6, 46.7, 40.9, 37.6, 32.4, 29.7, 27.9, 18.7, 13.7 ppm. **[α]$_D$** -6.32 cm^{-1} (*c* 1, CHCl$_3$). **IR** (film): 2964, 1754, 1720, 1451, 1365, 1261, 1153, 1029, 957, 744 cm^{-1}. **HRMS** (QToF): Calcd for C$_{47}$H$_{54}$ClPO$_{14}$Na [M + Na]$^+$ 931.2832; found 931.2884.

6.3.3 Synthesis of BODIPY Carbohydrate Photo-cages 3.29a-d

***p*-Tolyl 2-*O*-benzoyl-3,4-di-*O*-benzyl-1-thio-*α*-D-mannopyranoside (3.30)[143]**

3.12   **3.30**
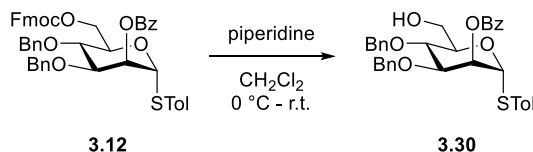
A solution of *p*-tolyl 2-*O*-benzoyl-3,4-di-*O*-benzyl-6-*O*-(9-fluorenylmethoxycarbonyl)-1-thio-*α*-D-mannopyranoside **3.12** (500 mg, 0.63 mmol, 1.0 equiv.) in anhydrous CH_2Cl_2 (12 mL) was cooled to 0 °C and a solution of piperidine (1.0 mL, 10.70 mmol, 17 equiv. in 4 mL anhydrous CH_2Cl_2) was added dropwise. The reaction mixture was stirred for 3 h at 0 °C, diluted with CH_2Cl_2 (50 mL) and washed with saturated aqueous citric acid (1 x 20 mL). The aqueous phase was extracted with CH_2Cl_2 (3 x 50 mL), the combined organic phase was washed with brine (50 mL), dried over Na_2SO_4, filtered and concentrated in *vacuo* to give product **3.30** (330 mg, 0.58 mmol, 92%) as a colourless oil after purification by column chromatography (SiO_2, Hex/EtOAc 3:1).

R*f* = 0.25 (Hex/EtOAc 3:1). **¹H NMR** (600 MHz, CDCl₃): δ 8.09 – 8.03 (m, 2H), 7.62 – 7.56 (m, 1H), 7.47 (t, J = 7.8 Hz, 2H), 7.39 – 7.23 (m, 12H), 7.12 (d, J = 8.0 Hz, 2H), 5.84 (dd, J = 2.9, 1.8 Hz, 1H), 5.51 (d, J = 1.7 Hz, 1H), 4.94 (d, J = 10.9 Hz, 1H), 4.80 (d, J = 11.3 Hz, 1H), 4.68 (d, J = 10.9 Hz, 1H), 4.62 (d, J = 11.4 Hz, 1H), 4.26 (dt, J = 9.3, 3.4 Hz, 1H), 4.11 – 4.01 (m, 2H), 3.90 – 3.79 (m, 2H), 2.32 (s, 3H), 1.79 (dd, J = 7.9, 5.5 Hz, 1H) ppm. **¹³C NMR** (151 MHz, CDCl₃): δ 165.7, 138.5, 138.2, 137.7, 133.4, 132.9, 130.1, 130.0, 129.8, 129.5, 128.6, 128.5, 128.5, 128.3, 128.2, 128.0, 127.9, 86.8, 78.5, 75.4, 74.3, 73.0, 71.8, 70.8, 62.1, 21.2 ppm.

***p*-Tolyl 2-*O*-benzoyl-3,4-di-*O*-benzyl-6-*O*-(8-(4,4'-dimethyl-1,3,5,7-tetramethyl-4-bora-3a,4a-diaza-*s*-indacenyl)methoxycarbonyl)-1-thio-*α*-D-mannopyranoside (3.29a)**
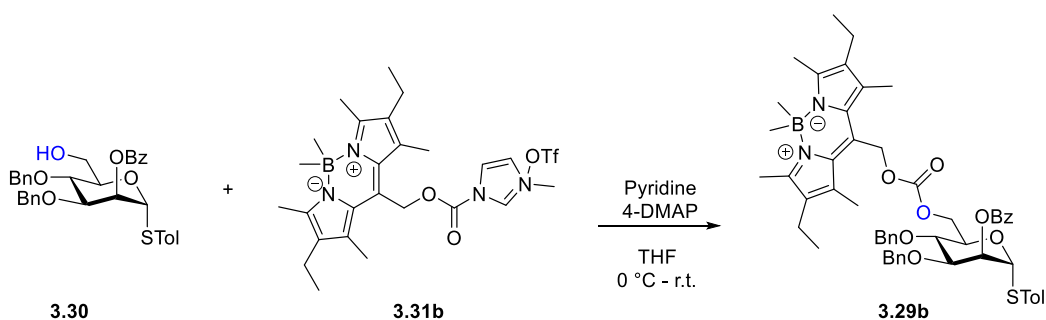

3.30   **3.31a**   **3.29a**
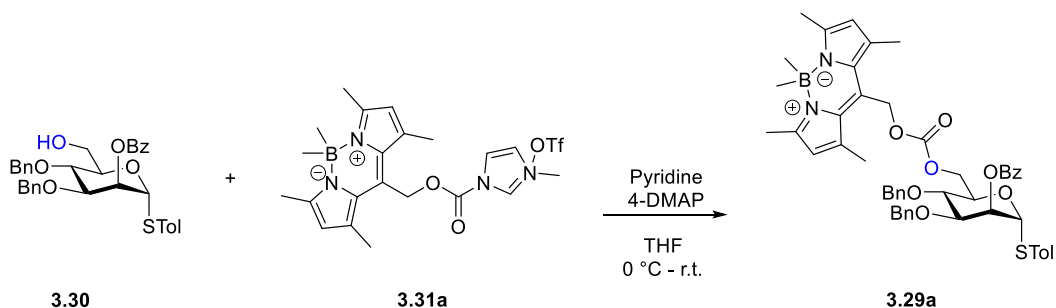
To a solution of mannose **3.30** (40 mg, 0.07 mmol, 1.0 equiv.) and pyridine (57 µL, 0.70 mmol, 10.0 equiv.) in anhydrous THF (5 mL) **3.31a** (41 mg, 0.08 mmol, 1.1 equiv.) was added in small portions at 0 °C followed by 4-DMAP (1 mg, 0.01 mmol, 0.1 equiv.). The reaction was warmed up to room temperature and was stirred overnight. The reaction mixture was diluted with ethyl

acetate and washed with water and brine. The organic phase was dried over Na$_2$SO$_4$, filtered, concentrated and purified by flash column chromatography (SiO$_2$, Hex/EtOAc 9:1 to 3:1) to give compound **3.29a** (30 mg, 0.04 mmol, 49%) as a red foam.

R$_f$ = 0.46 (Hex/EtOAc 3:1). **^{1}H NMR** (600 MHz, CDCl$_3$): δ 7.99 (d, J = 6.6 Hz, 2H), 7.40 (t, J = 7.4 Hz, 1H), 7.36 – 7.25 (m, 11H), 7.19 (t, J = 7.7 Hz, 2H), 7.04 (d, J = 7.9 Hz, 2H), 5.99 (s, 2H, BODIPY-C<u>H</u>), 5.83 (t, J = 2.3 Hz, 1H, <u>H-2</u>), 5.46 (d, J = 1.8 Hz, 1H, <u>H-1</u>), 5.45 – 5.39 (m, 2H, BODIPY-C<u>H$_2$</u>), 4.86 (dd, J = 78.7, 11.1 Hz, 2H, Ph-C<u>H$_2$</u>), 4.61 – 4.48 (m, 4H, Ph-C<u>H$_2$</u>, <u>H-6</u>, <u>H-6'</u>), 4.43 (ddd, J = 9.4, 4.1, 2.3 Hz, 1H, <u>H-5</u>), 4.08 – 3.99 (m, 2H, <u>H-3</u>, <u>H-4</u>), 2.46 (s, 6H, BODIPY-C<u>H$_3$</u>), 2.33 (s, 6H, BODIPY-C<u>H$_3$</u>), 2.24 (s, 3H, Tol-C<u>H$_3$</u>), 0.22 (s, 6H, B(C<u>H$_3$</u>)) ppm. **^{13}C NMR** (151 MHz, CDCl$_3$): δ 165.6, 155.0, 153.5, 138.4, 138.0, 137.6, 137.3, 133.3, 132.6, 132.1, 131.4, 130.1, 129.9, 129.5, 128.6, 128.5, 128.5, 128.3, 128.2, 128.0, 127.9, 123.0, 86.7, 78.4, 75.6, 74.2, 71.6, 70.7, 70.3, 66.9, 61.7, 21.2, 16.7, 16.0 ppm. **HRMS** (QToF): Calcd for C$_{51}$H$_{55}$BN$_2$O$_8$S [M + H]$^+$ 867.3845; found 867.3879.

_p_-Tolyl 2-_O_-benzoyl-3,4-di-_O_-benzyl-6-_O_-(8-(2,6-diethyl-4,4'-dimethyl-1,3,5,7-tetramethyl-4-bora-3a,4a-diaza-_s_-indacenyl)methoxycarbonyl)-1-thio-α-_D_-mannopyranoside (3.29b)
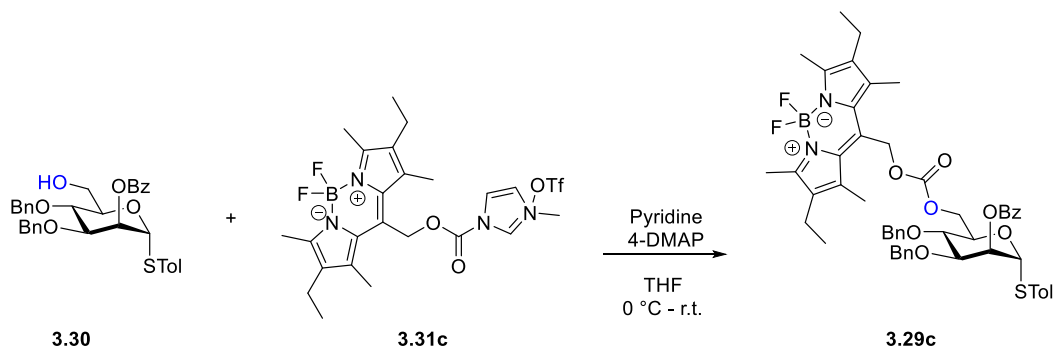

To a solution of mannose **3.30** (80 mg, 0.14 mmol, 2.0 equiv.) and pyridine (57 μL, 0.70 mmol, 10.0 equiv.) in anhydrous THF (5 mL) **3.31b** (41 mg, 0.07 mmol, 1.0 equiv.) was added in small portions at 0 °C followed by 4-DMAP (1 mg, 0.01 mmol, 0.1 equiv.). The reaction was warmed up to room temperature and was stirred overnight. The reaction mixture was diluted with ethyl acetate and washed with water and brine. The organic phase was dried over Na$_2$SO$_4$, filtered, concentrated and purified by flash column chromatography (SiO$_2$, Hex/EtOAc 9:1 to 3:1) to give compound **3.29b** (40 mg, 0.04 mmol, 62%) as a red foam.

R$_f$ = 0.49 (Hex/EtOAc 3:1). **^{1}H NMR** (600 MHz, CDCl$_3$): δ 7.97 (dt, J = 8.5, 1.1 Hz, 2H), 7.37 – 7.27 (m, 13H), 7.12 (tt, J = 7.3, 0.9 Hz, 2H), 7.04 (d, J = 7.9 Hz, 2H), 5.88 – 5.83 (m, 1H), 5.46 (dd, J = 4.2, 1.8 Hz, 3H), 4.86 (dd, J = 72.6, 11.0 Hz, 2H), 4.61 – 4.52 (m, 4H), 4.42 (dd, J = 7.6, 4.3 Hz, 1H), 4.08 – 4.01 (m, 2H), 2.43 (s, 6H), 2.28 (q, J = 7.6 Hz, 4H), 2.23 (s, 9H), 0.92 (t, J = 7.6 Hz, 6H), 0.24 (s, 6H) ppm. **^{13}C NMR** (151 MHz, CDCl$_3$): δ 165.6, 155.1, 152.0, 138.4,

138.0, 137.6, 133.6, 133.3, 132.6, 132.1, 131.0, 130.3, 130.1, 129.9, 129.6, 129.4, 128.6, 128.5, 128.5, 128.3, 128.1, 128.0, 86.7, 78.5, 75.7, 74.2, 71.6, 70.8, 70.1, 66.8, 62.3, 21.2, 17.5, 14.8, 14.7, 12.8 ppm. **HRMS** (QToF): Calcd for $C_{55}H_{64}BN_2O_8SNa$ [M + Na]$^+$ 945.4290; found 945.4369.

p-Tolyl 2-*O*-benzoyl-3,4-di-*O*-benzyl-6-*O*-(8-(2,6-diethyl-4,4'-difluoro-1,3,5,7-tetramethyl-4-bora-3a,4a-diaza-*s*-indacenyl)methoxycarbonyl)-1-thio-α-D-mannopyranoside (3.29c)

To a solution of mannose **3.30** (80 mg, 0.14 mmol, 2.0 equiv.) and pyridine (57 µL, 0.70 mmol, 10.0 equiv.) in anhydrous THF (5 mL) **3.31c** (41 mg, 0.07 mmol, 1.0 equiv.) was added in small portions at 0 °C followed by 4-DMAP (1 mg, 0.01 mmol, 0.1 equiv.). The reaction was warmed up to room temperature and was stirred overnight. The reaction mixture was diluted with ethyl acetate and washed with water and brine. The organic phase was dried over Na_2SO_4, filtered, concentrated and purified by flash column chromatography (SiO_2, Hex/EtOAc 9:1 to 3:1) to give compound **3.29c** (45 mg, 0.05 mmol, 69%) as a red foam**.**

R_f = 0.48 (Hex/EtOAc 3:1). **^{1}H NMR** (700 MHz, CDCl$_3$): δ 8.00 – 7.92 (m, 2H), 7.42 (tt, *J* = 7.4, 1.4 Hz, 1H), 7.36 – 7.26 (m, 12H), 7.21 – 7.15 (m, 2H), 7.07 – 7.03 (m, 2H), 5.87 – 5.84 (m, 1H), 5.45 (d, *J* = 2.0 Hz, 1H), 5.38 (s, 2H), 4.86 (dd, *J* = 88.1, 11.0 Hz, 2H), 4.64 – 4.57 (m, 3H), 4.52 (dd, *J* = 11.5, 3.9 Hz, 1H), 4.41 (ddd, *J* = 9.8, 4.0, 2.3 Hz, 1H), 4.05 (dd, *J* = 9.2, 2.8 Hz, 1H), 4.00 (t, *J* = 9.5 Hz, 1H), 2.50 (s, 6H), 2.30 – 2.23 (m, 7H), 2.20 (s, 6H), 0.92 (t, *J* = 7.6 Hz, 6H) ppm. **^{13}C NMR** (176 MHz, CDCl$_3$): δ 165.6, 155.4, 155.0, 138.4, 138.0, 137.6, 136.7, 133.8, 133.6, 132.5, 130.2, 130.1, 129.8, 129.3, 128.6, 128.6, 128.4, 128.3, 128.2, 128.1, 128.0, 86.8, 78.5, 75.6, 74.1, 71.6, 70.9, 70.2, 66.9, 61.4, 21.2, 17.2, 14.7, 12.8, 12.7 ppm. **^{19}F NMR** (659 MHz, CDCl$_3$): δ -145.72 (dd, *J* = 65.6, 32.2 Hz) ppm. **HRMS** (QToF): Calcd for $C_{53}H_{57}BF_2N_2O_8SNa$ [M + Na]$^+$ 953.3789; found 953.3829.

_p_-Tolyl 2-_O_-benzoyl-3,4-di-_O_-benzyl-6-_O_-(8-(2,6-diethyl-4,4'-dicyano-1,3,5,7-tetramethyl-4-bora-3a,4a-diaza-_s_-indacenyl)methoxycarbonyl)-1-thio-α-D-mannopyranoside (3.29d)
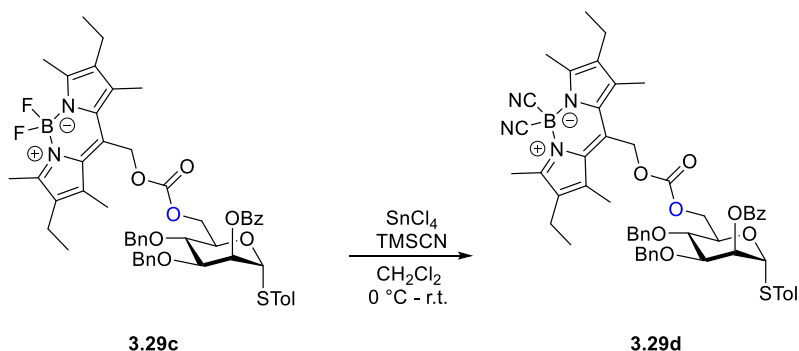
Tin tetrachloride (27 μL, 1 M in CH_2Cl_2) was added at 0 °C to a solution of **3.29c** (50 mg, 0.05 mmol, 1.0 equiv.) and trimethylsilyl cyanide (72 μL, 0.54 mmol, 10.0 equiv.) in anhydrous CH_2Cl_2 (2 mL). The reaction was stirred at room temperature for 2 h and was then quenched with water (1 mL). The mixture was extracted with CH_2Cl_2 (3 x 20 mL) and washed with saturated aqueous $NaHCO_3$ solution and water. The organic layer was dried over Na_2SO_4, filtered, concentrated and the residue was purified by column chromatography (SiO_2, Hex/EtOAc 3:1) to obtain **3.29d** (49 mg, 0.05 mmol, 97%) as a red foam.

R_f = 0.22 (Hex/EtOAc 3:1). **^{1}H NMR** (600 MHz, $CDCl_3$): δ 7.97 – 7.93 (m, 2H), 7.50 (tt, J = 7.5, 1.3 Hz, 1H), 7.38 – 7.32 (m, 4H), 7.32 – 7.26 (m, 8H), 7.17 (t, J = 7.7 Hz, 2H), 7.06 (d, J = 7.9 Hz, 2H), 5.85 (t, J = 2.4 Hz, 1H), 5.45 (d, J = 1.8 Hz, 1H), 5.37 (s, 2H), 4.93 (d, J = 10.8 Hz, 1H), 4.79 (d, J = 11.3 Hz, 1H), 4.66 (dd, J = 11.5, 2.3 Hz, 1H), 4.58 (t, J = 10.6 Hz, 2H), 4.51 (dd, J = 11.5, 3.7 Hz, 1H), 4.41 (dt, J = 10.0, 2.9 Hz, 1H), 4.05 (dd, J = 9.2, 2.8 Hz, 1H), 3.99 (t, J = 9.4 Hz, 1H), 2.66 (s, 6H), 2.30 (q, J = 7.6 Hz, 4H), 2.26 (s, 3H), 2.25 (s, 6H), 0.95 (t, J = 7.6 Hz, 6H) ppm. **^{13}C NMR** (151 MHz, $CDCl_3$): δ 165.5, 155.7, 154.8, 138.4, 138.2, 138.0, 137.5, 135.4, 133.7, 132.4, 131.2, 131.0, 130.1, 129.9, 129.6, 129.3, 128.6, 128.6, 128.3, 128.3, 128.2, 128.1, 128.0, 86.8, 78.4, 75.6, 74.0, 71.6, 70.8, 70.2, 67.0, 60.9, 21.3, 17.3, 14.6, 13.8, 12.8 ppm. **HRMS** (QToF): Calcd for $C_{55}H_{57}BN_4O_8SNa$ [M + Na]$^+$ 967.3882; found 967.3890.

6.3.4 Glycosylation Reactions of BODIPY Photo-cages

**1,2:3,4-Bis-O-(1-methylethylidene)-6-O-[2-*O*-benzoyl-3,4-di-*O*-benzyl-6-*O*-(8-(2,6-diethyl-4,4'-difluoro-1,3,5,7-tetramethyl-4-bora-3a,4a-diaza-*s*-indacenyl)methoxycarbonyl))-α-D-mannopyranosyl]-α-D-galactopyranoside (P4-SL335)**
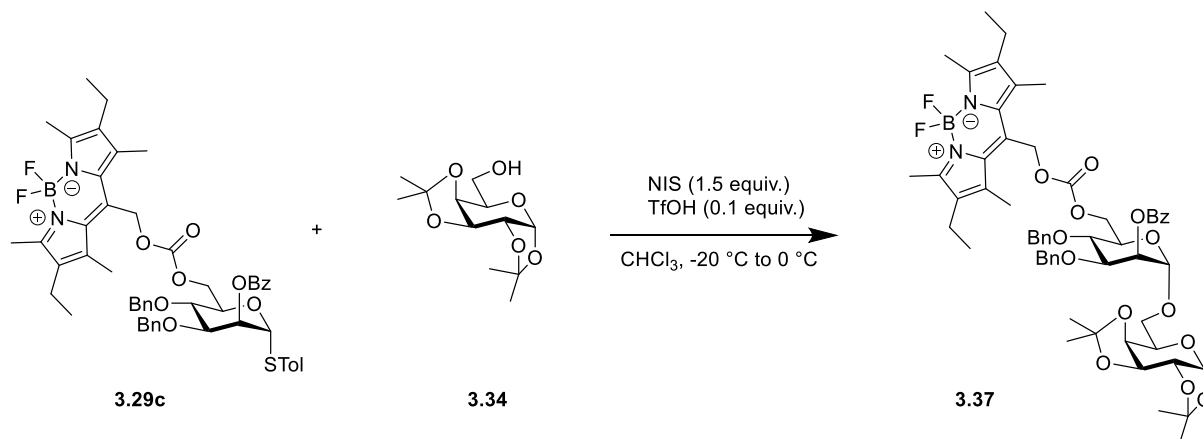
Donor **3.29c** (28.0 mg, 0.03 mmol, 1.0 equiv.) and **3.34** (8.6 mg, 0.03 mmol, 1.0 equiv.) were co-evaporated with anhydrous toluene (3 x 2 mL) and kept under high vacuum for two hours. Anhydrous CH_2Cl_2 (3 mL) was added and the mixture was stirred over activated molecular sieves (3 Å-AW) for 30 minutes at room temperature. The solution was cooled to -20 °C and NIS (10.2 mg, 0.05 mmol, 1.5 equiv.) was added followed by TfOH (20 µL of a 1% solution in CH_2Cl_2, 2 µmol, 0.1 equiv.) and the mixture was stirred for one hour, while it was allowed to warm to 0 °C. The reaction mixture was quenched with pyridine, diluted with CH_2Cl_2, filtered and was then washed with 10% Na_2SO_3 (10 mL). The aqueous phase was extracted with CH_2Cl_2 (3 x 10 mL), dried over Na_2SO_4 and concentrated. The residue was purified by column chromatography (SiO_2, Hex/EtOAc 9:1 to 3:1) to obtain compound **3.37** (27 mg, 0.03 mmol, 84%) as a red foam.

R*$_f$* = 0.18 (Hex/EtOAc 3:1). **^{1}H NMR** (600 MHz, $CDCl_3$): δ 7.98 – 7.89 (m, 2H), 7.44 – 7.08 (m, 13H), 5.66 – 5.62 (m, 1H), 5.51 (d, *J* = 4.9 Hz, 1H), 5.43 – 5.32 (m, 2H), 4.93 (d, *J* = 2.2 Hz, 1H), 4.90 – 4.74 (m, 3H), 4.70 – 4.46 (m, 5H), 4.32 (ddd, *J* = 5.0, 2.5, 0.8 Hz, 1H), 4.22 (dd, *J* = 7.9, 1.8 Hz, 1H), 4.11 (dd, *J* = 9.4, 2.8 Hz, 1H), 4.03 – 3.89 (m, 2H), 3.81 (dd, *J* = 10.4, 6.4 Hz, 1H), 3.75 – 3.68 (m, 1H), 2.48 (s, 6H), 2.27 – 2.17 (m, 10H), 1.52 (s, 3H), 1.42 (s, 3H), 1.34 (s, 3H), 1.33 (s, 3H), 0.91 (t, *J* = 7.7 Hz, 6H) ppm. **^{13}C NMR** (151 MHz, $CDCl_3$): δ 165.6, 155.3, 155.2, 138.2, 138.0, 136.7, 133.8, 133.5, 132.5, 129.8, 129.1, 128.5, 128.4, 128.3, 128.2, 128.1, 128.0, 127.8, 109.6, 108.8, 98.1, 96.4, 78.1, 75.5, 73.7, 71.5, 71.0, 70.7, 70.3, 68.4, 66.8, 66.6, 66.2, 61.4, 26.3, 26.1, 25.0, 24.6, 17.2, 14.7, 12.6 ppm. **^{19}F NMR** (564 MHz, $CDCl_3$): δ -145.71 (dd, *J* = 65.4, 31.1 Hz) ppm. **HRMS** (QToF): Calcd for $C_{58}H_{69}BF_2N_2O_{14}Na$ [M + Na]$^+$ 1089.4702; found 1089.5118.

1,2:3,4-Bis-*O*-(1-methylethylidene)-6-*O*-[2-*O*-benzoyl-3,4-di-*O*-benzyl-6-*O*-(8-(2,6-diethyl-4,4'-dicyano-1,3,5,7-tetramethyl-4-bora-3a,4a-diaza-*s*-indacenyl)methoxycarbonyl))-α-D-mannopyranosyl]-α-D-galactopyranoside (3.36)
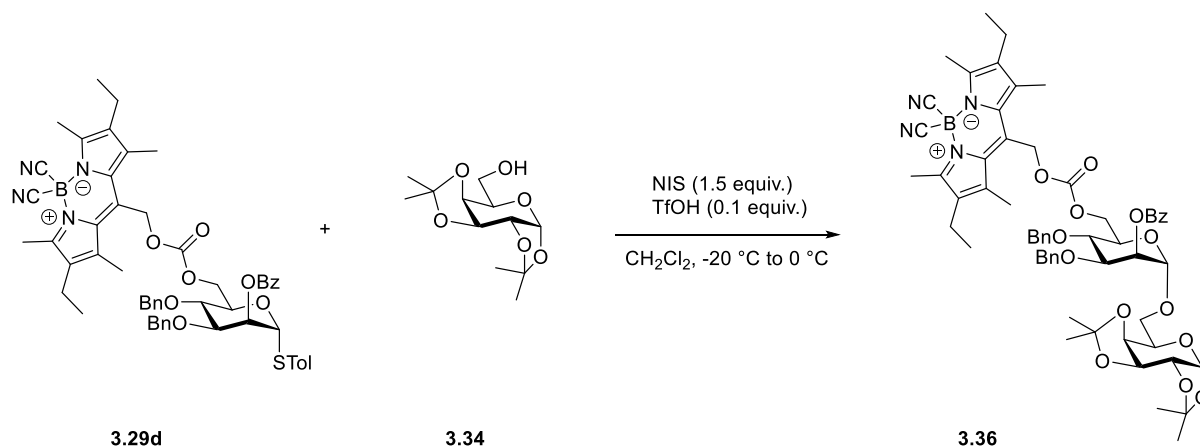
Donor **3.29d** (17.0 mg, 0.02 mmol, 1.0 equiv.) and **3.34** (4.7 mg, 0.02 mmol, 1.0 equiv.) were co-evaporated with anhydrous toluene (3 x 2 mL) and kept under high vacuum for two hours. Anhydrous CH_2Cl_2 (2 mL) was added and the mixture was stirred over activated molecular sieves (3 Å-AW) for 30 minutes at room temperature. The solution was cooled to -20 °C and NIS (6.1 mg, 0.03 mmol, 1.5 equiv.) was added followed by TfOH (2 µL of a 1% solution in CH_2Cl_2, 2 µmol, 0.1 equiv.) and the mixture was stirred for three hours, while it was allowed to warm to 0 °C. The reaction mixture was quenched with pyridine, diluted with CH_2Cl_2, filtered and was then washed with 10% Na_2SO_3 (10 mL). The aqueous phase was extracted with CH_2Cl_2 (3 x 10 mL), dried over Na_2SO_4 and concentrated. The residue was purified by column chromatography (SiO_2, Hex/EtOAc 9:1 to 1:1) to obtain compound **3.36** (17.5 mg, 0.02 mmol, 90%) as a red foam.

R*$_f$* = 0.10 (Hex/EtOAc 3:1). **^{1}H NMR** (400 MHz, CDCl$_3$): δ 7.94 (dd, *J* = 8.3, 1.3 Hz, 2H), 7.50 (s, 1H), 7.38 – 7.19 (m, 10H), 7.17 – 7.08 (m, 2H), 5.68 – 5.61 (m, 1H), 5.51 (d, *J* = 5.0 Hz, 1H), 5.43 – 5.28 (m, 2H), 4.95 – 4.84 (m, 2H), 4.82 – 4.44 (m, 6H), 4.32 (dd, *J* = 5.0, 2.4 Hz, 1H), 4.23 (dd, *J* = 7.9, 1.9 Hz, 1H), 4.16 – 4.07 (m, 1H), 4.02 – 3.67 (m, 5H), 2.65 (s, 6H), 2.35 – 2.21 (m, 10H), 1.53 (s, 3H), 1.42 (s, 3H), 1.34 (s, 3H), 1.33 (s, 3H), 0.95 (t, *J* = 7.6 Hz, 6H) ppm. **^{13}C NMR** (101 MHz, CDCl$_3$): δ 165.5, 155.7, 155.0, 138.2, 138.1, 137.9, 135.3, 133.7, 131.0, 130.0, 129.8, 129.2, 128.5, 128.4, 128.3, 128.2, 128.1, 128.0, 127.8, 109.5, 108.8, 98.1, 96.4, 78.0, 75.5, 73.7, 71.5, 71.0, 70.7, 70.2, 68.5, 66.9, 66.2, 60.9, 26.3, 26.1, 25.0, 24.6, 17.3, 14.6, 13.8, 12.8 ppm. **HRMS** (QToF): Calcd for $C_{60}H_{69}BN_4O_{14}Na$ [M + Na]$^+$ 1103.4796; found 1103.4791.

2-*O*-Benzoyl-3,4-di-*O*-benzyl-6-*O*-(8-(2,6-diethyl-4,4'-difluoro-1,3,5,7-tetramethyl-4-bora-3a,4a-diaza-s-indacenyl)methoxycarbonyl))-α-D-mannopyranosyl-(1→6)-2-*O*-benzoyl-3,4-di-*O*-benzyl-6-*O*-α-D-mannopyranosyl-(1→6)-1,2:3,4-bis-*O*-(1-methylethylidene)-α-D-galactopyranoside (3.38)
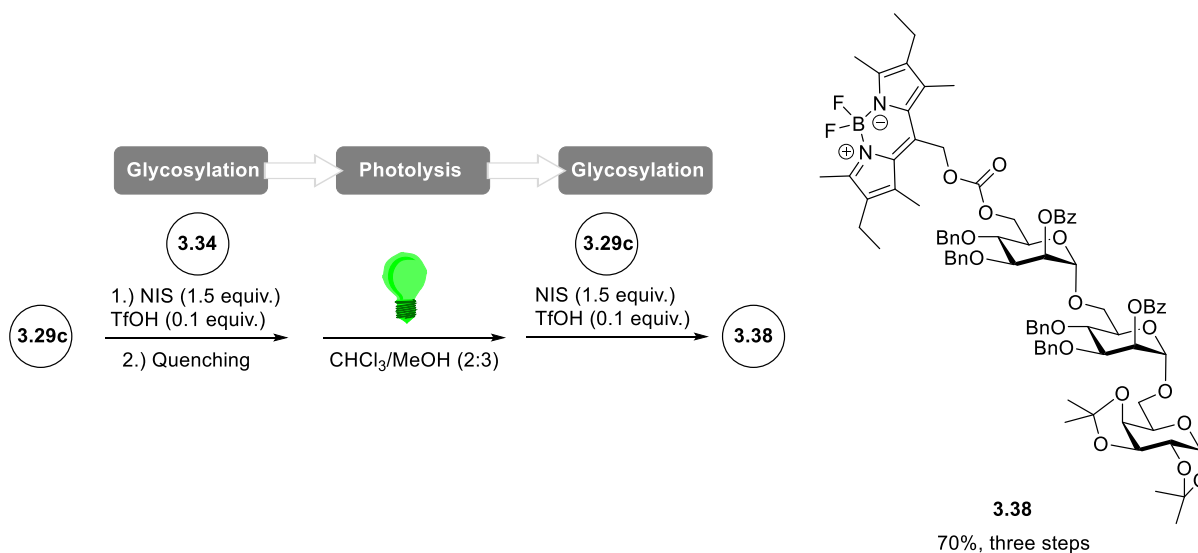
3.38
70%, three steps

Donor **3.29c** (28.0 mg, 0.03 mmol, 1.0 equiv.) and **3.34** (8.6 mg, 0.03 mmol, 1.0 equiv.) were co-evaporated with anhydrous toluene (3 x 2 mL) and kept under high vacuum for two hours. Anhydrous CH_2Cl_2 (4 mL) was added and the solution was cooled to -20 °C. NIS (18.2 mg, 0.08 mmol, 1.5 equiv.) was added followed by TfOH (48 µL of a 1% solution in CH_2Cl_2, 5 µmol, 0.1 equiv.) and the mixture was stirred for one hour, while it was allowed to warm to 0 °C. The reaction mixture was quenched with pyridine, filtered over a small plug of silica and the volatiles were removed under reduced pressure. The residue was redissolved in 5 mL of $CHCl_3$/MeOH (2:3) and was stirred for 3 h irradiated by green light from a LED lamp. Volatiles were removed under reduced pressure, donor **3.29c** (65 mg, 0.07 mmol, 1.3 equiv.) was added and the residue co-evaporated with anhydrous toluene (3 x 2 mL). Anhydrous CH_2Cl_2 (4 mL) was added and the solution was cooled to -20 °C. NIS (18.2 mg, 0.08 mmol, 1.5 equiv.) was added followed by TfOH (48 µL of a 1% solution in CH_2Cl_2, 5 µmol, 0.1 equiv.) and the mixture was stirred for one hour, while it was allowed to warm to 0 °C. The reaction mixture was quenched with pyridine, filtered over a small plug of silica and washed with 10% Na_2SO_3 (10 mL). The aqueous phase was extracted with CH_2Cl_2 (3 x 10 mL), dried over Na_2SO_4 and concentrated. The residue was purified by column chromatography (SiO_2, Hex/EtOAc 4:1 to 3:1) to obtain compound **3.38** (57 mg, 0.04 mmol, 70%) as a red foam.

R_f = 0.17 (Hex/EtOAc 3:1). **¹H NMR** (600 MHz, $CDCl_3$): δ 8.16 – 8.12 (m, 2H), 7.94 (dt, *J* = 8.4, 1.4 Hz, 2H), 7.52 – 7.47 (m, 3H), 7.40 – 7.01 (m, 23H), 5.78 (t, *J* = 2.5 Hz, 1H), 5.71 (dd, *J* = 3.3, 1.8 Hz, 1H), 5.51 (dd, *J* = 5.1, 1.9 Hz, 1H), 5.42 – 5.31 (m, 2H), 5.04 (d, *J* = 2.1 Hz, 1H), 4.99 (d, *J* = 1.8 Hz, 1H), 4.91 – 4.83 (m, 3H), 4.74 (d, *J* = 11.4 Hz, 1H), 4.65 – 4.49 (m, 4H),

4.41 (dd, J = 30.0, 11.4 Hz, 2H), 4.35 – 4.23 (m, 3H), 4.11 (d, J = 5.6 Hz, 1H), 4.09 – 4.02 (m, 2H), 4.01 – 3.91 (m, 3H), 3.84 – 3.78 (m, 2H), 3.72 (dt, J = 10.3, 5.7 Hz, 3H), 2.48 (s, 6H), 2.20 (d, J = 8.4 Hz, 10H), 1.54 (s, 3H), 1.43 (s, 3H), 1.33 (s, 3H), 1.32 (s, 3H), 0.91 – 0.85 (m, 6H) ppm. **^{13}C NMR** (151 MHz, CDCl$_3$): δ 165.8, 165.4, 155.3, 155.2, 138.5, 138.3, 138.1, 137.7, 136.7, 133.8, 133.5, 133.5, 132.5, 130.1, 130.0, 129.8, 128.8, 128.4, 128.4, 128.4, 128.3, 128.2, 128.1, 128.1, 127.8, 127.8, 127.6, 127.5, 109.6, 108.8, 98.4, 98.1, 96.4, 78.7, 77.8, 75.4, 75.2, 74.2, 73.5, 71.8, 71.0, 71.0, 70.7, 70.4, 69.0, 68.0, 66.6, 66.3, 66.1, 61.4, 32.1, 29.9, 26.3, 26.1, 25.0, 24.6, 22.8, 17.1, 14.7, 14.3, 12.8, 12.6 ppm. **^{19}F NMR** (564 MHz, CDCl$_3$): δ -145.69 (dd, J = 65.6, 30.2 Hz) ppm. **HRMS** (QToF): Calcd for C$_{85}$H$_{95}$BF$_2$N$_2$O$_{20}$Na [M + Na]$^+$ 1535.6432; found 1535.6710.

6.3.5 Photo-deprotections BODIPY Photo-cages 3.29a-d

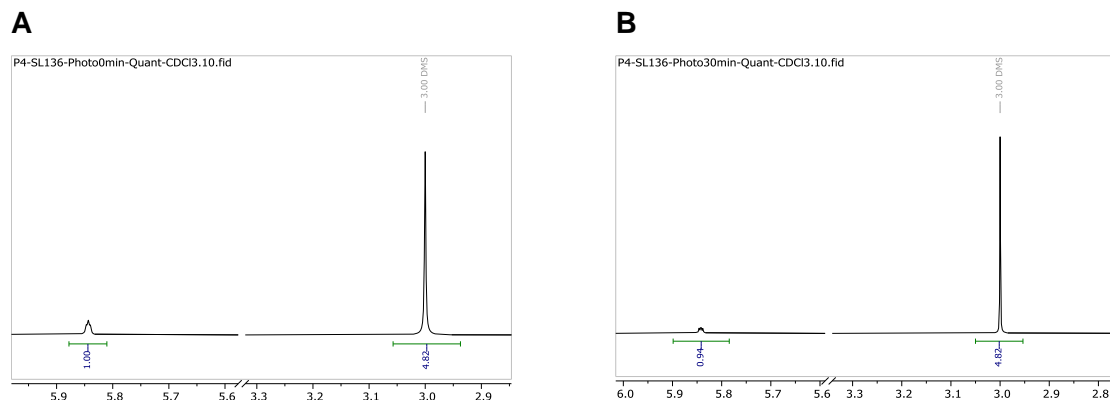### Photo-deprotection of 3.29a in CDCl₃ (500 W halogen lamp)

A

B

Figure S1. (**A**) Extract from ^{1}H-NMR-spectrum in CDCl$_3$ of **3.29a** before photo-deprotection for quantification. Dimethylsulfone DMS (6H) in relation to H-2 of **3.29a** (1H). (**B**) Extract from ^{1}H-NMR-spectrum in CDCl$_3$ of deprotected **3.29a** after 30 min photo-deprotection for quantification. Dimethylsulfone DMS (6H) in relation to H-2 of deprotected **3.29a** (1H) results in a yield of 94%.
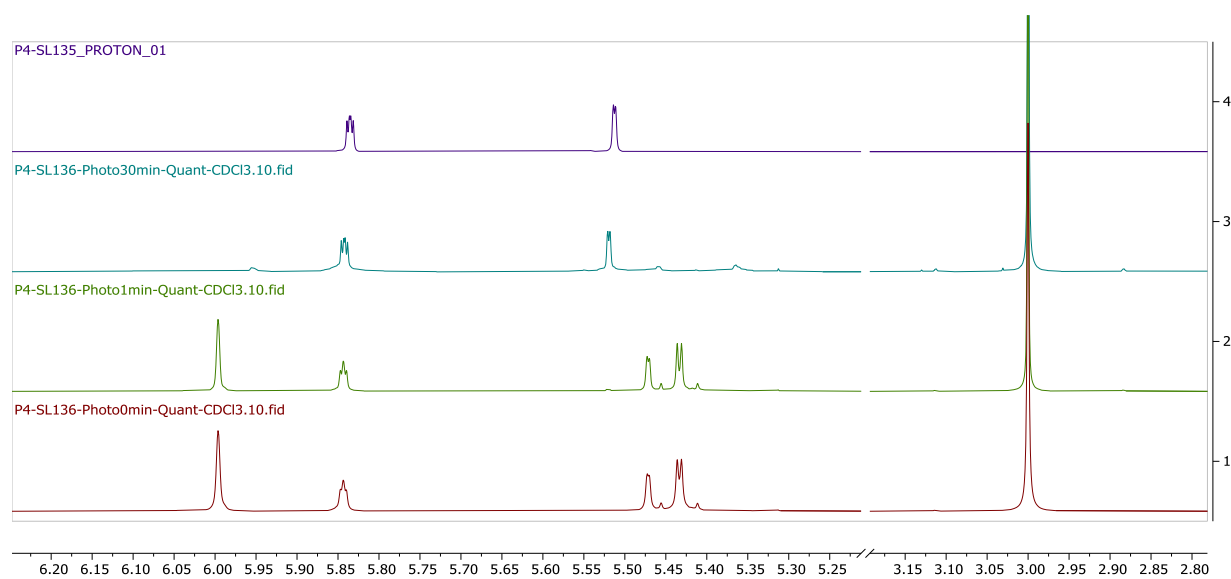
Figure S2. Zoom of stacked ^{1}H-NMR-spectra in CDCl$_3$ before (1), after 1 min (2) and 30 min (3) photo-deprotection of **3.29a** and reference-spectrum of the deprotected sugar (4).
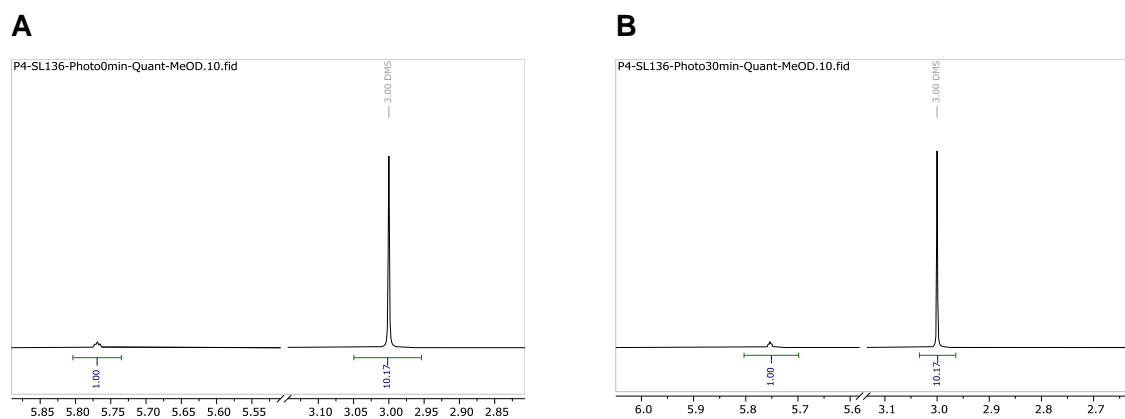
Photo-deprotection of 3.29a in MeOD (500 W halogen lamp)

A

B

Figure S3. (**A**) Extract from ^{1}H-NMR-spectrum in MeOD of **3.29a** before photo-deprotection for quantification. Dimethylsulfone DMS (6H) in relation to H-2 of **3.29a** (1H). (**B**) Extract from ^{1}H-NMR-spectrum in MeOD of deprotected **3.29a** after 30 min photo-deprotection for quantification. Dimethylsulfone DMS (6H) in relation to H-2 of deprotected **3.29a** (1H) results in a yield of 100%.
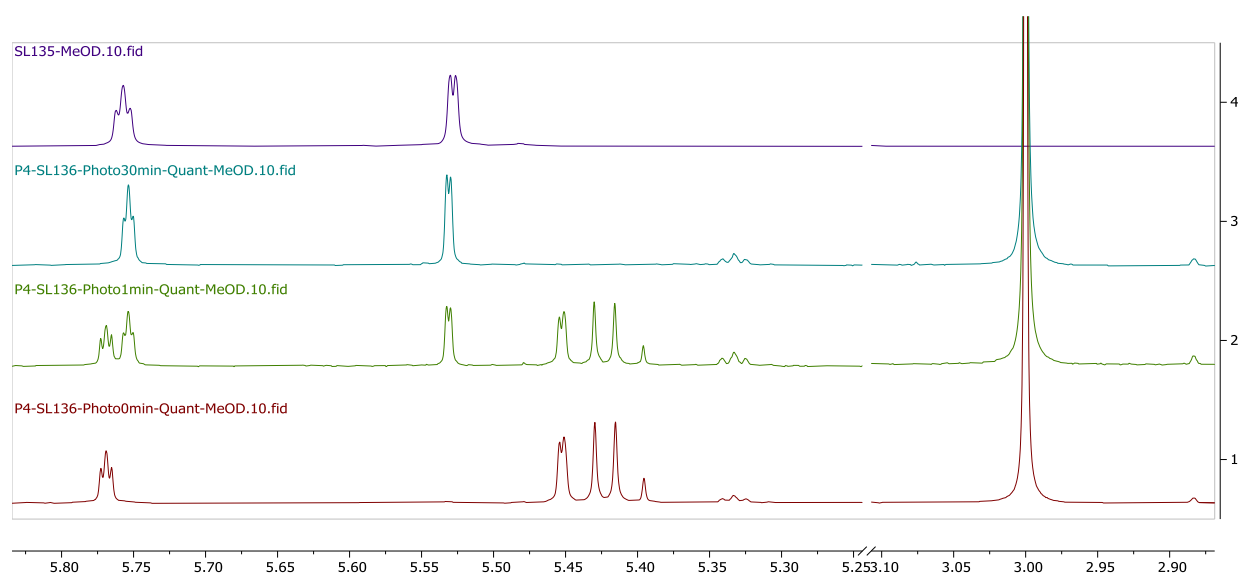

Figure S4. Zoom of stacked ^{1}H-NMR-spectra in MeOD before (1), after 1 min (2) and 30 min (3) photo-deprotection of **3.29a** and reference-spectrum of the deprotected sugar (4).
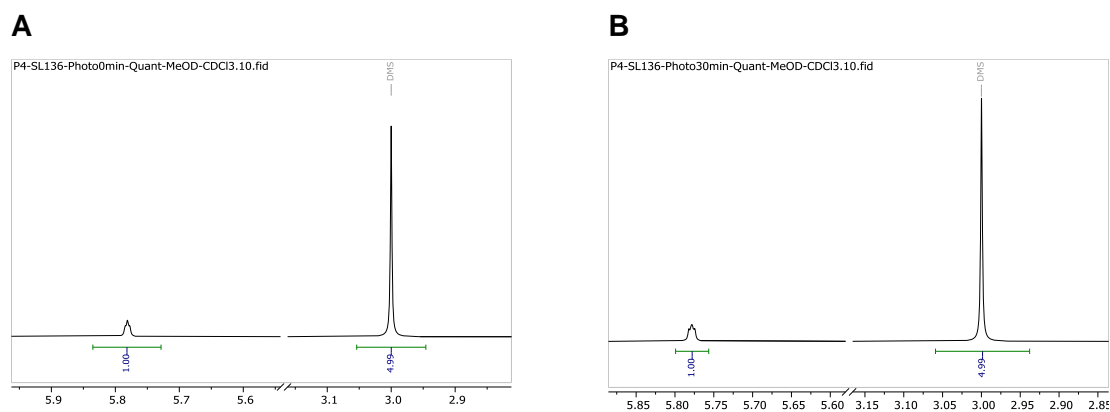
Photo-deprotection of 3.29a in MeOD:CDCl₃ (1:2) (500 W halogen lamp)

A

B

Figure S5. (**A**) Extract from ¹H-NMR-spectrum in MeOD:CDCl₃ (1:2) of **3.29a** before photo-deprotection for quantification. Dimethylsulfone DMS (6H) in relation to H-2 of **3.29a** (1H). (**B**) Extract from ¹H-NMR-spectrum in MeOD:CDCl₃ (1:2) of deprotected **3.29a** after 30 min photo-deprotection for quantification. Dimethylsulfone DMS (6H) in relation to H-2 of deprotected **3.29a** (1H) results in a yield of 100%.
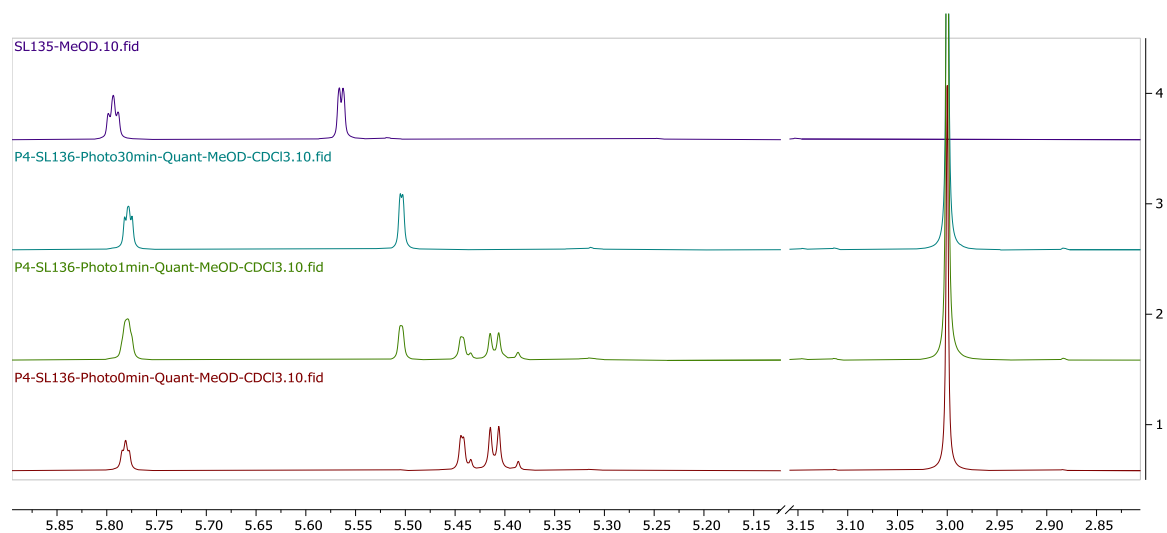

Figure S6. Zoom of stacked ¹H-NMR-spectra in MeOD:CDCl₃ (1:2) before (1), after 1 min (2) and 30 min (3) photo-deprotection of **3.29a** and reference-spectrum of the deprotected sugar (4).
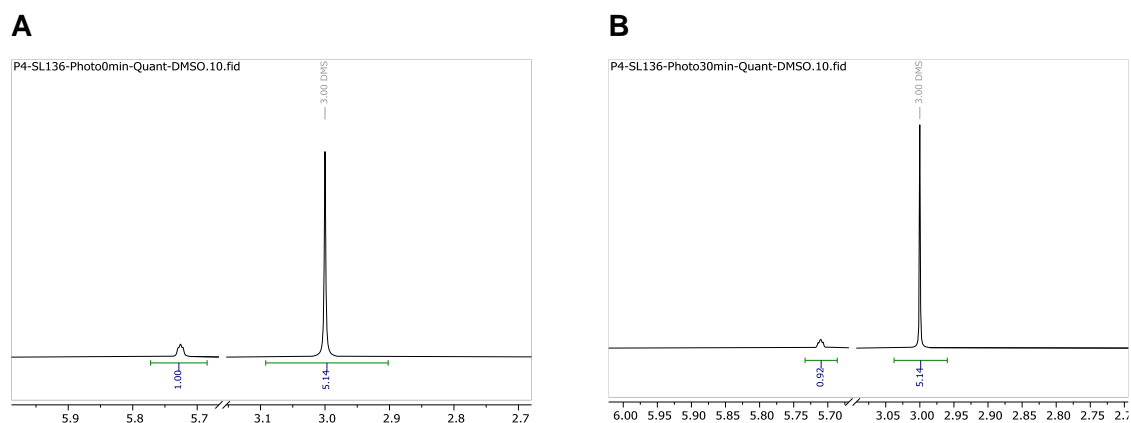
Photo-deprotection of 3.29a in DMSO (500 W halogen lamp)

A

B

Figure S7. (**A**) Extract from ^{1}H-NMR-spectrum in DMSO of **3.29a** before photo-deprotection for quantification. Dimethylsulfone DMS (6H) in relation to H-2 of **3.29a** (1H). (**B**) Extract from ^{1}H-NMR-spectrum in DMSO of deprotected **3.29a** after 30 min photo-deprotection for quantification. Dimethylsulfone DMS (6H) in relation to H-2 of deprotected **3.29a** (1H) results in a yield of 92%.
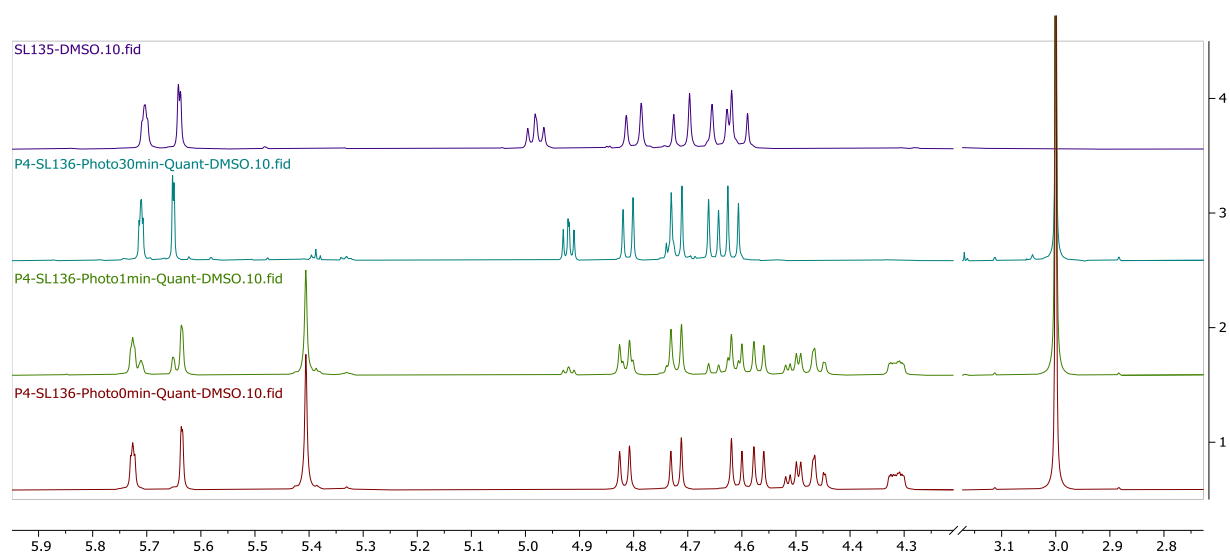

Figure S8. Zoom of stacked ^{1}H-NMR-spectra in DMSO before (1), after 1 min (2) and 30 min (3) photo-deprotection of **3.29a** and reference-spectrum of the deprotected sugar (4).
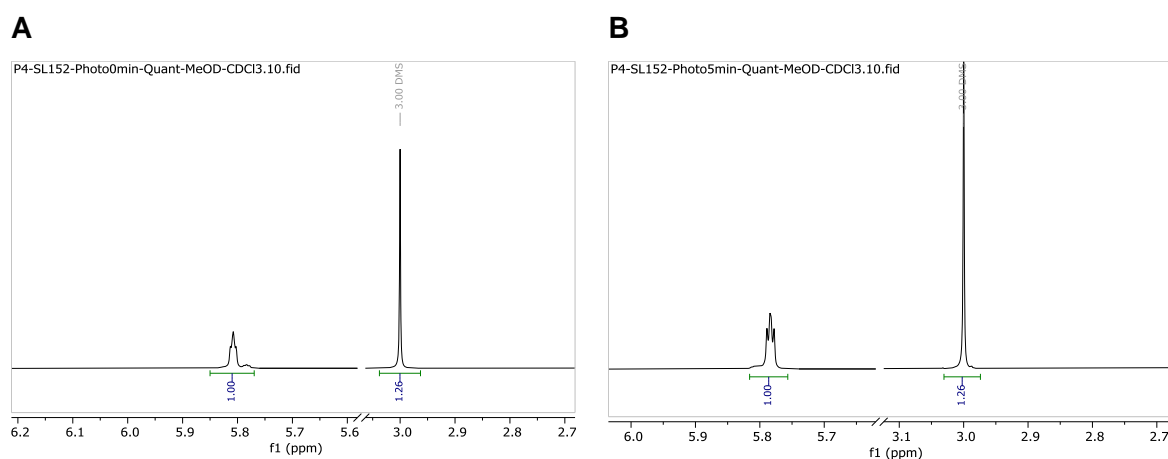
Photo-deprotection of 3.29b in MeOD:CDCl₃ (1:2) (500 W halogen lamp)

A

B

Figure S9. (**A**) Extract from ¹H-NMR-spectrum in MeOD:CDCl₃ (1:2) of **3.29b** before photo-deprotection for quantification. Dimethylsulfone DMS (6H) in relation to H-2 of **3.29b** (1H). (**B**) Extract from ¹H-NMR-spectrum in MeOD:CDCl₃ (1:2) of deprotected **3.29b** after 5 min photo-deprotection for quantification. Dimethylsulfone DMS (6H) in relation to H-2 of deprotected **3.29b** (1H) results in a yield of 100%.

Figure S10. Zoom of stacked ¹H-NMR-spectra in MeOD:CDCl₃ (1:2) before (1), after 1 min (2) and 5 min (3) photo-deprotection of **3.29b**.

Photo-deprotection of 3.29b in MeOD:CDCl$_3$ (1:2) (green LED lamp)
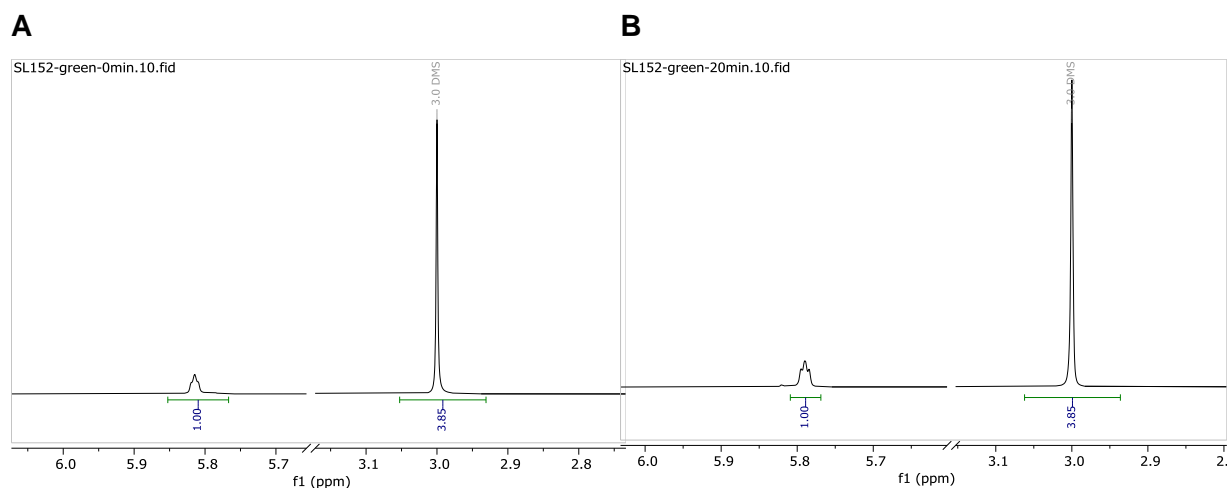
Figure S11. (**A**) Extract from ^{1}H-NMR-spectrum in MeOD:CDCl$_3$ (1:2) of **3.29b** before photo-deprotection for quantification. Dimethylsulfone DMS (6H) in relation to H-2 of **3.29b** (1H). (**B**) Extract from ^{1}H-NMR-spectrum in MeOD:CDCl$_3$ (1:2) of deprotected **3.29b** after 20 min photo-deprotection for quantification. Dimethylsulfone DMS (6H) in relation to H-2 of deprotected **3.29b** (1H) results in a yield of 100%.
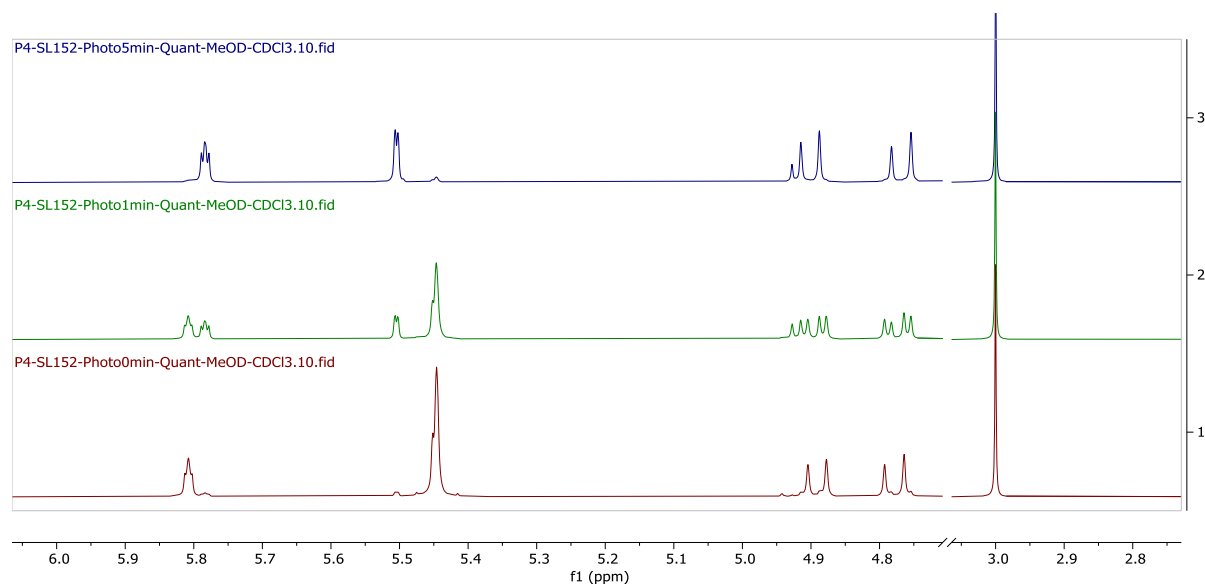

Figure S12. Zoom of stacked ^{1}H-NMR-spectra in MeOD:CDCl$_3$ (1:2) before (1), after 1 min (2), after 5 min (3), after 10 min (4) and 20 min (5) photo-deprotection of **3.29b**.

Photo-deprotection of 3.29c in MeOD:CDCl₃ (3:2) (500 W halogen lamp)

A

B

Figure S13. (**A**) Extract from ^{1}H-NMR-spectrum in MeOD:CDCl$_3$ (3:2) of **3.29c** before photo-deprotection for quantification. Dimethylsulfone DMS (6H) in relation to H-2 of **3.29c** (1H). (**B**) Extract from ^{1}H-NMR-spectrum in MeOD:CDCl$_3$ (1:2) of deprotected **3.29c** after 30 min photo-deprotection for quantification. Dimethylsulfone DMS (6H) in relation to H-2 of deprotected **3.29c** (1H) results in a yield of 16%.

Figure S14. Zoom of stacked ^{1}H-NMR-spectra in MeOD:CDCl$_3$ (3:2) before (1), after 1 min (2), after 5 min (3), after 15 min (4) and after 30 min (5) photo-deprotection of **3.29c**.

Photo-deprotection of 3.29c in MeOD:CDCl₃ (3:2) (green LED lamp)

A

B
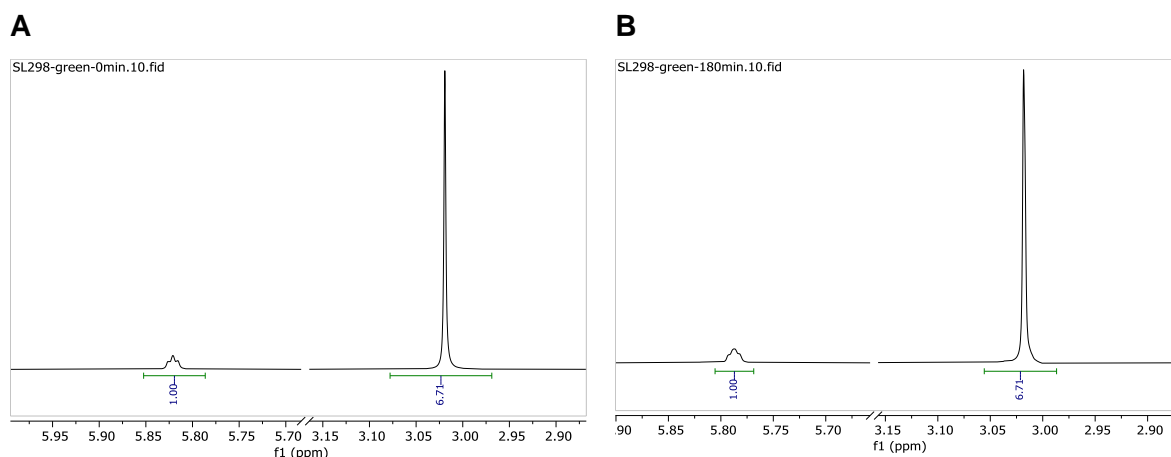
Figure S15. (**A**) Extract from ¹H-NMR-spectrum in MeOD:CDCl₃ (3:2) of **3.29c** before photo-deprotection for quantification. Dimethylsulfone DMS (6H) in relation to H-2 of **3.29c** (1H). (**B**) Extract from ¹H-NMR-spectrum in MeOD:CDCl₃ (1:2) of deprotected **3.29c** after 180 min photo-deprotection for quantification. Dimethylsulfone DMS (6H) in relation to H-2 of deprotected **3.29c** (1H) results in a yield of 100%.
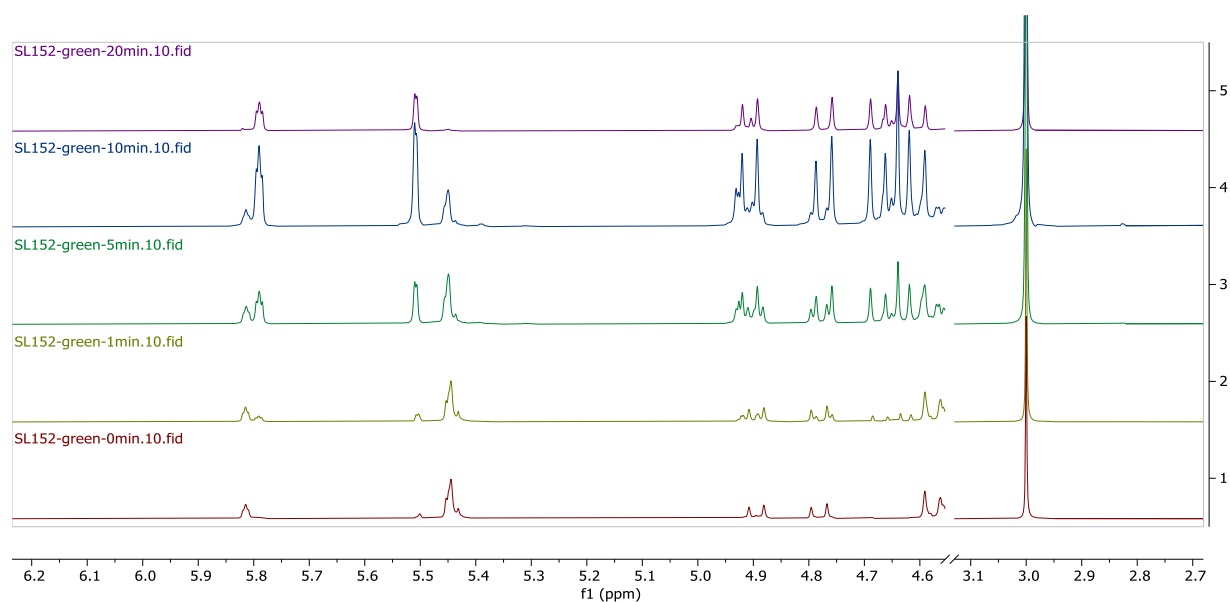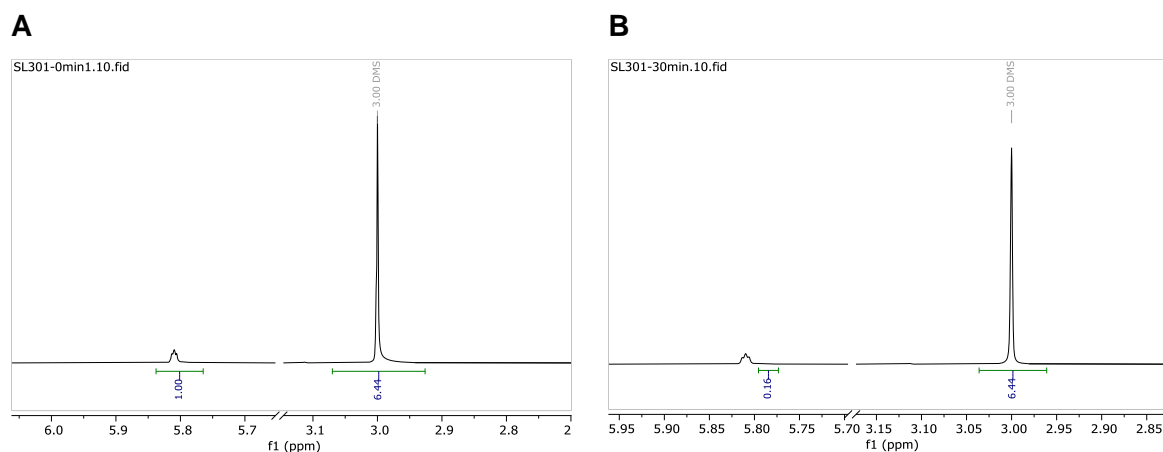

Figure S16. Zoom of stacked ¹H-NMR-spectra in MeOD:CDCl₃ (3:2) before (1), after 1 min (2), after 10 min (3), after 60 min (4), after 120 min (5) and after 180 min (6) photo-deprotection of **3.29c**.

Photo-deprotection of 3.29d in MeOD:CDCl₃ (3:2) (500 W halogen lamp)

A

B
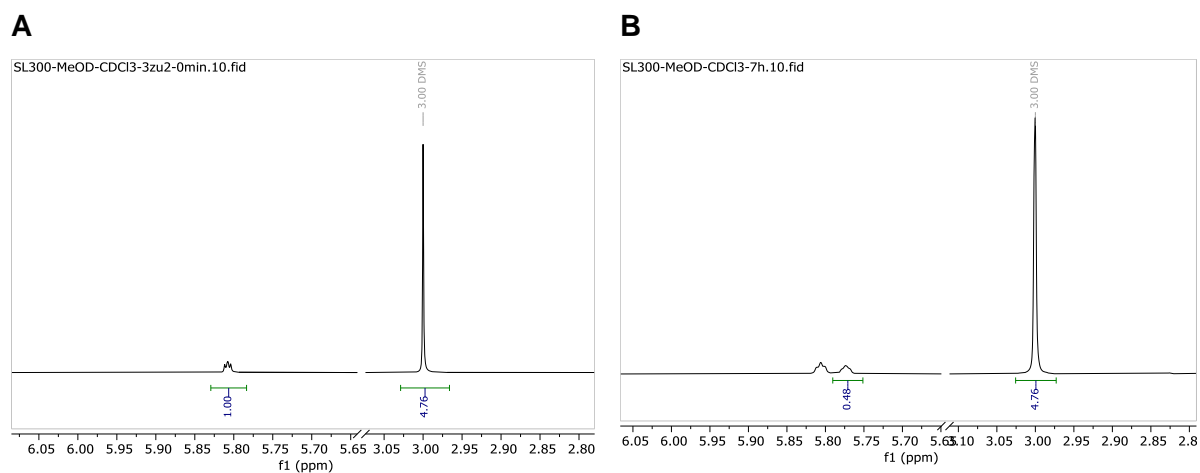
Figure S17. (**A**) Extract from ^{1}H-NMR-spectrum in MeOD:CDCl₃ (3:2) of **3.29d** before photo-deprotection for quantification. Dimethylsulfone DMS (6H) in relation to H-2 of **3.29d** (1H). (**B**) Extract from ^{1}H-NMR-spectrum in MeOD:CDCl₃ (1:2) of deprotected **3.29d** after 7 h photo-deprotection for quantification. Dimethylsulfone DMS (6H) in relation to H-2 of deprotected **3.29d** (1H) results in a yield of 48%.
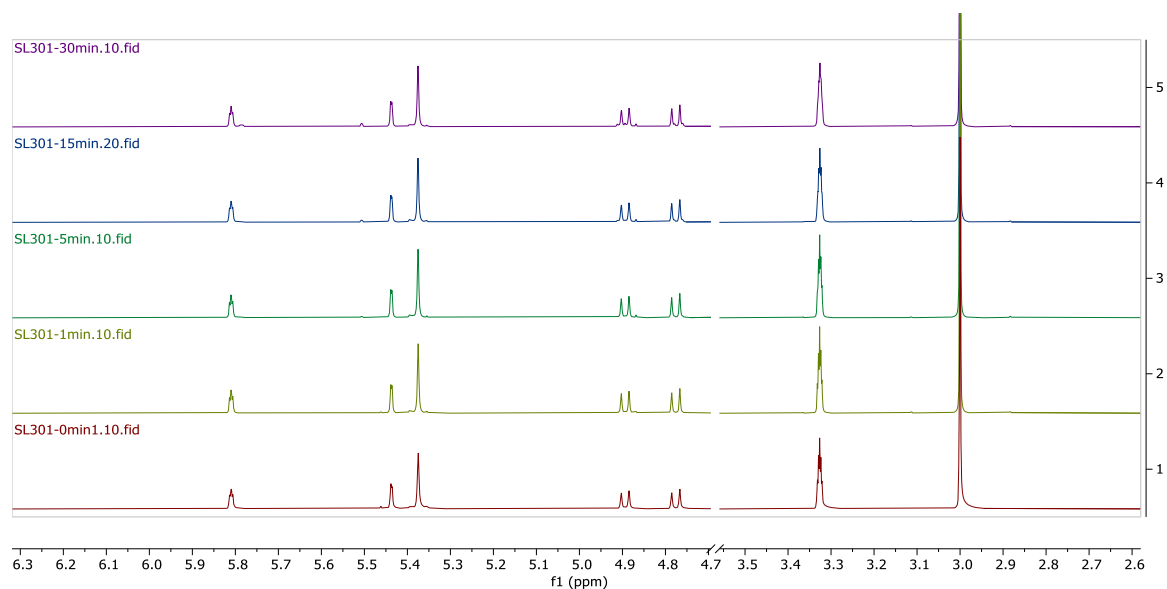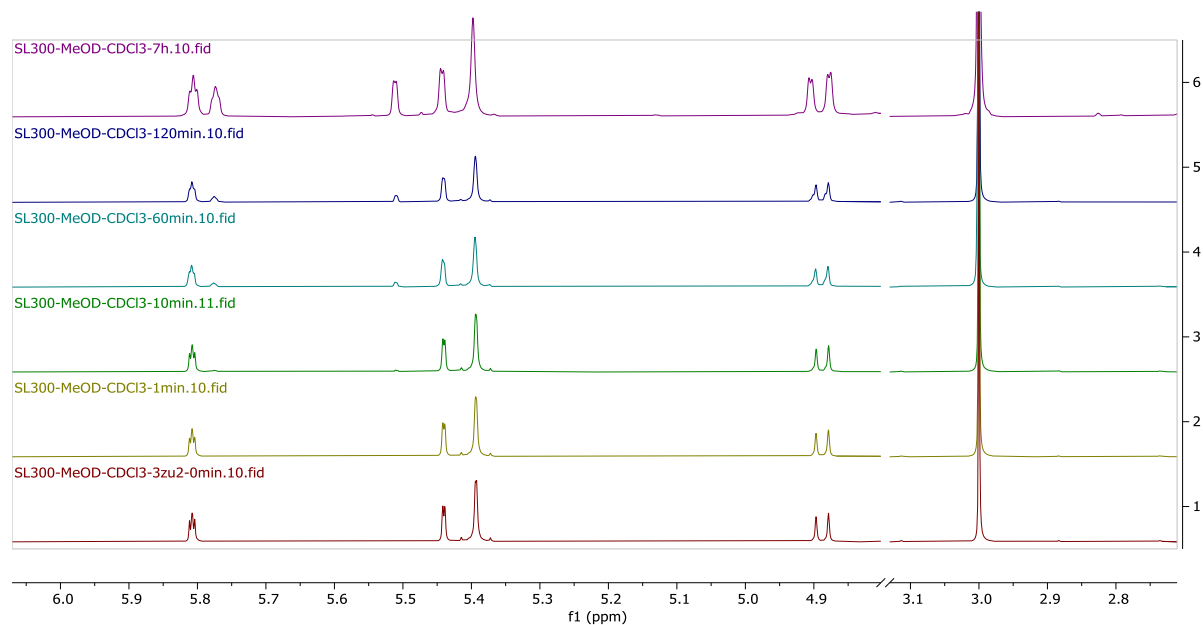

Figure S18. Zoom of stacked ^{1}H-NMR-spectra in MeOD:CDCl₃ (3:2) before (1), after 1 min (2), after 10 min (3), after 60 min (4), after 120 min (5) and after 7 h (6) photo-deprotection of **3.29d**.

Photo-deprotection of 3.29d in MeOD:CDCl$_3$ (3:2) (green LED lamp)

A

B
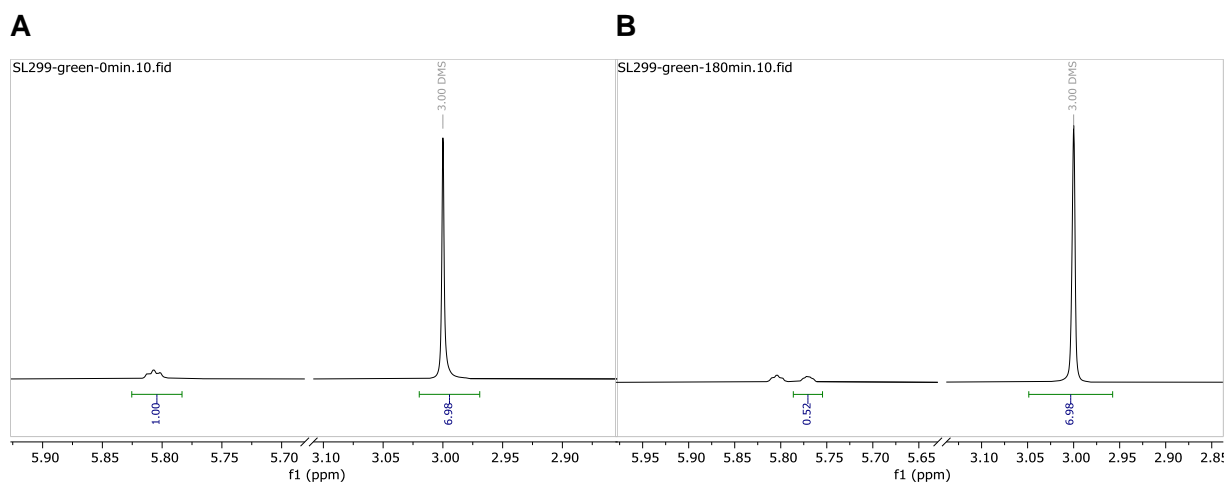
Figure S19. (**A**) Extract from ^{1}H-NMR-spectrum in MeOD:CDCl$_3$ (3:2) of **3.29d** before photo-deprotection for quantification. Dimethylsulfone DMS (6H) in relation to H-2 of **3.29d** (1H). (**B**) Extract from ^{1}H-NMR-spectrum in MeOD:CDCl$_3$ (1:2) of deprotected **3.29d** after 180 min photo-deprotection for quantification. Dimethylsulfone DMS (6H) in relation to H-2 of deprotected **3.29d** (1H) results in a yield of 52%.
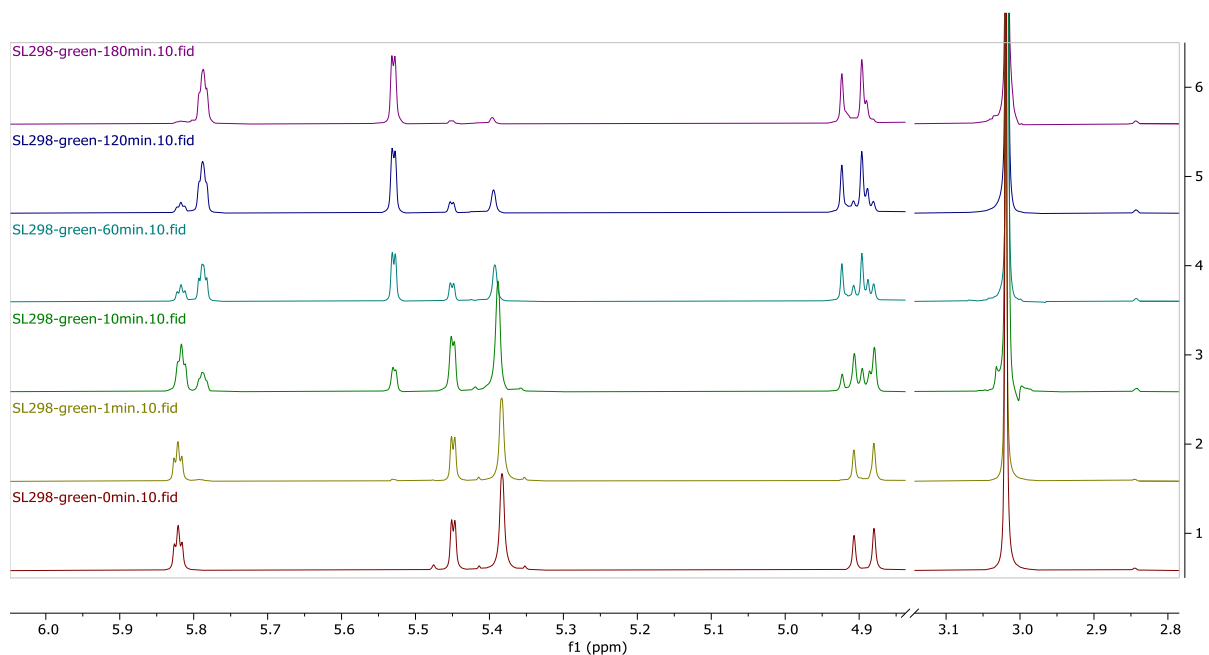

Figure S20. Zoom of stacked ^{1}H-NMR-spectra in MeOD:CDCl$_3$ (3:2) before (1), after 1 min (2), after 5 min (3), after 10 min (4), after 40 min (5), after 60 min (6) and after 180 min (7) photo-deprotection of **3.29d**.
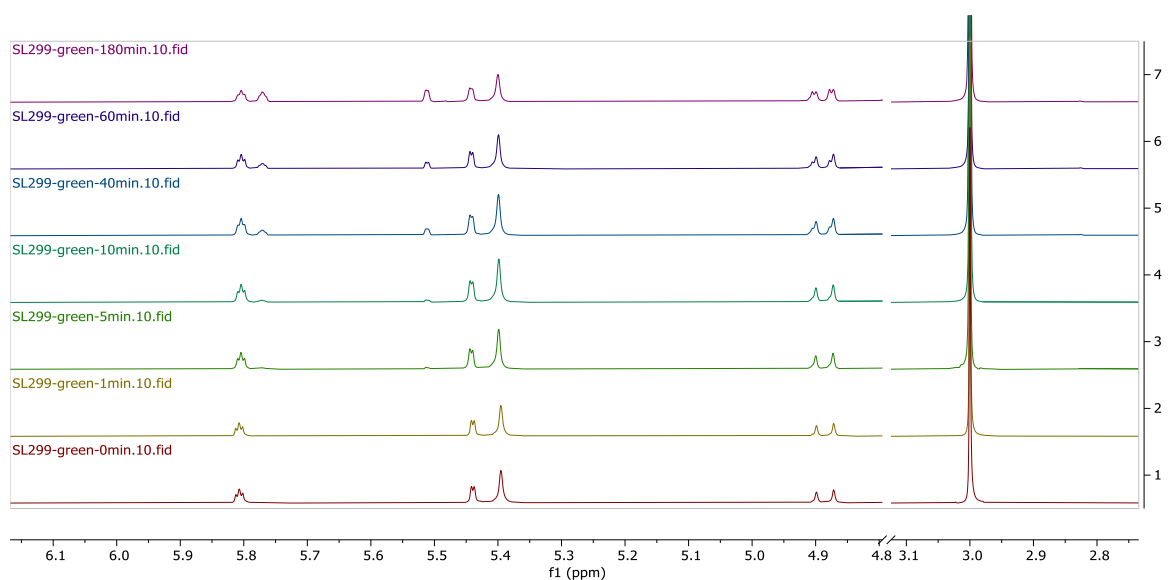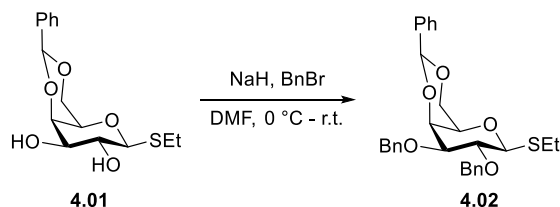
115

6.4 Preparation and Characterization of Compounds in Chapter 4

6.4.1 Synthesis of Building Blocks

Ethyl 2,3-bis-*O*-benzyl-4,6-*O*-[(*S*)-phenylmethylene]-1-thio-β-D-galactopyranoside[144] (4.02)

Galactose building block **4.01** (2.5 g, 8.00 mmol, 1.0 eq.) was dissolved in anhydrous DMF (15 mL). The stirred solution was cooled to 0 °C and sodium hydride (1.5 g, 37.61 mmol; 60% dispersion in mineral oil, 4.7 eq.) was added in small portions. After 30 min, benzyl bromide (2.85 mL, 24.01 mmol, 3.0 eq.) was added dropwise. The reaction mixture was allowed to warm to room temperature and was stirred overnight. Methanol (10 mL) was added, the reaction mixture was stirred for 10 min and afterwards diluted with EtOAc (50 mL). The organic layer was washed with water (2 x 30 mL). The aqueous phase was extracted with ethyl acetate (2 x 40 mL). The combined organic phase was washed with water (30 mL) followed by brine (30 mL), dried over Na_2SO_4 and concentrated. Product **4.02** (3.8 g, 7.71 mmol, 96%) was obtained as a colorless syrup after purification by column chromatography (SiO_2, Hex/EtOAc 9:1).

¹H NMR (400 MHz, $CDCl_3$) δ 7.58 – 7.51 (m, 2H), 7.46 – 7.28 (m, 13H), 5.48 (s, 1H), 4.93 – 4.83 (m, 2H), 4.76 (d, *J* = 2.0 Hz, 2H), 4.44 (d, *J* = 9.6 Hz, 1H), 4.31 (dd, *J* = 12.4, 1.6 Hz, 1H), 4.16 (dd, *J* = 3.6, 1.1 Hz, 1H), 3.97 (dd, *J* = 12.4, 1.8 Hz, 1H), 3.90 (t, *J* = 9.4 Hz, 1H), 3.60 (dd, *J* = 9.2, 3.5 Hz, 1H), 3.36 (q, *J* = 1.5 Hz, 1H), 2.92 – 2.70 (m, 2H), 1.34 (t, *J* = 7.5 Hz, 3H) ppm. **¹³C NMR** (101 MHz, $CDCl_3$) δ 138.5, 138.4, 138.0, 129.2, 128.5, 128.5, 128.3, 127.9, 127.9, 126.7, 101.6, 84.5, 81.1, 77.0, 75.9, 74.1, 71.9, 69.9, 69.5, 23.9, 15.2 ppm.

Ethyl 2,3-bis-*O*-benzyl-1-thio-β-D-galactopyranoside[145] (4.03)
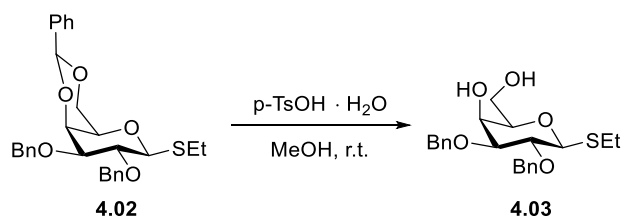
A mixture of **4.02** (750 mg, 1.52 mmol, 1.0 equiv.) and *p*-TsOH·H_2O (290 mg, 1.52 mmol, 1.0 equiv.) in MeOH (30 mL) was stirred at room temperature for 5 h. The mixture was diluted

with ethyl acetate (100 mL) and was washed with saturated aqueous NaHCO$_3$ (2 x 50 mL) and brine (50 mL). The organic layer was dried over Na$_2$SO$_4$, filtered and concentrated. Product **4.03** (560 mg, 1.38 mmol, 91%) was obtained as a white solid after purification by column chromatography (SiO$_2$, Hex/EtOAc 8:2 to 1:1).
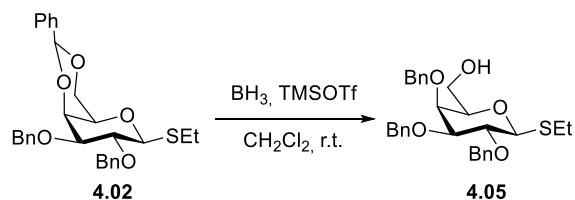
R_f = 0.23 (Hex/EtOAc 8:2). **^{1}H NMR** (400 MHz, CDCl$_3$) δ 7.44 – 7.27 (m, 10H), 4.92 – 4.74 (m, 2H), 4.73 (s, 2H), 4.44 (d, J = 9.7 Hz, 1H), 4.05 (dt, J = 3.3, 1.5 Hz, 1H), 4.00 – 3.74 (m, 2H), 3.67 (t, J = 9.3 Hz, 1H), 3.56 (dd, J = 9.0, 3.3 Hz, 1H), 3.52 – 3.45 (m, 1H), 2.86 – 2.69 (m, 2H), 2.66 (s, 1H), 2.19 (s, 1H), 1.32 (t, J = 7.4 Hz, 3H) ppm. **^{13}C NMR** (101 MHz, CDCl$_3$) δ 138.1, 137.7, 128.7, 128.5, 128.5, 128.2, 128.0, 128.0, 85.3, 82.3, 77.9, 77.8, 75.9, 72.3, 67.5, 62.9, 25.0, 15.2 ppm.

Ethyl 2,3,4-tris-*O*-benzyl-1-thio-β-D-galactopyranoside[146] (4.05)

To a solution of **4.02** (750 mg, 1.52 mmol, 1.0 equiv.) in anhydrous CH$_2$Cl$_2$ (10 mL) was added BH$_3$ (1 M solution in THF, 7.6 mL, 7.61 mmol, 5.0 equiv.) and TMSOTf (41 µL, 0.23 mmol, 0.15 equiv.). The mixture was stirred under argon atmosphere at room temperature for 4 h. Et$_3$N (1 mL) was added followed by MeOH until the evolution of H$_2$ ceased. The mixture was concentrated and coevaporated with MeOH (3 x 30 mL). Product **4.05** (650 mg, 1.31 mmol, 87%) was obtained as a white solid after purification by column chromatography (SiO$_2$, Hex/EtOAc 3:1).

R_f = 0.19 (Hex/EtOAc 3:1). **^{1}H NMR** (400 MHz, CDCl$_3$) δ 7.43 – 7.26 (m, 15H), 5.01 – 4.60 (m, 6H), 4.43 (d, J = 9.6 Hz, 1H), 3.89 – 3.80 (m, 2H), 3.81 – 3.74 (m, 1H), 3.58 (dd, J = 9.2, 2.8 Hz, 1H), 3.52 – 3.37 (m, 2H), 2.84 – 2.65 (m, 2H), 1.57 (s, 1H), 1.30 (t, J = 7.4 Hz, 3H) ppm. **^{13}C NMR** (101 MHz, CDCl$_3$) δ 138.4, 138.3, 138.3, 128.6, 128.6, 128.5, 128.5, 128.1, 127.9, 127.7, 85.6, 84.3, 78.7, 78.6, 75.9, 74.2, 73.2, 73.1, 62.3, 25.0, 15.2 ppm.

Ethyl 2,3,6-tris-*O*-benzyl-1-thio-β-D-galactopyranoside[147] (4.04)

117
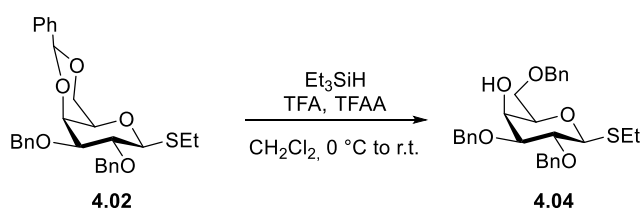
Compound **4.02** (1.00 g, 2.03 mmol, 1.0 equiv.) was co-evaporated with anhydrous toluene (2 x 3 mL), and dissolved in anhydrous CH_2Cl_2 (10 mL). Triethylsilane (1.93 mL, 12.18 mmol, 6.0 equiv.) and trifluoroacetic anhydride (0.29 mL, 2.03 mmol, 1.00 equiv.) were added and the solution was cooled to 0 °C. Trifluoroacetic acid (0.93 mL, 12.18 mmol, 6.00 equiv.) was added dropwise. The mixture was allowed to warm to room temperature and was stirred for 5 h. The solution was diluted with CH_2Cl_2 and quenched with saturated aqueous $NaHCO_3$ (20 mL). The aqueous phase was extracted with CH_2Cl_2 (2 x 30 mL) and the combined organic phase was washed with water (30 mL), dried over Na_2SO_4, filtered and concentrated. Product **4.04** (800 mg, 1.62 mmol, 80%) was obtained as a colorless syrup after purification by column chromatography (SiO_2, Hex/EtOAc 9:1 to 7:3).

R_f = 0.48 (Hex/EtOAc 7:3). **^{1}H NMR** (400 MHz, $CDCl_3$) δ 7.43 – 7.28 (m, 15H), 4.90 – 4.67 (m, 4H), 4.58 (s, 2H), 4.43 (d, J = 9.7 Hz, 1H), 4.10 (s, 1H), 3.83 – 3.63 (m, 3H), 3.61 – 3.51 (m, 2H), 2.84 – 2.68 (m, 2H), 2.52 (s, 1H), 1.31 (t, J = 7.5 Hz, 3H) ppm. **^{13}C NMR** (101 MHz, $CDCl_3$) δ 138.2, 138.0, 137.8, 128.7, 128.6, 128.5, 128.5, 128.5, 128.1, 128.0, 127.9, 127.9, 85.1, 82.4, 77.9, 76.9, 75.9, 73.8, 72.2, 69.4, 66.9, 24.9, 15.2 ppm.

Ethyl 2,3-bis-*O*-benzyl-4,6-bis(trifluoroacetate)-1-thio-β-D-galactopyranoside (4.06b)
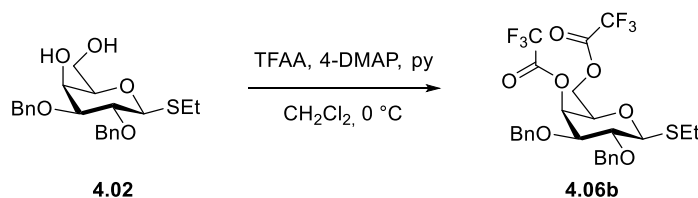

A stirred solution of **4.03** (150 mg, 0.37 mmol, 1.0 equiv.) in anhydrous CH_2Cl_2 (3 mL) was cooled to 0 °C and anhydrous pyridine (60 µL, 0.74 mmol, 2.0 equiv.), trifluoroacetic anhydride (105 µL, 0.74 mmol, 2.0 equiv.) and 4-DMAP (5 mg, 0.04 mmol, 0.10 equiv.) were added. The solution was stirred at 0 °C for 30 minutes before it was quenched with water (10 mL). The mixture was extracted with CH_2Cl_2 (3 x 10 mL) and the combined organic phases were washed with 1 N HCl (10 mL), dried over Na_2SO_4, filtered and concentrated. Product **4.06b** (130 mg, 0.22 mmol, 59%) was obtained as a colorless oil after purification by column chromatography (SiO_2, Hex/EtOAc 9:1 to 7:3).

R_f = 0.90 (Hex/EtOAc 3:1). **^{1}H NMR** (400 MHz, $CDCl_3$) δ 7.37 – 7.28 (m, 10H), 5.54 (d, J = 3.2 Hz, 1H), 4.88 – 4.80 (m, 1H), 4.77 – 4.70 (m, 2H), 4.63 – 4.56 (m, 1H), 4.54 – 4.43 (m, 2H), 4.35 (dd, J = 11.4, 5.6 Hz, 1H), 3.95 (t, J = 6.4 Hz, 1H), 3.75 – 3.67 (m, 1H), 3.59 (t, J = 9.4 Hz, 1H), 2.73 (qq, J = 13.7, 7.4 Hz, 2H), 1.31 (t, J = 7.5 Hz, 3H) ppm. **^{13}C NMR** (101 MHz, $CDCl_3$) δ 137.7, 136.9, 128.6, 128.5, 128.5, 128.3, 128.1, 85.7, 79.8, 77.0, 76.1, 73.0, 72.9,

71.5, 64.9, 25.1, 15.1 ppm. **^{19}F NMR** (376 MHz, CDCl$_3$) δ -74.60 (s), -74.86 (s) ppm. **HRMS** (QToF): Calcd for C$_{26}$H$_{26}$F$_6$O$_7$SNa [M + Na]$^+$ 619.1196; found 619.1201.

Ethyl 2,3,4-tris-*O*-benzyl-6-(trifluoroacetate)-1-thio-β-D-galactopyranoside (4.08b)

4.05   **4.08b**

A stirred solution of **4.05** (100 mg, 0.20 mmol, 1.0 equiv.) in anhydrous CH$_2$Cl$_2$ (3 mL) was cooled to 0 °C and anhydrous pyridine (20 µL, 0.24 mmol, 1.2 equiv.), trifluoroacetic anhydride (34 µL, 0.24 mmol, 1.2 equiv.) and 4-DMAP (2 mg, 0.02 mmol, 0.1 equiv.) were added. The solution was stirred at 0 °C for 30 minutes before it was quenched with water (10 mL). The mixture was extracted with CH$_2$Cl$_2$ (3 x 10 mL) and the combined organic phases were washed with 1 N HCl (10 mL), dried over Na$_2$SO$_4$, filtered and concentrated. Product **4.08b** (100 mg, 0.17 mmol, 84%) was obtained as a colorless solid after purification by column chromatography (SiO$_2$, Hex/EtOAc 9:1 to 7:3).

R$_f$ = 0.79 (Hex/EtOAc 3:1). **^{1}H NMR** (400 MHz, CDCl$_3$) δ 7.43 – 7.26 (m, 15H), 5.03 – 4.58 (m, 6H), 4.45 (d, J = 9.6 Hz, 1H), 4.55 – 4.06 (m, 2H), 3.84 (t, J = 9.4 Hz, 1H), 3.81 – 3.77 (m, 1H), 3.66 – 3.55 (m, 2H), 2.82 – 2.62 (m, 2H), 1.29 (t, J = 7.4 Hz, 3H) ppm. **^{13}C NMR** (101 MHz, CDCl$_3$) δ 138.2, 128.7, 128.5, 128.1, 128.0, 127.8, 85.6, 83.8, 78.4, 76.0, 75.2, 74.4, 73.6, 73.1, 66.9, 25.2, 15.2 ppm. **^{19}F NMR** (376 MHz, CDCl$_3$) δ -74.94 (s) ppm. **HRMS** (QToF): Calcd for C$_{31}$H$_{33}$F$_3$O$_6$SNa [M + Na]$^+$ 613.1842; found 613.1844.

Ethyl 2,3,6-tris-*O*-benzyl-4-(trifluoroacetate)-1-thio-β-D-galactopyranoside (4.07b)
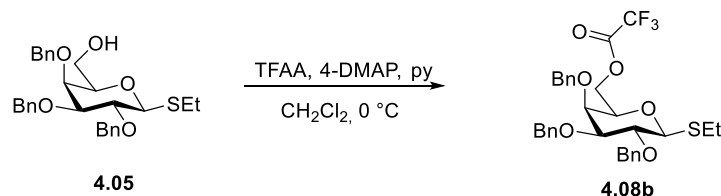

4.04   **4.07b**
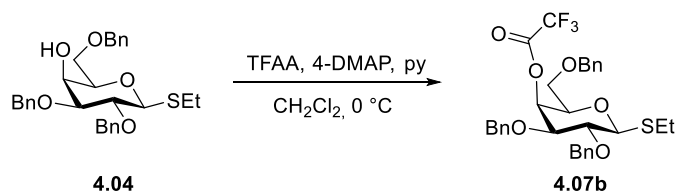
A stirred solution of **4.04** (130 mg, 0.30 mmol, 1.0 equiv.) in anhydrous CH$_2$Cl$_2$ (3 mL) was cooled to 0 °C and anhydrous pyridine (29 µL, 0.36 mmol, 1.2 equiv.), trifluoroacetic anhydride (51 µL, 0.36 mmol, 1.2 equiv.) and 4-DMAP (4 mg, 0.03 mmol, 0.1 equiv.) were added. The solution was stirred at 0 °C for 30 min before it was quenched with water (10 mL). The mixture was extracted with CH$_2$Cl$_2$ (3 x 10 mL) and the combined organic phases were washed with 1 N HCl (10 mL), dried over Na$_2$SO$_4$, filtered and concentrated. Product **4.07b** (100 mg, 0.17 mmol, 84%) was obtained as a colorless oil after purification by column chromatography (SiO$_2$, Hex/EtOAc 9:1 to 7:3).

R_f = 0.69 (Hex/EtOAc 3:1). **^{1}H NMR** (400 MHz, CDCl$_3$) δ 7.36 – 7.27 (m, 15H), 5.74 (d, J = 3.1 Hz, 1H), 4.85 – 4.71 (m, 3H), 4.57 – 4.42 (m, 4H), 3.80 (dd, J = 8.3, 5.7 Hz, 1H), 3.71 – 3.60 (m, 2H), 3.55 (t, J = 9.4 Hz, 1H), 3.45 (t, J = 8.8 Hz, 1H), 2.82 – 2.62 (m, 2H), 1.30 (t, J = 7.5 Hz, 3H) ppm. **^{13}C NMR** (101 MHz, CDCl$_3$) δ 137.9, 137.3, 137.2, 128.7, 128.5, 128.5, 128.2, 128.1, 128.0, 128.0, 85.5, 80.4, 77.3, 76.1, 74.7, 73.9, 72.4, 71.5, 67.1, 24.8, 15.1 ppm. **^{19}F NMR** (376 MHz, CDCl$_3$) δ -74.64 (s) ppm. **HRMS** (QToF): Calcd for C$_{31}$H$_{33}$F$_3$O$_6$SNa [M + Na]$^+$ 613.1842; found 613.1852.

Ethyl 2,3-bis-*O*-benzyl-4,6-bis(2,2-dimethylpropanoate)-1-thio-β-D-galactopyranoside (4.06a)
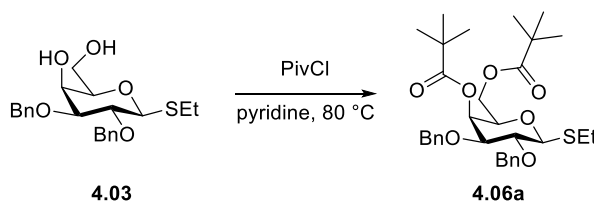
To a solution of **4.03** (140 mg, 0.35 mmol, 1.0 equiv.) in anhydrous pyridine (3 mL) pivaloyl chloride (1.5 mL, 12.13 mmol, 35.0 equiv.) was added. The mixture was stirred at 80 °C for two hours. The volatiles were evaporated. Product **4.06a** (150 mg, 0.26 mmol, 76%) was obtained as a colorless oil after purification by column chromatography (SiO$_2$, Hex/EtOAc 9:1).

R_f = 0.47 (Hex/EtOAc 9:1). **^{1}H NMR** (400 MHz, CDCl$_3$) δ 7.39 – 7.27 (m, 10H), 5.53 (d, J = 3.2 Hz, 1H), 4.84 – 4.70 (m, 3H), 4.53 – 4.44 (m, 2H), 4.11 (qd, J = 11.3, 6.8 Hz, 2H), 3.82 (t, J = 6.7 Hz, 1H), 3.62 (dd, J = 9.3, 3.2 Hz, 1H), 3.54 (t, J = 9.4 Hz, 1H), 2.84 – 2.63 (m, 2H), 1.31 (t, J = 7.4 Hz, 3H), 1.22 (s, 9H), 1.20 (s, 9H) ppm. **^{13}C NMR** (101 MHz, CDCl$_3$) δ 178.2, 177.6, 138.1, 137.9, 128.6, 128.4, 128.4, 128.2, 127.9, 127.8, 85.2, 81.1, 77.4, 75.9, 74.6, 71.9, 66.3, 62.2, 39.2, 38.9, 27.3, 27.2, 24.8, 15.2 ppm. **HRMS** (QToF): Calcd for C$_{32}$H$_{44}$O$_7$SNa [M + Na]$^+$ 595.2700; found 595.2701.

Ethyl 2,3,4-tris-*O*-benzyl-6-(2,2-dimethylpropanoate)-1-thio-β-D-galactopyranoside (4.08a)
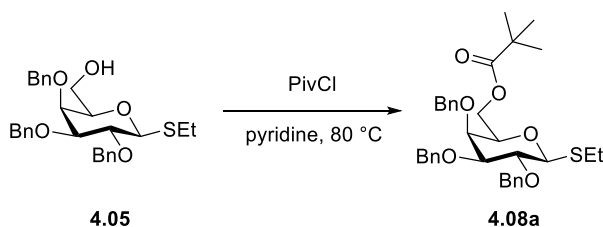
To a solution of **4.05** (150 mg, 0.30 mmol, 1.0 equiv.) in anhydrous pyridine (3 mL) pivaloyl chloride (0.75 mL, 6.06 mmol, 20.0 equiv.) was added. The mixture was stirred at 80 °C for

two hours. The volatiles were evaporated. Product **4.08a** (150 mg, 0.26 mmol, 85%) was obtained as a colorless oil after purification by column chromatography (SiO$_2$, Hex/EtOAc 9:1).

R$_f$ = 0.53 (Hex/EtOAc 3:1). **^{1}H NMR** (400 MHz, CDCl$_3$) δ 7.45 – 7.27 (m, 15H), 5.04 – 4.71 (m, 5H), 4.63 (d, J = 11.6 Hz, 1H), 4.44 (d, J = 9.7 Hz, 1H), 4.26 (dd, J = 11.2, 7.1 Hz, 1H), 4.06 (dd, J = 11.2, 5.6 Hz, 1H), 3.83 (t, J = 9.5 Hz, 1H), 3.79 – 3.76 (m, 1H), 3.60 – 3.50 (m, 2H), 2.84 – 2.63 (m, 2H), 1.30 (t, J = 7.4 Hz, 3H), 1.15 (s, 9H) ppm. **^{13}C NMR** (151 MHz, CDCl$_3$) δ 178.3, 138.5, 138.4, 138.4, 128.6, 128.6, 128.5, 128.4, 128.2, 127.9, 127.9, 127.8, 127.8, 85.4, 84.1, 78.6, 76.2, 75.9, 74.6, 74.1, 73.3, 63.4, 38.8, 27.3, 25.0, 15.2 ppm. **HRMS** (QToF): Calcd for C$_{34}$H$_{42}$O$_6$SNa [M + Na]$^+$ 601.2594; found 601.2610.

Ethyl 2,3,6-tris-*O*-benzyl-4-(2,2-dimethylpropanoate)-1-thio-β-D-galactopyranoside (4.07a)
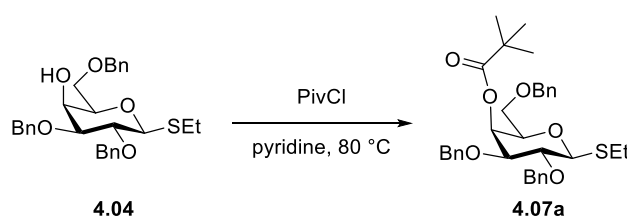
To a solution of **4.04** (100 mg, 0.20 mmol, 1.0 equiv.) in anhydrous pyridine (1.5 mL) pivaloyl chloride (0.50 mL, 6.06 mmol, 20.0 equiv.) was added. The mixture was stirred at 80 °C for two hours. The volatiles were evaporated. Product **4.07a** (110 mg, 0.19 mmol, 94%) was obtained as a colorless oil after purification by column chromatography (SiO$_2$, Hex/EtOAc 9:1).

R$_f$ = 0.49 (Hex/EtOAc 3:1). **^{1}H NMR** (600 MHz, CDCl$_3$) δ 7.37 – 7.26 (m, 14H), 5.64 (d, J = 2.3 Hz, 1H), 4.84 – 4.71 (m, 3H), 4.58 – 4.39 (m, 4H), 3.75 (d, J = 1.0 Hz, 1H), 3.64 – 3.50 (m, 3H), 3.46 (dd, J = 9.5, 6.9 Hz, 1H), 2.81 – 2.65 (m, 2H), 1.31 (t, J = 7.4 Hz, 3H), 1.19 (s, 9H) ppm. **^{13}C NMR** (151 MHz, CDCl$_3$) δ 177.6, 138.2, 138.1, 137.8, 128.6, 128.6, 128.4, 128.4, 128.2, 128.1, 127.9, 127.9, 127.7, 85.2, 81.5, 77.5, 76.1, 75.9, 73.9, 71.8, 68.5, 66.6, 39.2, 27.4, 24.7, 15.2 ppm. **HRMS** (QToF): Calcd for C$_{34}$H$_{42}$O$_6$SNa [M + Na]$^+$ 601.2594; found 601.2614.

Ethyl 2,3,4-tri-O-benzyl-6-methyl-1-thio-*β*-D-galactopyranoside (4.16)
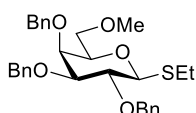
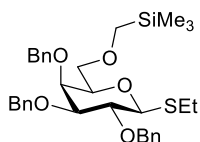**4.05** (100 mg, 0.20 mmol, 1.0 equiv.) was dissolved in anhydrous DMF (5 mL). The stirred solution was cooled to 0 °C and sodium hydride (10.0 mg, 0.24 mmol; 60% dispersion in mineral oil, 1.2 equiv.) was added. After 20 min, (bromomethyl)trimethylsilane (58 µL,

0.40 mmol, 2 equiv.) was added dropwise. The reaction mixture was allowed to warm to room temperature and was stirred for 30 min. Isopropanol (0.5 mL) was added, and the reaction mixture was diluted with ethyl acetate (5 mL). The organic layer was washed with water (10 mL), dried over Na_2SO_4 and concentrated to afford the undesired product **4.16** (90 mg, 0.17 mmol, 88%) as a colourless oil after purification by column chromatography (SiO_2, Hex/EtOAc 3:1).

R_f = 0.39 (Hex: AcOEt 3:1). **¹H NMR** (400 MHz, $CDCl_3$) δ 7.42 – 7.28 (m, 15H), 4.99 – 4.63 (m, 6H), 4.43 (d, J = 9.7 Hz, 1H), 3.93 (d, J = 2.8 Hz, 1H), 3.83 (t, J = 9.5 Hz, 1H), 3.57 (dd, J = 9.3, 2.9 Hz, 1H), 3.52 – 3.46 (m, 3H), 3.27 (s, 3H), 2.83 – 2.66 (m, 2H), 1.30 (t, J = 7.4 Hz, 3H) ppm. **¹³C NMR** (101 MHz, $CDCl_3$) δ 138.7, 138.3, 128.5, 128.5, 128.2, 127.8, 127.7, 127.6, 85.3, 84.0, 78.4, 75.8, 74.4, 73.3, 72.7, 71.1, 59.1, 24.9, 15.1 ppm.

Ethyl 2,3,4-tri-O-benzyl-1-thio-6-(trimethylsilyl)methyl-β-D-galactopyranoside (4.15)

4.05 (300 mg, 0.61 mmol, 1.0 equiv.) was dissolved in anhydrous THF (10 mL). The stirred solution was cooled to 0 °C and sodium hydride (24 mg, 0.61 mmol; 60% dispersion in mineral oil, 1.0 eq.) was added. After 20 min, (trimethylsilyl)methyl trifluoromethanesulfonate[148] (121 μL, 0.61 mmol, 1.0 equiv.) was added dropwise. The reaction mixture was allowed to warm to room temperature and was stirred over night. The reaction mixture was diluted with saturated aqueous NH_4Cl_4 and was extracted with CH_2Cl_2 (3 x 20 mL). The organic layer was dried over Na_2SO_4 and concentrated to afford **4.15** (49 mg, 0.08 mmol, 14%) as a colourless oil after purification by column chromatography (SiO_2, Hex/EtOAc 9:1), followed by HPLC purification (Hex/EtOAc 99:1, t_r = 6.4 min).

R_f = 0.39 (Hex/EtOAc 3:1).

¹H NMR (400 MHz, $CDCl_3$) δ 7.43 – 7.28 (m, 15H, 3 x $CH_2\underline{C_6H_5}$), 4.96 – 4.58 (m, 6H, 3 x $\underline{CH_2}C_6H_5$), 4.43 (d, J = 9.7 Hz, 1H, **H-1**), 3.86 (d, J = 2.9 Hz, 1H, **H-5**), 3.81 (t, J = 9.5 Hz, 1H, **H-2**), 3.60 – 3.49 (m, 4H, **H-6**, **H-6'**, **H-4**, **H-3**), 3.15 – 2.99 (m, 2H, $\underline{CH_2}$-TMS), 2.82 – 2.64 (m, 2H, $S\underline{CH_2}CH_3$), 1.29 (t, J = 7.4 Hz, 3H, $SCH_2\underline{CH_3}$), 0.01 (s, 9H, $Si(\underline{CH_3})_3$) ppm. **¹³C NMR** (101 MHz, $CDCl_3$) δ 139.0, 138.6, 138.4, 128.6, 128.5, 128.5, 128.3, 128.0, 127.9, 127.8, 127.7, 127.5 (3 x $CH_2\underline{C_6H_5}$), 85.3 (**C-1**), 84.1 (**C-3**), 78.6 (**C-2**), 77.0 (**C-4**), 75.9, 74.7, 74.2 (**C-5**), 73.5 (**C-6**), 72.8, 65.8 ($\underline{CH_2}$-TMS), 24.9 ($S\underline{CH_2}CH_3$), 15.2 ($SCH_2\underline{CH_3}$), -2.9 ($Si(\underline{CH_3})_3$) ppm. **[α]$_D$** -21.25 cm⁻¹ (c 1, $CHCl_3$). **IR** (film): 3033, 2865, 1498, 1455, 1362, 1249, 1210, 1102, 1029, 861, 733, 697 cm⁻¹. **HRMS (QToF):** Calcd for $C_{33}H_{44}O_5SSiNa$ [M + Na]⁺ 603.2571; found 603.2572.

Ethyl 6-C$_4$F$_9$-2,3,4-tri-*O*-benzyl-1-thio-*β*-D-galactopyranoside (4.17)
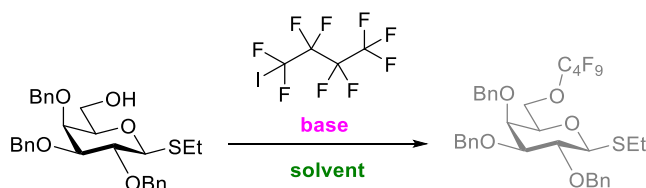
Table 1: Reaction conditions for the conversion of **4.05** (50 mg, 0.10 mmol, 1.0 equiv.) with 1,1,1,2,2,3,3,4,4-nonafluoro-4-iodobutane (C$_4$F$_9$I).

Entry	C$_4$F$_9$I	Base	Solvent	Temperature	Result
1	3.0 eq.	Cs$_2$CO$_3$ (3 eq.)	DMF	r. t.	N. C.
2	3.0 eq.	NaH (2 eq.)	DMF	0 °C - r. t.	N. C.
3	3.0 eq.	Cs$_2$CO$_3$ (3 eq.)	DMF	60 °C	N. C.
4	1.2 eq.	KOH (6 eq.)	DMSO	100 °C	N. C.
5	1.3 eq.	NaH (1.3 eq.)	DMF	0 °C - r. t.	N. C.
6	Solvent	KOH (5.0 eq.)	-	reflux	N. C.

4.05 (and Cs$_2$CO$_3$, entry 1 and 3) was dried in an ovendried flask under high vacuum for 30 min. Afterwards, **solvent** (2 mL) was added. For entry 2 and 5, the solution was cooled to 0 °C and sodium hydride (60% dispersion in mineral oil) was added and the suspension was stirred for 20 minutes. 1,1,1,2,2,3,3,4,4-nonafluoro-4-iodobutane was added and after 16 h und the conditions described in Table 1, no conversion (N. C.) was observed by ESI-MS, ^{1}H NMR and ^{19}F NMR analysis.

Ethyl 6-(4-methylbenzenesulfonate)-2,3,4-tris-*O*-benzyl-1-thio-β-D-galactopyranoside (4.19)
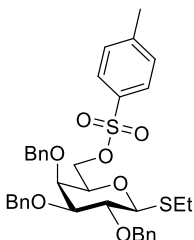
Tosyl chloride was purified before use in order to remove impurities of *p*-toluenesulfonic acid and HCl. Tosyl chloride (2 g) was dissolved in diethyl ether (50 mL) and the organic phase was washed with aqueous 10% NaOH (2 x 20 mL), then dried over Na$_2$SO$_4$ and crystallized by cooling the solution in powdered dry ice. The crystals were washed with cold diethyl ether and dried in *vacuo*.

To a stirred solution of **4.05** (200 mg, 0.40 mmol, 1.0 equiv.) and TsCl (304 mg, 1.62 mmol, 4.0 equiv.) in CH_2Cl_2 (2 mL) were added Et_3N (112 µL, 0.809 mmol, 2.0 equiv.) and catalytic DMAP (5 mg, 0.04 mmol, 0.1 equiv.). The reaction mixture was stirred for 4 h at room temperature. The solution was diluted with CH_2Cl_2 (20 mL) and was then washed with aq. HCl (1 M, 20 mL) and brine (2 x 20 mL). The organic phase was dried over Na_2SO_4 and concentrated in *vacuo* to afford compound **4.19** (206 mg, 0.32 mmol, 80%) as a colorless oil after purification by column chromatography (SiO_2, Hex/EtOAc 8:1 to 3:1).

R$_f$ = 0.20 (Hex/EtOAc 8:1). **¹H NMR** (400 MHz, $CDCl_3$) δ 7.78 – 7.72 (m, 1H), 7.42 – 7.29 (m, 15H), 7.25 – 7.19 (m, 2H), 4.99 – 4.48 (m, 6H), 4.41 (d, *J* = 9.6 Hz, 1H), 4.09 (dd, *J* = 9.9, 6.2 Hz, 1H), 3.97 (dd, *J* = 9.9, 6.5 Hz, 1H), 3.90 (d, *J* = 2.0 Hz, 1H), 3.79 (t, *J* = 9.5 Hz, 1H), 3.68 – 3.61 (m, 1H), 3.57 (dd, *J* = 9.3, 2.8 Hz, 1H), 2.79 – 2.60 (m, 2H), 2.45 (s, 3H), 1.29 (t, *J* = 7.5 Hz, 3H) ppm. **¹³C NMR** (101 MHz, $CDCl_3$) δ 145.1, 138.1, 138.1, 138.0, 132.3, 129.9, 128.5, 128.4, 128.4, 128.27, 128.0, 127.9, 127.8, 127.7, 127.6, 85.4, 83.6, 78.0, 75.8, 75.4, 74.4, 73.0, 72.9, 68.2, 24.9, 21.7, 15.1 ppm.

Ethyl 6-*O*-(2,2,2-trifluoroethyl)-2,3,4-tri-*O*-benzyl-1-thio-β-D-galactopyranoside (4.20)
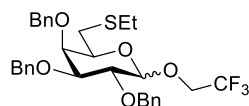
Compound **4.19** (190 mg, 0.293 mmol, 1.0 equiv.) was dissolved in 2,2,2-trifluoroethanol (1 mL) in an oven-dried 10 mL-pressure vessel. A sodium trifluoroethoxide solution (1.5 M) was prepared by adding sodium hydride (232 mg, 5.86 mmol, 60% dispersion in mineral oil) in small portions to 2,2,2-trifluoroethanol (4 mL) under rigorous stirring. Freshly prepared sodium trifluorethoxide solution (1.5 M, 2 mL, 10.0 equiv.) was added and the reaction was heated to 100 °C while stirring for 5 h in the closed pressure vessel. The reaction mixture was diluted with ethyl acetate (40 mL) and washed with water (20 mL) and brine (20 mL) successively. The organic layer was dried over Na_2SO_4 and the volatiles were evaporated in *vacuo* to afford an anomeric mixture of the undesired product **4.20** (91 mg, 0.16 mmol, 55%, α/β 6:1) as a colorless oil after purification by column chromatography (SiO_2, Hex/EtOAc 95:5 to 90:10).

R$_f$ = 0.37 (Hex/EtOAc 8:1).
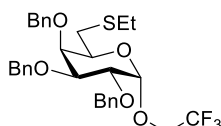
¹H NMR (400 MHz, $CDCl_3$) δ 7.36 – 7.20 (m, 15H), 4.94 (d, *J* = 11.3 Hz, 1H), 4.82 (d, *J* = 11.6 Hz, 1H), 4.77 (d, *J* = 4.2 Hz, 1H), 4.71 (d, *J* = 11.6 Hz, 1H), 4.58 (d, *J* = 11.9 Hz, 1H), 4.55 (d, *J* = 11.3 Hz, 1H), 3.71 (t, *J* = 6.9 Hz, 1H), 2.53 (ddd, *J* = 58.7, 13.5, 6.9 Hz, 2H), 2.43 (q, *J* = 7.4 Hz, 2H), 1.14 (t, *J* = 7.4 Hz, 3H) ppm. **¹³C NMR** (101 MHz, $CDCl_3$) δ 138.7, 138.4, 138.3,

128.5, 128.4, 128.4, 128.0, 127.8, 127.6, 127.5, 98.2, 78.9, 76.0, 75.3, 74.9, 73.5, 71.1, 65.1, 64.7, 64.4, 64.1, 31.9, 26.8, 14.7 ppm. **[α]$_D$** -14.93 cm^{-1} (*c* 1, CHCl$_3$). **IR** (film): 3066, 3033, 2928, 1498, 1455, 1350, 1278, 1144, 1080, 1028, 983, 913, 845, 736, 697 cm^{-1}. **HRMS** (QToF): Calcd for C$_{31}$H$_{35}$F$_3$O$_5$SNa [M + Na]$^+$ 599.2049; found 599.2059.
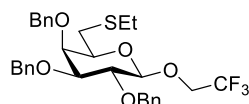
^{1}H NMR (400 MHz, CDCl$_3$) δ 7.39 – 7.27 (m, 15H), 5.04 – 4.66 (m, 6H), 4.47 (d, *J* = 7.6 Hz, 1H), 4.25 – 4.12 (m, 1H), 4.01 – 3.84 (m, 3H), 3.53 (dd, *J* = 9.8, 2.9 Hz, 1H), 3.40 (t, *J* = 6.4 Hz, 1H), 2.68 (ddd, *J* = 65.4, 13.5, 6.8 Hz, 2H), 2.55 – 2.48 (m, 2H), 1.22 (t, *J* = 7.4 Hz, 3H) ppm.
^{13}C NMR (101 MHz, CDCl$_3$) δ 138.4, 138.3, 138.3, 128.7, 128.6, 128.6, 128.4, 128.4, 127.9, 127.9, 127.8, 127.7, 104.1, 82.2, 78.9, 75.4, 75.2, 74.9, 73.9, 73.5, 71.2, 66.5, 66.2, 65.8, 65.5, 32.1, 27.1, 14.9 ppm.

1,2:3,4-Bis-*O*-(1-methylethylidene)-6-(2,2,2-trifluoroethoxy)-α-D-galactopyranose (4.23)
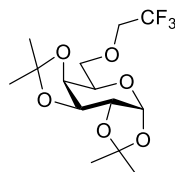
2,2,2-Trifluoroethanol (2.2 mL, 30.59 mmol, 8.0 equiv.) was dissolved in anhydrous THF (10 mL). The stirred solution was cooled to 0 °C and sodium hydride (0.32 g, 8.03 mmol; 60% dispersion in mineral oil, 2.1 equiv.) was added in small portions. After 15 minutes, a solution of triflated **4.22**[149] (1.5 g, 3.82 mmol, 1.0 equiv.) in anhydr. THF (6 mL) was added dropwise. The mixture was allowed to warm to room temperature and was stirred for 36 h. Acetic acid (0.24 mL, 4.21 mmol, 1.1 equiv.) was added to quench the reaction, the solvent was removed under reduced pressure and the residue was distributed between CH$_2$Cl$_2$ (30 mL) and water (30 mL). The aqueous phase was extracted with CH$_2$Cl$_2$ (3 x 30 mL), dried over Na$_2$SO$_4$ and concentrated. Product **4.23** (0.82 g, 2.34 mmol, 61%) was obtained as a colorless oil after purification by column chromatography (SiO$_2$, CH$_2$Cl$_2$).

**R$_f$** = 0.41 (CH$_2$Cl$_2$). **^{1}H NMR** (400 MHz, CDCl$_3$) δ 5.53 (d, *J* = 5.0 Hz, 1H), 4.61 (dd, *J* = 7.9, 2.4 Hz, 1H), 4.32 (dd, *J* = 5.0, 2.5 Hz, 1H), 4.24 (dd, *J* = 7.9, 1.9 Hz, 1H), 4.05 – 3.81 (m, 5H), 1.54 (s, 3H), 1.44 (s, 3H), 1.33 (s, 6H) ppm. **^{13}C NMR** (101 MHz, CDCl$_3$) δ 125.5, 122.7, 109.5, 108.9, 96.4, 71.6, 71.1, 70.7, 70.6, 69.5, 69.2, 68.9, 68.5, 67.4, 26.1, 26.1, 25.1, 24.5 ppm.
^{19}F NMR (376 MHz, CDCl$_3$) δ -74.39 (t, *J* = 8.6 Hz) ppm. **[α]$_D$** -65.45 cm^{-1} (*c* 1, CHCl$_3$). **IR** (film): 2993, 2941, 1459, 1385, 1282, 1257, 1214, 1162, 1111, 1010, 969, 894, 826 cm^{-1}.

1,2,3,4-Tetra-*O*-acetyl-6-(2,2,2-trifluoroethoxy)-α/β-D-galactopyranoside (4.24)
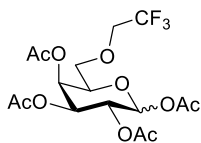
Compound **4.23** (0.50 g, 1.46 mmol, 1.0 equiv.) was dissolved in a mixture of trifluoroacetic acid and methanol (9:1, 25 mL) and stirred for one hour. The solvents were co-evaporated with toluene and chloroform under reduced pressure to obtain an anomeric mixture of deprotected **4.23**, which was used for the next step without further purification. Deprotected **4.23** (0.38 g, 1.45 mmol, 1.0 equiv.) was dissolved in pyridine (10 mL) at 0 °C and acetic anhydride (1.78 mL, 18.84 mmol, 13.0 equiv.) was added. The reaction mixture was allowed to warm to room temperature and was stirred overnight. The volatiles were removed in *vacuo* to obtain an anomeric mixture of **4.24** (0.50 g, 1.15 mmol, 79%, α/β 0.58:1.00) after purification by column chromatography (SiO$_2$, Hex/EtOAc 5:1).

R$_f$ = 0.35 (Hex/EtOAc 3:1). **^{1}H NMR** (400 MHz, CDCl$_3$) δ 6.35 (d, *J* = 2.7 Hz, 0.36H), 5.67 (d, *J* = 8.3 Hz, 0.63H), 5.52 (dd, *J* = 2.5, 1.3 Hz, 0.36H), 5.45 (dd, *J* = 3.4, 1.1 Hz, 0.63H), 5.32 (m, 1.5H), 5.07 (dd, *J* = 10.4, 3.4 Hz, 0.63H), 4.28 (td, *J* = 6.2, 1.5 Hz, 0.36H), 4.00 (td, *J* = 6.2, 1.2 Hz, 0.63H), 3.90 – 3.73 (m, 3H), 3.36 (d, *J* = 10.0 Hz, 0.63H), 2.14 – 1.98 (m, 12H) ppm. **^{13}C NMR** (101 MHz, CDCl$_3$) δ 170.1, 170.0, 169.9, 169.5, 169.1, 169.0, 127.9, 125.1, 122.3, 119.5, 118.1, 106.4, 100.6, 98.9, 97.1, 93.1, 92.2, 89.6, 81.8, 81.4, 80.7, 79.6, 78.9, 77.6, 76.5, 76.1, 75.6, 73.5, 72.8, 71.7, 70.8, 70.2, 70.0, 69.8, 68.9, 68.5, 67.8, 67.3, 67.0, 66.4, 55.3, 54.8, 20.9, 20.8, 20.6, 20.5 ppm. **[α]$_D$** 9.82 cm^{-1} (*c* 1, CHCl$_3$). **IR** (film): 3027, 2944, 1749, 1434, 1372, 1280, 1200, 1158, 1068, 1014, 950, 901 cm^{-1}. **HRMS** (QToF): Calcd for C$_{33}$H$_{44}$O$_5$SSiNa [M + Na]$^+$ 453.0979; found 453.0974.

2,3,4-Tri-*O*-acetyl-6-(2,2,2-trifluoroethoxy)-α-D-galactopyranosyl bromide (4.25)
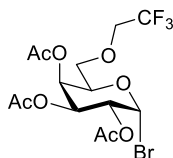
A solution of **4.24** (0.40 g, 0.93 mmol, 1.0 equiv.) in anhydrous CH$_2$Cl$_2$ (10 mL) was cooled to 0 °C and acetic anhydride (44 µL, 0.47 mmol, 0.5 equiv.). Afterwards, hydrobromic acid (4.22 mL, 33% in acetic acid, 25.0 equiv.) was added dropwise. The reaction mixture was allowed to warm to room temperature and stirred for 3 h. The reaction was then cooled to 0 °C, diluted with DCM and sat. aq. NaHCO$_3$ was added portion wise. The organic layer was separated and washed with brine, dried over Na$_2$SO$_4$, filtered and concentrated to obtain **4.25**

(0.37 g, 0.82 mmol, 88%) as a brown oil. Compound **4.25** was directly used for the following step without further purification.

R$_f$ = 0.66 (Hex/EtOAc 3:1). **¹H NMR** (400 MHz, CDCl$_3$) δ 6.70 (d, J = 4.0 Hz, 1H), 5.55 (dd, J = 3.3, 1.3 Hz, 1H), 5.40 (dd, J = 10.6, 3.3 Hz, 1H), 5.05 (dd, J = 10.6, 4.0 Hz, 1H), 4.44 (t, J = 6.2 Hz, 1H), 3.90 – 3.76 (m, 2H), 3.72 (d, J = 6.1 Hz, 2H), 2.14 (s, 3H), 2.11 (s, 3H), 2.01 (s, 3H) ppm. **¹³C NMR** (101 MHz, CDCl$_3$) δ 170.1, 169.7, 169.7, 88.1, 71.9, 68.8 (q, J = 34.4 Hz), 67.9, 67.8, 67.2, 20.7, 20.6, 20.5 ppm. **¹⁹F NMR** (376 MHz, CDCl$_3$) δ -74.13 (t, J = 8.7 Hz) ppm.

Ethyl 2,3,4-tri-*O*-benzyl-6-*O*-(2,2,2-trifluoroethoxy)-1-thio-*β*-D-galactopyranoside (4.18)
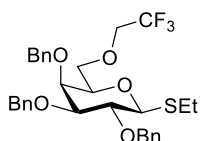
To a solution of ethanethiol (89 µL, 1.23 mmol, 1.5 equiv.) in anhydrous *N,N*-dimethylformamide (2 mL), sodium hydride (49 mg, 1.23 mmol; 60% dispersion in mineral oil, 1.5 equiv.) was added slowly at 0 °C. After stirring for 15 min, a solution of **4.25** (370 mg, 0.82 mmol, 1.0 equiv.) in *N,N*-dimethylformamide (2 mL), was added slowly. The reaction mixture was allowed to warm to room temperature and was stirred overnight. Then, the reaction mixture was diluted with CH$_2$Cl$_2$ (30 mL) and quenched with AcOH (50 µL). The organic phase was washed with brine (20 mL) was dried with Na$_2$SO$_4$, filtered and the solvent was removed in *vacuo* to afford thioglycosides **4.26** (0.35 mg, 0.81 mmol, 99%) after column chromatography (SiO$_2$, Hex/EtOAc 3:1). **R**$_f$ = 0.33 (Hex/EtOAc 3:1). To a solution of **4.26** (330 mg, 0.84 mmol, 1.0 equiv.) in MeOH (3 mL), sodium methoxide (0.5 M solution in MeOH, 2 mL, 1.00 mmol, 1.3 equiv.) was added. The mixture was stirred at room temperature for 4.5 h. Then Amberlite resin was added to quench. When the solution was neutralized, the reaction mixture was filtered and solvent was removed in *vacuo*. Deprotected **4.26** (180 mg, 0.59 mmol, 77%) was obtained as brown oil and was used for the next step without further purification. R$_f$ = 0.31 (CH$_2$Cl$_2$:MeOH:Acetone, 9:0.5:0.5). Deprotected **4.26** (160 mg, 0.52 mmol, 1.0 equiv.) was dissolved in anhydrous *N,N*-dimethylformamide (5 mL). The stirred solution was cooled to 0 °C and sodium hydride (104 mg, 2.61 mmol; 60% dispersion in mineral oil, 5.0 equiv.) was added in small portions. After 30 min, benzyl bromide (279 µL, 2.35 mmol, 4.5 equiv.) was added dropwise. The reaction mixture was allowed to warm to room temperature and was stirred for three hours. Acetic acid (0.5 mL) was added, and after 10 min, the reaction mixture was diluted with ethyl acetate (50 mL). The organic layer was washed with water (2 x 30 mL) and the aqueous phase was extracted with ethyl acetate (2 x 20 mL). The combined organic phase was dried over Na$_2$SO$_4$ and concentrated. Product **4.18** (152 mg, 0.26 mmol, 50%) was obtained as a white crystalline solid after purification by column

chromatography (SiO$_2$, Hex/EtOAc 95:5) followed by HPLC purification (Hex/EtOAc 98:2, t$_r$ = 8.5 min).

R$_f$ = 0.17 (Hex/EtOAc 95:5). **^{1}H NMR** (400 MHz, CDCl$_3$) δ 7.43 – 7.25 (m, 15H, 3 x CH$_2$C$_6$H$_5$), 5.02 – 4.57 (m, 6H, 3 x C$\underline{H_2}$C$_6$H$_5$), 4.44 (d, J = 9.7 Hz, 1H, **H-1**), 3.88 (dd, J = 2.9, 1.0 Hz, 1H, **H-4**), 3.82 (t, J = 9.5 Hz, 1H, **H-2**), 3.80 – 3.50 (m, 6H, C$\underline{H_2}$-CF$_3$, **H-6**, **H-6'**, **H-3**, **H-5**), 2.73 (qd, J = 12.6, 7.4 Hz, 2H, SC$\underline{H_2}$CH$_3$), 1.30 (t, J = 7.4 Hz, 3H, SCH$_2$C$\underline{H_3}$) ppm. **^{13}C NMR** (101 MHz, CDCl$_3$) δ 138.4, 138.2, 138.2, 128.5, 128.4, 128.3, 128.3, 128.2, 127.8, 127.7, 127.7, 127.6 (3 x CH$_2$$\underline{C_6H_5}$), 85.4 (**C-1**), 83.9 (**C-3**), 78.3 (**C-2**), 76.7 (**C-5**), 75.8 ($\underline{CH_2}$C$_6$H$_5$), 74.3 ($\underline{CH_2}$C$_6$H$_5$), 73.2 ($\underline{CH_2}$C$_6$H$_5$), 72.9 (**C-4**), 71.2 (**C-6**), 68.7 (q, J = 34.0 Hz, $\underline{CH_2}$-CF$_3$), 24.9 (S$\underline{CH_2}$CH$_3$), 15.0 (SCH$_2$$\underline{CH_3}$) ppm. **^{19}F NMR** (376 MHz, CDCl$_3$) δ -74.36 (t, J = 8.6 Hz). **[α]$_D$** − 8.81 cm^{-1} (c 1, CHCl$_3$) ppm. **IR** (film): 3274, 1631, 1456, 1363, 1279, 1254, 1069, 1043, 1029, 736, 698, 672 cm^{-1}. HRMS (QToF): Calcd for C$_{16}$H$_{23}$F$_3$O$_8$SNa [M + Na]$^+$ 599.2049; found 599.2055.

3,4,6-Tri-*O*-(2,2-dimethylpropanoate)-D-glucal (4.42a)
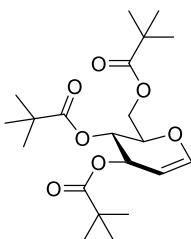
A suspension of unprotected glucal (100 mg, 0.68 mmol, 1.0 equiv.) in anhydrous CH$_2$Cl$_2$ (4 mL) was cooled to 0 °C and pivaloyl chloride (0.51 mL, 4.1 mmol, 6.0 equiv.) was added, followed by addition of 4-DMAP (8.4 mg, 0.07 mmol, 0.1 equiv.). The reaction mixture was allowed to warm to room temperature and was stirred overnight. The reaction was quenched with methanol (2 mL) and volatiles were removed under reduced pressure. The residue was redissolved in ethyl acetate (20 mL) and the organic phase was washed with water and brine, dried over Na$_2$SO$_4$, filtered and concentrated. Compound **4.42a** (150 mg, 0.68 mmol, 55%) was obtained as a white solid after purification by column chromatography (SiO$_2$, Hex/EtOAc 3:1).

^{1}H NMR (400 MHz, CDCl$_3$): δ 6.45 (dd, J = 6.2, 1.3 Hz, 1H), 5.33 – 5.24 (m, 2H), 4.81 (dd, J = 6.1, 3.1 Hz, 1H), 4.37 – 4.17 (m, 3H), 1.22 (s, 9H), 1.18 (s, 9H), 1.18 (s, 9H) ppm. **^{13}C NMR** (101 MHz, CDCl$_3$): δ 178.3, 178.0, 176.7, 145.8, 99.2, 74.3, 67.7, 66.8, 61.5, 39.0, 38.9, 38.9, 27.3, 27.2, 27.1 ppm. **HRMS** (QToF): Calcd for C$_{21}$H$_{34}$O$_7$Na [M + Na]$^+$ 421.2197 found 421.2217.

### 3,4,6-Tri-*O*-(2,2-dimethylpropanoate)-D-galactal (4.44a)
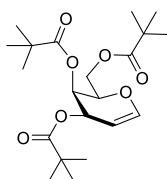
A suspension of unprotected galactal (100 mg, 0.68 mmol, 1.0 equiv.) in anhydrous CH_2Cl_2 (4 mL) was cooled to 0 °C and pivaloyl chloride (0.51 mL, 4.1 mmol, 6.0 equiv.) was added, followed by addition of 4-DMAP (8.4 mg, 0.07 mmol, 0.1 equiv.). The reaction mixture was allowed to warm to room temperature and was stirred overnight. The reaction was quenched with methanol (2 mL) and volatiles were removed under reduced pressure. The residue was redissolved in ethyl acetate (20 mL) and the organic phase was washed with water and brine, dried over Na_2SO_4, filtered and concentrated. Compound **4.44a** (152 mg, 0.68 mmol, 55%) was obtained as a white solid after purification by column chromatography (SiO_2, Hex/EtOAc 3:1).

¹H NMR (400 MHz, CDCl₃): δ 6.42 (dd, J = 6.3, 1.6 Hz, 1H), 5.54 – 5.47 (m, 1H), 5.43 (dd, J = 2.3, 1.2 Hz, 1H), 4.74 (ddd, J = 6.2, 3.1, 1.2 Hz, 1H), 4.41 – 4.29 (m, 2H), 4.20 – 4.07 (m, 1H), 1.23 (s, 9H), 1.21 (s, 9H), 1.19 (s, 9H) ppm. **¹³C NMR** (101 MHz, CDCl₃): δ 178.3, 177.8, 177.2, 145.2, 99.0, 73.1, 64.1, 61.7, 39.1, 38.9, 38.9, 27.3, 27.3, 27.3 ppm. **HRMS** (QToF): Calcd for $C_{21}H_{34}O_7Na$ [M + Na]⁺ 421.2197 found 421.2217.

3,4,6-Tri-*O*-levulinyl-D-glucal (4.42c)
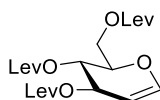
To a solution of glucal (100 mg, 0.68 mmol, 1.0 equiv.) and LevOH (0.42 mL, 4.10 mmol, 6.0 equiv.) in anhydrous CH_2Cl_2 (2 mL) was added dropwise a premixed solution of DIC (0.96 mL, 6.2 mmol, 9.0 equiv.) and 4-DMAP (17 mg, 0.14 mmol, 0.2 equiv.) in anhydrous CH_2Cl_2 (2 mL) at 0 °C. The reaction was stirred at room temperature overnight. The reaction mixture was filtered through Celite, the filtrate was washed with aqueous $NaHCO_3$ and the aqueous phase was extracted with CH_2Cl_2. The combined organic phase was dried over Na_2SO_4, filtered and concentrated. Compound **4.42c** (210 mg, 0.48 mmol, 70%) was obtained as a yellow syrup after purification by column chromatography (SiO_2, Hex/EtOAc 3:1).

¹H NMR (400 MHz, CDCl₃): δ 6.44 (dd, J = 6.2, 1.4 Hz, 1H), 5.41 – 5.34 (m, 1H), 5.23 (dd, J = 8.0, 6.1 Hz, 1H), 4.81 (dd, J = 6.2, 3.1 Hz, 1H), 4.40 – 4.31 (m, 1H), 4.29 – 4.19 (m, 2H), 2.81 – 2.70 (m, 6H), 2.70 – 2.51 (m, 6H), 2.18 (s, 3H), 2.17 (s, 3H), 2.17 (s, 3H) ppm. **¹³C NMR** (101 MHz, CDCl₃): δ 206.6, 206.3, 172.5, 172.3, 171.5, 145.8, 99.1, 74.1, 67.9, 67.3, 61.8,

38.0, 30.0, 29.9, 29.9, 29.3, 28.2, 28.0, 28.0 ppm. **HRMS** (QToF): Calcd for $C_{21}H_{28}O_{10}Na$ [M + Na]$^+$ 463.1575 found 463.1591.
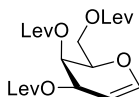
3,4,6-Tri-*O*-levulinyl-D-galactal (4.44c)

To a solution of galactal (100 mg, 0.68 mmol, 1.0 equiv.) and LevOH (0.42 mL, 4.10 mmol, 6.0 equiv.) in anhydrous CH_2Cl_2 (2 mL) was added dropwise a premixed solution of DIC (0.96 mL, 6.2 mmol, 9.0 equiv.) and 4-DMAP (17 mg, 0.14 mmol, 0.2 equiv.) in anhydrous CH_2Cl_2 (2 mL) at 0 °C. The reaction was stirred at room temperature overnight. The reaction mixture was filtered through Celite, the filtrate was washed with aqueous $NaHCO_3$ and the aqueous phase was extracted with CH_2Cl_2. The combined organic phase was dried over Na_2SO_4, filtered and concentrated. Compound **4.44c** (195 mg, 0.44 mmol, 65%) was obtained as a yellow syrup after purification by column chromatography (SiO_2, Hex/EtOAc 3:1).

^{1}H NMR (400 MHz, CDCl$_3$): δ 6.44 (dd, *J* = 6.3, 1.8 Hz, 1H), 5.56 – 5.47 (m, 1H), 5.40 (dt, *J* = 4.5, 1.5 Hz, 1H), 4.73 (ddd, *J* = 6.3, 2.8, 1.4 Hz, 1H), 4.36 – 4.25 (m, 2H), 4.25 – 4.13 (m, 1H), 2.84 – 2.44 (m, 12H), 2.20 – 2.14 (m, 9H) ppm. **^{13}C NMR** (101 MHz, CDCl$_3$): δ 206.7, 206.6, 206.4, 172.5, 172.3, 172.1, 157.3, 145.5, 98.9, 72.8, 64.2, 64.1, 62.1, 38.0, 37.9, 37.9, 29.9, 28.0, 27.9, 27.9 ppm. **HRMS** (QToF): Calcd for $C_{21}H_{28}O_{10}Na$ [M + Na]$^+$ 463.1575 found 463.1588.

3,4,6-Tri-*O*-benzoyl-D-glucal (4.42f)
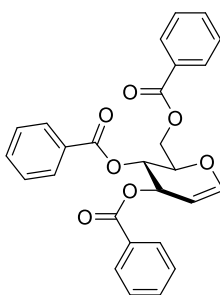
A suspension of unprotected glucal (30 mg, 0.21 mmol, 1.0 equiv.) in anhydrous pyridine (5 mL) was cooled to 0 °C and benzoyl chloride (0.14 mL, 1.23 mmol, 6.0 equiv.) was added, followed by addition of 4-DMAP (2.5 mg, 0.02 mmol, 0.1 equiv.). The reaction mixture was allowed to warm to room temperature and was stirred overnight, before it was diluted with water and extracted with ethyl acetate. The combined organic phase was washed with aqueous citric acid solution (10% v/v) and brine, dried over Na_2SO_4, filtered and concentrated.

Compound **4.42f** (80 mg, 0.17 mmol, 85%) was obtained as a colorless syrup after purification by column chromatography (SiO$_2$, Hex/EtOAc 9:1).

^{1}H NMR (400 MHz, CDCl$_3$): δ 8.09 – 7.94 (m, 5H), 7.59 – 7.37 (m, 10H), 6.61 (dd, *J* = 6.2, 1.4 Hz, 1H), 5.85 – 5.76 (m, 1H), 5.71 (ddd, *J* = 5.5, 2.7, 1.2 Hz, 1H), 5.12 (dd, *J* = 6.3, 3.5 Hz, 1H), 4.75 – 4.64 (m, 3H) ppm. **^{13}C NMR** (101 MHz, CDCl$_3$): δ 166.3, 166.0, 165.3, 146.1, 133.9, 133.7, 133.4, 130.3, 130.0, 129.9, 129.9, 129.7, 129.7, 129.3, 128.6, 128.6, 98.9, 74.0, 68.0, 67.6, 62.2 ppm. **HRMS** (QToF): Calcd for C$_{27}$H$_{22}$O$_7$Na [M + Na]$^+$ 481.1258 found 481.1266.
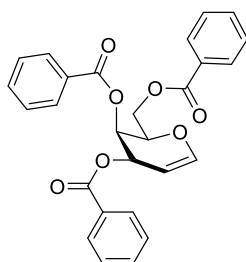
3,4,6-Tri-*O*-benzoyl-D-galactal (4.44f)

A suspension of unprotected galactal (50 mg, 0.34 mmol, 1.0 equiv.) in anhydrous pyridine (2 mL) was cooled to 0 °C and benzoyl chloride (0.24 mL, 2.05 mmol, 6.0 equiv.) was added, followed by addition of 4-DMAP (4.2 mg, 0.03 mmol, 0.1 equiv.). The reaction mixture was allowed to warm to room temperature and was stirred overnight, before it was diluted with water and extracted with ethyl acetate. The combined organic phase was washed with aqueous citric acid solution (10% v/v) and brine, dried over Na$_2$SO$_4$, filtered and concentrated. Compound **4.44f** (100 mg, 0.22 mmol, 64%) was obtained as a colorless syrup after purification by column chromatography (SiO$_2$, Hex/EtOAc 9:1).

^{1}H NMR (400 MHz, CDCl$_3$): δ 8.03 (ddd, *J* = 10.0, 8.4, 1.4 Hz, 4H), 7.94 – 7.84 (m, 2H), 7.64 – 7.39 (m, 7H), 7.38 – 7.29 (m, 2H), 6.63 (dd, *J* = 6.3, 1.6 Hz, 1H), 5.93 (dddd, *J* = 11.9, 4.5, 2.7, 1.4 Hz, 2H), 4.99 (ddd, *J* = 6.2, 2.9, 1.3 Hz, 1H), 4.80 (dd, *J* = 11.4, 7.7 Hz, 1H), 4.75 – 4.65 (m, 1H), 4.57 (dd, *J* = 11.4, 4.6 Hz, 1H) ppm. **^{13}C NMR** (101 MHz, CDCl$_3$): δ 166.4, 166.0, 165.7, 145.9, 133.6, 133.4, 133.3, 130.3, 130.1, 129.9, 129.8, 129.7, 129.7, 129.4, 128.6, 128.6, 128.5, 99.2, 73.2, 65.1, 62.7 ppm. **HRMS** (QToF): Calcd for C$_{27}$H$_{22}$O$_7$Na [M + Na]$^+$ 481.1258 found 481.1274.

3,4,6-Tri-*O*-benzyl-D-glucal (4.42d)
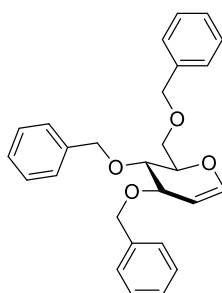
Unprotected glucal (50 mg, 0.34 mmol, 1.0 equiv.) was dissolved in anhydrous CH_2Cl_2 (3 mL). The stirred solution was cooled to 0 °C and sodium hydride (66 mg, 2.74 mmol; 60% dispersion in mineral oil, 8.0 eq.) was added in small portions. After 30 min, benzyl bromide (0.05 mL, 1.71 mmol, 5.0 eq.) was added dropwise. The reaction mixture was allowed to warm to room temperature and was stirred for 6 h. Methanol (5 mL) was added, the reaction mixture was stirred for 10 min and afterwards diluted with EtOAc (20 mL). The organic layer was washed with water (2 x 10 mL). The aqueous phase was extracted with ethyl acetate (2 x 10 mL). The combined organic phase was washed with water (10 mL) followed by brine (10 mL), dried over Na_2SO_4 and concentrated. Compound **4.42d** (110 mg, 0.34 mmol, 77%) was obtained as a colorless syrup after purification by column chromatography (SiO_2, Hex/EtOAc 9:1).

¹H NMR (400 MHz, $CDCl_3$): δ 7.41 – 7.28 (m, 15H), 6.43 (dd, *J* = 6.1, 1.5 Hz, 1H), 4.88 (dd, *J* = 6.1, 2.7 Hz, 1H), 4.87 – 4.81 (m, 1H), 4.69 – 4.66 (m, 1H), 4.65 – 4.62 (m, 1H), 4.60 – 4.54 (m, 3H), 4.22 (ddd, *J* = 6.2, 2.9, 1.5 Hz, 1H), 4.07 (ddd, *J* = 8.2, 5.0, 2.9 Hz, 1H), 3.91 – 3.73 (m, 3H) ppm. **¹³C NMR** (101 MHz, $CDCl_3$): δ 144.9, 138.5, 138.3, 138.1, 128.6, 128.5, 128.1, 127.9, 127.9, 127.8, 100.1, 75.9, 74.5, 73.9, 73.6, 72.3, 70.6, 68.7 ppm. **HRMS** (QToF): Calcd for $C_{27}H_{28}O_4Na$ [M + Na]⁺ 439.1880 found 439.2028.

3,4,6-Tri-*O*-benzyl-D-glucal (4.44d)

Unprotected galactal (50 mg, 0.34 mmol, 1.0 equiv.) was dissolved in anhydrous CH_2Cl_2 (3 mL). The stirred solution was cooled to 0 °C and sodium hydride (66 mg, 2.74 mmol; 60% dispersion in mineral oil, 8.0 eq.) was added in small portions. After 30 min, benzyl bromide (0.05 mL, 1.71 mmol, 5.0 eq.) was added dropwise. The reaction mixture was allowed to warm to room temperature and was stirred for 6 h. Methanol (5 mL) was added, the reaction mixture

was stirred for 10 min and afterwards diluted with EtOAc (20 mL). The organic layer was washed with water (2 x 10 mL). The aqueous phase was extracted with ethyl acetate (2 x 10 mL). The combined organic phase was washed with water (10 mL) followed by brine (10 mL), dried over Na_2SO_4 and concentrated. Compound **4.44d** (120 mg, 0.29 mmol, 84%) was obtained as a colorless syrup after purification by column chromatography (SiO_2, Hex/EtOAc 9:1).

^{1}H NMR (400 MHz, $CDCl_3$): δ 7.41 – 7.27 (m, 15H), 6.37 (dd, J = 6.3, 1.7 Hz, 1H), 4.92 – 4.82 (m, 2H), 4.71 – 4.61 (m, 3H), 4.61 – 4.33 (m, 2H), 4.23 – 4.15 (m, 2H), 3.98 – 3.92 (m, 1H), 3.78 (dd, J = 10.2, 7.2 Hz, 1H), 3.64 (dd, J = 10.1, 5.1 Hz, 1H) ppm. **^{13}C NMR** (101 MHz, $CDCl_3$): δ 144.3, 138.6, 138.5, 138.1, 128.5, 128.5, 128.3, 128.1, 127.8, 127.7, 127.6, 75.8, 73.6, 71.0, 68.6 ppm. **HRMS** (QToF): Calcd for $C_{27}H_{28}O_4Na$ [M + Na]$^+$ 439.1880 found 439.2034.

3,4,6-Tri-*O*-pentafluorobenzoyl-D-glucal (4.42h)
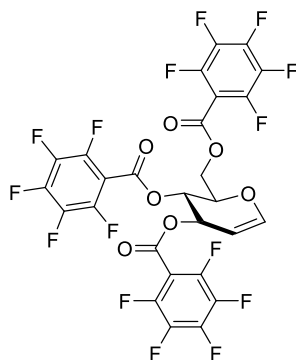
A suspension of unprotected glucal (20 mg, 0.14 mmol, 1.0 equiv.) in anhydrous pyridine (2 mL) was cooled to 0 °C and PFP-Cl (0.09 mL, 0.68 mmol, 5.0 equiv.) was added, followed by addition of 4-DMAP (1.7 mg, 0.01 mmol, 0.1 equiv.). The reaction mixture was allowed to warm to room temperature and was stirred overnight. The volatiles were removed and compound **4.42h** (32 mg, 0.04 mmol, 32%) was obtained as a colorless syrup after purification by column chromatography (SiO_2, Hex/EtOAc 9:1 to 3:1).

^{1}H NMR (700 MHz, $CDCl_3$): δ 6.60 (dd, J = 6.2, 1.6 Hz, 1H), 5.79 (ddd, J = 5.1, 3.3, 1.3 Hz, 1H), 5.70 (dd, J = 8.1, 5.8 Hz, 1H), 5.05 (dd, J = 6.2, 3.2 Hz, 1H), 4.77 (dd, J = 12.3, 5.2 Hz, 1H), 4.63 (dd, J = 12.4, 3.3 Hz, 1H), 4.54 (ddd, J = 8.3, 5.3, 3.2 Hz, 1H) ppm. **^{13}C NMR** (176 MHz, $CDCl_3$): δ 158.7, 158.6, 157.7, 146.8, 146.6, 146.5, 145.1, 144.5, 143.3, 143.0, 138.7, 138.6, 138.5, 137.3, 137.3, 137.1, 107.4, 107.2, 106.9, 106.8, 98.2, 73.4, 70.0, 69.0, 62.8 ppm. **^{19}F NMR** (659 MHz, $CDCl_3$): δ -137.21 (dt, J = 19.1, 5.4 Hz), -137.71 (dt, J = 19.1, 4.8 Hz), -146.45 (tt, J = 21.5, 6.0 Hz), -147.10 (tt, J = 20.3, 5.4 Hz), -147.28 (tt, J = 20.3,

5.4 Hz), -159.47 – -159.66 (m), -159.70 – -159.88 (m), -159.88 – -160.09 (m) ppm. **HRMS** (QToF): Calcd for $C_{27}H_7F_{15}O_7Na$ [M + Na]$^+$ 750.9844 found 750.9976.

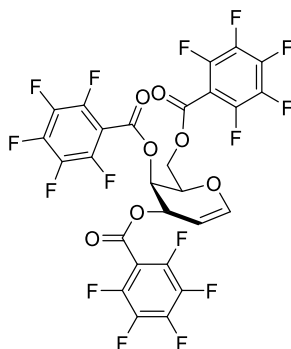### 3,4,6-Tri-*O*-pentafluorobenzoyl-D-galactal (4.44h)

A suspension of unprotected galactal (20 mg, 0.14 mmol, 1.0 equiv.) in anhydrous pyridine (2 mL) was cooled to 0 °C and PFP-Cl (0.09 mL, 0.68 mmol, 5.0 equiv.) was added, followed by addition of 4-DMAP (1.7 mg, 0.01 mmol, 0.1 equiv.). The reaction mixture was allowed to warm to room temperature and was stirred overnight. The volatiles were removed and compound **4.44h** (45 mg, 0.06 mmol, 45%) was obtained as a colorless syrup after purification by column chromatography (SiO$_2$, Hex/EtOAc 9:1 to 3:1).

^{1}H NMR (700 MHz, CDCl$_3$): δ 6.57 (dd, *J* = 6.3, 1.9 Hz, 1H), 5.97 (ddt, *J* = 4.5, 2.9, 1.4 Hz, 1H), 5.89 (dt, *J* = 4.2, 1.8 Hz, 1H), 4.94 (ddd, *J* = 6.3, 3.1, 1.3 Hz, 1H), 4.75 (dd, *J* = 11.3, 7.3 Hz, 1H), 4.68 – 4.55 (m, 2H) ppm. **^{19}F NMR** (659 MHz, CDCl$_3$): δ -137.14 – -137.42 (m), -146.56 (t, *J* = 20.9 Hz), -146.79 (tt, *J* = 20.3, 5.4 Hz), -147.25 (tt, *J* = 20.3, 5.4 Hz), -159.72 (td, *J* = 20.3, 6.0 Hz), -159.89 (dd, *J* = 20.3, 14.3 Hz), -160.02 (dd, *J* = 20.3, 14.3 Hz) ppm. **^{13}C NMR** (176 MHz, CDCl$_3$): δ 158.7, 158.6, 158.4, 146.8, 146.7, 146.6, 146.4, 145.3, 145.2, 145.0, 144.6, 144.5, 143.2, 143.0, 138.7, 138.5, 137.3, 137.2, 107.5, 107.4, 107.1, 107.1, 107.0, 106.9, 106.8, 97.9, 72.2, 66.0, 63.2 ppm. **HRMS** (QToF): Calcd for $C_{27}H_7F_{15}O_7Na$ [M + Na]$^+$ 750.9844 found 750.9890.
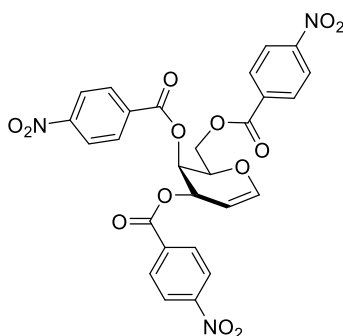
3,4,6-Tri-*O*-(*p*-nitrobenzoyl)-D-glucal (4.42g)
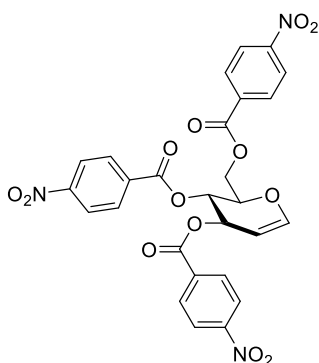
To a suspension of glucal (50 mg, 0.34 mmol, 1.0 equiv.) and 4-nitrobenzoic acid (343 mg, 2.05 mmol, 6.0 equiv.) in anhydrous CH_2Cl_2 (2 mL) was added dropwise a premixed solution of DIC (0.48 mL, 3.08 mmol, 9.0 equiv.) and 4-DMAP (8.36 mg, 0.07 mmol, 0.2 equiv.) in anhydrous CH_2Cl_2 (1 mL) at 0 °C. The reaction was stirred at room temperature overnight. The reaction mixture was filtered through Celite, the filtrate was washed with aqueous $NaHCO_3$ and the aqueous phase was extracted with CH_2Cl_2. The combined organic phase was dried over Na_2SO_4, filtered and concentrated. Compound **4.42g** (90 mg, 0.15 mmol, 44%) was obtained as a colorless syrup after purification by column chromatography (SiO_2, Hex/EtOAc 9:1 to 3:1).

¹H NMR (400 MHz, $CDCl_3$): δ 8.41 – 8.07 (m, 12H), 6.66 (dd, *J* = 6.2, 1.3 Hz, 1H), 5.89 – 5.78 (m, 2H), 5.11 (dd, *J* = 6.1, 3.4 Hz, 1H), 4.78 – 4.64 (m, 3H) ppm. **¹³C NMR** (101 MHz, $CDCl_3$): δ 164.4, 164.2, 163.6, 151.1, 146.7, 134.7, 134.2, 131.2, 131.1, 131.0, 123.9, 123.9, 123.8, 98.7, 73.9, 69.2, 68.6, 62.7 ppm.

3,4,6-Tri-*O*-(*p*-nitrobenzoyl)-D-galactal (4.44g)

To a suspension of galactal (50 mg, 0.34 mmol, 1.0 equiv.) and 4-nitrobenzoic acid (343 mg, 2.05 mmol, 6.0 equiv.) in anhydrous CH_2Cl_2 (2 mL) was added dropwise a premixed solution of DIC (0.48 mL, 3.08 mmol, 9.0 equiv.) and 4-DMAP (8.36 mg, 0.07 mmol, 0.2 equiv.) in anhydrous CH_2Cl_2 (1 mL) at 0 °C. The reaction was stirred at room temperature overnight. The reaction mixture was filtered through Celite, the filtrate was washed with aqueous $NaHCO_3$ and the aqueous phase was extracted with CH_2Cl_2. The combined organic phase was dried

over Na_2SO_4, filtered and concentrated. Compound **4.44g** (110 mg, 0.18 mmol, 54%) was obtained as a colorless syrup after purification by column chromatography (SiO_2, Hex/EtOAc 9:1 to 3:1).

¹H NMR (400 MHz, $CDCl_3$): δ 8.34 – 8.00 (m, 12H), 6.69 (dd, *J* = 6.2, 1.8 Hz, 1H), 5.97 (ddt, *J* = 27.7, 3.1, 2.1 Hz, 2H), 5.01 (ddd, *J* = 6.3, 2.7, 1.5 Hz, 1H), 4.82 – 4.70 (m, 2H), 4.59 (dd, *J* = 10.0, 3.6 Hz, 1H) ppm. **¹³C NMR** (101 MHz, $CDCl_3$): δ 164.4, 164.1, 164.0, 151.2, 150.9, 146.3, 134.7, 134.3, 131.1, 130.8, 123.8, 72.8, 65.9, 63.2 ppm.

3,4,6-Tri-*O*-(2-chloroacetyl)-D-glucal (4.42i)
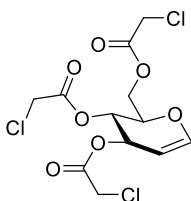
A suspension of unprotected glucal (20 mg, 0.14 mmol, 1.0 equiv.) in CH_2Cl_2 (3 mL) and anhydrous pyridine (0.14 mL, 1.71 mmol, 5.0 equiv.) was cooled to -20 °C and chloroacetyl chloride (0.07 mL, 0.82 mmol, 6.0 equiv.) was added. The reaction mixture was allowed to warm to 0 °C and was stirred for 5 h. The reaction mixture was diluted with water and extracted with ethyl acetate. The combined organic phase was washed with aqueous citric acid solution (10% v/v) and brine, dried over Na_2SO_4, filtered and concentrated. Compound **4.42i** (45 mg, 0.12 mmol, 87%) was obtained as a colorless syrup after purification by column chromatography (SiO_2, Hex/EtOAc 9:1 to 3:1).

¹H NMR (700 MHz, $CDCl_3$): δ 6.51 (dd, *J* = 6.1, 1.6 Hz, 1H), 5.50 (ddd, *J* = 5.3, 3.2, 1.5 Hz, 1H), 5.33 (dd, *J* = 8.0, 5.8 Hz, 1H), 4.89 (dd, *J* = 6.1, 3.2 Hz, 1H), 4.52 (dd, *J* = 12.2, 5.3 Hz, 1H), 4.41 – 4.32 (m, 2H), 4.11 (s, 2H), 4.08 (d, *J* = 2.2 Hz, 2H), 4.05 (s, 2H) ppm. **¹³C NMR** (176 MHz, $CDCl_3$): δ 167.1, 167.0, 166.4, 146.5, 98.4, 73.5, 69.3, 68.7, 62.7, 40.8, 40.7, 40.6 ppm.

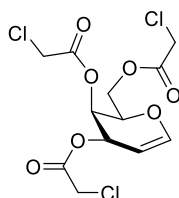### 3,4,6-Tri-*O*-(2-chloroacetyl)-D-glucal (4.44i)

A suspension of unprotected galactal (20 mg, 0.14 mmol, 1.0 equiv.) in CH_2Cl_2 (3 mL) and anhydrous pyridine (0.14 mL, 1.71 mmol, 5.0 equiv.) was cooled to -20 °C and chloroacetyl chloride (0.07 mL, 0.82 mmol, 6.0 equiv.) was added. The reaction mixture was allowed to warm to 0 °C and was stirred for 5 h. The reaction mixture was diluted with water and extracted

with ethyl acetate. The combined organic phase was washed with aqueous citric acid solution (10% v/v) and brine, dried over Na_2SO_4, filtered and concentrated. Compound **4.44i** (25 mg, 0.07 mmol, 49%) was obtained as a colorless syrup after purification by column chromatography (SiO_2, Hex/EtOAc 9:1 to 3:1).

¹H NMR (700 MHz, $CDCl_3$): δ 6.51 (dd, J = 6.1, 1.6 Hz, 1H), 5.50 (ddd, J = 5.3, 3.2, 1.5 Hz, 1H), 5.33 (dd, J = 8.0, 5.8 Hz, 1H), 4.89 (dd, J = 6.1, 3.2 Hz, 1H), 4.52 (dd, J = 12.2, 5.3 Hz, 1H), 4.41 – 4.32 (m, 2H), 4.11 (s, 2H), 4.08 (d, J = 2.2 Hz, 2H), 4.05 (s, 2H) ppm. **¹³C NMR** (176 MHz, $CDCl_3$): δ 167.1, 167.0, 166.4, 146.5, 98.4, 73.5, 69.3, 68.7, 62.7, 40.8, 40.7, 40.6 ppm.

Ethyl 2,3,6-tris-*O*-benzyl-1-thio-α-D-mannopyranoside[150] (4.30)
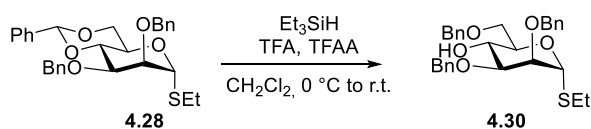
Mannose **4.28**[151] (500 mg, 1.0 mmol, 1.0 equiv.) was co-evaporated with anhydrous toluene (2 x 3 mL), and dissolved in anhydrous CH_2Cl_2 (15 mL). Triethylsilane (1.0 mL, 6.1 mmol, 6.0 equiv.) and trifluoroacetic anhydride (0.14 mL, 1.0 mmol, 1.0 equiv.) were added and the solution was cooled to 0 °C. Trifluoroacetic acid (0.45 mL, 6.1 mmol, 6.00 equiv.) was added dropwise. The mixture was allowed to warm to room temperature and was stirred for 5 h. The solution was diluted with CH_2Cl_2 and quenched with sat. aq. $NaHCO_3$ (40 mL). The aqueous phase was extracted with CH_2Cl_2 (2 x 60 mL) and the combined organic phase was washed with water (60 mL), dried over Na_2SO_4, filtered and concentrated. Product **4.30** (310 mg, 0.6 mmol, 62%) was obtained as a colorless syrup after purification by column chromatography (SiO_2, Hex/EtOAc 9:1 to 3:1).

R_f = 0.37 (Hex/EtOAc 3:1). **¹H NMR** (700 MHz, $CDCl_3$): δ 7.36 – 7.19 (m, 15H), 5.38 (s, 1H), 4.66 (d, J = 12.2 Hz, 1H), 4.63 – 4.49 (m, 4H), 4.43 (d, J = 11.7 Hz, 1H), 4.11 – 4.03 (m, 2H), 3.81 (dd, J = 3.2, 1.5 Hz, 1H), 3.75 (d, J = 3.9 Hz, 2H), 3.62 (dd, J = 8.7, 3.1 Hz, 1H), 2.65 – 2.50 (m, 2H), 1.23 (t, J = 7.4 Hz, 3H) ppm.

Ethyl 2,3,4-tris-*O*-benzyl-1-thio-α-D-mannopyranoside[152] (4.31)
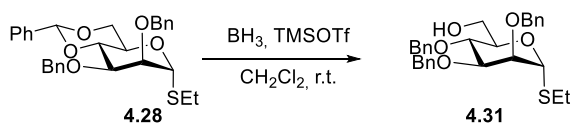
To a solution of **4.28** (500 mg, 1.0 mmol, 1.00 equiv.) in anhydrous CH_2Cl_2 (10 mL) was added BH_3 (1 M solution in THF, 5.1 mL, 5.1 mmol, 5.00 equiv.) and TMSOTf (28 μL, 0.15 mmol,

0.15 equiv.). The mixture was stirred under argon atmosphere at room temperature for 4 h. Et_3N (1 mL) was added followed by MeOH until the evolution of H_2 ceased. The mixture was concentrated and coevaporated with MeOH (3 x 30 mL). Compound **4.31** (370 mg, 0.7 mmol, 74%) was obtained as a white solid after purification by column chromatography (SiO_2, Hex/EtOAc 3:1).

R_f = 0.19 (Hex/EtOAc 3:1). **^{1}H NMR** (600 MHz, $CDCl_3$): δ 7.40 – 7.27 (m, 15H), 5.30 (d, J = 1.4 Hz, 1H), 4.95 (d, J = 10.9 Hz, 1H), 4.73 – 4.53 (m, 5H), 4.00 (dt, J = 5.0, 1.4 Hz, 2H), 3.89 – 3.77 (m, 4H), 2.63 – 2.49 (m, 2H), 1.23 (t, J = 7.4 Hz, 3H) ppm.

Ethyl 2,3-bis-*O*-benzyl-1-thio-α-D-mannopyranoside[153] (4.29)
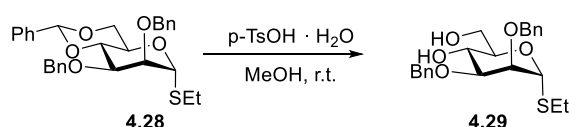
To a suspension of **4.28** (600 mg, 1.2 mmol, 1.0 equiv.) in MeOH (5 mL) was added p-TSA (116 mg, 0.6 mmol, 0.5 equiv.). The reaction mixture was sonicated for one hour at room temperature, after which pyridine (5 mL) was added. The solvent was removed and the residue was redissolved in ethyl acetate, washed with water, dried over Na_2SO_4, filtered and concentrated. Compound **4.29** (480 mg, 1.2 mmol, 97%) was obtained as a colorless oil after purification by column chromatography (SiO_2, Hex/EtOAc 3:1 to 2:3).

R_f = 0.13 (Hex/EtOAc 1:1). **^{1}H NMR** (600 MHz, $CDCl_3$): δ 7.39 – 7.28 (m, 10H), 5.35 (d, J = 1.6 Hz, 1H), 4.69 – 4.57 (m, 3H), 4.54 (dd, J = 11.7, 1.4 Hz, 1H), 4.43 (d, J = 11.6 Hz, 1H), 4.05 (t, J = 9.5 Hz, 1H), 4.02 – 3.95 (m, 1H), 3.91 – 3.81 (m, 4H), 3.65 (dd, J = 9.4, 3.1 Hz, 1H), 2.66 – 2.54 (m, 2H), 1.26 (td, J = 7.4, 1.3 Hz, 3H) ppm.

Ethyl 2,3,6-tris-*O*-benzyl-4-*O*-levulinyl-1-thio-α-D-mannopyranoside (4.33)
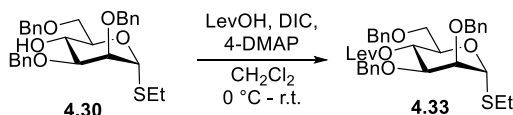
To a solution of **4.30** (150 mg, 0.3 mmol, 1.0 equiv.) and LevOH (0.06 mL, 0.6 mmol, 2.0 equiv.) in anhydrous CH_2Cl_2 (5 mL) was added dropwise a premixed solution of DIC (0.14 mL, 0.9 mmol, 3.0 equiv.) and DMAP (7 mg, 0.1 mmol, 0.2 equiv.) in anhydrous CH_2Cl_2 (5 mL) at 0 °C. The reaction was stirred at room temperature overnight. The reaction mixture was filtered through Celite, the filtrate was washed with aqueous $NaHCO_3$ and the aqueous phase was extracted with CH_2Cl_2. The combined organic phase was dried over Na_2SO_4, filtered and

concentrated. Compound **4.33** (160 mg, 0.3 mmol, 89%) was obtained as a colorless syrup after purification by column chromatography (SiO$_2$, Hex/EtOAc 9:1 to 1:1).

^{1}H NMR (700 MHz, CDCl$_3$): δ 7.37 – 7.22 (m, 15H), 5.40 (t, J = 9.7 Hz, 1H), 5.36 (d, J = 1.8 Hz, 1H), 4.67 (d, J = 4.4 Hz, 2H), 4.55 – 4.39 (m, 4H), 4.21 (ddd, J = 9.5, 5.9, 3.0 Hz, 1H), 3.81 (dd, J = 3.1, 1.8 Hz, 1H), 3.77 (dd, J = 9.5, 3.1 Hz, 1H), 3.66 – 3.55 (m, 2H), 2.70 – 2.55 (m, 4H), 2.43 (td, J = 6.7, 3.5 Hz, 2H), 2.12 (s, 3H), 1.26 (t, J = 7.4 Hz, 3H) ppm. **^{13}C NMR** (176 MHz, CDCl$_3$): δ 206.5, 171.9, 138.2, 128.5, 128.5, 128.3, 128.0, 127.9, 127.8, 127.8, 127.5, 82.1, 77.4, 76.1, 73.5, 72.4, 72.0, 70.7, 69.8, 69.4, 38.0, 29.9, 28.2, 25.4, 15.0 ppm. **HRMS** (QToF): Calcd for C$_{34}$H$_{40}$O$_7$SNa [M + Na]$^+$ 615.2387; found 615.2420.

Ethyl 2,3,4-tris-*O*-benzyl-6-*O*-levulinyl-1-thio-α-D-mannopyranoside (4.34)
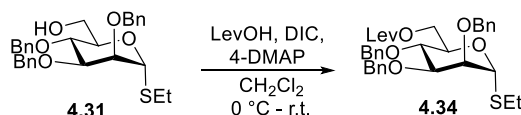
To a solution of **4.31** (150 mg, 0.3 mmol, 1.0 equiv.) and LevOH (0.06 mL, 0.6 mmol, 2.0 equiv.) in anhydrous CH$_2$Cl$_2$ (5 mL) was added dropwise a premixed solution of DIC (0.14 mL, 0.9 mmol, 3.0 equiv.) and DMAP (7 mg, 0.1 mmol, 0.2 equiv.) in anhydrous CH$_2$Cl$_2$ (5 mL) at 0 °C. The reaction was stirred at room temperature overnight. The reaction mixture was filtered through Celite, the filtrate was washed with aqueous NaHCO$_3$ and the aqueous phase was extracted with CH$_2$Cl$_2$. The combined organic phase was dried over Na$_2$SO$_4$, filtered and concentrated. Compound **4.34** (140 mg, 0.2 mmol, 78%) was obtained as a colorless syrup after purification by column chromatography (SiO$_2$, Hex/EtOAc 9:1 to 1:1).

^{1}H NMR (700 MHz, CDCl$_3$): δ 7.40 – 7.26 (m, 15H), 5.35 (d, J = 1.4 Hz, 1H), 4.92 (d, J = 10.8 Hz, 1H), 4.78 – 4.63 (m, 2H), 4.62 – 4.55 (m, 3H), 4.38 (d, J = 5.0 Hz, 1H), 4.31 (dd, J = 11.9, 2.2 Hz, 1H), 4.16 (ddd, J = 9.8, 5.0, 2.1 Hz, 1H), 3.95 – 3.90 (m, 1H), 3.86 – 3.81 (m, 2H), 2.71 (td, J = 6.7, 2.6 Hz, 2H), 2.65 – 2.51 (m, 4H), 2.14 (s, 3H), 1.25 (t, J = 7.4 Hz, 3H) ppm.**^{13}C NMR** (176 MHz, CDCl$_3$): δ 206.6, 172.7, 138.4, 138.2, 138.2, 128.6, 128.5, 128.3, 128.0, 128.0, 127.9, 127.9, 82.2, 80.5, 76.5, 75.3, 74.8, 72.2, 72.2, 70.4, 63.8, 38.0, 30.0, 28.1, 25.6, 15.1 ppm. **HRMS** (QToF): Calcd for C$_{34}$H$_{40}$O$_7$SNa [M + Na]$^+$ 615.2387; found 615.2417.

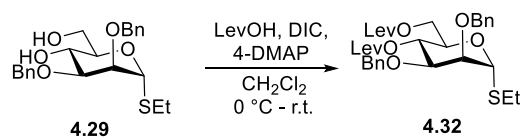### Ethyl 2,3-bis-*O*-benzyl-4,6-bis-*O*-levulinyl-1-thio-α-D-mannopyranoside (4.32)

To a solution of **4.29** (150 mg, 0.3 mmol, 1.0 equiv.) and LevOH (0.13 mL, 1.2 mmol, 4.0 equiv.) in anhydrous CH$_2$Cl$_2$ (5 mL) was added dropwise a premixed solution of DIC (0.28 mL,

1.8 mmol, 6.0 equiv.) and DMAP (8 mg, 0.1 mmol, 0.2 equiv.) in anhydrous CH_2Cl_2 (5 mL) at 0 °C. The reaction was stirred at room temperature overnight. The reaction mixture was filtered through Celite, the filtrate was washed with aqueous $NaHCO_3$ and the aqueous phase was extracted with CH_2Cl_2. The combined organic phase was dried over Na_2SO_4, filtered and concentrated. Compound **4.32** (170 mg, 0.3 mmol, 93%) was obtained as a colorless syrup after purification by column chromatography (SiO_2, Hex/EtOAc 9:1 to 1:1).

¹H NMR (700 MHz, $CDCl_3$): δ 7.37 – 7.25 (m, 10H), 5.39 (t, J = 9.6 Hz, 1H), 5.33 (d, J = 1.7 Hz, 1H), 4.67 (s, 2H), 4.55 – 4.42 (m, 2H), 4.25 – 4.18 (m, 2H), 4.15 – 4.10 (m, 1H), 3.81 (t, J = 2.5 Hz, 1H), 3.75 (dd, J = 9.6, 3.0 Hz, 1H), 2.78 – 2.44 (m, 10H), 2.15 (s, 3H), 2.14 (s, 3H), 1.26 (t, J = 7.4 Hz, 3H) ppm. **¹³C NMR** (176 MHz, $CDCl_3$): δ 206.7, 206.4, 172.5, 171.8, 138.1, 138.0, 128.5, 128.5, 128.0, 127.9, 127.9, 82.5, 77.3, 72.5, 72.1, 69.5, 68.5, 63.1, 38.0, 30.0, 28.1, 25.6, 15.1 ppm. **HRMS** (QToF): Calcd for $C_{32}H_{40}O_9SNa$ [M + Na]⁺ 623.2285; found 623.2310.

Ethyl 2,3-bis-*O*-benzyl-4,6-bis-*O*-levulinyl-1-thio-β-ᴅ-galactopyranoside (4.06c)
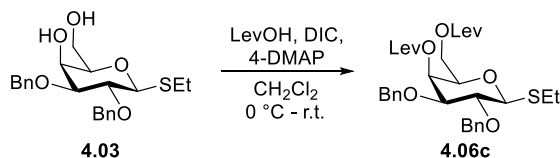
A solution of **4.03** (150 mg, 0.37 mmol, 1.0 equiv.) and LevOH (150 mL, 1.48 mmol, 4.0 equiv.) in anhydrous CH_2Cl_2 (5 mL) was cooled to 0 °C and was stirred for 5 minutes. A mixture of DCC (306 mg, 1.48 mmol, 4.0 equiv.) and 4-DMAP (9 mg, 0.07 mmol, 0.2 equiv.) in anhydrous CH_2Cl_2 (2 mL) was added dropwise. The reaction mixture was allowed to warm to room temperature und was stirred for 18 h. The mixture was filtered, washed with saturated aqueous $NaHCO_3$ (20 mL), dried over Na_2SO_4, filtered and concentrated. Product **4.06c** (210 mg, 0.35 mmol, 94%) was obtained as a colorless solid after purification by column chromatography (SiO_2, Hex/EtOAc 1:1).

¹H NMR (600 MHz, $CDCl_3$): δ 7.40 – 7.27 (m, 10H), 5.54 (dd, J = 3.4, 1.1 Hz, 1H), 4.84 – 4.74 (m, 2H), 4.73 (d, J = 11.2 Hz, 1H), 4.55 – 4.44 (m, 2H), 4.17 (ddd, J = 58.9, 11.3, 6.7 Hz, 2H), 3.77 (td, J = 6.7, 1.2 Hz, 1H), 3.62 (dd, J = 9.2, 3.3 Hz, 1H), 3.56 (t, J = 9.4 Hz, 1H), 2.82 – 2.63 (m, 8H), 2.60 – 2.53 (m, 2H), 2.19 (s, 3H), 2.16 (s, 3H), 1.32 (t, J = 7.4 Hz, 3H) ppm. **¹³C NMR** (151 MHz, $CDCl_3$): δ 206.6, 206.3, 172.5, 172.3, 138.2, 137.8, 128.5, 128.5, 128.3, 127.9, 127.9, 85.5, 80.8, 77.8, 76.0, 74.4, 72.0, 67.0, 62.3, 38.2, 38.1, 29.9, 28.2, 28.0, 25.2, 15.3 ppm. **HRMS** (QToF): Calcd for $C_{32}H_{40}O_9SNa$ [M + Na]⁺ 623.2285; found 623.2295.

Ethyl 2,3,6-tris-*O*-benzyl-4-*O*-levulinyl-1-thio-β-D-galactopyranoside (4.07c)
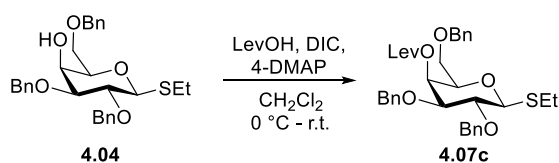
A solution of **4.04** (150 mg, 0.30 mmol, 1.0 equiv.) and LevOH (62 mL, 0.61 mmol, 2.0 equiv.) in anhydrous CH_2Cl_2 (5 mL) was cooled to 0 °C and was stirred for 5 minutes. A mixture of DCC (125 mg, 0.61 mmol, 2.0 equiv.) and 4-DMAP (3.7 mg, 0.03 mmol, 0.1 equiv.) in anhydrous CH_2Cl_2 (1 mL) was added dropwise. The reaction mixture was allowed to warm to room temperature und was stirred for 18 h. The mixture was filtered, washed with saturated aqueous $NaHCO_3$ (20 mL), dried over Na_2SO_4, filtered and concentrated. Product **4.07c** (150 mg, 0.25 mmol, 84%) was obtained as a colorless solid after purification by column chromatography (SiO_2, Hex/EtOAc 1:1).

**¹H NMR** (400 MHz, $CDCl_3$): δ 7.41 – 7.26 (m, 15H), 5.65 (d, *J* = 3.1 Hz, 1H), 4.84 – 4.71 (m, 3H), 4.56 – 4.43 (m, 4H), 3.71 (t, *J* = 6.5 Hz, 1H), 3.66 – 3.48 (m, 4H), 2.83 – 2.57 (m, 6H), 2.16 (s, 3H), 1.31 (t, *J* = 7.4 Hz, 3H) ppm. **¹³C NMR** (101 MHz, $CDCl_3$): δ 206.4, 172.2, 138.2, 137.9, 128.6, 128.5, 128.5, 128.5, 128.3, 128.0, 127.9, 127.9, 85.5, 81.1, 78.0, 76.0, 76.0, 73.9, 71.9, 68.4, 67.3, 38.2, 30.0, 28.1, 25.1, 15.2 ppm. **HRMS** (QToF): Calcd for $C_{34}H_{40}O_7SNa$ [M + Na]⁺ 615.2387; found 615.2394.

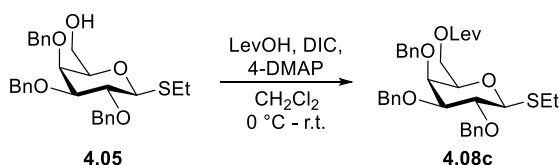**Ethyl 2,3,4-tris-*O*-benzyl-6-*O*-levulinyl-1-thio-β-D-galactopyranoside (4.08c)**

A solution of **4.05** (100 mg, 0.20 mmol, 1.0 equiv.) and LevOH (41 mL, 0.40 mmol, 2.0 equiv.) in anhydrous CH_2Cl_2 (5 mL) was cooled to 0 °C and was stirred for 5 minutes. A mixture of DCC (83 mg, 0.40 mmol, 2.0 equiv.) and 4-DMAP (2.5 mg, 0.02 mmol, 0.1 equiv.) in anhydrous CH_2Cl_2 (1 mL) was added dropwise. The reaction mixture was allowed to warm to room temperature und was stirred for 18 h. The mixture was filtered, washed with saturated aqueous $NaHCO_3$ (20 mL), dried over Na_2SO_4, filtered and concentrated. Product **4.08c** (100 mg, 0.17 mmol, 84%) was obtained as a colorless solid after purification by column chromatography (SiO_2, Hex/EtOAc 1:1).

¹H NMR (400 MHz, $CDCl_3$): δ 7.44 – 7.28 (m, 15H), 5.07 – 4.73 (m, 5H), 4.66 (d, *J* = 11.7 Hz, 1H), 4.43 (d, *J* = 9.7 Hz, 1H), 4.16 (ddd, *J* = 62.5, 11.2, 6.4 Hz, 2H), 3.90 – 3.79 (m, 2H), 3.67

– 3.47 (m, 2H), 2.86 – 2.61 (m, 4H), 2.48 (td, J = 6.3, 2.5 Hz, 2H), 2.17 (s, 3H), 1.30 (t, J = 7.4 Hz, 3H) ppm. ^{13}**C NMR** (101 MHz, CDCl$_3$): δ 206.7, 172.6, 138.5, 138.4, 138.3, 128.6, 128.6, 128.5, 128.4, 128.4, 127.9, 127.9, 127.8, 127.7, 85.5, 84.1, 78.4, 75.9, 75.9, 74.4, 73.2, 73.1, 63.5, 38.0, 30.0, 27.9, 25.1, 15.2 ppm. **HRMS** (QToF): Calcd for C$_{34}$H$_{40}$O$_7$SNa [M + Na]$^+$ 615.2387; found 615.2388.

6.4.2   AGA-Galactose Building Block 4.12

Ethyl   2-*O*-benzyl-3-*O*-(2-naphthalenylmethyl)-4,6-*O*-[(*S*)-phenylmethylene]-1-thio-β-D-galactopyranoside[154] (4.09)
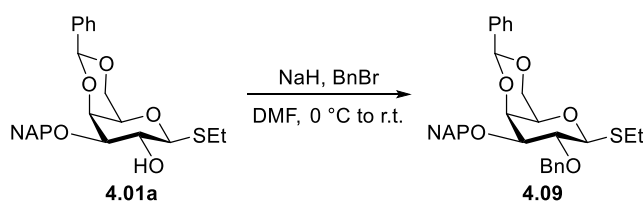
Compound **4.01a**[154] (7.4 g, 16.4 mmol, 1.0 equiv.) was dissolved in anhydrous DMF (75 mL). The stirred solution was cooled to 0 °C and sodium hydride (1.5 g, 24.6 mmol; 60% dispersion in mineral oil, 2.3 equiv.) was added in small portions. After 30 min, benzyl bromide (1.3 mL, 37.7 mmol, 1.5 equiv.) was added dropwise. The reaction mixture was allowed to warm to room temperature and was stirred overnight. Methanol (10 mL) was added, the reaction mixture was stirred for 10 min and afterwards diluted with ethyl acetate (100 mL). The organic layer was washed with water (2 x 100 mL). The aqueous phase was extracted with ethyl acetate (2 x 100 mL). The combined organic phase was washed with water (100 mL), dried over Na$_2$SO$_4$ and concentrated. Product **4.09** (8.8 g, 16.2 mmol, 99%) was obtained as a colorless solid after purification by column chromatography (SiO$_2$, Hex/EtOAc 3:1).

R$_f$ = 0.22 (Hex/EtOAc 3:1). ^{1}**H NMR** (700 MHz, CDCl$_3$) δ 7.87 – 7.78 (m, 3H), 7.74 – 7.69 (m, 1H), 7.57 – 7.29 (m, 13H), 5.48 (s, 1H), 4.96 – 4.87 (m, 4H), 4.44 (d, J = 9.7 Hz, 1H), 4.30 (dd, J = 12.3, 1.8 Hz, 1H), 4.17 (d, J = 3.7 Hz, 1H), 3.96 – 3.90 (m, 2H), 3.65 (dd, J = 9.2, 3.5 Hz, 1H), 3.35 – 3.32 (m, 1H), 2.90 – 2.73 (m, 2H), 1.34 (t, J = 7.5 Hz, 3H) ppm. ^{13}**C NMR** (176 MHz, CDCl$_3$) δ 138.6, 138.1, 135.9, 133.4, 133.2, 129.2, 128.5, 128.5, 128.4, 128.3, 128.0, 127.9, 127.8, 126.7, 126.7, 126.3, 126.1, 126.0, 101.7, 84.6, 81.1, 77.1, 75.9, 74.2, 72.1, 69.9, 69.5, 24.0, 15.2 ppm. **HRMS** (QToF): Calcd for C$_{33}$H$_{34}$O$_5$SNa [M + Na]$^+$ 565.2019; found 565.2018.

Ethyl 2,6-bis-*O*-benzyl-3-*O*-(2-naphthalenylmethyl)-1-thio-β-D-galactopyranoside[155] (4.09a)
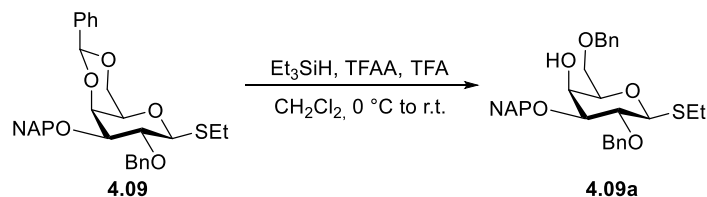
Compound **4.09** (2.0 g, 3.7 mmol, 1.0 equiv.) was co-evaporated with anhydrous toluene (2 x 3 mL), and dissolved in anhydrous CH_2Cl_2 (20 mL). Triethylsilane (3.5 mL, 22.1 mmol, 6.0 equiv.) and trifluoroacetic anhydride (0.52 mL, 3.7 mmol, 1.0 equiv.) were added and the solution was cooled to 0 °C. Trifluoroacetic acid (1.7 mL, 22.1 mmol, 6.0 equiv.) was added dropwise. The mixture was allowed to warm to room temperature and was stirred for 5 h. The solution was diluted with CH_2Cl_2 and quenched with saturated aqueous $NaHCO_3$ (40 mL). The aqueous phase was extracted with CH_2Cl_2 (2 x 60 mL) and the combined organic phase was washed with water (60 mL), dried over Na_2SO_4, filtered and concentrated. Product **4.09a** (1.8 g, 3.3 mmol, 90%) was obtained as a colorless syrup after purification by column chromatography (SiO_2, Hex/EtOAc 3:1 to 1:1).

R_f = 0.39 (Hex/EtOAc 1:1). **^{1}H NMR** (400 MHz, $CDCl_3$) δ 7.88 – 7.71 (m, 4H), 7.53 – 7.27 (m, 13H), 4.95 – 4.77 (m, 4H), 4.58 (s, 2H), 4.44 (d, *J* = 9.8 Hz, 1H), 4.14 (dd, *J* = 3.3, 1.1 Hz, 1H), 3.83 – 3.68 (m, 3H), 3.64 – 3.52 (m, 2H), 2.87 – 2.66 (m, 2H), 1.32 (t, *J* = 7.5 Hz, 3H) ppm. **^{13}C NMR** (101 MHz, $CDCl_3$) δ 138.3, 138.0, 135.3, 133.3, 133.2, 128.6, 128.5, 128.5, 128.0, 127.9, 127.9, 127.8, 126.8, 126.3, 126.2, 125.9, 85.2, 82.3, 78.0, 77.0, 76.0, 73.9, 72.3, 69.5, 67.1, 24.9, 15.3 ppm.

Ethyl 2,6-bis-*O*-benzyl-3-*O*-(2-naphthalenylmethyl)-4-(2,2-dimethylpropanoate)-1-thio-β-D-galactopyranoside (4.10)
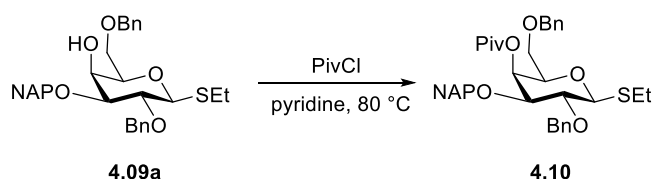
To a solution of **4.09a** (1.3 g, 2.4 mmol, 1.0 equiv.) in anhydrous pyridine (15 mL) pivaloyl chloride (1.5 mL, 12.0 mmol, 5.0 equiv.) was added. The mixture was stirred at 80 °C for two hours. The volatiles were evaporated. Product **4.10**(1.1 g, 1.7 mmol, **73%**) was obtained as a colorless oil after purification by column chromatography (SiO_2, Hex/EtOAc 9:1 to 3:1).

R_f = 0.43 (Hex/EtOAc 3:1). **^{1}H NMR** (400 MHz, $CDCl_3$) δ 7.84 – 7.68 (m, 4H), 7.50 – 7.41 (m, 3H), 7.39 – 7.27 (m, 10H), 5.68 (dd, *J* = 3.3, 1.1 Hz, 1H), 4.91 (d, *J* = 11.2 Hz, 1H), 4.80 (q, *J*

= 10.4 Hz, 2H), 4.63 (d, *J* = 11.2 Hz, 1H), 4.57 – 4.44 (m, 4H), 3.77 (ddd, *J* = 7.2, 5.8, 1.1 Hz, 1H), 3.67 (dd, *J* = 9.1, 3.3 Hz, 1H), 3.61 – 3.52 (m, 2H), 3.47 (dd, *J* = 9.5, 7.1 Hz, 1H), 1.31 (t, *J* = 7.5 Hz, 3H), 1.21 (s, 9H) ppm. ^{13}**C NMR** (101 MHz, CDCl$_3$) δ 177.7, 138.2, 135.6, 133.4, 133.1, 128.6, 128.6, 128.4, 128.2, 128.1, 127.9, 127.8, 127.0, 126.4, 126.1, 126.0, 85.2, 81.4, 77.0, 76.1, 75.9, 73.9, 71.9, 68.4, 66.6, 27.4, 24.7, 15.2 ppm. **HRMS** (QToF): Calcd for C$_{38}$H$_{44}$O$_6$SNa [M + Na]$^+$ 651.2751; found 651.2740.

Ethyl 2,6-bis-*O*-benzyl-4-(2,2-dimethylpropanoate)-1-thio-β-D-galactopyranoside (4.10a)
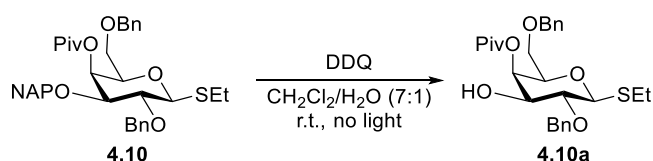
To a well stirred emulsion of **4.10** (1.3 g, 2.1 mmol, 1.0 equiv.) in CH$_2$Cl$_2$/water (7:1, 24 mL), was added DDQ (517 mg, 2.3 mmol, 1.1 equiv.) and the suspension was stirred at room temperature for 1.5 h protected from light. The mixture was diluted with CH$_2$Cl$_2$, washed with 10% Na$_2$S$_2$O$_3$ and saturated aqueous NaHCO$_3$ solution. The organic layer was dried over Na$_2$SO$_4$, filtered, concentrated and the residue was purified by column chromatography (SiO$_2$, Hex/EtOAc 9:1 to 3:1) to obtain compound **4.10a** (900 mg, 1.8 mmol, 89%) as a colorless solid.

^{1}**H NMR** (600 MHz, CDCl$_3$) δ 7.41 – 7.27 (m, 10H), 5.39 (dd, *J* = 3.4, 1.2 Hz, 1H), 4.93 (d, *J* = 11.0 Hz, 1H), 4.69 (d, *J* = 11.0 Hz, 1H), 4.53 – 4.43 (m, 3H), 3.82 – 3.76 (m, 2H), 3.55 (dd, *J* = 9.6, 6.2 Hz, 1H), 3.49 – 3.41 (m, 2H), 2.85 – 2.67 (m, 2H), 1.34 (t, *J* = 7.5 Hz, 3H), 1.18 (s, 9H) ppm. ^{13}**C NMR** (151 MHz, CDCl$_3$) δ 178.5, 137.9, 137.8, 128.8, 128.7, 128.6, 128.3, 128.0, 127.9, 85.1, 78.2, 76.3, 75.4, 74.1, 73.8, 69.8, 68.5, 39.3, 27.3, 25.0, 15.2 ppm. **HRMS** (QToF): Calcd for C$_{27}$H$_{36}$O$_6$SNa [M + Na]$^+$ 511.2125; found 511.2217.

Ethyl 2,6-bis-*O*-benzyl-4-(2,2-dimethylpropanoate)-4-*O*-fluorenylmethoxycarbonyl-1-thio-β-D-galactopyranoside (4.11)
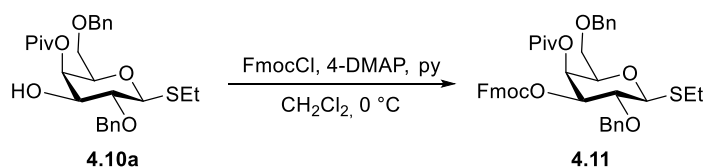
Compound **4.10a** was dissolved in anhydrous CH$_2$Cl$_2$ (20 mL) and anhydrous pyridine (0.41 mL, 5.12 mmol, 5.0 equiv.) was added followed by FmocCl (0.4 g, 1.54 mmol, 1.5 equiv.) at 0 °C. 4-DMAP (6 mg, 0.05 mmol, 0.05 equiv.) was added and the reaction mixture was stirred for one hour at 0 °C. Aqueous citric acid solution (10 mL) was added and the mixture was allowed to warm to room temperature. The aqueous phase was extracted with CH$_2$Cl$_2$ and the combined organic phase was dried over Na$_2$SO$_4$, filtered and concentrated. Compound

4.11 (600 mg, 0.84 mmol, 82%) was obtained as a white solid after purification by column chromatography (SiO$_2$, Hex/EtOAc 9:1 to 3:1).

^{1}H NMR (600 MHz, CDCl$_3$) δ 7.78 (ddt, J = 7.5, 2.0, 0.9 Hz, 2H), 7.63 (ddd, J = 9.2, 7.4, 0.9 Hz, 2H), 7.42 (tt, J = 7.5, 1.5 Hz, 2H), 7.38 – 7.26 (m, 12H), 5.62 (dd, J = 3.4, 1.1 Hz, 1H), 4.92 – 4.85 (m, 2H), 4.72 (d, J = 10.8 Hz, 1H), 4.57 – 4.43 (m, 4H), 4.34 – 4.25 (m, 2H), 3.88 (td, J = 6.4, 1.2 Hz, 1H), 3.67 (t, J = 9.6 Hz, 1H), 3.58 (dd, J = 9.6, 6.2 Hz, 1H), 3.46 (dd, J = 9.6, 6.5 Hz, 1H), 2.86 – 2.70 (m, 2H), 1.35 (t, J = 7.4 Hz, 3H), 1.22 (s, 9H) ppm. **^{13}C NMR** (151 MHz, CDCl$_3$) δ 177.5, 154.3, 143.8, 143.4, 141.4, 137.7, 137.6, 128.6, 128.5, 128.5, 128.0, 128.0, 127.9, 127.3, 127.3, 125.4, 125.3, 120.1, 85.2, 78.7, 75.9, 75.6, 75.5, 73.7, 70.3, 68.1, 67.7, 46.8, 39.3, 27.3, 25.0, 15.1 ppm. **HRMS** (QToF): Calcd for C$_{42}$H$_{46}$O$_8$SNa [M + Na]$^+$ 733.2806; found 733.2787.

Dibutoxyphosphoryloxy 2,6-bis-*O*-benzyl-4-(2,2-dimethylpropanoate)-4-*O*-fluorenylmethoxycarbonyl-α-D-galactopyranoside (4.12)
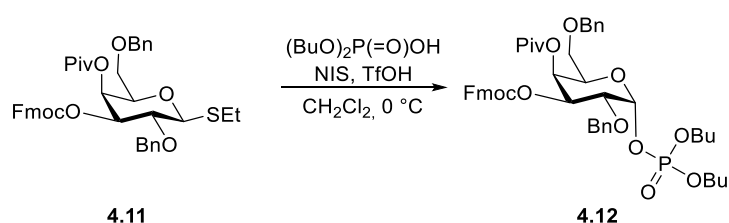
To a solution of **4.11** (300 mg, 0.4 mmol, 1.0 equiv.) and dibutyl phosphate (168 µL, 0.8 mmol, 2.0 equiv.) in anhydrous CH$_2$Cl$_2$ (4 mL) was added NIS (171 mg, 0.8 mmol, 1.5 equiv.) and TfOH (11 µL, 0.1 mmol, 0.3 equiv.) at 0 °C. The reaction was stirred for 1 h. To the reaction mixture was added 10% sodium thiosulfate solution. The bilayer mixture was extracted with CH$_2$Cl$_2$, dried with Na$_2$SO$_4$, filtered, concentrated and purified by flash column chromatography (SiO$_2$, Hex/EtOAc 3:1 to 2:3) to give title compound **4.12** (290 mg, 0.3 mmol, 80%) as a colorless foam.

R$_f$ = 0.16 (Hex/EtOAc 3:1). **^{1}H NMR** (600 MHz, CDCl$_3$) δ 7.77 (ddt, J = 7.6, 1.8, 0.9 Hz, 2H), 7.63 (tt, J = 7.5, 1.0 Hz, 2H), 7.41 (t, J = 7.1 Hz, 2H), 7.37 – 7.24 (m, 12H), 5.96 (dd, J = 7.3, 3.4 Hz, 1H), 5.63 (dd, J = 3.4, 1.5 Hz, 1H), 5.16 (dd, J = 10.4, 3.3 Hz, 1H), 4.81 – 4.62 (m, 2H), 4.56 – 4.36 (m, 4H), 4.35 – 4.24 (m, 2H), 4.09 – 3.97 (m, 4H), 3.88 (dt, J = 10.4, 2.9 Hz, 1H), 3.54 – 3.39 (m, 2H), 1.61 – 1.53 (m, 4H), 1.40 – 1.23 (m, 4H), 1.14 (s, 9H), 0.86 (dt, J = 15.0, 7.4 Hz, 6H) ppm. **^{13}C NMR** (151 MHz, CDCl$_3$) δ 177.4, 154.3, 143.8, 143.4, 141.4, 137.7, 137.3, 128.5, 128.5, 128.2, 128.1, 128.0, 128.0, 127.9, 127.3, 127.2, 125.4, 125.4, 120.2, 95.2, 73.7, 73.7, 72.7, 70.3, 69.8, 68.0, 67.8, 46.8, 39.2, 32.2, 27.2, 18.7, 13.7 ppm. **HRMS** (QToF): Calcd for C$_{48}$H$_{59}$O$_{12}$PNa [M + Na]$^+$ 881.3636; found 881.3759.

α-D-Galactopyranosyl-(1→3)-α-D-galactopyranosyl-(1→3)-α-D-galactopyranose (4.14)
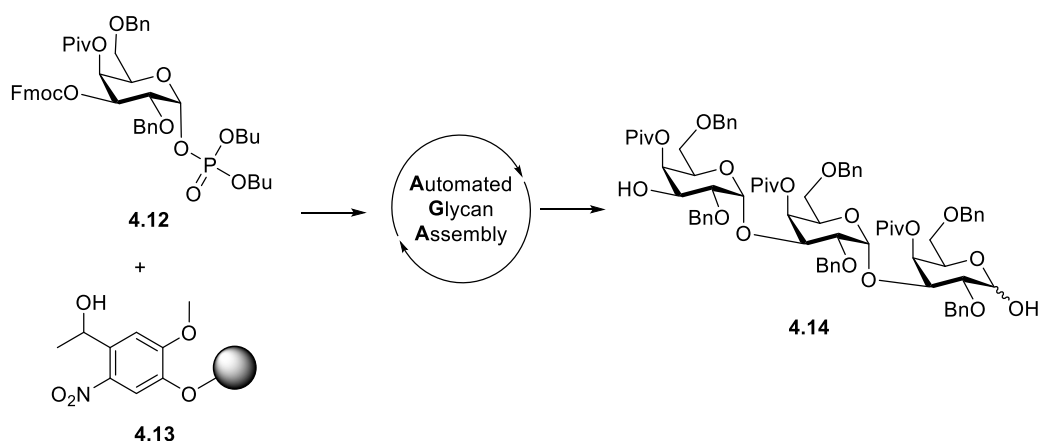
Repeat	Building Blocks	Modules	Notes	
2x		**I** – Acidic Wash		
	4.12 (2 x 4.7 equiv.)	**IIb** – Glycosylation with glycosyl phosphate	-35 °C (T_1) 5min (t_1)	-20 °C (T_2) 50 min (t_2)
		III – Capping **IVc** – Fmoc Deprotection		
1x		**I** – Acidic Wash		
	4.12 (9.4 equiv.)	**IIb** – Glycosylation with glycosyl phosphate – 2 cycles	-35 °C (T_1) 5min (t_1)	-20 °C (T_2) 50 min (t_2)
		III – Capping **IVc** – Fmoc Deprotection		

Trisaccharide **4.14** (12.5 mg, 0.014 mmol, 69%, α-only) was obtained as a colorless oil after photo-cleavage from solid-support following **Method A** and purification by normal-phase HPLC (**Method B-1b**, t_R = 9.1 to 9.8 min).

^{1}H NMR (700 MHz, CDCl$_3$) δ 7.40 – 7.20 (m, 30H), 5.54 (d, J = 3.2 Hz, 1H), 5.27 (dd, J = 6.6, 3.5 Hz, 3H), 5.23 (d, J = 3.4 Hz, 1H), 5.12 (d, J = 3.4 Hz, 1H), 4.77 – 4.70 (m, 2H), 4.59 – 4.56 (m, 3H), 4.54 – 4.42 (m, 5H), 4.38 (s, 1H), 4.36 – 4.32 (m, 4H), 4.30 – 4.25 (m, 3H), 3.91 (dd, J = 10.1, 3.5 Hz, 1H), 3.84 (dd, J = 10.3, 3.4 Hz, 1H), 3.78 (dd, J = 10.1, 3.5 Hz, 1H), 3.57 – 3.26 (m, 6H), 1.15 (s, 9H), 1.09 (s, 9H), 1.02 (s, 9H) ppm. **^{13}C NMR** (176 MHz, CDCl$_3$) δ 178.1, 177.4, 177.3, 138.3, 138.2, 138.1, 138.0, 137.9, 137.6, 128.7, 128.6, 128.5, 128.5, 128.5, 128.4, 128.3, 128.0, 128.0, 127.9, 127.7, 127.5, 93.1, 92.9, 91.9, 75.3, 74.7, 73.7, 73.2, 73.0, 72.7, 72.3, 70.5, 70.1, 69.8, 69.0, 68.6, 68.5, 68.3, 68.1, 68.0, 67.5, 66.8, 66.3, 39.2, 39.1, 39.0, 27.3, 27.2, 27.2 ppm. **HRMS** (QToF): Calcd for C$_{75}$H$_{92}$O$_{19}$Na [M + Na]$^+$ 1319.6125; found 1319.6166.

6.4.3 Alpha/beta-Ratio Determination

General Procedure for Glycosylations
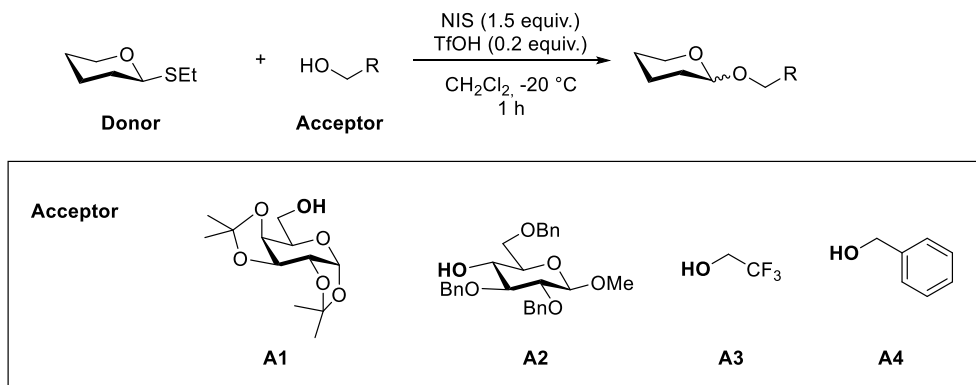
Donor (35 µmol, 1.0 equiv.) and the acceptor **A1** or **A2** (35 µmol, 1.0 equiv.) were co-evaporated with anhydrous toluene (3 x 2 mL) and kept under high vacuum for one hour. Anhydrous CH_2Cl_2 (2 mL) was added and if acceptor **A1** or **A2** were not used, acceptor **A3** or **A4** (175 µmol, 5 equiv.) was added and the mixture was stirred over activated molecular sieves (3 Å-AW) for 30 minutes at room temperature. The solution was cooled to -20 °C and NIS (52 µmol, 1.5 equiv.) was added followed by TfOH (60 µL of a 1% solution in CH_2Cl_2, 7 µmol, 0.2 equiv.) and the mixture was stirred for 1 h at -20 °C. The reaction mixture was quenched with pyridine, diluted with CH_2Cl_2, filtered and was then washed with 10% $Na_2S_2O_3$ (10 mL). The aqueous phase was extracted with CH_2Cl_2 (3 x 10 mL), dried over Na_2SO_4 and concentrated. The residue was purified by HPLC using **Method B-2**.

Determination of Alpha/Beta Ratios and Purification

Alpha/beta ratios were determined using HPLC and $^1H/^{13}C$/HSQC NMR spectroscopy.

Analytical NP-HPLC for alpha/beta ratio determination (Method B-2a)

Analytical NP-HPLC was conducted on an Agilent 1200 Series system. A YMC-Diol-300-NP column (150 mm x 4.600 mm I.D.) was used with a flow rate of 1.00 mL/min and hexanes/EtOAc as eluent (16 min linear gradient 2 to 25% EtOAc in hexanes, 2 min linear gradient 25 to 70% EtOAc in hexanes, 2 min isocratic 70% EtOAc).

Preparative NP-HPLC of Crude Material (Method B-2b)

Preparative NP-HPLC was conducted on an Agilent 1200 Series system. A YMC-Diol-300-NP column (150 mm x 20 mm I.D.) was used at a flow rate of 15.00 mL/min with hexane/EtOAc as eluent (16 min linear gradient 2 to 25% EtOAc in hexanes, 2 min linear gradient 25 to 70% EtOAc in hexanes, 2 min isocratic 70% EtOAc).

Analytical Data

1,2:3,4-Bis-*O*-(1-methylethylidene)-6-*O*-[2,3,4-tris-*O*-benzyl-6-(2,2-dimethylpropanoate)-α/β-D-galactopyranosyl]-α-D-galactopyranoside (4.08a-A1)
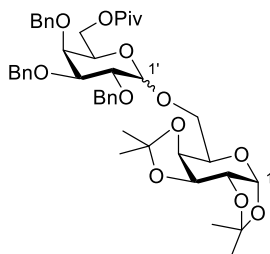
The title compound was prepared according to the general glycosylation procedure. Product **4.08a-A1** (20 mg, 26 µmol, 75%, **α/β 53:47**) was obtained as a colorless oil after purification using **Method-2b** (t_R (α) = 9.8 min, t_R (β) = 9.1 min).

Data of the anomeric mixture:

^{1}H NMR (600 MHz, CDCl$_3$) δ 7.47 – 7.27 (m, 30H), 5.56 (d, *J* = 5.0 Hz, 1H, **H$_1$(β)**), 5.50 (d, *J* = 5.0 Hz, 1H, **H$_1$(α)**), 5.05 (d, *J* = 11.1 Hz, 1H), 5.00 (d, *J* = 3.7 Hz, 1H, **H$_1$'(α)**), 4.97 (dd, *J* = 11.3, 5.1 Hz, 2H), 4.87 (dd, *J* = 18.6, 11.9 Hz, 2H), 4.79 – 4.70 (m, 5H), 4.62 (d, *J* = 11.5 Hz, 1H), 4.60 – 4.56 (m, 3H), 4.41 (d, *J* = 7.7 Hz, 1H, **H$_1$'(β)**), 4.32 – 4.28 (m, 3H), 4.28 – 4.24 (m, 1H), 4.23 – 4.16 (m, 2H), 4.13 – 4.00 (m, 8H), 3.97 (dd, *J* = 10.0, 2.8 Hz, 1H), 3.88 – 3.82 (m, 2H), 3.76 (d, *J* = 6.6 Hz, 1H), 3.73 – 3.66 (m, 3H), 3.55 – 3.49 (m, 2H), 1.51 (s, 3H), 1.48 (s, 3H), 1.43 (s, 4H), 1.32 (s, 3H), 1.31 (s, 6H), 1.30 (s, 3H), 1.17 (s, 9H), 1.15 (s, 9H) ppm. **^{13}C NMR** (151 MHz, CDCl$_3$) δ 178.2, 139.1, 139.0, 138.8, 138.7, 138.6, 138.5, 137.3, 128.7, 128.6, 128.5, 128.5, 128.4, 128.4, 128.3, 128.3, 127.9, 127.8, 127.8, 127.8, 127.7, 127.7, 127.7, 127.6, 127.5, 109.5, 109.4, 108.7, 108.6, 104.8 (**C$_1$'(β)**), 97.5 (**C$_1$'(α)**), 96.5 (**C$_1$(β)**), 96.4 (**C$_1$(α)**), 82.0, 79.2, 79.0, 76.5, 75.5, 74.9, 74.9, 74.7, 74.0, 73.7, 73.5, 72.9, 72.1, 71.6, 71.1, 70.9, 70.8, 70.8, 70.7, 69.9, 69.7, 68.7, 67.8, 67.6, 66.6, 66.2, 63.3, 62.7, 38.8, 27.4, 27.3, 26.3, 26.2, 26.1, 25.2, 25.1, 24.6, 24.6 ppm. **HRMS** (QToF): Calcd for C$_{44}$H$_{56}$O$_{12}$Na [M + Na]$^+$ 799.3664; found 799.3670.

1,2:3,4-Bis-*O*-(1-methylethylidene)-6-*O*-[2,3-bis-*O*-benzyl-4,6-bis-(2,2-dimethylpropanoate)-α/β-D-galactopyranosyl]-α-D-galactopyranoside (4.06a-A1)
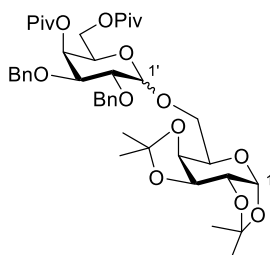
The title compound was prepared according to the general glycosylation procedure. Product **4.06a-A1** (19 mg, 24 μmol, 69%, **α/β 80:20**) was obtained as a colorless oil after purification using **Method-2b** (t_R (α) = 7.6 min, t_R (β) = 8.6 min).

Data of the major isomer (α):

¹H NMR (600 MHz, CDCl₃) δ 7.35 – 7.26 (m, 10H), 5.56 (dd, J = 3.5, 1.4 Hz, 1H), 5.51 (d, J = 5.0 Hz, 1H, **H₁**), 4.97 (d, J = 3.5 Hz, 1H, **H₁'**), 4.80 – 4.67 (m, 3H), 4.59 (ddd, J = 7.7, 5.3, 2.4 Hz, 1H), 4.54 (d, J = 10.8 Hz, 1H), 4.34 – 4.26 (m, 3H), 4.08 (dd, J = 11.0, 7.1 Hz, 1H), 4.05 – 3.97 (m, 3H), 3.82 – 3.72 (m, 3H), 1.52 (s, 3H), 1.44 (s, 3H), 1.33 – 1.32 (m, 6H), 1.21 (s, 9H), 1.15 (s, 9H) ppm. **¹³C NMR** (151 MHz, CDCl₃) δ 178.1, 176.9, 138.5, 138.4, 128.4, 128.3, 128.0, 128.0, 127.8, 127.5, 109.4, 108.7, 98.1 (**C₁'**), 96.4 (**C₁**), 76.1, 74.9, 73.2, 72.0, 71.1, 70.8, 70.7, 67.3, 67.1, 67.0, 66.5, 62.2, 39.2, 38.9, 27.3, 27.3, 26.3, 26.2, 25.1, 24.7 ppm. **HRMS** (QToF): Calcd for C₄₂H₅₈O₁₃Na [M + Na]⁺ 793.3796; found 793.3786.

1,2:3,4-Bis-*O*-(1-methylethylidene)-6-*O*-[2,3,6-tris-*O*-benzyl-4-(2,2-dimethylpropanoate)-α/β-D-galactopyranosyl]-α-D-galactopyranoside (4.07a-A1)
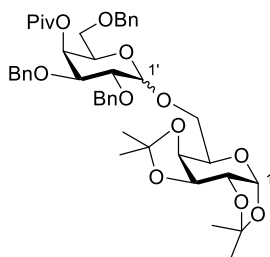
The title compound was prepared according to the general glycosylation procedure. Product **4.07a-A1** (22 mg, 28 μmol, 82%, **α/β 96:4**) was obtained as a colorless oil after purification using **Method-2b** (t_R (α) = 7.9 min).

Data of the major isomer (α):

¹H NMR (600 MHz, CDCl₃) δ 7.35 – 7.24 (m, 15H), 5.63 (dd, J = 3.4, 1.3 Hz, 1H), 5.51 (d, J = 5.1 Hz, 1H, **H₁**), 4.98 (d, J = 3.7 Hz, 1H, **H₁'**), 4.79 – 4.67 (m, 3H), 4.58 (dd, J = 7.9, 2.4 Hz, 1H), 4.52 (t, J = 10.7 Hz, 2H), 4.48 – 4.43 (m, 1H), 4.34 (dd, J = 7.9, 1.9 Hz, 1H), 4.30 (dd, J = 5.0, 2.4 Hz, 1H), 4.23 (td, J = 6.5, 1.3 Hz, 1H), 4.04 (td, J = 6.7, 1.9 Hz, 1H), 3.98 (dd, J = 10.0, 3.3 Hz, 1H), 3.85 – 3.80 (m, 1H), 3.80 – 3.70 (m, 2H), 3.46 (ddd, J = 42.0, 9.6, 6.5 Hz, 2H), 1.53 (s, 3H), 1.43 (s, 3H), 1.33 (s, 3H), 1.32 (s, 3H), 1.12 (s, 9H) ppm. **¹³C NMR** (151 MHz, CDCl₃) δ 177.5, 138.7, 138.6, 138.0, 128.5, 128.4, 128.2, 128.1, 128.0, 128.0, 127.8, 127.7, 127.5, 109.3, 108.7, 98.1 (**C₁'**), 96.4 (**C₁**), 76.5, 75.1, 73.6, 73.1, 71.8, 71.0, 70.8, 70.8, 68.5, 67.9, 67.6, 66.8, 66.5, 66.2, 39.1, 29.8, 27.3, 26.3, 26.2, 25.1, 24.8 ppm. **HRMS** (QToF): Calcd for C₄₄H₅₆O₁₂Na [M + Na]⁺ 799.3664; found 799.3693.

1,2:3,4-Bis-*O*-(1-methylethylidene)-6-*O*-[2,3,6-tris-*O*-benzyl-4-(trifluoroacetate)-α/β-ᴅ-galactopyranosyl]-α-ᴅ-galactopyranoside (4.07b-A1)

The title compound was prepared according to the general glycosylation procedure. Product **4.07b-A1** (18 mg, 23 μmol, 67%, **α/β 85:15**) was obtained as a colorless oil after purification using **Method-2b** ($t_R(α)$ = 6.0 min, $t_R(β)$ = 9.1 min).

Data of the major isomer (α):

¹H NMR (600 MHz, CDCl₃) δ 7.37 – 7.26 (m, 15H), 5.74 (dd, *J* = 3.4, 1.3 Hz, 1H), 5.49 (d, *J* = 5.0 Hz, 1H, **H₁**), 4.94 (d, *J* = 3.7 Hz, 1H, **H₁'**), 4.75 (dt, *J* = 11.6, 3.4 Hz, 2H), 4.67 (d, *J* = 12.0 Hz, 1H), 4.61 – 4.54 (m, 2H), 4.53 – 4.43 (m, 2H), 4.33 – 4.25 (m, 3H), 4.06 – 3.98 (m, 2H), 3.80 – 3.68 (m, 3H), 3.54 (dd, *J* = 9.3, 5.6 Hz, 1H), 3.41 (dd, *J* = 9.2, 8.3 Hz, 1H), 1.51 (s, 3H), 1.43 (s, 3H), 1.33 (s, 3H), 1.30 (s, 3H) ppm. **¹³C NMR** (151 MHz, CDCl₃) δ 138.4, 138.0, 137.6, 128.6, 128.4, 128.1, 128.0, 127.9, 127.8, 127.8, 109.5, 108.8, 98.0 (**C₁'**), 96.5 (**C₁**), 75.7, 75.2, 73.8, 73.4, 72.9, 72.6, 71.1, 70.8, 70.7, 67.4, 67.3, 66.6, 66.4, 29.9, 26.3, 26.2, 25.1, 24.7 ppm. **¹⁹F NMR** (564 MHz, CDCl₃) δ -74.85 (s) ppm. **HRMS** (QToF): Calcd for C₄₁H₄₇F₃O₁₂Na [M + Na]⁺ 811.2912; found 811.2944.

1,2:3,4-Bis-*O*-(1-methylethylidene)-6-*O*-[2,3,4-tris-*O*-benzyl-6-(trifluoroacetate)-α/β-ᴅ-galactopyranosyl]-α-ᴅ-galactopyranoside (4.08b-A1)
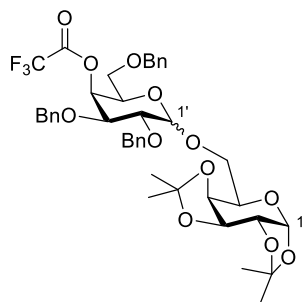

The title compound was prepared according to the general glycosylation procedure. Product **4.08b-A1** (15 mg, 19 μmol, 56%, **α/β 53:47**) was obtained as a colorless oil after purification using **Method-2b** ($t_R(α)$ = 8.3 min, $t_R(β)$ = 9.0 min).

Data of the anomeric mixture:

1H NMR (600 MHz, CDCl$_3$) δ 7.46 – 6.98 (m, 30H), 5.56 (d, J = 5.0 Hz, 1H. **H$_1$(β)**), 5.46 (d, J = 5.0 Hz, 1H, **H$_1$(α)**), 5.05 (d, J = 11.0 Hz, 1H, **H$_1$'(α)**), 4.98 (dd, J = 11.6, 7.3 Hz, 2H), 4.93 (d, J = 3.6 Hz, 1H), 4.88 (dd, J = 14.2, 11.7 Hz, 2H), 4.81 – 4.71 (m, 5H), 4.63 – 4.55 (m, 4H), 4.51 – 4.42 (m, 3H, **H$_1$'(β)**), 4.29 (ddd, J = 15.8, 5.0, 2.4 Hz, 2H), 4.24 – 4.19 (m, 2H), 4.18 – 4.03 (m, 5H), 3.98 (dd, J = 12.7, 9.8 Hz, 2H), 3.88 – 3.82 (m, 2H), 3.78 – 3.66 (m, 4H), 3.61 (t, J = 6.2 Hz, 1H), 3.54 (dd, J = 9.7, 2.9 Hz, 1H), 1.48 (s, 6H), 1.44 (s, 3H), 1.42 (s, 3H), 1.31 (s, 3H), 1.31 (s, 3H), 1.30 (s, 3H), 1.30 (s, 4H) ppm. **13C NMR** (151 MHz, CDCl$_3$) δ 139.0, 138.8, 138.6, 138.5, 138.2, 138.0, 128.7, 128.6, 128.6, 128.5, 128.3, 128.1, 128.1, 128.0, 127.9, 127.8, 127.8, 127.8, 127.7, 127.6, 109.5, 109.5, 108.8, 108.6, 104.8 (**C$_1$'(β)**), 97.7 (**C$_1$'(α)**), 96.5 (**C$_1$(β)**), 96.4 (**C$_1$(α)**), 81.7, 79.0, 78.8, 76.4, 74.9, 74.7, 74.5, 74.5, 73.9, 73.8, 73.3, 73.0, 71.6, 71.5, 71.3, 70.9, 70.9, 70.6, 69.8, 67.8, 67.7, 67.6, 66.9, 66.5, 66.4, 26.2, 26.2, 26.1, 26.0, 25.2, 25.0, 24.6, 24.5 ppm. **19F NMR** (564 MHz, CDCl$_3$) δ -74.9 (s), -74.9 (s) ppm. **HRMS** (QToF): Calcd for C$_{41}$H$_{47}$F$_3$O$_{12}$Na [M + Na]$^+$ 811.2939; found 811.2912.

2,2,2-Trifluoroethyl 2,3,4-tris-*O*-benzyl-6-(2,2-dimethylpropanoate)-α/β-D-galactopyranoside (4.08a-A3)
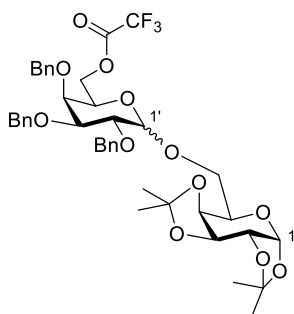

The title compound was prepared according to the general glycosylation procedure. Product **4.08a-A3** (18 mg, 29 µmol, 85%, **α/β 82:18**) was obtained as a colorless oil after purification using **Method-2b** (t$_R$ (α) = 6.7 min).

Data of the major isomer (α):

1H NMR (600 MHz, CDCl$_3$) δ 7.42 – 7.27 (m, 15H), 4.99 (d, J = 11.2 Hz, 1H), 4.93 – 4.81 (m, 3H), 4.75 (d, J = 11.6 Hz, 1H, **H$_1$**), 4.66 (d, J = 12.2 Hz, 1H), 4.59 (d, J = 11.3 Hz, 1H), 4.17 (dd, J = 11.4, 7.5 Hz, 1H), 4.11 – 4.01 (m, 2H), 3.98 – 3.81 (m, 5H), 1.17 (s, 9H) ppm. **13C NMR** (151 MHz, CDCl$_3$) δ 178.2, 138.7, 138.5, 138.2, 128.6, 128.5, 128.4, 128.1, 128.0, 127.8, 127.7, 98.2 (**C$_1$**), 78.6, 76.2, 75.3, 74.9, 73.8, 73.6, 69.6, 63.7, 38.8, 27.2 ppm. **19F NMR** (564 MHz, CDCl$_3$) δ -73.61 (t, J = 8.7 Hz) ppm. **HRMS** (QToF): Calcd for C$_{34}$H$_{39}$F$_3$O$_7$Na [M + Na]$^+$ 639.2540; 639.2535.

2,2,2-Trifluoroethyl 2,3-bis-*O*-benzyl-4,6-bis-(2,2-dimethylpropanoate)-α/β-D-galactopyranoside (4.06a-A3)
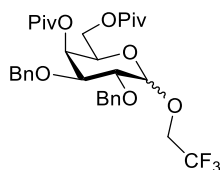
The title compound was prepared according to the general glycosylation procedure. Product **4.06a-A3** (13 mg, 21 μmol, 61%, **α/β 96:4**) was obtained as a colorless oil after purification using **Method-2b** (t_R (α) = 4.5 min).

Data of the major isomer (α):

¹H NMR (600 MHz, CDCl₃) δ 7.33 – 7.27 (m, 10H), 5.56 (dd, *J* = 3.5, 1.4 Hz, 1H), 4.88 (s, 1H, **H₁**), 4.82 (d, *J* = 12.2 Hz, 1H), 4.72 (d, *J* = 10.8 Hz, 1H), 4.64 (d, *J* = 12.2 Hz, 1H), 4.55 (d, *J* = 10.7 Hz, 1H), 4.16 (td, *J* = 6.5, 1.4 Hz, 1H), 4.10 – 4.02 (m, 2H), 3.99 (dd, *J* = 10.1, 3.4 Hz, 1H), 3.93 (q, *J* = 8.6 Hz, 2H), 3.76 (dd, *J* = 10.0, 3.7 Hz, 1H), 1.19 (s, 9H), 1.16 (s, 9H) ppm. **¹³C NMR** (151 MHz, CDCl₃) δ 178.1, 177.4, 138.2, 138.1, 128.5, 128.3, 128.2, 128.1, 128.0, 127.7, 98.6 (**C₁**), 75.8, 74.4, 73.7, 72.2, 68.0, 67.1, 62.5, 39.2, 38.9, 27.3, 27.2 ppm. **¹⁹F NMR** (564 MHz, CDCl₃) δ -73.63 (t, *J* = 8.7 Hz) ppm. **HRMS** (QToF): Calcd for C₃₂H₄₁F₃O₈Na [M + Na]⁺ 633.2646; found 633.2651.

2,2,2-Trifluoroethyl 2,3,6-tris-*O*-benzyl-4-(2,2-dimethylpropanoate)-α/β-D-galactopyranoside (4.07a-A3)
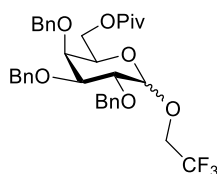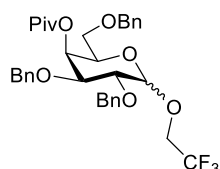

The title compound was prepared according to the general glycosylation procedure. Product **4.07a-A3** (15 mg, 24 μmol, 71%, **α/β 97:3**) was obtained as a colorless oil after purification using **Method-2b** (t_R (α) = 5.5 min).

Data of the major isomer (α):

¹H NMR (600 MHz, CDCl₃) δ 7.37 – 7.27 (m, 15H), 5.62 (dd, *J* = 3.4, 1.3 Hz, 1H), 4.90 (d, *J* = 3.7 Hz, 1H, **H₁**), 4.81 (d, *J* = 12.2 Hz, 1H), 4.73 (d, *J* = 10.8 Hz, 1H), 4.64 (d, *J* = 12.2 Hz, 1H), 4.55 – 4.50 (m, 2H), 4.45 (d, *J* = 11.8 Hz, 1H), 4.11 (td, *J* = 6.3, 1.3 Hz, 1H), 4.00 – 3.91 (m, 3H), 3.76 (dd, *J* = 10.0, 3.7 Hz, 1H), 3.50 – 3.41 (m, 2H), 1.13 (s, 9H) ppm. **¹³C NMR** (151 MHz, CDCl₃) δ 177.4, 138.4, 138.3, 137.8, 128.6, 128.5, 128.3, 128.1, 128.1, 128.0, 127.9, 127.6, 98.6 (**C₁**), 76.1, 74.6, 73.8, 73.6, 72.0, 68.8, 68.6, 67.4, 39.1, 27.3 ppm. **¹⁹F NMR**

(564 MHz, CDCl$_3$) δ -73.54 (t, *J* = 8.7 Hz). **HRMS** (QToF): Calcd for C$_{34}$H$_{39}$F$_3$O$_7$Na [M + Na]$^+$ 639.2540; found 639.2535.

2,2,2-Trifluoroethyl 2,3,4-tris-*O*-benzyl-6-(trifluoroacetate)-α/β-D-galactopyranoside (4.08b-A3)

The title compound was prepared according to the general glycosylation procedure. Product **4.08b-A3** (14 mg, 22 µmol, 66%, **α/β 96:4**) was obtained as a colorless oil.

Data of the major isomer (α):

^{1}H NMR (600 MHz, CDCl$_3$) δ 7.45 – 7.26 (m, 15H), 5.00 (d, *J* = 11.6 Hz, 1H), 4.92 (d, *J* = 11.6 Hz, 1H), 4.86 – 4.75 (m, 3H, **H$_1$**), 4.69 – 4.57 (m, 2H), 4.44 (dd, *J* = 11.3, 7.9 Hz, 1H), 4.07 (ddd, *J* = 11.4, 6.9, 3.9 Hz, 2H), 4.01 – 3.92 (m, 2H), 3.90 – 3.83 (m, 3H) ppm. **^{13}C NMR** (151 MHz, CDCl$_3$) δ 157.1, 156.8, 138.4, 138.2, 137.7, 128.5, 128.5, 128.4, 128.1, 128.0, 127.9, 127.8, 127.6, 115.3, 113.4, 98.3 (**C$_1$**), 78.1, 76.0, 74.6, 74.2, 73.9, 73.6, 68.7, 66.8, 64.8 (q, *J* = 35.0 Hz) ppm. **^{19}F NMR** (564 MHz, CDCl$_3$) δ -73.87 (t, *J* = 8.7 Hz), -75.11 ppm.

2,2,2-Trifluoroethyl 2,3,6-tris-*O*-benzyl-4-(trifluoroacetate)-α-D-galactopyranoside (4.07b-A3)

The title compound was prepared according to the general glycosylation procedure. Product **4.07b-A3** (15 mg, 24 µmol, 71%, **α-only**) was obtained as a colorless oil.

Data of the major isomer (α):

^{1}H NMR (600 MHz, CDCl$_3$) δ 7.38 – 7.26 (m, 15H), 5.73 (dd, *J* = 3.2, 1.3 Hz, 1H), 4.85 (d, *J* = 3.7 Hz, 1H, **H$_1$**), 4.83 – 4.72 (m, 2H), 4.61 (dd, *J* = 11.5, 2.2 Hz, 2H), 4.53 – 4.41 (m, 2H), 4.14 (ddd, *J* = 7.3, 5.7, 1.3 Hz, 1H), 4.03 (dd, *J* = 10.0, 3.3 Hz, 1H), 3.91 (qd, *J* = 8.6, 2.8 Hz, 2H), 3.77 (dd, *J* = 10.0, 3.7 Hz, 1H), 3.52 (dd, *J* = 9.4, 5.8 Hz, 1H), 3.42 (dd, *J* = 9.3, 7.9 Hz, 1H) ppm. **^{13}C NMR** (151 MHz, CDCl$_3$) δ 156.92 (q, *J* = 42.4 Hz), 138.1, 137.7, 137.3, 128.7, 128.6, 128.5, 128.2, 128.2, 128.1, 127.9, 127.9, 113.8, 98.7 (**C$_1$**), 75.3, 74.8, 73.9, 73.9, 72.8, 72.5,

67.5, 67.3, 65.3 (q, J = 35.0 Hz) ppm. **^{19}F NMR** (564 MHz, CDCl$_3$) δ -73.69 (t, J = 8.7 Hz), -74.82 ppm. **HRMS** (QToF): Calcd for C$_{31}$H$_{30}$F$_6$O$_7$Na [M + Na]$^+$ 651.1788; found 651.1815.

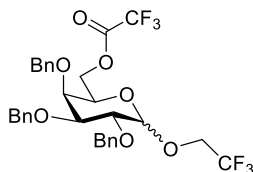**Benzyl 2,3,4-tris-*O*-benzyl-6-(2,2-dimethylpropanoate)-α/β-D-galactopyranoside (4.08a-A4)**

The title compound was prepared according to the general glycosylation procedure. Product **4.08a-A4** (18 mg, 29 μmol, 83%, **α/β 36:64**) was obtained as a colorless oil after purification using **Method-2b** (t$_R$ (α/ β) = 6.7 min).

Data of the anomeric mixture:

^{1}H NMR (600 MHz, CDCl$_3$) δ 7.44 – 7.27 (m, 26H), 5.03 – 4.88 (m, 4H, **H$_1$(α)**), 4.85 – 4.69 (m, 5H), 4.68 – 4.52 (m, 4H), 4.45 (d, J = 7.7 Hz, 1H, **H$_1$(β)**), 4.31 (dd, J = 11.1, 7.0 Hz, 1H), 4.18 (dd, J = 11.2, 7.4 Hz, 1H), 4.13 – 3.95 (m, 3H), 3.91 (dd, J = 9.7, 7.7 Hz, 1H), 3.88 – 3.85 (m, 1H), 3.74 (d, J = 2.8 Hz, 1H), 3.57 – 3.49 (m, 2H), 1.19 (s, 4H), 1.19 (s, 9H) ppm. **^{13}C NMR** (151 MHz, CDCl$_3$) δ 178.2, 138.9, 138.8, 138.6, 138.6, 138.5, 138.4, 137.6, 137.2, 128.5, 128.5, 128.5, 128.4, 128.4, 128.3, 128.3, 128.1, 128.0, 127.9, 127.8, 127.7, 102.7 **C$_1$(β)**, 95.7 **C$_1$(α)**, 82.3, 79.6, 79.2, 76.5, 75.5, 75.3, 74.9, 74.7, 73.9, 73.7, 73.6, 73.3, 72.3, 70.9, 68.9, 68.7, 63.8, 63.2, 38.9, 27.3 ppm. **HRMS** (QToF): Calcd for C$_{39}$H$_{44}$O$_7$Na [M + Na]$^+$ 647.2979; found 647.2974.

Benzyl 2,3-bis-*O*-benzyl-4,6-bis-(2,2-dimethylpropanoate)-α/β-D-galactopyranoside (4.06a-A4)
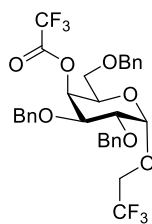

The title compound was prepared according to the general glycosylation procedure. Product **4.06a-A4** (18 mg, 29 μmol, 83%, **α/β 66:34**) was obtained as a colorless oil after purification using **Method-2b** (t$_R$ (α) = 5.0 min, t$_R$ (β) = 5.6 min).

Data of the anomeric mixture:

^{1}H NMR (600 MHz, CDCl$_3$) δ 7.46 – 7.27 (m, 22H), 5.59 (d, J = 2.9 Hz, 1H), 5.50 (d, J = 3.4 Hz, 1H), 5.01 – 4.87 (m, 2H, **H$_1$(α)**), 4.83 – 4.67 (m, 5H), 4.64 – 4.49 (m, 4H, **H$_1$(β)**), 4.29 –

4.12 (m, 2H), 4.12 – 4.04 (m, 3H), 3.83 (t, J = 6.8 Hz, 1H), 3.75 (dd, J = 10.0, 3.7 Hz, 1H), 3.66 – 3.55 (m, 1H), 1.25 (s, 4H), 1.25 (s, 9H), 1.23 (s, 4H), 1.18 (d, J = 0.8 Hz, 9H) ppm. **^{13}C NMR** (151 MHz, CDCl$_3$) δ 178.2, 178.1, 177.7, 177.5, 138.6, 138.4, 138.4, 138.1, 137.4, 137.0, 128.6, 128.6, 128.4, 128.4, 128.3, 128.3, 128.3, 128.1, 128.1, 128.0, 127.8, 127.7, 127.6, 102.5 **C_1(β)**, 96.1 **C_1(α)**, 79.4, 78.7, 76.4, 75.4, 74.9, 73.5, 72.2, 72.2, 71.2, 71.1, 69.1, 67.4, 67.3, 66.2, 62.6, 62.1, 39.2, 39.1, 38.9, 27.3, 27.3, 27.3 ppm. **HRMS** (QToF): Calcd for C$_{37}$H$_{46}$O$_8$Na [M + Na]$^+$ 641.3085; found 641.3082.

Benzyl 2,3,6-tris-*O*-benzyl-4-(2,2-dimethylpropanoate)-α/β-D-galactopyranoside (4.07a-A4)
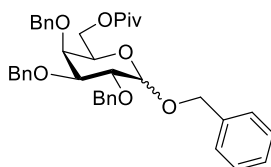

The title compound was prepared according to the general glycosylation procedure. Product **4.07a-A4** (16 mg, 26 µmol, 74%, **α/β 68:32**) was obtained as a colorless oil after purification using **Method-2b** (t_R (α) = 6.8 min, t_R (β) = 8.1 min).

Data of the major isomer (α):

^{1}H NMR (600 MHz, CDCl$_3$) δ 7.43 – 7.25 (m, 15H), 5.61 (d, J = 3.0 Hz, 1H), 4.99 – 4.83 (m, 2H, **H_1**), 4.77 – 4.66 (m, 4H), 4.63 – 4.42 (m, 6H), 4.16 (t, J = 6.4 Hz, 1H), 4.03 (dd, J = 10.0, 3.3 Hz, 1H), 3.77 – 3.69 (m, 1H), 3.64 – 3.50 (m, 2H), 3.43 (dd, J = 6.3, 1.2 Hz, 2H), 1.12 (s, 9H) ppm. **^{13}C NMR** (151 MHz, CDCl$_3$) δ 177.5, 138.5, 138.0, 137.3, 128.6, 128.5, 128.5, 128.3, 128.3, 128.1, 127.9, 127.7, 127.6, 96.4 (**C_1**), 76.7, 75.1, 73.8, 73.5, 72.0, 69.3, 68.8, 68.3, 67.7, 39.1, 27.3 ppm. **HRMS** (QToF): Calcd for C$_{39}$H$_{44}$O$_7$Na [M + Na]$^+$ 647.2979; found 647.2978.

Benzyl 2,3,6-tris-*O*-benzyl-4-(trifluoroacetate)-α/β-D-galactopyranoside (4.07b-A4)
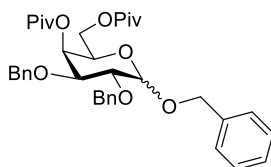

The title compound was prepared according to the general glycosylation procedure. Product **4.07b-A4** (10 mg, 16 µmol, 47%, **α/β 54:46**) was obtained as a colorless oil after purification using **Method-2b** (t_R (α/ β) = 6.1 min).

Data of the anomeric mixture:

¹H NMR (600 MHz, CDCl₃) δ 7.38 – 7.19 (m, 39H), 5.70 (dd, *J* = 3.4, 1.4 Hz, 1H), 5.66 (q, *J* = 1.3 Hz, 1H), 4.92 (d, *J* = 11.9 Hz, 1H), 4.88 – 4.82 (m, 2H), 4.77 – 4.39 (m, 13H), 4.13 (ddd, *J* = 7.4, 5.7, 1.4 Hz, 1H), 4.06 (dd, *J* = 10.0, 3.3 Hz, 1H), 3.76 (ddd, *J* = 8.3, 5.5, 1.1 Hz, 1H), 3.70 (dd, *J* = 10.0, 3.7 Hz, 1H), 3.64 (dd, *J* = 9.2, 5.6 Hz, 1H), 3.60 (dd, *J* = 4.5, 1.6 Hz, 2H), 3.50 (dd, *J* = 9.3, 8.2 Hz, 1H), 3.42 (dd, *J* = 9.2, 5.8 Hz, 1H), 3.37 (dd, *J* = 9.3, 7.9 Hz, 1H) ppm. **¹³C NMR** (151 MHz, CDCl₃) δ 170.2, 170.1, 157.3, 157.2, 157.0, 156.9, 138.4, 138.3, 137.9, 137.5, 137.4, 137.3, 137.2, 137.1, 132.6, 130.1, 128.7, 128.6, 128.6, 128.5, 128.4, 128.3, 128.2, 128.1, 128.0, 127.9, 127.8, 127.8, 102.6, 96.5, 78.7, 75.8, 75.6, 75.2, 74.0, 73.7, 72.9, 72.7, 71.5, 71.2, 69.8, 67.5, 67.2, 67.0 ppm. **¹⁹F NMR** (564 MHz, CDCl₃) δ -74.58, -74.80 ppm. **HRMS** (QToF): Calcd for $C_{36}H_{35}F_3O_7Na$ [M + Na]⁺ 659.2227; found 659.2225.

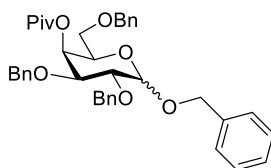### Benzyl 2,3,4-tris-*O*-benzyl-6-(trifluoroacetate)-α/β-D-galactopyranoside (4.08b-A4)

The title compound was prepared according to the general glycosylation procedure. Product **4.08b-A4** (11 mg, 17 µmol, 50%, **α/β 50:50**) was obtained as a colorless oil after purification using **Method-2b** (t$_R$ (α) = 5.7 min, t$_R$ (β) = 6.0 min).

Data of the anomeric mixture:

¹H NMR (600 MHz, CDCl₃) δ 7.44 – 7.26 (m, 40H), 5.00 (dd, *J* = 11.7, 6.3 Hz, 2H), 4.98 – 4.89 (m, 4H), 4.84 (d, *J* = 11.7 Hz, 1H), 4.76 (ddd, *J* = 20.7, 11.3, 2.1 Hz, 4H), 4.70 – 4.61 (m, 4H), 4.61 – 4.50 (m, 4H), 4.45 (d, *J* = 7.6 Hz, 1H), 4.41 (dd, *J* = 11.1, 7.5 Hz, 1H), 4.14 (dd, *J* = 11.2, 5.1 Hz, 1H), 4.09 – 4.05 (m, 1H), 4.04 – 3.99 (m, 2H), 3.92 (dd, *J* = 9.7, 7.6 Hz, 1H), 3.86 (dd, *J* = 2.6, 1.4 Hz, 1H), 3.75 (dd, *J* = 3.0, 1.3 Hz, 1H), 3.60 (ddd, *J* = 7.4, 5.1, 1.3 Hz, 1H), 3.53 (dd, *J* = 9.7, 2.9 Hz, 1H) ppm. **¹³C NMR** (151 MHz, CDCl₃) δ 157.1 (q, *J* = 42.5 Hz), 138.7, 138.6, 138.5, 138.4, 138.0, 137.9, 137.2, 137.0, 128.7, 128.6, 128.6, 128.6, 128.6, 128.5, 128.5, 128.4, 128.3, 128.2, 128.2, 128.2, 128.1, 128.0, 128.0, 127.9, 127.8, 127.8, 127.8, 127.7, 115.5, 115.5, 113.6, 113.6, 102.4, 95.9, 82.0, 79.4, 79.0, 76.5, 75.4, 74.7, 74.5, 74.0, 73.9, 73.4, 72.9, 71.6, 70.9, 69.1, 68.1, 67.1, 66.8 ppm. **¹⁹F NMR** (564 MHz, CDCl₃) δ -74.87, -74.87 ppm. **HRMS** (QToF): Calcd for $C_{36}H_{35}F_3O_7Na$ [M + Na]⁺ 659.2227; found 659.2225.

Methyl *O*-**[2,3,4-tris-***O***-benzyl-6-(2,2-dimethylpropanoate)-α/β-D-galactopyranosyl]-(1→4)-2,3,6-tri-***O***-benzyl-β-D-glucopyranoside (4.08a-A2)**
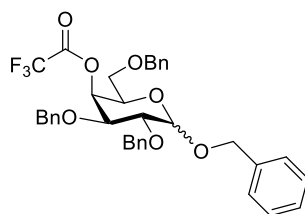

The title compound was prepared according to the general glycosylation procedure. Product **4.08a-A2** (28 mg, 28 μmol, 81%, **α/β 74:26**) was obtained as a colorless oil after purification using **Method-2b** (t_R (α) = 10.7 min, t_R (β) = 10.7 min).

Data of the major isomer (α):

¹H NMR (700 MHz, CDCl$_3$) δ 7.38 – 7.27 (m, 25H), 7.20 – 7.16 (m, 5H), 5.71 (d, *J* = 3.8 Hz, 1H, **H$_1$'**), 4.94 – 4.86 (m, 3H), 4.81 – 4.72 (m, 3H), 4.69 – 4.54 (m, 6H), 4.50 (d, *J* = 12.3 Hz, 1H), 4.36 (d, *J* = 7.7 Hz, 1H, **H$_1$**), 4.18 (dd, *J* = 11.1, 7.2 Hz, 1H), 4.00 (d, *J* = 3.8 Hz, 2H), 3.90 – 3.66 (m, 6H), 3.63 (ddd, *J* = 9.8, 5.9, 2.4 Hz, 1H), 3.60 (s, 3H), 3.45 (dd, *J* = 9.1, 7.7 Hz, 1H), 1.21 (s, 9H) ppm. **¹³C NMR** (176 MHz, CDCl$_3$) δ 178.1, 138.8, 138.7, 138.5, 138.4, 138.3, 138.3, 128.5, 128.5, 128.5, 128.4, 128.4, 128.3, 128.2, 128.0, 127.9, 127.7, 127.6, 127.6, 126.8, 104.6 (**C$_1$**), 97.2 (**C$_1$'**), 84.8, 82.5, 78.9, 75.7, 75.1, 74.8, 74.7, 74.6, 74.1, 73.8, 73.4, 73.3, 70.2, 69.1, 63.5, 57.1, 38.9, 27.5 ppm. **HRMS** (QToF): Calcd for C$_{60}$H$_{68}$O$_{12}$Na [M + Na]$^+$ 1003.4603; found 1003.4612.

Methyl *O*-**[2,3-bis-***O***-benzyl-4,6-bis-(2,2-dimethylpropanoate)-α/β-D-galactopyranosyl]-(1→4)-2,3,6-tri-***O***-benzyl-β-D-glucopyranoside (4.06a-A2)**
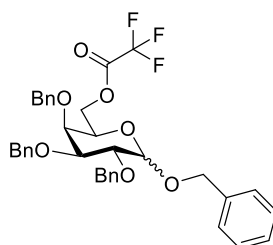

The title compound was prepared according to the general glycosylation procedure. Product **4.06a-A2** (26 mg, 27 μmol, 76%, **α/β 89:11**) was obtained as a colorless oil after purification using **Method-2b** (t_R (α) = 9.6 min, t_R (β) = 9.6 min).

Data of the major isomer (α):

¹H NMR (700 MHz, CDCl$_3$) δ 7.43 – 7.17 (m, 20H), 7.16 – 7.01 (m, 5H), 5.65 (d, *J* = 3.7 Hz, 1H, **H$_1$'**), 5.39 (dd, *J* = 3.3, 1.7 Hz, 1H), 4.95 – 4.82 (m, 2H), 4.79 (d, *J* = 11.7 Hz, 1H), 4.67 (d, *J* = 12.3 Hz, 1H), 4.61 (dd, *J* = 11.1, 4.9 Hz, 2H), 4.57 (d, *J* = 11.0 Hz, 1H), 4.51 (t, *J* = 11.7 Hz, 2H), 4.38 – 4.31 (m, 2H, **H$_1$**), 4.07 (td, *J* = 6.9, 1.8 Hz, 1H), 3.95 – 3.92 (m, 2H), 3.80 (dd, *J* = 10.3, 3.3 Hz, 1H), 3.77 – 3.72 (m, 2H), 3.69 (dd, *J* = 10.7, 5.1 Hz, 1H), 3.65 – 3.59 (m, 1H), 3.57 (s, 3H), 3.46 – 3.39 (m, 1H), 1.20 (s, 9H), 1.10 (s, 9H) ppm. **¹³C NMR** (176 MHz, CDCl$_3$)

δ 178.0, 177.5, 139.0, 138.5, 138.2, 138.2, 138.0, 128.6, 128.4, 128.4, 128.3, 128.2, 128.2, 128.1, 128.0, 127.9, 127.7, 127.6, 127.6, 127.2, 126.7, 104.7 (C_1), 97.3 (C_1'), 84.8, 82.5, 76.1, 74.8, 74.4, 74.3, 74.0, 73.8, 73.5, 73.3, 72.0, 69.8, 67.3, 66.9, 62.3, 57.2, 39.1, 38.9, 27.4, 27.3 ppm. **HRMS** (QToF): Calcd for $C_{58}H_{70}O_{13}Na$ [M + Na]$^+$ 997.4709; found 997.4714.

Methyl O-[2,3,6-tris-O-benzyl-4-(2,2-dimethylpropanoate)-α/β-D-galactopyranosyl]-(1→4)-2,3,6-tri-O-benzyl-β-D-glucopyranoside (4.07a-A2)
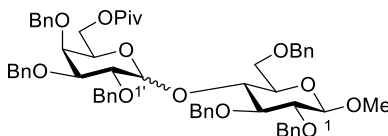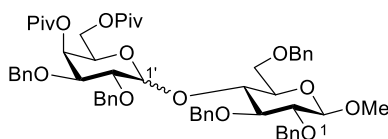

The title compound was prepared according to the general glycosylation procedure. Product **4.07a-A2** (29 mg, 30 µmol, 87%, **α/β 96:4**) was obtained as a colorless oil after purification using **Method-2b** (t_R (α) = 11.9 min, t_R (β) = 11.9 min).

Data of the major isomer (α):

¹H NMR (700 MHz, CDCl$_3$) δ 7.38 – 7.15 (m, 25H), 7.14 – 7.01 (m, 5H), 5.68 (d, J = 3.9 Hz, 1H, **H$_1'$**), 5.52 (dd, J = 3.3, 1.5 Hz, 1H), 4.92 (d, J = 11.8 Hz, 1H), 4.83 (dd, J = 21.5, 11.3 Hz, 2H), 4.66 – 4.59 (m, 3H), 4.57 (d, J = 11.0 Hz, 1H), 4.48 (dd, J = 12.0, 5.9 Hz, 2H), 4.41 (d, J = 11.7 Hz, 1H), 4.33 (d, J = 2.7 Hz, 1H), 4.32 (s, 1H, **H$_1$**), 4.29 (d, J = 11.7 Hz, 1H), 4.03 (t, J = 6.5 Hz, 1H), 3.96 (t, J = 9.1 Hz, 1H), 3.80 (dd, J = 10.2, 3.2 Hz, 1H), 3.79 – 3.74 (m, 2H), 3.71 (dd, J = 10.8, 5.0 Hz, 1H), 3.63 (dd, J = 10.2, 3.9 Hz, 1H), 3.59 (td, J = 4.8, 2.5 Hz, 1H), 3.57 (s, 3H), 3.45 (dd, J = 9.1, 7.6 Hz, 1H), 3.41 – 3.35 (m, 1H), 3.31 (dd, J = 9.1, 7.0 Hz, 1H), 1.07 (s, 9H) ppm. **¹³C NMR** (176 MHz, CDCl$_3$) δ 177.5, 139.2, 138.5, 138.5, 138.3, 138.1, 138.0, 128.5, 128.5, 128.4, 128.3, 128.3, 128.2, 128.1, 128.1, 127.9, 127.9, 127.7, 127.7, 127.6, 127.5, 127.1, 126.7, 104.6 (**C$_1$**), 97.7(**C$_1'$**), 84.9, 82.6, 76.6, 74.8, 74.5, 74.4, 74.0, 73.9, 73.8, 73.4, 73.3, 71.8, 69.8, 68.5, 67.3, 57.1, 39.1, 27.3 ppm. **HRMS** (QToF): Calcd for $C_{60}H_{68}O_{12}Na$ [M + Na]$^+$ 1003.4603; found 1003.4614.

Methyl O-[2,3,6-tris-O-benzyl-4-(trifluoroacetate)-α/β-D-galactopyranosyl]-(1→4)-2,3,6-tri-O-benzyl-β-D-glucopyranoside (4.07b-A2)

The title compound was prepared according to the general glycosylation procedure. Product **4.07b-A2** (23 mg, 23 µmol, 69%, **α/β 97:3**) was obtained as a colorless oil after purification using **Method-2b** (t_R (α) = 11.2 min, t_R (β) = 11.2 min).

Data of the major isomer (α):

¹H NMR (700 MHz, CDCl₃) δ 7.39 – 7.21 (m, 23H), 7.22 – 7.12 (m, 5H), 7.12 – 7.08 (m, 2H), 5.72 (d, *J* = 3.8 Hz, 1H, **H₁'**), 5.68 (dd, *J* = 3.3, 1.4 Hz, 1H), 4.91 (dd, *J* = 35.1, 11.3 Hz, 2H), 4.78 (d, *J* = 11.6 Hz, 1H), 4.70 – 4.57 (m, 4H), 4.56 (d, *J* = 12.0 Hz, 1H), 4.50 (d, *J* = 11.6 Hz, 1H), 4.40 (dd, *J* = 25.0, 11.2 Hz, 2H), 4.35 (d, *J* = 7.7 Hz, 1H), 4.26 (d, *J* = 11.6 Hz, 1H, **H₁**), 4.17 (ddd, *J* = 8.5, 5.4, 1.5 Hz, 1H), 4.04 (t, *J* = 9.1 Hz, 1H), 3.92 (dd, *J* = 10.2, 3.1 Hz, 1H), 3.81 – 3.71 (m, 3H), 3.67 (dd, *J* = 10.2, 3.8 Hz, 1H), 3.60 (s, 3H), 3.58 (ddd, *J* = 9.6, 4.1, 2.6 Hz, 1H), 3.48 (dd, *J* = 9.1, 7.7 Hz, 1H), 3.41 (dd, *J* = 8.8, 5.5 Hz, 1H), 3.31 (t, *J* = 8.7 Hz, 1H) ppm. **¹³C NMR** (176 MHz, CDCl₃) δ 157.00 (q, *J* = 42.6 Hz), 138.8, 138.4, 138.4, 137.8, 137.7, 137.5, 128.6, 128.5, 128.5, 128.4, 128.3, 128.3, 128.3, 128.2, 128.1, 128.1, 128.0, 128.0, 127.9, 127.8, 127.8, 127.7, 127.3, 126.8, 114.73 (q, *J* = 286.3 Hz), 104.7 (**C₁**), 97.3 (**C₁'**), 84.9, 82.6, 76.0, 74.8, 74.4, 74.3, 74.2, 73.8, 73.6, 72.8, 72.5, 72.4, 69.5, 67.3, 67.1, 57.1 ppm. **¹⁹F NMR** (659 MHz, CDCl₃) δ -74.79 (s) ppm. **HRMS** (QToF): Calcd for C₅₇H₅₉F₃O₁₂Na [M + Na]⁺ 1015.3851; found 1015.3853.

Methyl *O*-**[2,3,4-tris-*O*-benzyl-6-(trifluoroacetate)-α/β-ᴅ-galactopyranosyl]-(1→4)-2,3,6-tri-*O*-benzyl-β-ᴅ-glucopyranoside (4.08b-A2)**
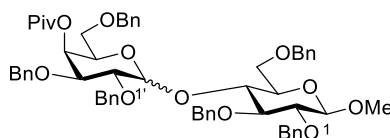

The title compound was prepared according to the general glycosylation procedure. Product **4.08b-A2** (20 mg, 20 μmol, 59%, **α/β 74:26**) was obtained as a colorless oil after purification using **Method-2b** (t*ᵣ* (α) = 9.9 min, t*ᵣ* (β) = 9.9 min).

Data of the major isomer (α):

¹H NMR (700 MHz, CDCl₃) δ 7.38 – 7.26 (m, 20H), 7.23 – 7.13 (m, 10H), 5.73 (d, *J* = 3.8 Hz, 1H, **H₁'**), 4.94 – 4.87 (m, 3H), 4.77 – 4.72 (m, 3H), 4.67 (dd, *J* = 15.7, 11.7 Hz, 3H), 4.60 (d, *J* = 11.1 Hz, 1H), 4.54 (dd, *J* = 14.0, 11.6 Hz, 2H), 4.48 (d, *J* = 12.3 Hz, 1H), 4.36 (d, *J* = 7.7 Hz, 1H, **H₁**), 4.32 – 4.25 (m, 1H), 3.98 (dd, *J* = 10.2, 3.9 Hz, 1H), 3.91 (dd, *J* = 11.0, 5.2 Hz, 1H), 3.88 – 3.76 (m, 4H), 3.68 – 3.64 (m, 1H), 3.60 (s, 3H), 3.46 (dd, *J* = 9.1, 7.6 Hz, 1H) ppm. **¹³C NMR** (176 MHz, CDCl₃) δ 156.95 (q, *J* = 42.4 Hz), 138.8, 138.5, 138.5, 138.5, 138.2, 137.9, 128.6, 128.6, 128.5, 128.4, 128.4, 128.2, 128.1, 128.0, 127.9, 127.8, 127.7, 127.7, 127.6, 127.6, 126.7, 114.55 (q, *J* = 285.5 Hz), 104.6 (**C₁**), 97.3 (**C₁'**), 84.8, 82.4, 78.7, 75.5, 74.7, 74.5, 74.5, 74.0, 73.9, 73.5, 73.4, 73.4, 69.9, 68.4, 66.9, 57.2 ppm. **¹⁹F NMR** (659 MHz, CDCl₃) δ -74.57 (s). **HRMS** (QToF): Calcd for C₅₇H₅₉F₃O₁₂Na [M + Na]⁺ 1015.3851; found 1015.3860.

1,2:3,4-Bis-*O*-(1-methylethylidene)-6-*O*-[2,3,4-tris-*O*-benzyl-*O*-(2,2,2-trifluoroethoxy)-α/β-D-galactopyranosyl]-α-D-galactopyranoside (4.18-A1)
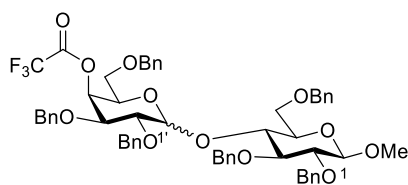

The title compound was prepared according to the general glycosylation procedure. Product **4.18-A1** (23 mg, 30 µmol, 86%, **α/β 60:40**) was obtained as a colorless oil after purification using **Method-2b**.

Data of the anomeric mixture:

^{1}H NMR (600 MHz, CDCl$_3$): δ 7.43 – 7.22 (m, 30H), 5.52 (d, *J* = 5.0 Hz, 1H, **H$_1$(β)**), 5.47 (d, *J* = 5.0 Hz, 1H, **H$_1$(α)**), 5.02 (d, *J* = 11.1 Hz, 1H), 4.92 (d, *J* = 11.5 Hz, 4H, **H$_1$'(α)**), 4.84 – 4.49 (m, 15H, **H$_1$'(β)**), 4.40 (dd, *J* = 26.3, 7.7 Hz, 2H), 4.33 – 4.23 (m, 3H), 4.18 (dd, *J* = 7.9, 1.9 Hz, 1H), 4.12 – 3.53 (m, 24H), 3.48 (ddd, *J* = 9.9, 5.1, 2.1 Hz, 2H), 1.47 (s, 3H), 1.45 (s, 3H), 1.40 (s, 3H), 1.39 (s, 3H), 1.29 – 1.26 (m, 12H) ppm. **^{13}C NMR** (151 MHz, CDCl$_3$): δ 139.0, 138.9, 138.7, 138.7, 138.6, 138.6, 138.5, 138.5, 138.5, 138.1, 137.6, 137.6, 137.5, 128.7, 128.7, 128.6, 128.5, 128.5, 128.5, 128.4, 128.4, 128.3, 128.3, 128.2, 128.1, 128.0, 127.9, 127.8, 127.7, 127.7, 127.6, 127.6, 127.5, 109.5, 109.4, 108.7, 108.7, 104.7 **C$_1$'(β)**, 102.9, 98.5, 97.8 (**C$_1$'(α)**), 96.5 (**C$_1$(β)**), 96.4 (**C$_1$(α)**), 76.4, 75.4, 74.9, 74.8, 74.7, 74.5, 74.5, 73.5, 73.4, 73.4, 73.4, 73.2, 73.0, 72.4, 71.5, 71.3, 71.2, 71.1, 70.9, 70.8, 70.7, 70.6, 69.7, 69.3, 69.1, 69.0, 69.0, 68.9, 68.9, 68.8, 68.8, 68.7, 68.6, 67.5, 67.1, 66.3, 26.2, 26.1, 26.1, 26.1, 25.2, 25.0, 24.6, 24.5 ppm. **^{19}F NMR** (564 MHz, CDCl$_3$): δ -74.24 – -74.36 (m). **HRMS** (QToF): Calcd for C$_{41}$H$_{49}$F$_3$O$_{11}$Na [M + Na]$^+$ 797.3119; found 797.3192.

1,2:3,4-Bis-*O*-(1-methylethylidene)-6-*O*-[2,3,4-tris-*O*-benzyl-*O*-(2,2,2-trifluoroethoxy)-α/β-D-galactopyranosyl]-α-D-galactopyranoside (4.15-A1)
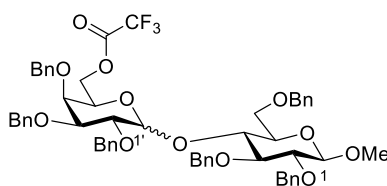

The title compound was prepared according to the general glycosylation procedure. Product **4.15-A1** (18 mg, 23 µmol, 67%, **α/β 60:40**) was obtained as a colorless oil after purification using **Method-2b**.

Data of the anomeric mixture:

^{1}H NMR (600 MHz, CDCl$_3$): δ 7.47 – 7.27 (m, 28H), 5.56 (d, J = 5.0 Hz, 1H, **H$_1$(β)**), 5.52 (d, J = 5.0 Hz, 1H, **H$_1$(α)**), 5.08 – 4.90 (m, 4H, **H$_1$'(α)**), 4.83 (dd, J = 26.5, 11.9 Hz, 2H), 4.78 – 4.67 (m, 5H), 4.65 – 4.29 (m, 10H, **H$_1$'(β)**), 4.24 – 3.36 (m, 21H), 3.20 – 3.00 (m, 4H), 1.52 (s, 3H), 1.49 (s, 3H), 1.44 (s, 6H), 1.37 – 1.29 (m, 12H), 0.03 (s, 9H), 0.02 (s, 7H) ppm. **^{13}C NMR** (151 MHz, CDCl$_3$): δ 139.1, 139.0, 138.9, 138.4, 138.1, 137.7, 128.7, 128.7, 128.6, 128.5, 128.4, 128.4, 128.3, 128.2, 128.2, 128.1, 128.0, 127.9, 127.9, 127.8, 127.6, 127.6, 127.5, 127.5, 127.4, 109.4, 109.3, 108.7, 108.6, 104.8 (**C$_1$'(β)**), 100.4 (**C$_1$'(α)**), 97.5 (**C$_1$(β)**), 96.5 (**C$_1$(α)**), 96.4, 82.0, 79.3, 79.0, 76.6, 76.5, 75.5, 75.1, 74.9, 74.3, 74.2, 73.3, 73.2, 73.1, 72.9, 72.7, 72.3, 71.6, 71.3, 70.9, 70.7, 70.6, 69.7, 68.8, 67.5, 66.2, 65.9, 65.8, 65.7, 64.5, 29.9, 26.3, 26.2, 26.1, 25.2, 25.1, 24.7, 24.5, -2.9, -2.9 ppm. **HRMS** (QToF): Calcd for C$_{53}$H$_5$O$_{11}$SiNa [M + Na]$^+$ 801.3641; found 801.3669.

1,2:3,4-Bis-*O*-(1-methylethylidene)-6-*O*-[2,3,4-tris-*O*-benzyl-6-*O*-levulinyl-α/β-D-galactopyranosyl]-α-D-galactopyranoside (4.08c-A1)
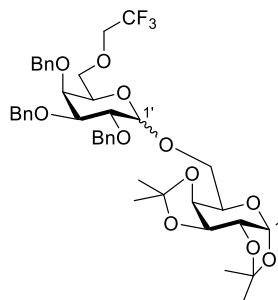
The title compound was prepared according to the general glycosylation procedure. Product **4.08c-A1** (19 mg, 24 µmol, 71%, **α/β 19:81**) was obtained as a colorless oil after purification using **Method-2b**.

Data of the major isomer (β):

^{1}H NMR (600 MHz, CDCl$_3$): δ 7.49 – 7.27 (m, 15H), 5.56 (d, J = 5.0 Hz, 1H, **H$_1$**), 5.06 (d, J = 11.1 Hz, 1H), 4.95 (dd, J = 11.6, 1.8 Hz, 1H), 4.84 (d, J = 11.9 Hz, 1H), 4.74 (dd, J = 11.6, 7.9 Hz, 2H), 4.65 (d, J = 11.6 Hz, 1H), 4.58 (dd, J = 7.9, 2.4 Hz, 1H), 4.41 (d, J = 7.7 Hz, 1H, **H$_1$'**), 4.30 (dd, J = 4.9, 2.4 Hz, 1H), 4.25 – 4.19 (m, 2H), 4.15 – 4.06 (m, 3H), 3.84 (dd, J = 9.8, 7.7 Hz, 1H), 3.80 (dd, J = 2.9, 1.1 Hz, 1H), 3.69 (dd, J = 10.6, 7.5 Hz, 1H), 3.58 – 3.48 (m, 2H), 2.71 (td, J = 6.6, 3.0 Hz, 2H), 2.58 – 2.41 (m, 2H), 2.17 (s, 3H), 1.49 (s, 3H), 1.44 (s, 3H), 1.32 (s, 3H), 1.31 (s, 3H) ppm. **^{13}C NMR** (151 MHz, CDCl$_3$): δ 206.6, 172.5, 139.1, 138.7, 138.5, 128.7, 128.7, 128.5, 128.4, 128.3, 127.9, 127.8, 127.7, 127.6, 127.5, 109.5, 108.8, 104.8 (**C$_1$'**), 96.5 (**C$_1$**), 82.0, 79.1, 74.9, 74.5, 73.5, 73.3, 72.1, 71.6, 70.9, 70.7, 69.8, 67.6, 63.2, 38.1, 30.0, 27.9, 26.1, 25.2, 24.6 ppm. **HRMS** (QToF): Calcd for C$_{44}$H$_{54}$O$_{13}$Na [M + Na]$^+$ 813.3457; found 813.3478.

1,2:3,4-Bis-*O*-(1-methylethylidene)-6-*O*-[2,3-bis-*O*-benzyl-4,6-bis-*O*-levulinyl-α/β-D-galactopyranosyl]-α-D-galactopyranoside (4.06c-A1)
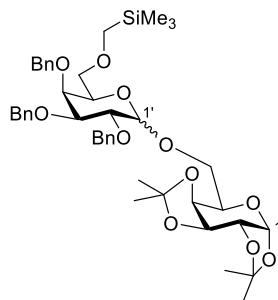

The title compound was prepared according to the general glycosylation procedure. Product **4.06c-A1** (21 mg, 26 µmol, 79%, **α/β 87:13**) was obtained as a colorless oil after purification using **Method-2b**.

Data of the major isomer (α):

^{1}H NMR (600 MHz, CDCl$_3$): δ 7.44 – 7.26 (m, 10H), 5.55 (dd, J = 3.5, 1.3 Hz, 1H, **H$_1$**), 5.51 (d, J = 5.0 Hz, 1H), 4.97 (d, J = 3.6 Hz, 1H, **H$_1$'**), 4.81 – 4.67 (m, 3H), 4.63 – 4.53 (m, 2H), 4.34 – 4.27 (m, 2H), 4.26 – 4.21 (m, 1H), 4.11 (dd, J = 6.7, 2.8 Hz, 2H), 4.04 – 3.99 (m, 1H), 3.97 (dd, J = 10.0, 3.4 Hz, 1H), 3.75 (ddd, J = 10.0, 5.1, 3.0 Hz, 3H), 2.75 – 2.53 (m, 8H), 2.18 (s, 3H), 2.11 (s, 3H), 1.51 (s, 3H), 1.44 (s, 3H), 1.32 (s, 3H), 1.31 (s, 3H) ppm. **^{13}C NMR** (151 MHz, CDCl$_3$): δ 206.6, 206.3, 172.4, 172.2, 138.7, 138.3, 128.4, 128.4, 128.1, 127.8, 127.7, 127.7, 109.4, 108.7, 97.9 (**C$_1$'**), 96.4 (**C$_1$**), 75.9, 75.5, 73.1, 72.2, 71.0, 70.8, 70.7, 68.1, 67.1, 66.7,

66.3, 62.5, 38.2, 38.1, 30.0, 29.9, 28.2, 28.0, 26.3, 26.2, 25.1, 24.7 ppm. **HRMS** (QToF): Calcd for $C_{42}H_{54}O_{15}Na$ [M + Na]$^+$ 821.3355; found 821.3372.

1,2:3,4-Bis-*O*-(1-methylethylidene)-6-*O*-[2,3,6-tris-*O*-benzyl-4-*O*-levulinyl-α/β-D-galactopyranosyl]-α-D-galactopyranoside (4.07c-A1)
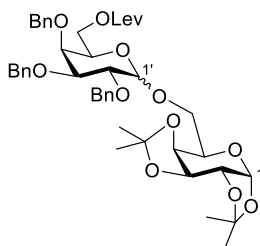

The title compound was prepared according to the general glycosylation procedure. Product **4.07c-A1** (19 mg, 24 µmol, 72%, **α/β 45:55**) was obtained as a colorless oil after purification using **Method-2b**.

Data of the anomeric mixture:

^{1}H NMR (600 MHz, CDCl$_3$): δ 7.43 – 7.25 (m, 28H), 5.64 (dd, *J* = 3.4, 1.3 Hz, 1H), 5.56 (dd, *J* = 3.1, 1.1 Hz, 1H), 5.55 (d, *J* = 5.0 Hz, 1H, **H$_1$(β)**), 5.49 (d, *J* = 5.0 Hz, 1H, **H$_1$(α)**), 5.03 – 4.93 (m, 2H), 4.79 – 4.65 (m, 5H), 4.60 – 4.39 (m, 9H), 4.32 – 4.24 (m, 3H, **H$_1$'(β)**), 4.23 – 3.92 (m, 6H), 3.84 – 3.65 (m, 6H), 3.62 – 3.40 (m, 6H), 2.82 – 2.50 (m, 8H), 2.11 (s, 3H), 2.08 (s, 3H), 1.50 (s, 3H), 1.49 (s, 3H), 1.42 (s, 3H), 1.42 (s, 3H), 1.32 – 1.28 (m, 12H) ppm. **^{13}C NMR** (151 MHz, CDCl$_3$): δ 206.4, 172.3, 172.1, 139.0, 138.8, 138.5, 138.1, 128.6, 128.6, 128.5, 128.4, 128.4, 128.4, 128.2, 128.2, 128.1, 128.1, 127.9, 127.8, 127.8, 127.7, 127.7, 127.6, 127.5, 109.5, 109.4, 108.8, 108.7, 104.7 (**C$_1$'(β)**), 97.9 (**C$_1$'(α)**), 96.5 (**C$_1$(β)**), 96.5 (**C$_1$(α)**), 79.0, 78.6, 76.3, 75.6, 75.0, 73.9, 73.7, 73.0, 72.2, 72.1, 72.1, 71.6, 71.0, 70.9, 70.8, 70.8, 70.6, 70.1, 68.5, 68.4, 68.2, 67.7, 67.5, 67.3, 66.8, 66.1, 38.2, 30.0, 29.9, 28.2, 26.3, 26.2, 26.2, 26.1, 25.2, 25.1, 24.8, 24.6 ppm. **HRMS** (QToF): Calcd for $C_{44}H_{54}O_{13}Na$ [M + Na]$^+$ 813.3457; found 813.3493.

1,2:3,4-Bis-*O*-(1-methylethylidene)-6-*O*-[2,3,6-tris-*O*-benzyl-4-*O*-levulinyl-α/β-D-mannopyranosyl]-α-D-galactopyranoside (4.33-A1)
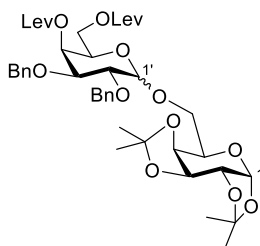

The title compound was prepared according to the general glycosylation procedure. Product **4.33-A1** (22 mg, 28 μmol, 82%, **α/β 40:60**) was obtained as a colorless oil after purification using **Method-2b**.

Data of the major isomer (β):

¹H NMR (600 MHz, CDCl$_3$): δ 7.47 – 7.44 (m, 1H), 7.35 – 7.22 (m, 14H), 5.60 (d, *J* = 4.9 Hz, 1H, **H$_1$**), 5.29 (t, *J* = 9.8 Hz, 1H), 4.92 (dd, *J* = 66.5, 12.5 Hz, 2H), 4.68 – 4.45 (m, 4H, **H$_1$'**), 4.41 (d, *J* = 12.4 Hz, 1H), 4.34 (dt, *J* = 5.9, 3.0 Hz, 1H), 4.21 (td, *J* = 11.8, 3.1 Hz, 3H), 4.11 (dt, *J* = 8.3, 2.3 Hz, 1H), 3.99 (d, *J* = 3.1 Hz, 1H), 3.73 – 3.58 (m, 3H), 3.50 (ddd, *J* = 9.7, 6.2, 3.5 Hz, 1H), 3.39 (dd, *J* = 9.8, 3.1 Hz, 1H), 2.60 (t, *J* = 6.7 Hz, 2H), 2.48 – 2.39 (m, 2H), 2.11 (s, 3H), 1.50 (s, 3H), 1.44 (s, 3H), 1.34 (s, 3H), 1.32 (s, 3H) ppm. **¹³C NMR** (151 MHz, CDCl$_3$): δ 206.5, 172.0, 138.5, 138.4, 138.0, 128.7, 128.4, 128.4, 128.3, 128.0, 127.8, 127.7, 127.7, 127.5, 109.6, 108.9, 102.2 (**C$_1$'**), 96.5 (**C$_1$**), 78.7, 74.3, 73.8, 73.7, 72.5, 71.7, 71.0, 70.9, 70.6, 70.5, 70.1, 69.5, 68.2, 38.0, 29.9, 28.1, 26.2, 26.1, 25.2, 24.5 ppm. **HRMS** (QToF): Calcd for C$_{44}$H$_{54}$O$_{13}$Na [M + Na]⁺ 813.3457; found 813.3506.

1,2:3,4-Bis-*O*-(1-methylethylidene)-6-*O*-[2,3-bis-*O*-benzyl-4,6-bis-*O*-levulinyl-α/β-D-mannopyranosyl]-α-D-galactopyranoside (4.32-A1)
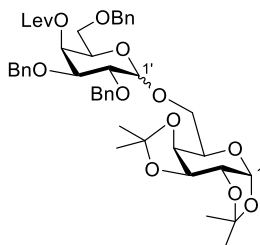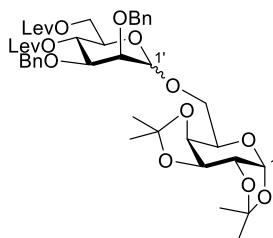

The title compound was prepared according to the general glycosylation procedure. Product **4.32-A1** (16 mg, 20 μmol, 60%, **α/β 52:48**) was obtained as a colorless oil after purification using **Method-2b** (t$_R$ (α) = 9.8 min, t$_R$ (β) = 9.1 min).

Data of the anomeric mixture:

¹H NMR (700 MHz, CDCl₃): δ 7.48 – 7.10 (m, 30H), 5.56 (t, J = 4.1 Hz, 1H), 5.49 (t, J = 4.1 Hz, 1H), 5.45 – 5.35 (m, 1H), 5.31 (s, 1H), 4.98 – 4.90 (m, 2H), 4.83 (d, J = 12.4 Hz, 1H), 4.73 – 4.38 (m, 7H), 4.34 – 4.05 (m, 7H), 3.99 – 3.58 (m, 5H), 2.64 – 2.47 (m, 16H), 2.18 (t, J = 1.8 Hz, 3H), 2.14 – 2.11 (m, 9H), 1.49 (s, 3H), 1.46 (s, 3H), 1.44 – 1.42 (m, 3H), 1.41 (s, 3H), 1.33 – 1.32 (m, 3H), 1.30 (s, 3H), 1.18 (t, J = 1.8 Hz, 3H), 1.18 – 1.17 (m, 3H) ppm. **¹³C NMR** (176 MHz, CDCl₃): δ 206.8, 206.4, 177.2, 172.6, 172.3, 170.9, 154.1, 138.5, 138.4, 138.3, 138.1, 137.9, 137.8, 128.6, 128.4, 128.3, 128.0, 127.9, 127.7, 127.6, 127.5, 109.6, 108.7, 102.3, 97.8, 96.5, 92.2, 78.5, 76.3, 74.5, 73.8, 73.4, 73.0, 72.7, 72.0, 71.2, 70.9, 70.7, 70.1, 69.4, 68.4, 68.2, 67.7, 65.9, 63.3, 63.1, 62.8, 43.0, 38.8, 38.1, 30.0, 29.8, 29.7, 28.2, 28.1, 26.2, 26.1, 25.2, 24.7, 24.5, 22.4, 20.8 ppm. **HRMS** (QToF): Calcd for $C_{42}H_{54}O_{15}Na$ [M + Na]⁺ 821.3355; found 821.3416.

1,2:3,4-Bis-*O*-(1-methylethylidene)-6-*O*-[2,3,4-tris-*O*-benzyl-6-*O*-levulinyl-α/β-D-mannopyranosyl]-α-D-galactopyranoside (4.34-A1)
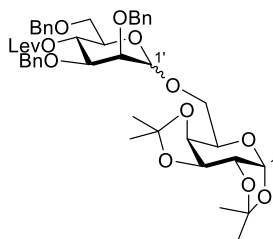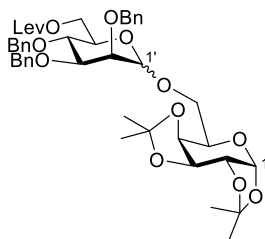

The title compound was prepared according to the general glycosylation procedure. Product **4.34-A1** (22 mg, 28 μmol, 72%, **α/β 37:63**) was obtained as a colorless oil after purification using **Method-2b**.

Data of the major isomer (β):

¹H NMR (600 MHz, CDCl₃): δ 7.80 – 7.44 (m, 1H), 7.35 – 7.22 (m, 14H), 5.65 (d, J = 4.9 Hz, 1H, **H₁**), 5.29 (t, J = 9.8 Hz, 1H), 4.92 (dd, J = 66.5, 12.5 Hz, 2H), 4.68 – 4.42 (m, 4H, **H₁'**), 4.41 (d, J = 12.4 Hz, 1H), 4.34 (dt, J = 5.9, 3.0 Hz, 1H), 4.21 (td, J = 11.8, 3.1 Hz, 3H), 4.11 (dt, J = 8.3, 2.3 Hz, 1H), 3.99 (d, J = 3.1 Hz, 1H), 3.73 – 3.58 (m, 3H), 3.50 (ddd, J = 9.7, 6.2, 3.5 Hz, 1H), 3.39 (dd, J = 9.8, 3.1 Hz, 1H), 2.60 (t, J = 6.7 Hz, 2H), 2.48 – 2.39 (m, 2H), 2.11 (s, 3H), 1.50 (s, 3H), 1.44 (s, 3H), 1.34 (s, 3H), 1.32 (s, 3H) ppm. **¹³C NMR** (151 MHz, CDCl₃): δ 206.5, 172.0, 138.5, 138.4, 138.0, 128.7, 128.4, 128.4, 128.3, 128.0, 127.8, 127.7, 127.7, 127.5, 109.6, 108.9, 102.2 (**C₁'**), 96.5 (**C₁**), 78.7, 74.3, 73.8, 73.7, 72.5, 71.7, 71.0, 70.9, 70.6, 70.5, 70.1, 69.5, 68.2, 38.0, 29.9, 28.1, 26.2, 26.1, 25.2, 24.5 ppm. **HRMS** (QToF): Calcd for $C_{44}H_{54}O_{13}Na$ [M + Na]⁺ 813.3457; found 813.3506.

6.5 Preparation and Characterization of Compounds in Chapter 5

6.5.1 Automated Glycan Assembly of *P. Gingivalis* LPS Fragments

5-Amino-pentyl α-D-glucopyranosyl-(1→4)-α-L-rhamnopyranosyl-(1→3)-2-acetamido-2-deoxy-β-D-galactopyranosyl-(1→3)-α-D-galactopyranoside (LPS-1)

Repeat	Building Blocks	Modules	Notes	
1x	**5.03** (2 x 5.0 equiv.)	**I** – Acidic Wash **IIa** – Glycosylation with thioglycoside – 2 cycles **III** – Capping **IVa** – Fmoc Deprotection - 2 cycles	-40 °C (T_1) -10 °C (T_2)	10 min (t_1) 50 min (t_2)
1x	**5.02** (2 x 5.0 equiv.)	**I** – Acidic Wash **IIa** – Glycosylation with thioglycoside – 2 cycles **III** – Capping **IVa** – Fmoc Deprotection - 2 cycles	-40 °C (T_1) -20 °C (T_2)	30 min (t_1) 20 min (t_2)
1x	**5.04b** (2 x 5.0 equiv.)	**I** – Acidic Wash **IIa** – Glycosylation with thioglycoside – 2 cycles **III** – Capping **IVa** – Fmoc Deprotection	-20 °C (T_1) 0 °C (T_2)	10 min (t_1) 30 min (t_2)
1x	**5.05** (2 x 5.0 equiv.)	**I** – Acidic Wash **IIa** – Glycosylation with thioglycoside – 2 cycles	-20 °C (T_1) 0 °C (T_2)	5 min (t_1) 30 min (t_2)

Protected **LPS-1** (22 mg, 0.011 mmol, crude yield: 81%) was obtained as a colorless oil after photo-cleavage from solid-support following **Method A-1**. Deprotection of **LPS-1** following **Method C** and **D** and purification by reverse-phase HPLC (**Method E-1**, t_R = 18.8 min) afforded deprotected compound **LPS-1** (1.1 mg, 0.002 mmol, 11%) as a white solid after lyophilization.

¹H NMR (700 MHz, D₂O): δ 4.97 – 4.92 (m, 1H), 4.85 – 4.80 (m, 1H), 4.79 (s, 1H), 4.63 (d, J = 8.2 Hz, 1H), 4.10 (s, 1H), 4.01 – 3.55 (m, 19H), 3.49 – 3.42 (m, 2H), 3.43 – 3.35 (m, 2H), 2.94 – 2.89 (m, 2H), 1.95 (s, 3H), 1.64 – 1.57 (m, 4H), 1.40 – 1.34 (m, 2H), 1.27 (d, J = 6.2 Hz, 3H) ppm. **¹³C NMR** (176 MHz, D₂O): δ 174.9, 102.5, 102.0, 99.7, 98.4, 81.0, 79.0, 75.0, 72.7, 70.7,

70.5, 69.3, 68.7, 68.4, 67.8, 67.3, 61.2, 60.9, 60.1, 51.8, 39.4, 28.1, 26.6, 22.4, 22.2, 16.9 ppm.

HRMS (QToF): Calcd for $C_{31}H_{57}N_2O_{20}$ [M + H]$^+$ 777.3499; found 777.3508.

5-Amino-pentyl α-D-galactopyranosyl-(1→6)-α-D-glucopyranosyl-(1→4)-α-L-rhamnopyranosyl-(1→3)-2-acetamido-2-deoxy-β-D-galactopyranoside (LPS-2)

Repeat	Building Blocks	Modules	Notes	
1x	**5.02** (2 x 5.0 equiv.)	**I** – Acidic Wash		
		IIa – Glycosylation with thioglycoside – 2 cycles	-40 °C (T$_1$)	30 min (t$_1$)
			-20 °C (T$_2$)	20 min (t$_2$)
		III – Capping		
		IVc – Fmoc Deprotection - 2 cycles		
1x	**5.04b** (2 x 5.0 equiv.)	**I** – Acidic Wash		
		IIa – Glycosylation with thioglycoside – 2 cycles	-20 °C (T$_1$)	10 min (t$_1$)
			0 °C (T$_2$)	30 min (t$_2$)
		III – Capping		
		IVc – Fmoc Deprotection		
1x	**5.05** (2 x 5.0 equiv.)	**I** – Acidic Wash		
		IIa – Glycosylation with thioglycoside – 2 cycles	-20 °C (T$_1$)	5 min (t$_1$)
			0 °C (T$_2$)	30 min (t$_2$)
		III – Capping		
		IVe – ClAc Deprotection		
1x	**5.03** (2 x 5.0 equiv.)	**I** – Acidic Wash		
		IIa – Glycosylation with thioglycoside – 2 cycles	-40 °C (T$_1$)	10 min (t$_1$)
			-10 °C (T$_2$)	50 min (t$_2$)

Protected **LPS-2** (26 mg, 0.012 mmol, crude yield: 86%) was obtained as a colorless oil after photo-cleavage from solid-support following **Method A-1**. Deprotection of **LPS-2** following **Method C** and **D** and purification by reverse-phase HPLC (**Method E-1**, t_R = 18.9 min) afforded deprotected compound **LPS-2** (1.5 mg, 0.002 mmol, 15%) as a white solid after lyophilization.

^{1}H NMR (700 MHz, D$_2$O): δ 5.00 (d, J = 4.0 Hz, 1H), 4.94 (d, J = 3.8 Hz, 1H), 4.83 (s, 1H), 4.47 (d, J = 8.6 Hz, 1H), 4.19 – 4.15 (m, 1H), 3.99 – 3.40 (m, 23H), 2.97 – 2.92 (m, 2H), 2.00 (s, 3H), 1.67 – 1.60 (m, 2H), 1.59 – 1.54 (m, 2H), 1.40 – 1.33 (m, 2H), 1.31 (d, J = 6.3 Hz, 3H) ppm.
^{13}C NMR (176 MHz, D$_2$O): δ 174.4, 102.0, 101.0, 99.7, 98.1, 80.9, 78.9, 75.0, 72.8, 71.4, 70.9, 70.6, 70.4, 69.9, 69.4, 69.1, 68.7, 68.4, 68.3, 67.5, 65.4, 61.0, 60.8, 51.4, 39.2, 28.0, 26.3,

22.1, 22.0, 16.7 ppm. **HRMS** (QToF): Calcd for $C_{31}H_{57}N_2O_{20}$ [M + H]$^+$ 777.3499; found 777.3489.

5-Amino-pentyl 2-acetamido-2-deoxy-β-D-galactopyranosyl-(1→3)-α-D-galactopyranosyl-(1→6)-α-D-glucopyranosyl-(1→4)-α-L-rhamnopyranoside (LPS-3)

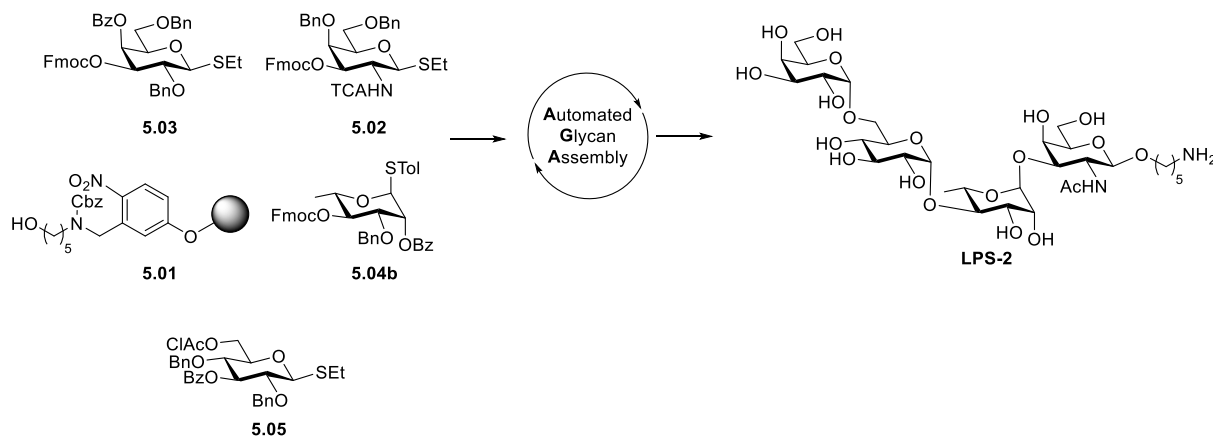| Repeat	Building Blocks	Modules	Notes	
1x	**5.04b** (2 x 5.0 equiv.)	**I** – Acidic Wash **IIa** – Glycosylation with thioglycoside – 2 cycles	-20 °C (T$_1$) 0 °C (T$_2$)	10 min (t$_1$) 30 min (t$_2$)
		III – Capping **IVc** – Fmoc Deprotection		
1x	**5.05** (2 x 5.0 equiv.)	**I** – Acidic Wash **IIa** – Glycosylation with thioglycoside – 2 cycles	-20 °C (T$_1$) 0 °C (T$_2$)	5 min (t$_1$) 30 min (t$_2$)
		III – Capping **IVe** – ClAc Deprotection		
1x	**5.03** (2 x 5.0 equiv.)	**I** – Acidic Wash **IIa** – Glycosylation with thioglycoside – 2 cycles	-40 °C (T$_1$) -10 °C (T$_2$)	10 min (t$_1$) 50 min (t$_2$)
		III – Capping **IVc** – Fmoc Deprotection		
1x	**5.02** (3 x 5.0 equiv.)	**I** – Acidic Wash **IIa** – Glycosylation with thioglycoside – 3 cycles	-40 °C (T$_1$) -20 °C (T$_2$)	30 min (t$_1$) 20 min (t$_2$)

Protected **LPS-3** (27 mg, 0.012 mmol, crude yield: 92%) was obtained as a colorless oil after photo-cleavage from solid-support following **Method A-1**. Deprotection of **LPS-3** following **Method C** and **D** and purification by reverse-phase HPLC (**Method E-1**, t$_R$ = 19.4 min) afforded deprotected compound **LPS-3** (1.8 mg, 0.002 mmol, 18%) as a white solid after lyophilization.

^{1}H NMR (700 MHz, D$_2$O): δ 5.01 (d, J = 3.9 Hz, 1H), 4.91 (d, J = 3.9 Hz, 1H), 4.76 – 4.74 (m, 1H), 4.60 (d, J = 8.5 Hz, 1H), 4.19 – 4.14 (m, 2H), 3.98 (dd, J = 11.3, 3.5 Hz, 1H), 3.94 – 3.60 (m, 18H), 3.57 – 3.48 (m, 3H), 3.44 (t, J = 9.4 Hz, 1H), 2.96 (t, J = 7.7 Hz, 2H), 1.99 (s, 2H), 1.68 – 1.56 (m, 4H), 1.41 (d, J = 7.9 Hz, 2H), 1.33 (d, J = 6.3 Hz, 3H) ppm. **^{13}C NMR** (176 MHz, D$_2$O): δ 175.1, 103.2, 99.7, 99.4, 98.1, 81.1, 79.1, 74.9, 72.9, 71.3, 70.7, 70.5, 70.4, 69.2, 69.1,

69.0, 67.6, 67.5, 67.4, 65.1, 60.9, 52.6, 39.2, 28.0, 26.5, 22.3, 22.2, 16.6 ppm. **HRMS** (QToF): Calcd for $C_{31}H_{57}N_2O_{20}$ [M + H]$^+$ 777.3499; found 777.3501.

5-Amino-pentyl α-L-rhamnopyranosyl-(1→3)-2-acetamido-2-deoxy-β-D-galactopyranosyl-(1→3)-α-D-galactopyranosyl-(1→6)-α-D-glucopyranoside (LPS-4)

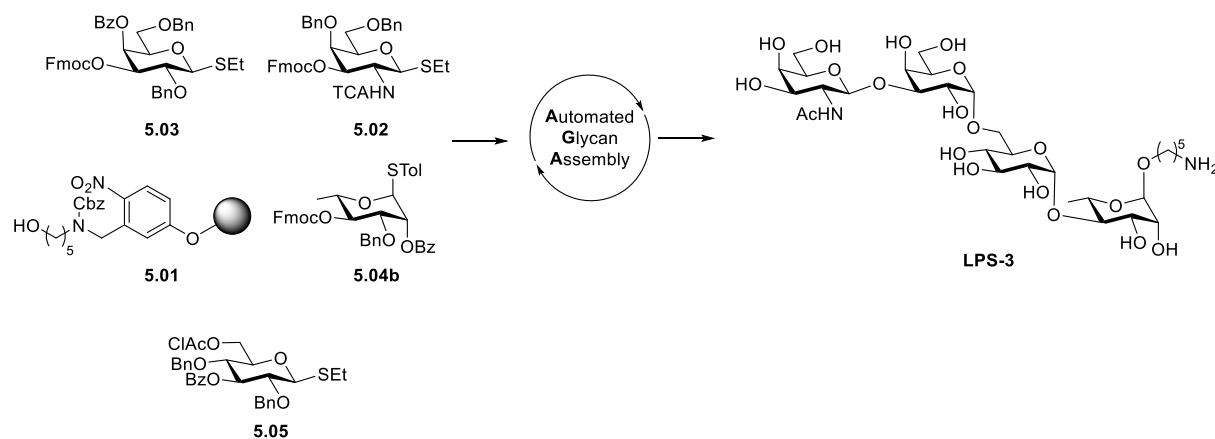| Repeat	Building Blocks	Modules	Notes	
1x	**5.05** (2 x 5.0 equiv.)	I – Acidic Wash		
		IIa – Glycosylation with thioglycoside – 2 cycles	-20 °C (T$_1$) 0 °C (T$_2$)	5 min (t$_1$) 30 min (t$_2$)
		III – Capping IVe – ClAc Deprotection		
1x	**5.03** (2 x 5.0 equiv.)	I – Acidic Wash		
		IIa – Glycosylation with thioglycoside – 2 cycles	-40 °C (T$_1$) -10 °C (T$_2$)	10 min (t$_1$) 50 min (t$_2$)
		III – Capping IVc – Fmoc Deprotection		
1x	**5.02** (2 x 5.0 equiv.)	I – Acidic Wash		
		IIa – Glycosylation with thioglycoside – 2 cycles	-40 °C (T$_1$) -20 °C (T$_2$)	30 min (t$_1$) 20 min (t$_2$)
		III – Capping IVc – Fmoc Deprotection		
1x	**5.04b** (2 x 5.0 equiv.)	I – Acidic Wash		
		IIa – Glycosylation with thioglycoside – 2 cycles	-20 °C (T$_1$) 0 °C (T$_2$)	10 min (t$_1$) 30 min (t$_2$)

Protected **LPS-4** (17 mg, 0.012 mmol, crude yield: 57%) was obtained as a colorless oil after photo-cleavage from solid-support following **Method A-1**. Deprotection of **LPS-4** following **Method C** and **D** and purification by reverse-phase HPLC (**Method E-1**, t$_R$ = 19.4 min) afforded deprotected compound **LPS-3** (0.8 mg, 0.001 mmol, 8%) as a white solid after lyophilization.

^{1}H NMR (700 MHz, D$_2$O): δ 4.88 (d, *J* = 3.8 Hz, 1H), 4.86 (d, *J* = 4.1 Hz, 1H), 4.64 (d, *J* = 8.5 Hz, 1H), 4.15 (s, 1H), 4.02 – 3.83 (m, 6H), 3.82 – 3.59 (m, 14H), 3.52 – 3.44 (m, 3H), 3.36 (t, *J* = 9.7 Hz, 1H), 2.93 (t, *J* = 7.6 Hz, 2H), 1.97 (s, 3H), 1.63 (p, *J* = 7.4 Hz, 4H), 1.40 (dt, *J* = 16.0, 8.4 Hz, 2H), 1.20 (d, *J* = 6.3 Hz, 3H) ppm. **^{13}C NMR** (176 MHz, D$_2$O): δ 174.8, 102.6,

102.3, 98.2, 98.1, 73.3, 70.0, 69.1, 67.9, 60.9, 51.8, 46.5, 39.4, 38.7, 28.0, 26.6, 22.5, 16.6 ppm. **HRMS** (QToF): Calcd for $C_{31}H_{57}N_2O_{20}$ $[M + H]^+$ 777.3499; found 777.3502.

5-Amino-pentyl α-D-galactopyranoside (LPS-11)

Repeat	Building Blocks	Modules	Notes	
1x	**5.03** (2 x 5.0 equiv.)	**I** – Acidic Wash **IIa** – Glycosylation with thioglycoside – 2 cycles	-40 °C (T_1) -10 °C (T_2)	10 min (t_1) 50 min (t_2)

Protected **LPS-11** (8 mg, 0.012 mmol, crude yield: 87%) was obtained as a colorless oil after photo-cleavage from solid-support following **Method A-1**. Deprotection of **LPS-11** following **Method C** and **D** and purification by reverse-phase HPLC (**Method E-1**, t_R = 13.5 min) afforded deprotected compound **LPS-11** (1.2 mg, 0.004 mmol, 18%) as a white solid after lyophilization.

¹H NMR (700 MHz, D$_2$O): δ 4.95 (d, J = 3.4 Hz, 1H), 3.98 (d, J = 3.2 Hz, 1H), 3.93 (t, J = 6.2 Hz, 1H), 3.87 – 3.81 (m, 2H), 3.78 – 3.72 (m, 3H), 3.54 (dt, J = 10.0, 6.2 Hz, 1H), 3.01 (t, J = 7.6 Hz, 2H), 1.75 – 1.62 (m, 4H), 1.53 – 1.42 (m, 2H) ppm. **¹³C NMR** (176 MHz, D$_2$O): δ 98.2, 70.9, 69.5, 69.3, 68.3, 67.8, 61.3, 39.4, 28.0, 26.5, 22.4 ppm. **HRMS** (QToF): Calcd for $C_{11}H_{24}NO_6$ $[M + H]^+$ 266.1598; found 266.1726.

5-Amino-pentyl α-D-glucopyranoside (LPS-8)

Repeat	Building Blocks	Modules	Notes	
1x	**5.05** (2 x 5.0 equiv.)	**I** – Acidic Wash **IIa** – Glycosylation with thioglycoside – 2 cycles	-20 °C (T_1) 0 °C (T_2)	5 min (t_1) 30 min (t_2)

Protected **LPS-8** (5 mg, 0.006 mmol, crude yield: 46%) was obtained as a colorless oil after photo-cleavage from solid-support following **Method A-1**. Deprotection of **LPS-8** following

Method C and **D** and purification by reverse-phase HPLC (**Method E-1**, t_R = 12.8 min) afforded deprotected compound **LPS-8** (0.9 mg, 0.003 mmol, 25%) as a white solid after lyophilization.

^{1}H NMR (700 MHz, D$_2$O): δ 4.92 (d, J = 3.8 Hz, 1H), 3.86 (dd, J = 12.3, 2.4 Hz, 1H), 3.78 – 3.65 (m, 4H), 3.59 – 3.52 (m, 2H), 3.41 (dd, J = 10.1, 9.1 Hz, 1H), 3.02 (t, J = 7.6 Hz, 2H), 1.72 – 1.63 (m, 4H), 1.54 – 1.41 (m, 2H) ppm. **^{13}C NMR** (176 MHz, D$_2$O): δ 97.9, 73.0, 71.7, 71.1, 69.5, 67.6, 60.5, 39.2, 28.0, 26.4, 22.4 ppm. **HRMS** (QToF): Calcd for C$_{11}$H$_{24}$NO$_6$ [M + H]$^+$ 266.1598; found 266.1750.

5-Amino-pentyl 2-acetamido-2-deoxy-β-D-galactopyranosyl-(1→3)-α-D-galactopyranoside (LPS-6)

Repeat	Building Blocks	Modules	Notes	
1x	**5.03** (2 x 5.0 equiv.)	**I** – Acidic Wash		
		IIa – Glycosylation with thioglycoside – 2 cycles	-40 °C (T$_1$)	10 min (t$_1$)
			-10 °C (T$_2$)	50 min (t$_2$)
		III – Capping		
		IVc – Fmoc Deprotection		
1x	**5.02** (2 x 5.0 equiv.)	**I** – Acidic Wash		
		IIa – Glycosylation with thioglycoside – 2 cycles	-40 °C (T$_1$)	30 min (t$_1$)
			-20 °C (T$_2$)	20 min (t$_2$)
		III – Capping		
		IVc – Fmoc Deprotection		

Protected **LPS-6** (11 mg, 0.009 mmol, crude yield: 67%) was obtained as a colorless oil after photo-cleavage from solid-support following **Method A-1**. Deprotection of **LPS-6** following **Method C** and **D** and purification by reverse-phase HPLC (**Method E-1**, t_R = 15.6 min) afforded deprotected compound **LPS-6** (1.1 mg, 0.002 mmol, 17%) as a white solid after lyophilization.

^{1}H NMR (700 MHz, D$_2$O): δ 4.92 (d, J = 3.8 Hz, 1H), 4.65 (d, J = 8.4 Hz, 1H), 4.20 (d, J = 3.2 Hz, 1H), 3.97 – 3.86 (m, 5H), 3.83 – 3.71 (m, 6H), 3.70 – 3.65 (m, 1H), 3.54 (dt, J = 9.9, 6.2 Hz, 1H), 3.01 (t, J = 7.6 Hz, 2H), 2.04 (s, 3H), 1.74 – 1.63 (m, 4H), 1.53 – 1.42 (m, 2H) ppm. **^{13}C NMR** (176 MHz, D$_2$O): δ 175.2, 103.1, 98.4, 79.0, 75.0, 70.8, 70.5, 69.3, 67.8, 67.3, 61.2, 61.0, 52.7, 39.4, 28.1, 26.5, 22.4, 22.3 ppm. **HRMS** (QToF): Calcd for C$_{19}$H$_{37}$N$_2$O$_{11}$ [M + H]$^+$ 469.2392; found 469.2402.

5-Amino-pentyl α-L-rhamnopyranosyl-(1→3)-2-acetamido-2-deoxy-β-D-galactopyranosyl-(1→3)-α-D-galactopyranoside (LPS-5)
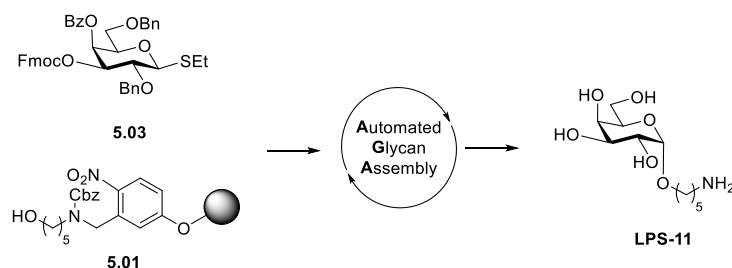

Repeat	Building Blocks	Modules	Notes	
1x	**5.03** (2 x 5.0 equiv.)	**I** – Acidic Wash **IIa** – Glycosylation with thioglycoside – 2 cycles **III** – Capping **IVc** – Fmoc Deprotection - 2 cycles	-40 °C (T$_1$) -10 °C (T$_2$)	10 min (t$_1$) 50 min (t$_2$)
1x	**5.02** (2 x 5.0 equiv.)	**I** – Acidic Wash **IIa** – Glycosylation with thioglycoside – 2 cycles **III** – Capping **IVc** – Fmoc Deprotection - 2 cycles	-40 °C (T$_1$) -20 °C (T$_2$)	30 min (t$_1$) 20 min (t$_2$)
1x	**5.04b** (2 x 5.0 equiv.)	**I** – Acidic Wash **IIa** – Glycosylation with thioglycoside – 2 cycles	-20 °C (T$_1$) 0 °C (T$_2$)	10 min (t$_1$) 30 min (t$_2$)

Protected **LPS-5** (16 mg, 0.011 mmol, crude yield: 79%) was obtained as a colorless oil after photo-cleavage from solid-support following **Method A-1**. Deprotection of **LPS-5** following **Method C** and **D** and purification by reverse-phase HPLC (**Method E-1**, t$_R$ = 17.4 min) afforded deprotected compound **LPS-5** (1.2 mg, 0.002 mmol, 15%) as a white solid after lyophilization.

^{1}H NMR (700 MHz, D$_2$O): δ 4.83 (d, J = 3.9 Hz, 1H), 4.80 (s, 1H), 4.65 (d, J = 8.5 Hz, 1H), 4.11 (d, J = 3.4 Hz, 1H), 3.96 (dd, J = 11.0, 8.5 Hz, 1H), 3.89 – 3.56 (m, 14H), 3.46 (dt, J = 10.1, 6.3 Hz, 1H), 3.36 (t, J = 9.7 Hz, 1H), 2.93 (t, J = 7.6 Hz, 2H), 1.97 (s, 3H), 1.61 (dt, J = 12.3, 6.1 Hz, 4H), 1.38 (q, J = 8.7 Hz, 2H), 1.20 (d, J = 6.2 Hz, 3H) ppm. **^{13}C NMR** (176 MHz, D$_2$O): δ 174.9, 102.5, 102.3, 98.4, 79.0, 78.6, 75.0, 71.9, 70.5, 70.4, 70.0, 69.3, 67.8, 67.6, 67.3, 61.2, 60.9, 51.8, 39.4, 28.1, 26.5, 22.4, 22.2, 16.6 ppm. **HRMS** (QToF): Calcd for C$_{25}$H$_{47}$N$_2$O$_{15}$ [M + H]$^+$ 615.2971; found 615.2974.

5-Amino-pentyl β-D-galactopyranosyl-(1→3)-α-D-galactopyranosyl-(1→6)-α-D-glucopyranoside (LPS-7)

Repeat	Building Blocks	Modules	Notes	
1x	**5.05** (2 x 5.0 equiv.)	**I** – Acidic Wash		
		IIa – Glycosylation with thioglycoside – 2 cycles	-20 °C (T₁)	5 min (t₁)
			0 °C (T₂)	30 min (t₂)
		III – Capping		
		IVe – ClAc Deprotection		
1x	**5.03** (2 x 5.0 equiv.)	**I** – Acidic Wash		
		IIa – Glycosylation with thioglycoside – 2 cycles	-40 °C (T₁)	10 min (t₁)
			-10 °C (T₂)	50 min (t₂)
		III – Capping		
		IVc – Fmoc Deprotection		

Protected **LPS-7** (12 mg, 0.010 mmol, crude yield: 76%) was obtained as a colorless oil after photo-cleavage from solid-support following **Method A-1**. Deprotection of **LPS-7** following **Method C** and **D** and purification by reverse-phase HPLC (**Method E-1**, t_R = 17.4 min) afforded deprotected compound **LPS-7** (0.56 mg, 0.013 mmol, 10%) as a white solid after lyophilization.

^{1}H NMR (700 MHz, D$_2$O): δ 4.93 (d, J = 3.7 Hz, 1H), 4.88 (d, J = 3.8 Hz, 1H), 3.96 – 3.91 (m, 3H), 3.85 – 3.76 (m, 3H), 3.73 – 3.66 (m, 4H), 3.64 (t, J = 9.4 Hz, 1H), 3.55 – 3.44 (m, 3H), 2.96 (t, J = 7.6 Hz, 2H), 1.69 – 1.60 (m, 4H), 1.48 – 1.36 (m, 2H). **^{13}C NMR** (176 MHz, D$_2$O): δ 98.0, 97.9, 73.3, 71.1, 70.9, 70.2, 69.3, 69.1, 68.3, 67.8, 65.5, 61.0, 39.3, 28.0, 26.5, 22.4. **HRMS** (QToF): Calcd for C$_{17}$H$_{34}$NO$_{11}$ [M + H]$^+$ 428.2126; found 428.2142.

5-Amino-pentyl α-(1→2)-L-trirhamnopyranoside (5.06)
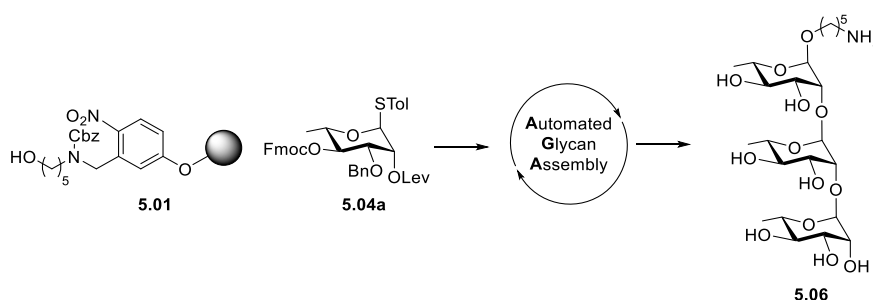
Repeat	Building Blocks	Modules	Notes	
3x	**5.04a** (3 x 3.0 equiv.)	**I** – Acidic Wash		
		IIa – Glycosylation with thioglycoside – 2 cycles	-20 °C (T_1) 0 °C (T_2)	10 min (t_1) 30 min (t_2)
		III – Capping		
		IVb – Lev Deprotection		

Protected **5.06** (35 mg, 0.022 mmol, crude yield: 80%) was obtained as a colorless oil after photo-cleavage from solid-support following **Method A-1**. Deprotection of **5.06** following **Method C** and **D** and purification by reverse-phase HPLC (**Method E-1**, t_R = 17.4 min) afforded deprotected compound **5.06** (6 mg, 0.011 mmol, 41%) as a white solid after lyophilization.

^{1}H NMR (700 MHz, D_2O): δ 5.12 (d, J = 1.8 Hz, 1H), 4.98 (d, J = 1.8 Hz, 1H), 4.88 (d, J = 1.7 Hz, 1H), 4.09 (ddd, J = 11.5, 3.4, 1.7 Hz, 2H), 3.95 – 3.88 (m, 2H), 3.86 (dd, J = 9.8, 3.4 Hz, 1H), 3.82 – 3.67 (m, 5H), 3.56 (dt, J = 10.0, 6.1 Hz, 1H), 3.53 – 3.40 (m, 3H), 3.01 (t, J = 7.6 Hz, 2H), 1.76 – 1.61 (m, 4H), 1.53 – 1.41 (m, 2H), 1.31 (d, J = 6.3 Hz, 3H), 1.30 (d, J = 6.2 Hz, 3H), 1.28 (d, J = 6.2 Hz, 3H) ppm. **^{13}C NMR** (176 MHz, D_2O): δ 102.2, 100.9, 98.4, 72.1, 72.1, 72.0, 70.2, 70.1, 70.0, 69.8, 69.3, 69.1, 68.8, 67.7, 39.4, 28.0, 26.6, 22.4, 16.6 ppm. **HRMS** (QToF): Calcd for $C_{23}H_{44}NO_{13}$ [M + H]$^+$ 542.2807; found 542.2811.

6.5.2 Synthesis of Rhamnose Building Blocks 5.04a and 5.04b

4-Methylphenyl 2,3-*O*-(1-methylethylidene)-4-*O*-(2-naphthalenylmethyl)-1-thio-α-L-rhamnopyranoside (5.12)
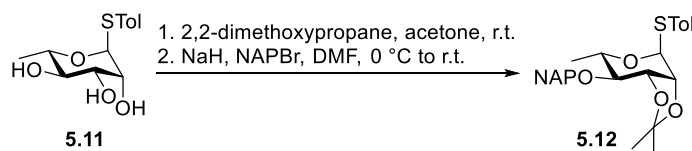
Rhamnopyranose **5.11**[156] (4.13 g, 15.3 mmol, 1.0 equiv.) was dissolved in anhydr. acetone (60 mL). 2,2,-Dimethoxypropane (7.5 mL, 61.2 mmol, 4.0 equiv.) was added followed by para-toluenesulfonic acid (582 mg, 3.1 mmol, 0.2 equiv.). The reaction mixture was stirred for 6 h at room temperature. Then, it was quenched by the addition of sat. aq. NaHCO$_3$, filtered and concentrated under reduced pressure. The residue was extracted with CH$_2$Cl$_2$ (2 x 100 mL), dried over Na$_2$SO$_4$, filtered and concentrated. 2,3-Isopropylidene product (3.7 g, 11.9 mmol, 78%) was obtained as a colorless solid after purification by column chromatography (Hex:AcOEt 3:1). R$_f$ = 0.48 (Hex:AcOEt, 3:1). The residue (3.7 g, 11.9 mmol, 1.0 equiv.) was dissolved in anhydrous *N,N*-dimethylformamide (40 mL). The stirred solution was cooled to 0 °C and sodium hydride (1.1 g, 27.4 mmol; 60% dispersion in mineral oil, 2.3 eq.) was added in small portions. After 30 min, NAPBr (4.0 g, 17.9 mmol, 1.5 equiv.) was added. The reaction

mixture was allowed to warm to room temperature and was stirred over night. Methanol (10 mL) was added, the reaction mixture was stirred for 10 min and afterwards diluted with ethyl acetate (100 mL). The organic layer was washed with water (2 x 100 mL). The aqueous phase was extracted with ethyl acetate (2 x 100 mL). The combined organic phase was washed with water (100 mL), dried over Na_2SO_4 and concentrated. Product **5.12** (4.0 g, 8.9 mmol, 75%) was obtained as a colorless oil after purification by column chromatography (SiO_2, Hex/EtOAc 9:1 to 3:1).

R_f = 0.8 (Hex/EtOAc 1:1). **^{1}H NMR** (400 MHz, CDCl$_3$) δ 7.88 – 7.83 (m, 4H), 7.56 – 7.46 (m, 3H), 7.42 – 7.37 (m, 2H), 7.17 – 7.12 (m, 2H), 5.71 (s, 1H), 4.98 (dd, J = 108.5, 11.8 Hz, 2H), 4.41 – 4.39 (m, 1H), 4.23 (dd, J = 9.8, 6.2 Hz, 1H), 3.42 – 3.35 (m, 1H), 1.55 (s, 3H), 1.43 (s, 3H), 1.30 (d, J = 6.2 Hz, 3H) ppm. **^{13}C NMR** (101 MHz, CDCl$_3$) δ 137.9, 135.8, 133.3, 133.1, 132.6, 129.9, 129.8, 128.2, 128.0, 127.8, 126.9, 126.2, 126.0, 109.5, 84.3, 81.5, 78.6, 76.8, 73.2, 66.2, 28.2, 26.6, 21.2, 17.9 ppm. **HRMS** (QToF): Calcd for $C_{27}H_{30}O_4SNa$ [M + Na]$^+$ 473.1757; found 473.1743.

4-Methylphenyl 4-*O*-(2-naphthalenylmethyl)-1-thio-α-L-rhamnopyranoside (5.13)
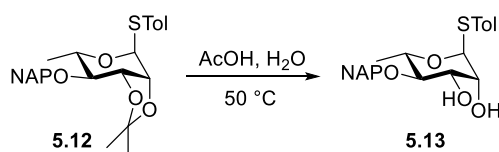
2,3-Isopropylidene **5.12** (4.0 g, 8.8 mmol, 1.0 equiv.) was dissolved in acetic acid/water (9:1, 50 mL) solution and reacted for 18 h at 50 °C. The mixture was concentrated and purified by column chromatography (SiO_2, Hex/EtOAc 3:1 to 1:1) to obtain compound **5.13** (3.6 g, 1.7 mmol, 99%) as a colorless syrup.

R_f = 0.27 (Hex/EtOAc 1:1). **^{1}H NMR** (400 MHz, CDCl$_3$) δ 7.90 – 7.76 (m, 4H), 7.53 – 7.46 (m, 3H), 7.40 – 7.31 (m, 2H), 7.12 (dd, J = 8.2, 4.1 Hz, 2H), 5.41 (d, J = 1.7 Hz, 1H), 4.92 (d, J = 3.2 Hz, 2H), 4.32 – 4.23 (m, 1H), 4.19 (dd, J = 3.4, 1.6 Hz, 1H), 3.97 (dd, J = 9.1, 3.4 Hz, 1H), 3.47 (t, J = 9.2 Hz, 1H), 2.33 (s, 3H), 1.39 (d, J = 6.2 Hz, 3H) ppm. **^{13}C NMR** (101 MHz, CDCl$_3$) δ 137.9, 135.7, 133.4, 133.2, 132.3, 130.3, 130.0, 129.9, 128.7, 128.1, 127.9, 126.9, 126.4, 126.3, 125.9, 87.9, 82.0, 75.3, 72.7, 72.0, 68.7, 21.3, 18.1 ppm. **HRMS** (QToF): Calcd for $C_{24}H_{26}O_4SNa$ [M + Na]$^+$ 433.1444; found 433.1432.

4-Methylphenyl 3-*O*-benzyl-4-*O*-(2-naphthalenylmethyl)-1-thio-α-L-rhamnopyranoside (5.14)
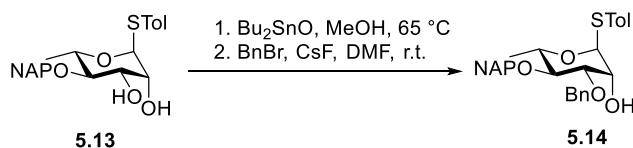
Diol **5.13** (7.0 g, 17.1 mmol, 1.0 equiv.) was dissolved in MeOH (100 mL) and Bu_2SnO (8.5 g, 34.2 mmol, 2.0 equiv.) was added. The reaction mixture was then heated up to 65 °C and stirred at the same temperature overnight. The reaction mixture was co-evaporated with toluene and dried under high vacuum. The crude was dissolved in DMF (100 mL) and benzyl bromide (2.45 mL, 20.5 mmol, 1.2 equiv.), and CsF (3.4 g, 22.2 mmol, 1.3 equiv.) were added to the stirred reaction mixture at room temperature under argon atmosphere. The reaction was stirred at room temperature for 5 h and then diluted with EtOAc, passed through a short plug of silica gel and dried under vacuum. Compound **5.14** (8.4 g, 16.8 mmol, 98%) was obtained as a colorless oil after purification by column chromatography (SiO_2, Hex/EtOAc 9:1 to 3:1).

R_f = 0.41 (Hex/EtOAc 3:1). **^{1}H NMR** (400 MHz, $CDCl_3$) δ 7.86 – 7.76 (m, 4H), 7.53 – 7.43 (m, 3H), 7.41 – 7.32 (m, 7H), 7.12 (d, *J* = 8.2 Hz, 2H), 5.47 (d, *J* = 1.8 Hz, 1H), 4.94 (dd, *J* = 91.4, 11.2 Hz, 2H), 4.74 (s, 2H), 4.31 – 4.20 (m, 2H), 3.91 (dd, *J* = 9.0, 3.2 Hz, 1H), 3.59 (t, *J* = 9.3 Hz, 1H), 2.33 (s, 3H), 1.34 (d, *J* = 6.2 Hz, 3H) ppm. **^{13}C NMR** (101 MHz, $CDCl_3$) δ 137.8, 137.7, 135.9, 133.4, 133.1, 132.2, 130.3, 130.0, 128.8, 128.3, 128.2, 128.1, 128.1, 127.8, 126.8, 126.2, 126.1, 126.0, 87.5, 80.3, 80.2, 75.6, 72.3, 70.2, 68.8, 21.3, 18.0 ppm. **HRMS** (QToF): Calcd for $C_{31}H_{32}O_4SNa$ [M + Na]$^+$ 523.1913; found 523.1924.

4-Methylphenyl 3-*O*-benzyl-2-*O*-levulinyl-4-*O*-fluorenylmethoxycarbonyl-1-thio-α-L-rhamnopyranoside (5.15a)
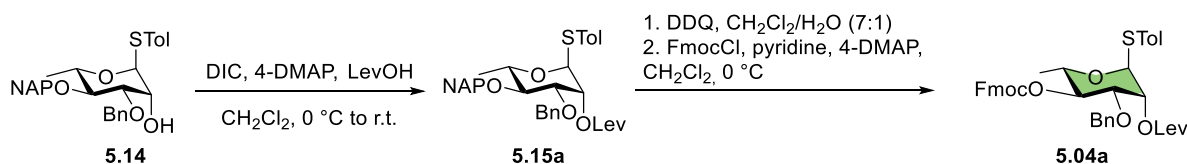
To a solution of **5.14** (800 mg, 1.6 mmol, 1.0 equiv.) and LevOH (0.33 mL, 3.2 mmol, 2.0 equiv.) in anhydrous CH_2Cl_2 (15 mL) was added DIC (0.75 mL, 4.8 mmol, 3.0 equiv.) and 4-DMAP (39 mg, 0.32 mmol, 0.2 equiv.) at 0 °C. The reaction was stirred at room temperature overnight. The reaction mixture was filtered through Celite, the filtrate was washed with aqueous $NaHCO_3$ and the aqueous phase was extracted with CH_2Cl_2. The combined organic phase was dried over Na_2SO_4, filtered and concentrated. Sugar **5.15a** (810 mg, 1.35 mmol, 85%) was obtained as a colorless syrup after purification by column chromatography (SiO_2, Hex/EtOAc 3:1). R_f =

0.35 (Hex: EtOAc 3:1). To a well stirred emulsion of sugar **5.15a** (810 mg, 1.3 mmol, 1.0 equiv.) in CH_2Cl_2/water (7:1, 24 mL), was added DDQ (337 mg, 1.5 mmol, 1.1 equiv.) and the suspension was stirred at room temperature for 1.5 h protected from light. The mixture was diluted with CH_2Cl_2, washed with 10% $Na_2S_2O_3$ and saturated aqueous $NaHCO_3$ solution. The organic layer was dried over Na_2SO_4, filtered, concentrated and the residue was purified by column chromatography (SiO_2, Hex/EtOAc 9:1 to 3:1) to obtain **3-OH-sugar** (620 mg, 1.4 mmol, quant.) as a colorless solid. R_f = 0.35 (Hex:AcOEt 3:1). To a solution of **3-OH-sugar** (620 g, 1.4 mmol, 1.0 equiv.) and anhydrous pyridine (0.55 mL, 6.7 mmol, 5.0 equiv.) in anhydrous CH_2Cl_2 (15 mL) at 0 °C was added FmocCl (524 mg, 2.0 mmol, 1.5 equiv.) followed by 4-DMAP (8 mg, 0.1 mmol, 0.05 equiv.) was added and the reaction mixture was stirred for two hours at 0 °C. Aqueous citric acid solution (10 mL) was added and the mixture was allowed to warm to room temperature. The aqueous phase was extracted with CH_2Cl_2 and the combined organic phase was dried over Na_2SO_4, filtered and concentrated. Compound **5.04a** (840 mg, 1.2 mmol, 91%) was obtained as a white solid after purification by column chromatography (SiO_2, Hex/EtOAc 19:1 to 3:1).

R_f = 0.25 (Hex/EtOAc 3:1). **^{1}H NMR** (400 MHz, $CDCl_3$): δ 7.79 (d, J = 7.5 Hz, 2H), 7.67 – 7.57 (m, 2H), 7.46 – 7.36 (m, 2H), 7.35 – 7.30 (m, 4H), 7.26 – 7.20 (m, 5H), 7.12 (d, J = 7.9 Hz, 2H), 5.57 (dd, J = 3.3, 1.7 Hz, 1H), 5.35 (d, J = 1.6 Hz, 1H), 4.88 (t, J = 9.8 Hz, 1H), 4.65 (d, J = 11.9 Hz, 1H), 4.52 – 4.40 (m, 3H), 4.35 (dd, J = 9.8, 6.2 Hz, 1H), 4.26 (t, J = 7.2 Hz, 1H), 3.88 (dd, J = 9.7, 3.2 Hz, 1H), 2.68 (ddd, J = 10.8, 5.1, 1.3 Hz, 4H), 2.33 (s, 3H), 2.15 (s, 3H), 1.26 (d, J = 6.2 Hz, 3H) ppm. **^{13}C NMR** (101 MHz, $CDCl_3$): δ 206.44, 171.98, 154.99, 143.51, 143.31, 141.45, 138.30, 137.41, 132.49, 130.09, 129.59, 128.50, 128.07, 127.99, 127.34, 125.23, 120.25, 86.32, 74.97, 71.56, 70.41, 70.13, 67.50, 46.94, 38.10, 29.93, 28.24, 21.29, 17.43 ppm. **[α]$_D$** -39.32 cm^{-1} (c 1, $CHCl_3$). **IR** (film): 3067, 2872, 1749, 1723, 1603, 1495, 1451, 1386, 1246, 1152, 1102, 986, 848, 784, 738, 698 cm^{-1}. **HRMS** (QToF): Calcd for $C_{40}H_{40}O_8SNa$ [M + Na]$^+$ 703.2336; found 703.2354.

4-Methylphenyl 2-*O*-benzoyl 3-*O*-benzyl-4-*O*-fluorenylmethoxycarbonyl-1-thio-α-L-rhamnopyranoside (5.04b)
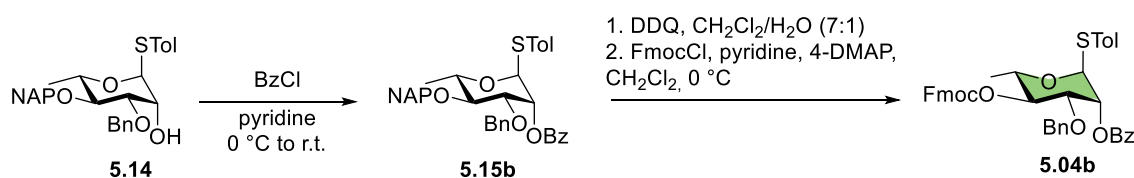

To a solution of **5.14** (5.0 g, 10.0 mmol, 1.0 equiv.) in anhydrous pyridine (10 mL), BzCl (3.48 mL, 30.0 mmol, 3.0 equiv.) was added at 0 °C under an argon atmosphere. The mixture was allowed to warm to room temperature and stirred for 16 h. The reaction mixture was diluted with water and extracted with ethyl acetate. The combined organic phase was washed with

aqueous citric acid solution (10% v/v) and brine, dried over Na_2SO_4, filtered and concentrated. The benzoylated **5.15b** (5.6 g, 9.3 mmol, 93%) was obtained as a colorless syrup after purification by column chromatography (SiO_2, Hex/EtOAc 9:1). R_f = 0.41 (Hex/EtOAc 9:1). To a well stirred emulsion of **5.15b** (5.5 g, 9.1 mmol, 1.0 equiv.) in CH_2Cl_2/water (7:1, 48 mL), was added DDQ (1.3 g, 10.0 mmol, 1.1 equiv.) and the suspension was stirred at room temperature for 1.5 h protected from light. The mixture was diluted with CH_2Cl_2, washed with 10% aqueous $Na_2S_2O_3$ and saturated aqueous $NaHCO_3$ solution. The organic layer was dried over Na_2SO_4, filtered, concentrated and the residue was purified by column chromatography (SiO_2, Hex/EtOAc 9:1 to 3:1) to obtain the **4-OH-sugar** (3.8 g, 6.5 mmol, 71%) as a colorless solid. R_f = 0.41 (Hex/EtOAc 3:1). To a solution of **4-OH-sugar** (3.8 g, 8.2 mmol, 1.0 equiv.) and anhydrous pyridine (3.31 mL, 40.9 mmol, 5.0 equiv.) in anhydrous CH_2Cl_2 (60 mL) at 0 °C was added FmocCl (3.2 g, 1.5 mmol, 1.5 equiv.) followed by 4-DMAP (50 mg, 0.4 mmol, 0.05 equiv.) was added and the reaction mixture was stirred for two hours at 0 °C. Aqueous citric acid solution (30 mL) was added and the mixture was allowed to warm to room temperature. The aqueous phase was extracted with CH_2Cl_2 and the combined organic phase was dried over Na_2SO_4, filtered and concentrated. Compound **5.04b** (4.9 g, 7.1 mmol, 87%) was obtained as a white solid after purification by column chromatography (SiO_2, Hex/EtOAc 19:1 to 3:1).

R$_f$ = 0.69 (Hex/EtOAc 3:1). **^{1}H NMR** (600 MHz, $CDCl_3$): δ 8.10 – 8.05 (m, 2H), 7.79 (d, J = 7.5 Hz, 2H), 7.66 – 7.53 (m, 3H), 7.49 – 7.39 (m, 4H), 7.38 – 7.25 (m, 6H), 7.22 (q, J = 2.5 Hz, 3H), 7.13 (d, J = 8.2 Hz, 2H), 5.80 (dd, J = 3.3, 1.7 Hz, 1H), 5.50 (d, J = 1.8 Hz, 1H), 5.06 (t, J = 9.8 Hz, 1H), 4.65 (dd, J = 94.5, 12.1 Hz, 2H), 4.47 (d, J = 7.3 Hz, 2H), 4.42 (dd, J = 9.8, 6.2 Hz, 1H), 4.26 (t, J = 7.2 Hz, 1H), 4.01 (dd, J = 9.7, 3.3 Hz, 1H), 2.33 (s, 3H), 1.32 (d, J = 6.3 Hz, 3H) ppm. **^{13}C NMR** (151 MHz, $CDCl_3$): δ 165.8, 155.0, 143.5, 143.3, 141.5, 141.4, 138.3, 137.4, 133.5, 132.5, 130.1, 130.1, 129.7, 129.6, 128.6, 128.5, 128.1, 127.9, 127.3, 125.2, 125.2, 120.2, 86.6, 77.4, 75.0, 71.6, 70.9, 70.1, 67.7, 47.0, 21.3, 17.6 ppm. **[α]$_D$** -54.58 cm^{-1} (c 1, $CHCl_3$). **IR** (film): 3067, 2924, 1752, 1721, 1585, 1494, 1451, 1385, 1244, 1176, 1090, 988, 848, 758, 740, 709 cm^{-1}. **HRMS** (QToF): Calcd for $C_{42}H_{38}O_7SNa$ [M + Na]$^+$ 709.2230; found 709.2250.

6.5.3 Synthesis of Galactose Building Block 5.03

Ethyl 2-*O*-benzyl-3-*O*-(2-naphthalenylmethyl)-4,6-*O*-[(*S*)-phenylmethylene]-1-thio-β-D-galactopyranoside[154] (5.08)
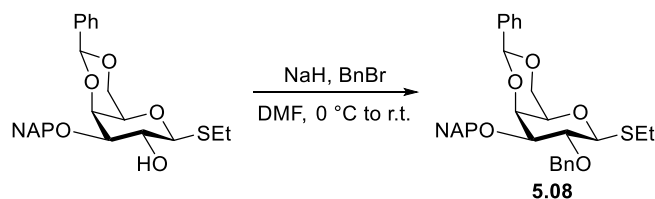
2-OH-galactose[154] (7.4 g, 16.4 mmol, 1.0 equiv.) was dissolved in anhydrous DMF (75 mL). The stirred solution was cooled to 0 °C and sodium hydride (1.5 g, 24.6 mmol; 60% dispersion in mineral oil, 2.3 equiv.) was added in small portions. After 30 min, benzyl bromide (1.3 mL, 37.7 mmol, 1.5 equiv.) was added dropwise. The reaction mixture was allowed to warm to room temperature and was stirred overnight. Methanol (10 mL) was added, the reaction mixture was stirred for 10 min and afterwards diluted with ethyl acetate (100 mL). The organic layer was washed with water (2 x 100 mL). The aqueous phase was extracted with ethyl acetate (2 x 100 mL). The combined organic phase was washed with water (100 mL), dried over Na_2SO_4 and concentrated. Product **5.08** (8.8 g, 16.2 mmol, **99%**) was obtained as a colorless solid after purification by column chromatography (SiO_2, Hex/EtOAc 3:1).

R$_f$ = 0.22 (Hex/EtOAc 3:1). **¹H NMR** (700 MHz, CDCl$_3$) δ 7.87 – 7.78 (m, 3H), 7.74 – 7.69 (m, 1H), 7.57 – 7.29 (m, 13H), 5.48 (s, 1H), 4.96 – 4.87 (m, 4H), 4.44 (d, *J* = 9.7 Hz, 1H), 4.30 (dd, *J* = 12.3, 1.8 Hz, 1H), 4.17 (d, *J* = 3.7 Hz, 1H), 3.96 – 3.90 (m, 2H), 3.65 (dd, *J* = 9.2, 3.5 Hz, 1H), 3.35 – 3.32 (m, 1H), 2.90 – 2.73 (m, 2H), 1.34 (t, *J* = 7.5 Hz, 3H) ppm. **¹³C NMR** (176 MHz, CDCl$_3$) δ 138.6, 138.1, 135.9, 133.4, 133.2, 129.2, 128.5, 128.5, 128.4, 128.3, 128.0, 127.9, 127.8, 126.7, 126.7, 126.3, 126.1, 126.0, 101.7, 84.6, 81.1, 77.1, 75.9, 74.2, 72.1, 69.9, 69.5, 24.0, 15.2 ppm. **HRMS** (QToF): Calcd for $C_{33}H_{34}O_5SNa$ [M + Na]⁺ 565.2019; found 565.2018.

Ethyl 4-*O*-benzoyl-2,6-bis-*O*-benzyl-3-*O*-(2-naphthalenylmethyl)-1-thio-β-D-galactopyranoside (5.09)
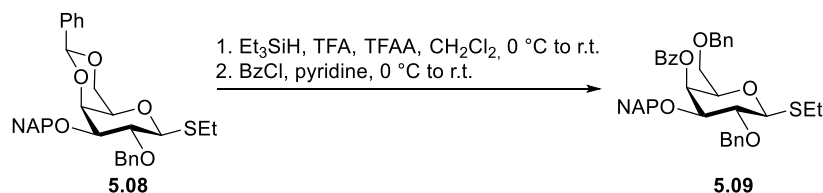
Compound **5.08** (2.0 g, 3.7 mmol, 1.0 equiv.) was co-evaporated with anhydrous toluene (2 x 3 mL), and dissolved in anhydrous CH_2Cl_2 (20 mL). Triethylsilane (3.5 mL, 22.1 mmol, 6.0 equiv.) and trifluoroacetic anhydride (0.52 mL, 3.7 mmol, 1.0 equiv.) were added and the solution was cooled to 0 °C. Trifluoroacetic acid (1.7 mL, 22.1 mmol, 6.0 equiv.) was added

dropwise. The mixture was allowed to warm to room temperature and was stirred for 5 h. The solution was diluted with CH_2Cl_2 and quenched with saturated aqueous $NaHCO_3$ (40 mL). The aqueous phase was extracted with CH_2Cl_2 (2 x 60 mL) and the combined organic phase was washed with water (60 mL), dried over Na_2SO_4, filtered and concentrated. **4-OH-galactose** (1.8 g, 3.3 mmol, 90%) was obtained as a colorless syrup after purification by column chromatography (SiO_2, Hex/EtOAc 3:1 to 1:1). R_f = 0.39 (Hex/EtOAc 1:1). **4-OH-galactose** (1.4 g, 2.6 mmol, 1.0 equiv.) was dissolved in pyridine (20 mL) and the solution was cooled to 0 °C. Benzoyl chloride (0.89 mL, 7.7 mmol, 3.0 equiv.) was added under an argon atmosphere. The reaction mixture was allowed to warm to room temperature and was stirred for 16 h. The reaction was quenched by addition of water and the aqueous layer was extracted with ethyl acetate. The combined organic phase was washed with 1.0 M HCl and brine, dried over Na_2SO_4, filtered and concentrated. Compound **5.09** (1.2 g, 1.8 mmol, 72%) was obtained as a colorless oil after purification by column chromatography (SiO_2, Hex/EtOAc 9:1 to 3:1).

R_f = 0.31 (Hex/EtOAc 3:1). **^{1}H NMR** (400 MHz, $CDCl_3$): δ 8.16 – 7.98 (m, 3H), 7.81 – 7.68 (m, 3H), 7.65 – 7.56 (m, 2H), 7.52 – 7.13 (m, 14H), 5.94 (dd, J = 3.3, 1.0 Hz, 1H), 5.02 (d, J = 11.6 Hz, 1H), 4.89 – 4.66 (m, 3H), 4.57 – 4.36 (m, 3H), 3.84 (d, J = 1.2 Hz, 1H), 3.77 (d, J = 3.3 Hz, 1H), 3.75 – 3.61 (m, 2H), 3.58 (d, J = 7.1 Hz, 1H), 2.78 – 2.66 (m, 2H), 1.34 (t, J = 7.5 Hz, 3H) ppm. **^{13}C NMR** (101 MHz, $CDCl_3$): δ 165.9, 138.2, 137.7, 135.4, 133.8, 133.3, 133.1, 130.3, 130.2, 130.0, 128.6, 128.5, 128.5, 128.2, 128.1, 127.9, 127.0, 126.3, 126.0, 125.9, 99.7, 85.6, 81.1, 77.9, 77.4, 76.2, 76.0, 73.9, 71.9, 68.4, 67.6, 25.1, 15.2 ppm. **HRMS** (QToF): Calcd for $C_{40}H_{40}O_6SNa$ [M + Na]$^+$ 671.2438; found 671.2488.

Ethyl 4-*O*-benzoyl-2,6-bis-*O*-benzyl-3-*O*-fluorenylmethoxycarbonyl-1-thio-β-D-galactopyranoside (5.03)
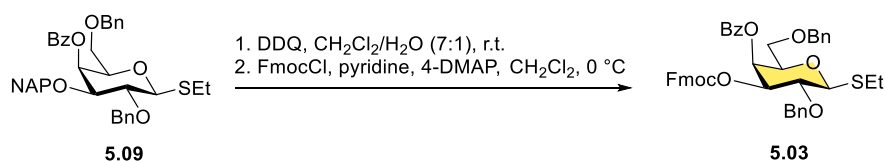
To a well stirred emulsion of **5.09** (1.8 g, 2.8 mmol, 1.0 equiv.) in CH_2Cl_2/water (7:1, 24 mL), was added DDQ (692 mg, 3.1 mmol, 1.1 equiv.) and the suspension was stirred at room temperature for 1.5 h protected from light. The mixture was diluted with CH_2Cl_2, washed with aqueous 10% $Na_2S_2O_3$ and saturated aqueous $NaHCO_3$ solution. The organic layer was dried over Na_2SO_4, filtered, concentrated and the residue was purified by column chromatography (SiO_2, Hex/EtOAc 9:1 to 3:1) to obtain the title compound (1.1 g, 2.2 mmol, 78%) as a colorless solid. R_f = 0.35 (Hex/EtOAc 3:1). To a solution of **4-OH-sugar** (1.1 g, 2.2 mmol, 1.0 equiv.) and anhydrous pyridine (0.87 mL, 10.8 mmol, 5.0 equiv.) in anhydrous CH_2Cl_2 (15 mL) at 0 °C

was added FmocCl (838 mg, 3.2 mmol, 1.5 equiv.) followed by 4-DMAP (13 mg, 0.11 mmol, 0.05 equiv.) and the reaction mixture was stirred for two hours at 0 °C. Aqueous citric acid solution (10 mL) was added and the mixture was allowed to warm to room temperature. The aqueous phase was extracted with CH_2Cl_2 and the combined organic phase was dried over Na_2SO_4, filtered and concentrated. Compound **5.03** (1.2 g, 1.6 mmol, 76%) was obtained as a white solid after purification by column chromatography (SiO_2, Hex/EtOAc 19:1 to 3:1).

R_f = 0.5 (Hex/EtOAc 3:1). **^{1}H NMR** (400 MHz, $CDCl_3$): δ 8.10 – 8.03 (m, 2H), 7.76 (ddt, J = 7.7, 1.9, 0.9 Hz, 2H), 7.63 (d, J = 7.4 Hz, 1H), 7.60 – 7.52 (m, 2H), 7.49 (t, J = 7.8 Hz, 2H), 7.44 – 7.31 (m, 4H), 7.31 – 7.12 (m, 10H), 5.90 (dd, J = 3.4, 1.1 Hz, 1H), 5.00 (dd, J = 9.6, 3.4 Hz, 1H), 4.88 (d, J = 10.5 Hz, 1H), 4.71 (d, J = 10.5 Hz, 1H), 4.66 – 4.56 (m, 2H), 4.39 (d, J = 12.0 Hz, 1H), 4.31 (t, J = 7.4 Hz, 1H), 4.19 (dd, J = 10.3, 8.3 Hz, 1H), 3.98 (td, J = 6.4, 1.1 Hz, 1H), 3.81 (t, J = 9.7 Hz, 1H), 3.59 (ddd, J = 33.9, 9.6, 6.4 Hz, 2H), 2.93 – 2.74 (m, 2H), 1.37 (t, J = 7.4 Hz, 3H) ppm. **^{13}C NMR** (101 MHz, $CDCl_3$): δ 165.77, 154.36, 143.97, 143.20, 141.42, 141.29, 137.75, 137.57, 133.52, 130.26, 129.56, 128.62, 128.47, 128.28, 127.99, 127.97, 127.94, 127.87, 127.85, 127.31, 127.23, 125.67, 125.34, 120.10, 85.56, 78.91, 76.29, 75.97, 75.90, 73.69, 70.48, 68.54, 68.03, 46.78, 25.37, 15.21 ppm. **[α]$_D$** 14.29 cm^{-1} (*c* 1, $CHCl_3$). **IR** (film): 3066, 2927, 2869, 1750, 1726, 1603, 1497, 1451, 1388, 1274, 1246, 1096, 1070, 1026, 984, 907, 758, 737, 697 cm^{-1}. **HRMS** (QToF): Calcd for $C_{44}H_{42}O_8SNa$ [M + Na]$^+$ 753.2493; found 753.2518.

6.5.4   Synthesis of Glucose Building Block 5.05

Ethyl 2-*O*-benzyl-4,6-*O*-[(*S*)-phenylmethylene]-1-thio-β-D-glucopyranoside[157] (5.16a)
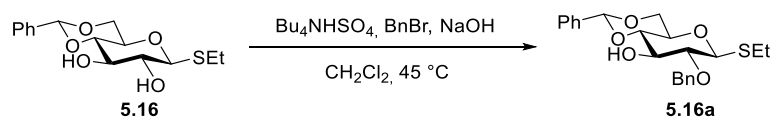
Tetrabutylammonium hydrogen sulfate (2.2 g, 6.4 mmol, 0.5 equiv.), benzyl bromide (1.68 mL, 14.1 mmol, 1.1 equiv., filtered using a short aluminium oxide column before use) and 5% aqueous NaOH (33 mL) was added to a stirred solution of ethyl 4,6-*O*-benzylidene-1-thio-β-D-glucopyranoside (4.0 g, 12.8 mmol, 1.0 equiv.) in CH_2Cl_2 (300 mL). The mixture was heated to 45 °C and was stirred for 8 h. The mixture was allowed to cool down to room temperature and the organic phase was separated from the aqueous phase. The aqueous phase was extracted with CH_2Cl_2 (2 x 100 mL) and the combined organic phase was washed with brine (100 mL), dried over Na_2SO_4, filtered and concentrated. 3-OH-galactose **5.16a** (2.6 g, 6.5 mmol, 50%) was obtained as a colorless solid after purification by column chromatography (SiO_2, toluene/EtOAc 95:5 to 9:1). All spectra are in accordance with literature spectra.

R_f = 0.42 (Toluene/EtOAc 9:1). **¹H NMR** (400 MHz, CDCl₃): δ 7.54 – 7.28 (m, 10H), 5.52 (s, 1H), 4.87 (dd, J = 68.7, 10.8 Hz, 2H), 4.57 (d, J = 9.8 Hz, 1H), 4.35 (dd, J = 10.4, 4.9 Hz, 1H), 3.89 (t, J = 8.8 Hz, 1H), 3.76 (t, J = 10.2 Hz, 1H), 3.56 (d, J = 9.3 Hz, 1H), 3.45 (d, J = 5.0 Hz, 1H), 3.38 (dd, J = 9.8, 8.3 Hz, 1H), 2.87 – 2.68 (m, 2H), 1.34 (t, J = 7.5 Hz, 3H) ppm. **HRMS** (QToF): Calcd for $C_{22}H_{26}O_5SNa$ [M + Na]⁺ 425.1393; found 425.1389.

Ethyl 3-*O*-benzoyl-2,4-bis-*O*-benzyl-1-thio-β-D-glucopyranoside (5.18)
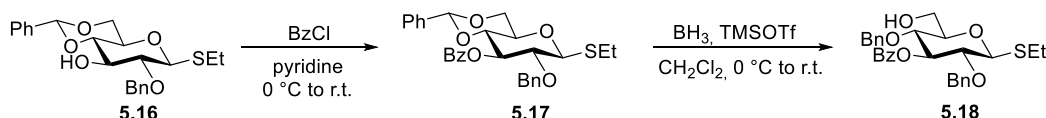
3-OH-Galactose **5.16a** (2.6 g, 6.5 mmol, 1.0 equiv.) was dissolved in pyridine (30 mL) and the solution was cooled to 0 °C. Benzoyl chloride (2.26 mL, 19.4 mmol, 3.0 equiv.) was added under an argon atmosphere. The reaction mixture was allowed to warm to room temperature and was stirred for 16 h. The reaction was quenched by addition of water and the aqueous layer was extracted with ethyl acetate (3 x 100 mL). The combined organic phase was washed with 1.0 M HCl and brine, dried over Na_2SO_4, filtered and concentrated. Compound **5.17** (3.1 g, 6.1 mmol, 95%) was obtained as a colorless oil after purification by column chromatography (SiO₂, Hex/EtOAc 9:1 to 3:1). R_f = 0.29 (Hex/EtOAc 9:1). Compound **5.17** (1.0 g, 2.0 mmol, 1.0 equiv.) was co-evaporated by anhydrous toluene and dried for 2 h at high vacuum. Then, it was dissolved in anhydrous CH_2Cl_2 (25 mL) and the mixture was stirred over activated molecular sieves (3 Å-AW) for 30 minutes at room temperature. The mixture was cooled to 0 °C and BH₃ (1 M solution in THF, 9.9 mL, 9.9 mmol, 5.0 equiv.) and TMSOTf (53 µL, 0.29 mmol, 0.15 equiv.) were added dropwise. The mixture was allowed to warm to room temperature and stirred under an argon atmosphere for 4 h. Et₃N (1 mL) was added followed by MeOH until the evolution of H₂ ceased. The mixture was concentrated and co-evaporated with MeOH (3 x 30 mL). 6-OH-sugar **5.18** (805 mg, 1.6 mmol, 80%) was obtained as a white solid after purification by column chromatography (SiO₂, Hex/EtOAc 3:1).

R_f = 0.18 (Hex/EtOAc 3:1). **¹H NMR** (600 MHz, CDCl₃): δ 8.02 – 7.97 (m, 2H), 7.61 – 7.55 (m, 1H), 7.48 – 7.41 (m, 2H), 7.20 – 7.07 (m, 10H), 5.58 (t, J = 9.2 Hz, 1H), 4.79 (d, J = 10.7 Hz, 1H), 4.62 (d, J = 9.7 Hz, 1H), 4.55 (s, 2H), 4.54 (d, J = 10.7 Hz, 1H), 3.92 (dd, J = 12.2, 2.6 Hz, 1H), 3.80 – 3.72 (m, 2H), 3.54 – 3.47 (m, 2H), 2.84 – 2.73 (m, 2H), 1.33 (t, J = 7.5 Hz, 3H) ppm. **¹³C NMR** (151 MHz, CDCl₃): δ 165.6, 137.4, 133.3, 130.1, 129.9, 128.6, 128.5, 128.4, 128.1, 127.9, 85.4, 79.5, 79.2, 78.0, 75.7, 75.1, 74.8, 62.0, 25.6, 15.3 ppm. **HRMS** (QToF): Calcd for $C_{29}H_{32}O_6SNa$ [M + Na]⁺ 531.1812; found 531.1830.

Ethyl 3-*O*-benzoyl-2,4-bis-*O*-benzyl-6-*O*-(2-chloroacetyl)-1-thio-β-ᴅ-glucopyranoside (5.05)

5.18 → **5.05**
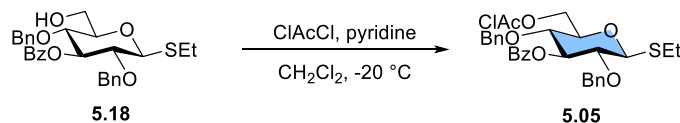
To a solution of 6-OH-sugar **5.18** (1.5 g, 2.9 mmol, 1.0 equiv.) and anhydrous pyridine (1.19 mL, 14.8 mmol, 5.0 equiv.) in anhydrous CH_2Cl_2 (20 mL) at -20 °C was added chloroacetyl chloride (0.47 mL, 5.9 mmol, 2.0 equiv.). The reaction was stirred for 10 min, aqueous citric acid solution (2 mL) was added and the mixture was allowed to warm to room temperature. Water was added and the aqueous phase was extracted with CH_2Cl_2 (3 x 50 mL). The combined organic phase was dried over Na_2SO_4, filtered and concentrated. Compound **5.05** (1.4 g, 2.4 mmol, 81%) was obtained as a light-yellow solid after purification by column chromatography (SiO_2, Hex/EtOAc 9:1 to 3:1).

R_f = 0.44 (Hex/EtOAc 3:1). **^{1}H NMR** (600 MHz, $CDCl_3$): δ 8.05 – 8.00 (m, 2H), 7.62 – 7.56 (m, 1H), 7.46 (t, J = 7.8 Hz, 2H), 7.20 (dd, J = 4.9, 1.9 Hz, 3H), 7.12 (dq, J = 5.5, 3.0 Hz, 7H), 5.59 (t, J = 8.8 Hz, 1H), 4.79 (d, J = 10.7 Hz, 1H), 4.64 – 4.51 (m, 3H), 4.48 – 4.43 (m, 2H), 4.29 (dd, J = 11.9, 4.6 Hz, 1H), 4.03 (q, J = 14.8 Hz, 2H), 3.68 (t, J = 6.4 Hz, 2H), 3.53 (t, J = 9.4 Hz, 1H), 2.77 (dtt, J = 20.1, 12.6, 7.4 Hz, 2H), 1.33 (t, J = 7.4 Hz, 3H) ppm. **^{13}C NMR** (151 MHz, $CDCl_3$): δ 167.1, 165.6, 137.3, 137.0, 133.4, 129.9, 128.7, 128.6, 128.5, 128.5, 128.4, 128.3, 127.9, 85.4, 79.3, 78.1, 76.5, 75.7, 75.1, 74.7, 64.8, 40.9, 25.6, 15.2 ppm. **[α]$_D$** 24.1 cm^{-1} (*c* 1, $CHCl_3$). **IR** (film): 3066, 2962, 2884, 1761, 1722, 1602, 1453, 1406, 1335, 1266, 1248, 1199, 1135, 1061, 1027, 998, 916, 805, 753, 700 cm^{-1}. **HRMS** (QToF): Calcd for $C_{31}H_{33}ClO_7SNa$ [M + Na]$^+$ 607.1528; found 607.1539.

6.6 Human Sera and Saliva Sample Collection and Characterization

6.6.1 General Information

Sera and saliva of periodontitis patients (infected (I), 16 people), recovered periodontitis patients (treated (T), 6 people) and parodontal healthy patients (healthy (H), 20 people) were provided by Prof. Dr. Henrik Domisch and used for the immunological evaluation of the synthesized glycans in glycan microarray experiments.

6.6.2 Sera Collection

The sera collection was conducted by Dr. Kim Stolte, Zahnklinik Charité Berlin. For the collection of sera, 5 mL venous blood per puncture was withdrawn using serum tubes (Vacuette, 5 mL CAT serum Sep Clot Activator, Greiner). After taking of the blood sample, the filled tubes rested vertically for 30 min at room temperature to ensure coagulation, followed by

centrifugation (15 minutes, 1300 x g). Afterwards, the serum was transfered to Eppendorf tubes and stored at -20 °C before use.

6.7 Glycan Microarrays

6.7.1 Printing of Microarray-Slides

Amine-terminated oligosaccharides were immobilized on commercial N-hydroxysuccinimide (NHS) ester-activated microarray slides (CodeLink Activated Slides; SurModics) using a piezoelectric microarray spotting device (S3; Scienion) such that 64 identical subarrays can be contained on each slide. Before the spotting, glycan solutions were prepared (0.1 mM, in 50 mM sodium phosphate buffer, pH 8.5). Slides were incubated in a humid chamber for 24 h at room temperature to complete coupling reactions. The next day, slides were quenched in 100 mM ethanolamine in 50 mM sodium phosphate buffer, pH 9, for one hour at room temperature. Afterwards, the slides were washed with deionized water (3 x), dried by centrifugation (300 x g, 5 min) and stored at 4 °C in a black box until use.

6.7.2 Glycan Microarray Experiments

The microarray slides with immobilized glycans were blocked with 1% BSA-PBS for one hour at room temperature. Afterwards, the slides were washed with PBS (3 x) and dried by centrifugation. A FlexWell 64 grid was applied and slides were incubated with human serum (dilution 1:10 in 1% BSA-PBS) and saliva (undiluted) in triplicate in a humid chamber for one hour at room temperature. Wells were washed with PBS-Tween (3 x) followed by incubation with fluorescence-labeled secondary antibody (Goat anti-Human IgG, Fc-AF 647, SouthernBiotech) in a light-protected humidity chamber for 60 minutes at room temperature. The slides were washed tree times with PBS-Tween (3 x). Then, the grids were removed and washed in a Petri dish with PBS-Tween for 2 minutes and rinsing (total 3 x) followed by washing with deionized water for 2 minutes and rinsing (total 3 x). The slides were dried by centrifugation (300 x g, 5 min). Afterwards, the slides were scanned with a GenePix 4300A microarray scanner (Molecular Devices, Sunnyvale, CA, USA). The Image analysis was carried out using GenePix Pro 7 software (Molecular Devices).

6.7.3 Statistical Analysis

Graphing and statistical analysis (two-sided unpaired t tests) were performed using OriginPro® 2021b.
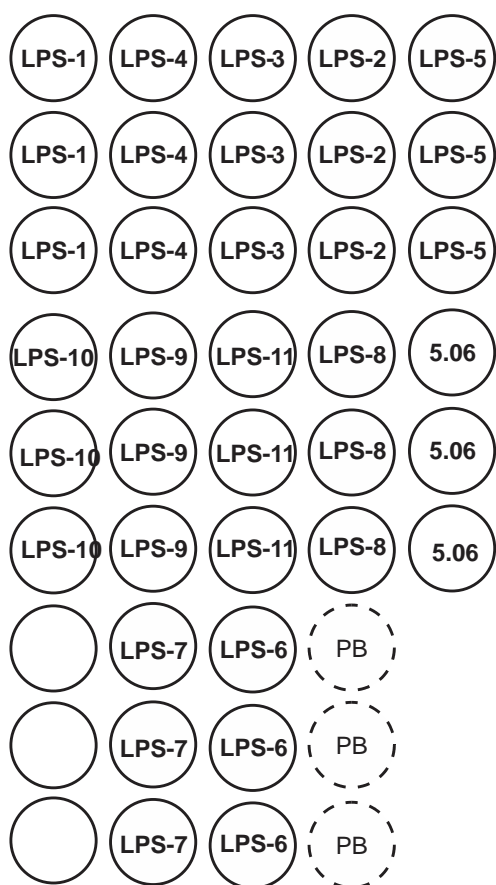
Scheme 1: Microarray printing pattern of *P. gingivalis* glycans **LPS1-11** and **5.06** using 0.1 mM printing concentration. PB – Printing buffer.

7   References

[1]   L. Petrus, M. A. Noordermeer, *Green Chem.* **2006**, *8*, 861-867.
[2]   R. A. Dwek, *Chem. Rev.* **1996**, *96*, 683-720.
[3]   M. A. Schmidt, L. W. Riley, I. Benz, *Trends Microb.* **2003**, *11*, 554-561.
[4]   A. D. McNaught, A. Wilkinson, IUPAC. Compendium of Chemical Terminology, 2nd ed. (the "Golden Book") **1997**.
[5]   S. Hanson, M. Best, M. C. Bryan, C.-H. Wong, *Trends Biochem. Sci.* **2004**, *29*, 656-663.
[6]   R. E. Reyes, C. R. González, R. C. Jiménez, M. O. Herrera, A. A. Andrade, D. Karunaratne, *The complex world of polysaccharides* **2012**.
[7]   a) H. S. Hahm, M. K. Schlegel, M. Hurevich, S. Eller, F. Schuhmacher, J. Hofmann, K. Pagel, P. H. Seeberger, *Proc. Natl. Acad. Sci. U.S.A.* **2017**, *114*, E3385; b) O. J. Plante, E. R. Palmacci, P. H. Seeberger, *Science* **2001**, *291*, 1523.
[8]   a) M. H. Caruthers, *Science* **1985**, *230*, 281-285; b) S. A. Scaringe, F. E. Wincott, M. H. Caruthers, *J. Am. Chem. Soc.* **1998**, *120*, 11820-11821.
[9]   R. Merrifield, *Science* **1965**, *150*, 178-185.
[10]   Y. Zhu, M. Delbianco, P. H. Seeberger, *J. Am. Chem. Soc.* **2021**, *143*, 9758-9768.
[11]   M. Guberman, M. Bräutigam, P. H. Seeberger, *Chem. Sci.* **2019**, *10*, 5634-5640.
[12]   H. S. Hahm, C.-F. Liang, C.-H. Lai, R. J. Fair, F. Schuhmacher, P. H. Seeberger, *J. Org. Chem.* **2016**, *81*, 5866-5877.
[13]   a) M. W. Weishaupt, S. Matthies, M. Hurevich, C. L. Pereira, H. S. Hahm, P. H. Seeberger, *Beilstein J. Org. Chem.* **2016**, *12*, 1440-1446; b) J. Louçano, P. Both, A. Marchesi, L. del Bino, R. Adamo, S. Flitsch, M. Salwiczek, *RSC Adv.* **2020**, *10*, 23668-23674.
[14]   G. Fittolani, E. Shanina, M. Guberman, P. H. Seeberger, C. Rademacher, M. Delbianco, *Angew. Chem. Int. Ed.* **2021**, *60*, 13302-13309.
[15]   a) H. S. Hahm, F. Broecker, F. Kawasaki, M. Mietzsch, R. Heilbronn, M. Fukuda, P. H. Seeberger, *Chem* **2017**, *2*, 114-124; b) T. Tyrikos-Ergas, E. T. Sletten, J.-Y. Huang, P. H. Seeberger, M. Delbianco, *Chem. Sci.* **2022**, *13*, 2115-2120.
[16]   a) P. Dallabernardina, F. Schuhmacher, P. H. Seeberger, F. Pfrengle, *Org. Biomol. Chem.* **2016**, *14*, 309-313; b) M. P. Bartetzko, F. Pfrengle, *ChemBioChem* **2019**, *20*, 877-885; c) F. Pfrengle, in *The Plant Cell Wall*, Springer, **2020**, 503-512.
[17]   N. M. Sabbavarapu, P. H. Seeberger, *J. Org. Chem.* **2021**, *86*, 7280-7287.
[18]   A. Fleming, *Brit. Med. J.* **1941**, *2*, 386.
[19]   J. Needham, *Science and civilisation in China, Vol. 5*, Cambridge University Press, **1974**.
[20]   D. Baxby, *Vaccine* **1999**, *17*, 301-307.
[21]   W. H. Assembly, *Assignment Child.* **1983**, 119-122.
[22]   A. J. Pollard, E. M. Bijker, *Nat. Rev. Immunol.* **2021**, *21*, 83-100.

[23]   a) A. O. Tzianabos, R. W. Finberg, Y. Wang, M. Chan, A. B. Onderdonk, H. J. Jennings, D. L. Kasper, *J. Biol. Chem.* **2000**, *275*, 6733-6740; b) B. Schumann, R. Pragani, C. Anish, C. L. Pereira, P. H. Seeberger, *Chem. Sci.* **2014**, *5*, 1992-2002.

[24]   a) M. Patel, C. k. Lee, *Cochrane Database Syst. Rev.* **2005**; b) S. Moberley, J. Holden, D. P. Tatham, R. M. Andrews, *Cochrane Database Syst. Rev.* **2013**.

[25]   E. Malito, B. Bursulaya, C. Chen, P. L. Surdo, M. Picchianti, E. Balducci, M. Biancucci, A. Brock, F. Berti, M. J. Bottomley, *Proc. Natl. Acad. Sci. U.S.A.* **2012**, *109*, 5229-5234.

[26]   A. A. Lindberg, *Vaccine* **1999**, *17*, S28-S36.

[27]   C. L. Trotter, J. McVernon, M. E. Ramsay, C. G. Whitney, E. K. Mulholland, D. Goldblatt, J. Hombach, M.-P. Kieny, *Vaccine* **2008**, *26*, 4434-4445.

[28]   F. S. Hassane, A. Phalipon, M. Tanguy, C. Guerreiro, F. Bélot, B. Frisch, L. A. Mulard, F. Schuber, *Vaccine* **2009**, *27*, 5419-5426.

[29]   X. Liu, S. Siegrist, M. Amacker, R. Zurbriggen, G. Pluschke, P. H. Seeberger, *ACS Chem. Biol.* **2006**, *1*, 161-164.

[30]   D. Safari, M. Marradi, F. Chiodo, H. A. Th Dekker, Y. Shan, R. Adamo, S. Oscarson, G. T. Rijkers, M. Lahmann, J. P. Kamerling, *Nanomed. J.* **2012**, *7*, 651-662.

[31]   P. H. Seeberger, *Chem. Rev.* **2021**, *121*, 3598-3626.

[32]   A. Geissner, C. Anish, P. H. Seeberger, *Curr. Opin. Chem. Biol.* **2014**, *18*, 38-45.

[33]   S. F. Ahmed, A. A. Quadeer, M. R. McKay, *Viruses* **2020**, *12*, 254.

[34]   K. M. Matz, A. Marzi, H. Feldmann, *Expert Rev.Vaccines* **2019**, *18*, 1229-1242.

[35]   J. Danglad-Flores, S. Leichnitz, E. T. Sletten, A. Abragam Joseph, K. Bienert, K. Le Mai Hoang, P. H. Seeberger, *J. Am. Chem. Soc.* **2021**, *143*, 8893-8901.

[36]   E. T. Sletten, J. Danglad-Flores, S. Leichnitz, A. Abragam Joseph, P. H. Seeberger, *Carbohydr. Res.* **2022**, *511*, 108489.

[37]   a) B. Ghosh, S. S. Kulkarni, *Chem.: Asian J.* **2020**, *15*, 450-462; b) M. Guberman, P. H. Seeberger, *J. Am. Chem. Soc.* **2019**, *141*, 5581-5592.

[38]   P. Klán, T. Solomek, C. G. Bochet, A. Blanc, R. Givens, M. Rubina, V. Popik, A. Kostikov, J. Wirz, *Chem. Rev.* **2013**, *113*, 119-191.

[39]   A. M. Smith, M. C. Mancini, S. Nie, *Nat. Nanotechnol.* **2009**, *4*, 710-711.

[40]   J. Zhao, S. Lin, Y. Huang, J. Zhao, P. R. Chen, *J. Am. Chem. Soc.* **2013**, *135*, 7410-7413.

[41]   J. S. Katz, J. A. Burdick, *Macromol. Biosci.* **2010**, *10*, 339-348.

[42]   a) J. H. Kaplan, G. Ellis-Davies, *Proc. Natl. Acad. Sci. U.S.A.* **1988**, *85*, 6571-6575; b) J. Engels, E. J. Schlaeger, *J. Med. Chem.* **1977**, *20*, 907-911.

[43]   C.-H. Park, R. S. Givens, *J. Am. Chem. Soc.* **1997**, *119*, 2453-2463.

[44]   A. J. Ackmann, J. M. Fréchet, *Chem. Commun.* **1996**, 605-606.

[45]   J. C. Sheehan, R. M. Wilson, *J. Am. Chem. Soc.* **1964**, *86*, 5277-5281.

[46]   S. Arumugam, V. V. Popik, *J. Am. Chem. Soc.* **2009**, *131*, 11892-11899.

[47] L. Zayat, M. G. Noval, J. Campi, C. I. Calero, D. J. Calvo, R. Etchenique, *ChemBioChem* **2007**, *8*, 2035-2038.

[48] P. Stacko, P. Šebej, A. T. Veetil, P. Klán, *Org. Lett.* **2012**, *14*, 4918-4921.

[49] a) J. P. Olson, M. R. Banghart, B. L. Sabatini, G. C. Ellis-Davies, *J. Am. Chem. Soc.* **2013**, *135*, 15948-15954; b) L. Fournier, C. Gauron, L. Xu, I. Aujard, T. Le Saux, N. Gagey-Eilstein, S. Maurin, S. Dubruille, J.-B. Baudin, D. Bensimon, *ACS Chem. Biol.* **2013**, *8*, 1528-1536.

[50] a) J. A. Peterson, C. Wijesooriya, E. J. Gehrmann, K. M. Mahoney, P. P. Goswami, T. R. Albright, A. Syed, A. S. Dutton, E. A. Smith, A. H. Winter, *J. Am. Chem. Soc,* **2018**, *140*, 7343-7346; b) T. Slanina, P. Shrestha, E. Palao, D. Kand, J. A. Peterson, A. S. Dutton, N. Rubinstein, R. Weinstain, A. H. Winter, P. Klán, *J. Am. Chem. Soc,* **2017**, *139*, 15168-15175; c) D. Kand, P. Liu, M. X. Navarro, L. J. Fischer, L. Rousso-Noori, D. Friedmann-Morvinski, A. H. Winter, E. W. Miller, R. Weinstain, *J. Am. Chem. Soc,* **2020**, *142*, 4970-4974; d) P. Shrestha, K. C. Dissanayake, E. J. Gehrmann, C. S. Wijesooriya, A. Mukhopadhyay, E. A. Smith, A. H. Winter, *J. Am. Chem. Soc.* **2020**, *142*, 15505-15512; e) J. A. Peterson, D. Yuan, A. H. Winter, *J. Org. Chem.* **2021**, *86*, 9781-9787.

[51] a) A. Barattucci, C. M. A. Gangemi, A. Santoro, S. Campagna, F. Puntoriero, P. Bonaccorsi, *Org. Biomol. Chem.* **2022**, *20*, 2742-2763; b) C. Uriel, C. Permingeat, J. Ventura, E. Avellanal-Zaballa, J. Bañuelos, I. García-Moreno, A. M. Gómez, J. C. Lopez, *Eur. J. Chem.* **2020**, *26*, 5388-5399.

[52] M. Guberman, P. H. Seeberger, *J. Am. Chem. Soc.* **2019**, *141*, 5581-5592.

[53] S. Eller, M. Collot, J. Yin, H. S. Hahm, P. H. Seeberger, *Angew. Chem. Int. Ed.* **2013**, *52*, 5858-5861.

[54] Y. Yu, A. Kononov, M. Delbianco, P. H. Seeberger, *Chem. Eur. J.* **2018**, *24*, 6075-6078.

[55] a) K. Ágoston, G. M. Watt, P. Fügedi, *Tetrahedron Lett.* **2015**, *56*, 5010-5012; b) C.-H. Wong, X.-S. Ye, Z. Zhang, *J. Am. Chem. Soc.* **1998**, *120*, 7137-7138; c) F. Compostella, S. Ronchi, L. Panza, S. Mariotti, L. Mori, G. De Libero, F. Ronchetti, *Chem. Eur. J.* **2006**, *12*, 5587-5595; d) W. Muramatsu, K. Mishiro, Y. Ueda, T. Furuta, T. Kawabata, *Eur. J. Org. Chem.* **2010**, *2010*, 827-831.

[56] P. J. Garegg, T. Iversen, S. Oscarson, *Carbohydr. Res.* **1976**, *50*, C12-C14.

[57] K. Ágoston, G. M. Watt, P. Fügedi, *Tetrahedron Lett.* **2015**, *56*, 5010-5012.

[58] a) A. G. Volbeda, H. A. V. Kistemaker, H. S. Overkleeft, G. A. van der Marel, D. V. Filippov, J. D. C. Codée, *J. Org. Chem.* **2015**, *80*, 8796-8806; b) Y. Li, B. Roy, X. Liu, *Chem. Commun.* **2011**, *47*, 8952-8954.

[59] D. Schmidt, F. Schuhmacher, A. Geissner, P. H. Seeberger, F. Pfrengle, *Chem. Eur. J.* **2015**, *21*, 5709-5713.

[60] T. Hansen, H. Elferink, J. M. A. van Hengst, K. J. Houthuijs, W. A. Remmerswaal, A. Kromm, G. Berden, S. van der Vorm, A. M. Rijs, H. S. Overkleeft, D. V. Filippov, F. P. J. T. Rutjes, G. A. van der Marel, J.

Martens, J. Oomens, J. D. C. Codée, T. J. Boltje, *Nat. Commun.* **2020**, *11*, 2664.

[61] R. Kurucz, P. H. Seeberger, D. Varón Silva, in *Encyclopedia of Malaria* (Eds.: M. Hommel, P. G. Kremsner), Springer New York, New York, NY, **2021**, pp. 1-13.

[62] S. Lin, T. L. Lowary, *Org. Lett.* **2020**, *22*, 7645-7649.

[63] a) V. N. Thota, M. J. Ferguson, R. P. Sweeney, T. L. Lowary, *Angew. Chem. Int. Ed.* **2018**, *57*, 15592-15596; b) L. Wang, M. Dong, T. L. Lowary, *J. Org. Chem.* **2015**, *80*, 2767-2780.

[64] S. S. Kulkarni, C.-C. Wang, N. M. Sabbavarapu, A. R. Podilapu, P.-H. Liao, S.-C. Hung, *Chem. Rev.* **2018**, *118*, 8025-8104.

[65] Y. Feng, J. Wu, G. Chen, Y. Chai, *Org. Lett.* **2020**, *22*, 2564-2568.

[66] A. Das, N. Jayaraman, *Carbohydr. Res.* **2021**, *508*, 108404.

[67] J. Wang, Y. Feng, T. Sun, Q. Zhang, Y. Chai, *J. Org. Chem.* **2022**, *87*, 3402-3421.

[68] a) M. M. Nielsen, C. M. Pedersen, *Chem. Rev.* **2018**, *118*, 8285-8358; b) E. Söderberg, J. Westman, S. Oscarson, *J. Carbohydr. Chem.* **2001**, *20*, 397-410.

[69] a) H. Shimizu, Y. Yoshimura, H. Hinou, S.-I. Nishimura, *Tetrahedron* **2008**, *64*, 10091-10096; b) N. Ferlin, L. Duchet, J. Kovensky, E. Grand, *Carbohydr. Res.* **2008**, *343*, 2819-2821.

[70] M. A. Rosenthal, D. Rischin, G. McArthur, K. Ribbons, B. Chong, J. Fareed, G. Toner, M. D. Green, R. L. Basser, *Ann. Oncol.* **2002**, *13*, 770-776.

[71] K. Greis, C. Kirschbaum, S. Leichnitz, S. Gewinner, W. Schöllkopf, G. von Helden, G. Meijer, P. H. Seeberger, K. Pagel, *Org. Lett.* **2020**, *22*, 8916-8919.

[72] H. S. Hahm, M. Hurevich, P. H. Seeberger, *Nat. Commun.* **2016**, *7*, 12482.

[73] a) B. S. Komarova, M. V. Orekhova, Y. E. Tsvetkov, N. E. Nifantiev, *Carbohydr. Res.* **2014**, *384*, 70-86; b) Z. Li, L. Zhu, J. Kalikanda, *Tetrahedron Lett.* **2011**, *52*, 5629-5632; c) K. Fukase, Y. Nakai, T. Kanoh, S. Kusumoto, *Synlett* **1998**, *1998*, 84-86; d) A. Demchenko, T. Stauch, G.-J. Boons, *Synlett* **1997**, *1997*, 818-820; e) S. Chatterjee, S. Moon, F. Hentschel, K. Gilmore, P. H. Seeberger, *J. Am. Chem. Soc.* **2018**, *140*, 11942-11953.

[74] E. Mucha, A. I. González Flórez, M. Marianski, D. A. Thomas, W. Hoffmann, W. B. Struwe, H. S. Hahm, S. Gewinner, W. Schöllkopf, P. H. Seeberger, G. von Helden, K. Pagel, *Angew. Chem. Int. Ed.* **2017**, *56*, 11248-11251.

[75] E. Mucha, M. Marianski, F.-F. Xu, D. A. Thomas, G. Meijer, G. von Helden, P. H. Seeberger, K. Pagel, *Nat. Commun.* **2018**, *9*, 4174.

[76] M. Marianski, E. Mucha, K. Greis, S. Moon, A. Pardo, C. Kirschbaum, D. A. Thomas, G. Meijer, G. von Helden, K. Gilmore, P. H. Seeberger, K. Pagel, *Angew. Chem. Int. Ed.* **2020**, *59*, 6166-6171.

[77] T. Hansen, H. Elferink, J. M. A. van Hengst, K. J. Houthuijs, W. A. Remmerswaal, A. Kromm, G. Berden, S. van der Vorm, A. M. Rijs, H. S.

Overkleeft, D. V. Filippov, F. Rutjes, G. A. van der Marel, J. Martens, J. Oomens, J. D. C. Codee, T. J. Boltje, *Nat. Commun.* **2020**, *11*, 2664.

[78] S. van der Vorm, T. Hansen, J. M. A. van Hengst, H. S. Overkleeft, G. A. van der Marel, J. D. C. Codee, *Chem. Soc. Rev.* **2019**, *48*, 4688-4706.

[79] M. Marianski, E. Mucha, K. Greis, S. Moon, A. Pardo, C. Kirschbaum, D. A. Thomas, G. Meijer, G. von Helden, K. Gilmore, P. H. Seeberger, K. Pagel, *Angew. Chem. Int. Ed.* **2020**, *59*, 6166-6171.

[80] a) E. Mucha, A. Stuckmann, M. Marianski, W. B. Struwe, G. Meijer, K. Pagel, *Chem. Sci.* **2019**, *10*, 1272-1284; b) M. Grabarics, M. Lettow, C. Kirschbaum, K. Greis, C. Manz, K. Pagel, *Chem. Rev.* **2021**.

[81] K. Kappler, T. Hennet, *Genes Immun.* **2020**, *21*, 224-239.

[82] a) X. Zou, C. Qin, C. L. Pereira, G. Tian, J. Hu, P. H. Seeberger, J. Yin, *Chem. Eur. J.* **2018**, *24*, 2868-2872; b) N. Paramonov, D. Bailey, M. Rangarajan, A. Hashim, G. Kelly, M. A. Curtis, E. F. Hounsell, *Eur. J. Biochem.* **2001**, *268*, 4698-4707.

[83] I. V. Alabugin, M. Manoharan, *J. Org. Chem.* **2004**, *69*, 9011-9024.

[84] R. L. Kreeger, P. R. Menard, E. A. Sans, H. Shechter, *Tetrahedron Lett.* **1985**, *26*, 1115-1118.

[85] R. D. Chambers, in *Fluorine in Organic Chemistry*, **2004**, pp. 122-136.

[86] a) M. Collot, J. Savreux, J.-M. Mallet, *Tetrahedron* **2008**, *64*, 1523-1535; b) Z. Li, J. C. Gildersleeve, *J. Am. Chem. Soc.* **2006**, *128*, 11612-11619.

[87] C. Li, Y. Sun, J. Zhang, Z. Zhao, G. Yu, H. Guan, *Carbohydr. Res.* **2013**, *376*, 15-23.

[88] J. R. Falck, J. Yu, H.-S. Cho, *Tetrahedron Lett.* **1994**, *35*, 5997-6000.

[89] G. S. Forman, A. E. McConnell, R. P. Tooze, W. Janse van Rensburg, W. H. Meyer, M. M. Kirk, C. L. Dwyer, D. W. Serfontein, *Organometallics* **2005**, *24*, 4528-4542.

[90] Z. Rappoport, M. Frankel, *CRC handbook of tables for organic compound identification*, **1967**.

[91] L. Eberson, M. P. Hartshorn, O. Persson, *Journal of the Chemical Society, Perkin Transactions 2* **1995**, 1735-1744.

[92] C. Alex, A. V. Demchenko, *Chem. Rec.* **2021**, *21*, 3278-3294.

[93] Y. Zhang, H. He, Z. Chen, Y. Huang, G. Xiang, P. Li, X. Yang, G. Lu, G. Xiao, *Angew. Chem. Int. Ed.* **2021**, *133*, 12705-12714.

[94] a) Ö. Yilmaz, *Microbiology (Reading, England)* **2008**, *154*, 2897; b) F. Mei, M. Xie, X. Huang, Y. Long, X. Lu, X. Wang, L. Chen, *Pathogens* **2020**, *9*, 944.

[95] R. P. Darveau, G. Hajishengallis, M. A. Curtis, *J. Dent. Res.* **2012**, *91*, 816-820.

[96] T. Maekawa, J. L. Krauss, T. Abe, R. Jotwani, M. Triantafilou, K. Triantafilou, A. Hashim, S. Hoch, M. A. Curtis, G. Nussbaum, *Cell Host Microbe* **2014**, *15*, 768-778.

[97] A. Chopra, S. G. Bhat, K. Sivaraman, *J. Oral Microbiol.* **2020**, *12*, 1801090.

[98] C. O. Igboin, A. L. Griffen, E. J. Leys, *J. Clin. Microbiol.* **2009**, *47*, 3073-3081.

[99]   a) M. L. Laine, A. J. Van Winkelhoff, *Oral Microbiology and Immunology* **1998**, *13*, 322-325; b) S. Jain, R. P. Darveau, *Periodontol. 2000* **2010**, *54*, 53-70.

[100]   M. Enersen, K. Nakano, A. Amano, *J. Oral Microbiol.* **2013**, *5*, 20265.

[101]   E. Jeong, J.-Y. Lee, S.-J. Kim, J. Choi, *J. Periodontal Res.* **2012**, *47*, 811-816.

[102]   W. Xu, W. Zhou, H. Wang, S. Liang, *Adv. Protein Chem. Struct. Biol.* **2020**, *120*, 45-84.

[103]   a) M. J. Gui, S. G. Dashper, N. Slakeski, Y.-Y. Chen, E. C. Reynolds, *Mol. Oral Microbiol.* **2016**, *31*, 365-378; b) Z. Zhang, D. Liu, S. Liu, S. Zhang, Y. Pan, *Front. Cell. Infect. Microbiol.* **2021**, *10*.

[104]   M. Gui, S. Dashper, N. Slakeski, Y. Y. Chen, E. Reynolds, *Mol. Oral Microbiol.* **2016**, *31*, 365-378.

[105]   P. E. Petersen, H. Ogawa, *Periodontol. 2000* **2012**, *60*, 15-39.

[106]   H. N. Newman, *J. Dent. Res.* **1996**, *75*, 1912-1919.

[107]   a) L. Winning, G. J. Linden, *BDJ Team* **2015**, *2*, 15163; b) F. Q. Bui, C. L. C. Almeida-da-Silva, B. Huynh, A. Trinh, J. Liu, J. Woodward, H. Asadi, D. M. Ojcius, *Biomed. J.* **2019**, *42*, 27-35.

[108]   a) L. Forner, T. Larsen, M. Kilian, P. Holmstrup, *Journal of Clinical Periodontology* **2006**, *33*, 401-407; b) E. Berggreen, H. Wiig, *J. Dent. Res.* **2013**, *92*, 1074-1080.

[109]   A. Kriauciunas, A. Gleiznys, D. Gleiznys, G. Janužis, *Cureus* **2019**, *11*.

[110]   a) E. V. Kozarov, B. R. Dorn, C. E. Shelburne, W. A. Dunn, A. Progulske-Fox, *Arterioscler. Thromb. Vasc. Biol.* **2005**, *25*, e17-e18; b) M. Benedyk, P. M. Mydel, N. Delaleu, K. Płaza, K. Gawron, A. Milewska, K. Maresz, J. Koziel, K. Pyrc, J. Potempa, *J. Innate Immun.* **2016**, *8*, 185-198; c) K. Yamatake, M. Maeda, T. Kadowaki, R. Takii, T. Tsukuba, T. Ueno, E. Kominami, S. Yokota, K. Yamamoto, *Infect. Immun.* **2007**, *75*, 2090-2100; d) J. Gnanasekaran, A. Binder Gallimidi, E. Saba, K. Pandi, L. Eli Berchoer, E. Hermano, S. Angabo, H. a. Makkawi, A. Khashan, A. Daoud, M. Elkin, G. Nussbaum, *Cancers* **2020**, *12*, 2331; e) A. R. El-Awady, B. Miles, E. Scisci, Z. B. Kurago, C. D. Palani, R. M. Arce, J. L. Waller, C. A. Genco, C. Slocum, M. Manning, P. V. Schoenlein, C. W. Cutler, *PLOS Pathogens* **2015**, *11*, e1004647; f) S. S. Dominy, C. Lynch, F. Ermini, M. Benedyk, A. Marczyk, A. Konradi, M. Nguyen, U. Haditsch, D. Raha, C. Griffin, L. J. Holsinger, S. Arastu-Kapur, S. Kaba, A. Lee, M. I. Ryder, B. Potempa, P. Mydel, A. Hellvard, K. Adamowicz, H. Hasturk, G. D. Walker, E. C. Reynolds, R. L. M. Faull, M. A. Curtis, M. Dragunow, J. Potempa, *Sci. Adv.* **2019**, *5*, eaau3333.

[111]   L. L. Humphrey, R. Fu, D. I. Buckley, M. Freeman, M. Helfand,   *J. Gen. Intern. Med.* **2008**, *23*, 2079.

[112]   A. Burns, S. Iliffe, *BMJ* **2009**, *338*, b158.

[113]   G. Livingston, A. Sommerlad, V. Orgeta, S. G. Costafreda, J. Huntley, D. Ames, C. Ballard, S. Banerjee, A. Burns, J. Cohen-Mansfield, C. Cooper, N. Fox, L. N. Gitlin, R. Howard, H. C. Kales, E. B. Larson, K. Ritchie, K. Rockwood, E. L. Sampson, Q. Samus, L. S. Schneider, G. Selbæk, L. Teri, N. Mukadam, *The Lancet* **2017**, *390*, 2673-2734.

[114] I. Olsen, S. K. Singhrao, *J. Oral Microbiol.* **2020**, *12*, 1820834.

[115] I. Olsen, M. A. Taubman, S. K. Singhrao, *J. Oral Microbiol.* **2016**, *8*, 33029.

[116] S. G. de Aquino, S. Abdollahi-Roodsaz, M. I. Koenders, F. A. J. van de Loo, G. J. M. Pruijn, R. J. Marijnissen, B. Walgreen, M. M. Helsen, L. A. van den Bersselaar, R. S. de Molon, M. J. A. Campos, F. Q. Cunha, J. A. Cirelli, W. B. van den Berg, *J. Immunol.* **2014**, *192*, 4103.

[117] R. de Oliveira Ferreira, R. de Brito Silva, M. B. Magno, A. P. C. P. S. Carvalho Almeida, N. C. F. Fagundes, L. C. Maia, R. R. Lima, *Ther. Adv. Musculoskelet. Dis.* **2019**, *11*, 1759720X19858514.

[118] S. Kaur, R. Bright, S. M. Proudman, P. M. Bartold, *Seminars in Arthritis and Rheumatism* **2014**, *44*, 113-122.

[119] a) D. Polak, A. Wilensky, G. N. Antonoglou, L. Shapira, M. Goldstein, C. Martin, *J. Clin. Periodontol.* **2020**, *47*, 303-319; b) L. Nibali, V. P. Koidou, M. Nieri, L. Barbato, U. Pagliaro, F. Cairo, *J. Clin. Periodontol.* **2020**, *47*, 320-351; c) E. Ertugal, **2017**; dP. J. Hanes, J. P. Purvis, *Ann. Periodontol.* **2003**, *8*, 79-98.

[120] a) M. Madan, B. Bishayi, M. Hoge, E. Messas, S. Amar, *Atherosclerosis* **2007**, *190*, 62-72; b) S. Amar, S.-c. Wu, M. Madan, *J. Immunol. Res.* **2009**, *182*, 1584.

[121] T. Guevara, A. Rodríguez-Banqueri, A. M. Lasica, M. Ksiazek, B. A. Potempa, J. Potempa, F. X. Gomis-Rüth, *Sci. Rep.* **2019**, *9*, 4935.

[122] a) M. Li, Y. Wang, Y. Sun, H. Cui, S. J. Zhu, H.-J. Qiu, Immunol. Lett. **2020**, *217*, 116-125; b) Y. Shimizu, T. Iwasaki, T. Tajima, E. Yuba, K. Kono, S. Watarai, *J. Vet. Med. Sci.* **2016**, 16-0338; c) R. Nakao, H. Hasegawa, B. Dongying, M. Ohnishi, H. Senpuku, *Vaccine* **2016**, *34*, 4626-4634; d) R. Nakao, H. Hasegawa, K. Ochiai, S. Takashiba, A. Ainai, M. Ohnishi, H. Watanabe, H. Senpuku, *PloS one* **2011**, *6*, e26163; e) P.-F. Liu, W. Shi, W. Zhu, J. W. Smith, S.-L. Hsieh, R. L. Gallo, C.-M. Huang, *Vaccine* **2010**, *28*, 3496-3505; f) V. Vaernewyck, B. Arzi, N. N. Sanders, E. Cox, B. Devriendt, *Front. Immunol.* **2021**, *12*.

[123] M. W. Russell, P. L. Ogra, *Mucosal Vaccines* **2020**, 3-17.

[124] a) Y. Koizumi, T. Kurita-Ochiai, S. Oguchi, M. Yamamoto, *Infect. Immun.* **2008**, *76*, 2958-2965; b) M. Hagiwara, T. Kurita-Ochiai, R. Kobayashi, T. Hashizume-Takizawa, K. Yamazaki, M. Yamamoto, *J. Dent. Res.* **2014**, *93*, 382-387.

[125] M. F. Haurat, J. Aduse-Opoku, M. Rangarajan, L. Dorobantu, M. R. Gray, M. A. Curtis, M. F. Feldman, *J. Biol. Chem.* **2011**, *286*, 1269-1276.

[126] C. R. H. Raetz, C. Whitfield, *Annu. Rev. Biochem.* **2002**, *71*, 635-700.

[127] N. Paramonov, D. Bailey, M. Rangarajan, A. Hashim, G. Kelly, M. A. Curtis, E. F. Hounsell, *FEBS J.* **2001**, *268*, 4698-4707.

[128] T. Ogawa, Y. Kusumoto, S. Hamada, J. R. McGhee, H. Kiyono, *Clin. Exp. Immunol.* **1990**, *82*, 318-325.

[129] M. Marianski, E. Mucha, K. Greis, S. Moon, A. Pardo, C. Kirschbaum, D. A. Thomas, G. Meijer, G. von Helden, K. Gilmore, P. H. Seeberger, K. Pagel, *Angew. Chem. Int. Ed.* **2020**, *59*, 6166-6171.

[130] I. C. Lee, M. M. L. Zulueta, C.-R. Shie, S. D. Arco, S.-C. Hung, *Org. Biomol. Chem.* **2011**, *9*, 7655-7658.

[131] O. T. Tuck, E. T. Sletten, J. Danglad-Flores, P. H. Seeberger, *Angew. Chem. Int. Ed.* **2022**, *61*, e202115433.

[132] M. P. Bartetzko, F. Schuhmacher, H. S. Hahm, P. H. Seeberger, F. Pfrengle, *Org. Lett.* **2015**, *17*, 4344-4347.

[133] J. Danglad-Flores, S. Leichnitz, E. T. Sletten, A. Abragam Joseph, K. Bienert, K. Le Mai Hoang, P. H. Seeberger, *J. Am. Chem. Soc.* **2021**, *143*, 8893-8901.

[134] M. S. Tonetti, H. Greenwell, K. S. Kornman, *J. Periodontol.* **2018**, *89 Suppl 1*, S159-s172.

[135] R. T. Sheridan, J. Hudon, J. A. Hank, P. M. Sondel, L. L. Kiessling, *ChemBioChem* **2014**, *15*, 1393-1398.

[136] a) P. BRANDTZAEG, *Ann. N. Y. Acad. Sci.* **2007**, *1098*, 288-311; b) P. Hettegger, J. Huber, K. Paßecker, R. Soldo, U. Kegler, C. Nöhammer, A. Weinhäusel, *PloS one* **2019**, *14*, e0218456-e0218456.

[137] a) D. Barrett, *Adv. Pediatr.* **1985**, *32*, 139-158; b) Q. Vos, A. Lees, Z. Q. Wu, C. Snapper, J. Mond, *Immunol. Rev.* **2000**, *176*, 154-170.

[138] a) T. B. Tomasi Jr, *Annu. Rev. Med.* **1970**, *21*, 281-298; b) S. J. Hägewald, D. L. W. Fishel, C. E. B. Christan, J.-P. Bernimoulin, A. Kage, *Eur. J. Oral Sci.* **2003**, *111*, 203-208.

[139] a) S. Zhang, M. Sella, J. Sianturi, P. Priegue, D. Shen, P. H. Seeberger, *Angew. Chem. Int. Ed.* **2021**, *60*, 14679-14692; b) P. Kaplonek, L. Yao, K. Reppe, F. Voß, T. Kohler, F. Ebner, A. Schäfer, U. Blohm, P. Priegue, M. Bräutigam, C. L. Pereira, S. G. Parameswarappa, M. Emmadi, P. Ménová, M. Witzenrath, S. Hammerschmidt, S. Hartmann, L. E. Sander, P. H. Seeberger, *Vaccine* **2022**, *40*, 1038-1046.

[140] S. V. Durbin, W. S. Wright, J. C. Gildersleeve, *ACS omega* **2018**, *3*, 16882-16891.

[141] K. Le Mai Hoang, A. Pardo-Vargas, Y. Zhu, Y. Yu, M. Loria, M. Delbianco, P. H. Seeberger, *J. Am. Chem. Soc.* **2019**, *141*, 9079-9086.

[142] M. Gude, J. Ryf, P. D. White, *Lett. Pept. Sci.* **2002**, *9*, 203-206.

[143] D. Wang, D.-C. Xiong, X.-S. Ye, *Chin. Chem. Lett.* **2018**, *29*, 1340-1342.

[144] C. Alex, S. Visansirikul, A. V. Demchenko, *Org. Biomol. Chem.* **2020**, *18*, 6682-6695.

[145] E. M. Scanlan, M. M. Mackeen, M. R. Wormald, B. G. Davis, *J. Am. Chem. Soc,* **2010**, *132*, 7238-7239.

[146] K. Daragics, P. Fügedi, *Tetrahedron Lett.* **2009**, *50*, 2914-2916.

[147] A. A. Sherman, Y. V. Mironov, O. N. Yudina, N. E. Nifantiev, *Carbohydr. Res.* **2003**, *338*, 697-703.

[148] E. Vedejs, G. Martinez, *J. Am. Chem. Soc.* **1979**, *101*, 6452-6454.

[149] W. Xie, G. Tanabe, J. Akaki, T. Morikawa, K. Ninomiya, T. Minematsu, M. Yoshikawa, X. Wu, O. Muraoka, *Bioorg. Med. Chem.* **2011**, *19*, 2015-2022.

[150] P. J. Garegg, I. Kvarnström, A. Niklasson, G. Niklasson, S. C. Svensson, *J. Carbohydr. Chem.* **1993**, *12*, 933-953.

[151] L. Van Huy, C. Tanaka, T. Imai, S. Yamasaki, T. Miyamoto, *ACS Med. Chem. Lett.* **2018**, *10*, 44-49.

[152] L. Zou, R. B. Zheng, T. L. Lowary, *Beilstein J. Org. Chem.* **2012**, *8*, 1219-1226.

[153] D. Crich, A. A. Bowers, *J. Org. Chem.* **2006**, *71*, 3452-3463.

[154] G. Tian, J. Hu, C. Qin, L. Li, X. Zou, J. Cai, P. H. Seeberger, J. Yin, *Angew. Chem. Int. Ed.* **2020**, *59*, 13362-13370.

[155] J. Hofmann, H. S. Hahm, P. H. Seeberger, K. Pagel, *Nature* **2015**, *526*, 241-244.

[156] H. R. Elsaidi, T. L. Lowary, *Chemm Sci.* **2015**, *6*, 3161-3172.

[157] L. K. Mydock, M. N. Kamat, A. V. Demchenko, *Org. Lett.* **2011**, *13*, 2928-2931.

8   Appendix

8.1   List of Publications

Parts of this thesis were already published in:

"Expedited synthesis of mannose-6-phosphate containing oligosaccharides"
Eric T. Sletten, José Danglad Flores, **Sabrina Leichnitz**, Abragam A. Joseph, Peter H. Seeberger, *Carbohydrate. Res.* **2022**, *511*, 108489.

"Microwave-assisted Automated Glycan Assembly"
José Danglad Flores[‡], **Sabrina Leichnitz**[‡], Eric T. Sletten[‡], Abragam A. Joseph, Klaus Bienert, Kim Le M Le Mai Hoang, Peter H. Seeberger, *J. Am. Chem. Soc.* **2021**, *143* (23), 8893–8901.

"Direct Experimental Characterization of the Ferrier Glycosyl Cation in the Gas Phase"
Kim Greis, Carla Kirschbaum, **Sabrina Leichnitz**, Sandy Gewinner, Wieland Schöllkopf, Gert von Helden, Gerard Meijer, Peter H. Seeberger, Kevin Pagel, *Org. Lett.* **2020**, *22* (22), 8916-8919.

Parts of this thesis are in preparation for the manuscripts:

"Green Light Labile BODIPY Protecting Groups for the Synthesis of Glycans."

Sabrina Leichnitz, Arthur Winter, Peter H. Seeberger

"The Effect of Electron Density in Acyl Protecting Groups on the Selectivity of Galactosylations."

Kim Greis[‡], **Sabrina Leichnitz**[‡], Carla Kirschbaum, Gerard Meijer, Gert von Helden, Peter H. Seeberger, Kevin Pagel,

"Automated Glycan Assembly of *Porphyromonas Gingivalis* LPS Epitopes for Vaccine Design."

Sabrina Leichnitz, Kim-Natalie Stolte, Katrin Sellrie, José Danglad-Flores, Henrik Dommisch, Peter H. Seeberger

Published manuscript before the start of this dissertation:

"A fluorescence assay for the detection of hydrogen peroxide and hydroxyl radicals generated by metallonucleases."

Sabrina Leichnitz, Julian Heinrich, Nora Kulak, *Chem. Commun.* **2018,** *54* (95), 13411-13414.

[‡]These authors contributed equally.

8.2 Curriculum Vitae

Aus Gründen des Datenschutzes ist der Lebenslauf in der Online-Version nicht enthalten.